Steering Product Formation in High-Pressure Anaerobic Digestion Systems

The role of elevated partial pressure of carbon dioxide (pCO2)

Ceron Chafla, P.S.

DOI
10.4233/uuid:851366e2-88e2-4d9e-8831-35a8dfe450df

Publication date
2022

Document Version
Final published version

Citation (APA)
Ceron Chafla, P. S. (2022). *Steering Product Formation in High-Pressure Anaerobic Digestion Systems: The role of elevated partial pressure of carbon dioxide (pCO2)*. [Dissertation (TU Delft), Delft University of Technology]. https://doi.org/10.4233/uuid:851366e2-88e2-4d9e-8831-35a8dfe450df

STEERING PRODUCT FORMATION IN HIGH PRESSURE ANAEROBIC DIGESTION SYSTEMS:

THE ROLE OF ELEVATED PARTIAL PRESSURE OF CARBON DIOXIDE (pCO_2)

Pamela Cerón Chafla

GHENT UNIVERSITY

TU Delft

Steering Product Formation in High-Pressure Anaerobic Digestion Systems

The role of elevated partial pressure of carbon dioxide (pCO_2)

Pamela S. CERON CHAFLA

Steering Product Formation in High-Pressure Anaerobic Digestion Systems

The role of elevated partial pressure of carbon dioxide (pCO_2)

Dissertation

For the purpose of obtaining the degree of doctor
at Delft University of Technology
by the authority of the Rector Magnificus Prof. dr. ir. T. H. J. J. van der Hagen
chair of the Board for Doctorates
to be defended publicly on
Thursday 14th of July, 2022 at 15:00 o'clock

by

Pamela Stefanía CERON CHAFLA
Master of Science in Environmental Technology and Engineering
Ghent University, Belgium - UCTP, Czech Republic - IHE Delft, The Netherlands
born in Riobamba, Ecuador

This dissertation has been approved by:
Prof. dr.ir J.B. van Lier (promotor)
Prof. dr. ir. K. Rabaey (promotor)
Dr. ir. R.E.F. Lindeboom (copromotor)

Composition of the doctoral committee:

Rector Magnificus	Chairperson
Prof. dr. ir. J.B. van Lier	Delft University of Technology, promotor
Prof. dr. ir. K. Rabaey	Ghent University, promotor
Dr. ir. R.E.F. Lindeboom	Delft University of Technology, copromotor

Independent members:

Prof. dr. ir. E.I.P. Volcke	Ghent University, Belgium
Prof. dr. ir. G.J.W. Euverink	University of Groningen, The Netherlands
Prof. dr. ir. M.K. de Kreuk	Delft University of Technology
Dr. ir. M. Winkler	University of Washington, United States

Reserve member:

Prof. dr. ir. L.C. Rietveld	Delft University of Technology

The doctoral research has been carried out in the context of an agreement on joint doctoral supervision between Ghent University, Belgium and Delft University of Technology, the Netherlands.

The doctoral research was performed at the Water Management Department, Faculty of Civil Engineering and Geosciences, Delft University of Technology. It included a six months research stay at the Centre for Microbial Ecology and Technology (CMET), Faculty of Bioscience Engineering, Ghent University. The research project was funded by the European Union's Horizon 2020 research and innovation program under the Marie Skłodowska-Curie grant agreement No 676070 (SuPER-W). This communication reflects only the author's view, and the Research Executive Agency of the EU is not responsible for any use that may be made of the information it contains.

Cover design: Ariana M. Ceron Chafla

Printed in the Netherlands by Proefschrift-aio.nl

ISBN: 978-94-93270-78-7

An electronic version of this dissertation is available at http://repository.tudelft.nl

Table of Contents

Summary

Anaerobic processes such as Anaerobic Digestion (AD) and mixed culture fermentation (MCF) are important technologies in the bioeconomy context since they can be used to convert (waste) biomass feedstock into gaseous energy carriers and chemical commodities, theoretically without the use of any additional energy source. AD is a multi-step bioconversion process pursuing organic matter stabilization whose final product, *i.e.*, biogas, can be used as an energy source. On the other hand, MCF employs open mixed cultures under non-sterilized conditions to produce carboxylates, *i.e.,* short and medium-chain organic acids, which will serve as chemical building blocks after downstream processing.

Limitations of biogas production are associated with the low CH_4 content (≈50-60%), presence of impurities (like H_2S) and unsuitable final pressure for direct connection to national grids. Thus, in recent years, the topic of biogas upgrading to biomethane (i.e., CH_4>90%) has gained momentum and in-situ and ex-situ alternatives have been proposed with differences in financial and technical viability as well as achieved final CH_4 content. While for the carboxylate production, major limitations are associated with process selectivity, presence of trace pollutants and too low broth concentrations for direct application inducing a need for "wet" and energy-intensive downstream processing.

High-Pressure Anaerobic digestion (HPAD) is an innovative technology designed for simultaneous digestion and biogas upgrading. HPAD takes advantage of the large differences in solubility between biogas constituents, *i.e.,* CH_4 and CO_2. Consequently, CH_4 will predominantly remain in the gas phase after a pressure increase, whereas ionisable gases like CO_2 and H_2S will increasingly dissolve in the liquid. Thus, from a biogas production perspective, the proposed technology accomplishes higher CH_4 content in the gas phase at the cost of increased dissolved CO_2 levels. The process's overall performance under elevated pCO_2 has not been adequately addressed. Mechanistic explanations for the role of increased dissolved CO_2 in the fermentation process remain speculative, partially due to the limited amount of published experimental work on high-pressure fermentation with open cultures. Since CO_2 exerts multiple roles in biological systems, increased dissolved CO_2 could impact the kinetic and energetic feasibility of the reaction chain in AD and MCF, as well as the microbial community dynamics. These effects constitute a notorious knowledge gap that requires urgent attention.

In this thesis, we examined the role of elevated CO_2 partial pressure (pCO_2) in anaerobic processes, based on the premise that due to its multiple roles in biological systems, elevated pCO_2 could be exploited to deliberately steer towards biogas or selective carboxylates production. **Chapter 1** describes the background and problem analysis and gives an overview

of relevant concepts for operation at elevated CO2 in the context of high-pressure AD and MCF and the scope of the research.

In the content chapters of this thesis, we start examining the effect of elevated pCO_2 in syntrophic conversions**. Chapter 2** deals with a kinetic and thermodynamic analysis of the syntrophic conversion of propionate and butyrate. Results showed that increasing pCO_2 from 0.3 to 8.0 bar in lab-scale batch reactors decreased the maximum substrate utilization rate ($r_{s\max}$) for both syntrophic oxidations. It is then proposed that these kinetic limitations are linked to an increased overall Gibbs free energy change ($\Delta G_{Overall}$), leading to a redistribution of the available biochemical energy among syntrophic partners. However, these kinetic and bioenergetics constraints only helped to a certain extent to explain the observed effects during syntrophic conversions under elevated pCO_2. Thus, incorporating physiological limitations on growth exerted by increased acidity and inhibition due to higher concentrations of undissociated volatile fatty acids is proposed to complement the initial explanatory mechanism.

A latent issue in high-pressure operation is the uncertainty that observable effects can be either attributed to an increase in total operational pressure or to modifications of partial pressure of gas components in the headspace. In addition, the possibility of developed tolerance to pressure (piezotolerance) due to prior exposure to other environmental stress factors has been limitedly addressed. In **Chapter 3**, we investigate carboxylate production and stress-response to mild hydrostatic pressure (MHP), considering incubation temperature and halotolerance of a marine sediment inoculum (MSI) and an anaerobic digester inoculum (ADI). Results showed that MHP effects on microbial growth, activity and community structure were strongly temperature-dependent. In contrast to low and high temperatures, incubation at moderate temperatures in concomitance with MHP did not limit biomass yield and carboxylates production. Thus, a cross-resistance effect from incubation temperature and halotolerance is proposed. Moreover, results revealed that temperature impacts the microbial community structure during the enrichment period, and only slight differences were observed after subsequent microbiome exposure to MHP.

Chapter 4 builds upon the understanding of cross-tolerance effects gained in chapter 3 and moves towards studying the effects of elevated pCO_2 on the conversion of more complex substrates. Here directional selection, *i.e.,* adaptive laboratory evolution (ALE), under increasing substrate load, is proposed as a strategy to restructure the microbial community. Also, to induce cross-protection mechanisms to enable glucose and glycerol conversion under elevated pCO_2. After the ALE process, the evolved inoculum showed differences in carbon flux distribution under elevated pCO_2. Glucose conversion correlated with higher cell density and viability, whereas glycerol addition led to high propionate production, whose enabled conversion reflected in an increased CH_4 yield. High CH_4 yield in the evolved inoculum was

ascribed to biomass adaptation and a restructured, more resilient microbial community. The evolved community was characterized by increased abundance in *Methanosaeta* and syntrophic propionate oxidizing bacteria (SPOB). Among the SPOB, the *Smithella* genus showed predominance, particularly after using glycerol as the substrate.

Throughout this study, it was observed that operational conditions could restructure the microbial community. For example, biomass adaptation at increasing substrate to biomass (S/X) ratios at atmospheric conditions showed to be advantageous for CH_4 production under elevated pCO_2. Thus, it was imperative to study the interaction of elevated pCO_2 with other operational conditions. **Chapter 5** investigated whether interaction effects between substrate type, high S/X ratio, and the presence of an external electron donor (formate) could influence the possible steering effect of pCO_2. It was hypothesized that we could limit CH_4 production while promoting carboxylates production with this strategy. The results evidenced that the interaction effect between high substrate concentration (to increase S/X ratio) and elevated pCO_2, while having formate present as additional electron donor, was significant to explain differences in metabolite predominance and cell density. Furthermore, the product spectrum was influenced by microbial community composition, which itself was modified by the interaction of pCO_2 and the presence of formate as additional electron donor. The latter interaction effect also showed statistical significance in explaining differences in succinate production.

Finally, in **Chapter 6**, the most relevant results from this thesis are interlinked and comprehensively discussed. The outlook for future research in HPAD and high-pressure MCF is presented in conjunction with envisioned roles for elevated pCO_2 in AD and MCF in the context of negative emissions technologies.

Samenvatting

Anaerobe processen zoals anaerobe gisting en fermentatie met gemende culturen (GCF) zijn belangrijke technologieën in de bio-economie, aangezien zij kunnen worden gebruikt om (afval) biomassa om te zetten in energie en chemische halffabricaten. Anaerobe gisting is een meertraps bioconversieproces waarbij organisch materiaal wordt gestabiliseerd en waarvan het eindproduct, biogas, als energiebron kan worden gebruikt. Fermentatie maakt gebruik van open gemengde culturen onder niet-steriele condities met als doel om organische zuren met korte en middellange keten te produceren, die kunnen dienen als halffabricaten voor de chemische industrie.

De beperkingen van de conventionele biogasproductie houden verband met het lage CH_4-gehalte (≈50-60%), de onzuiverheid van het biogas door aanwezigheid van bijvoorbeeld H_2S en de ongeschikte einddruk voor directe aansluiting op het regionale en nationale aardgasnetwerk. De laatste jaren is dan ook veel aandacht besteed aan de opwaardering van biogas tot biomethaan (d.w.z. CH_4>90%) en er zijn in-situ en ex-situ alternatieven voorgesteld met verschillen in financiële en technische haalbaarheid en in het gerealiseerde CH_4-gehalte. De belangrijkste beperkingen voor de productie van korte en middenlange vetzuren zijn de selectiviteit van het proces, de onzuiverheid van het product en te lage concentraties in het fermentatiemedium voor directe toepassing. Daarom energie-intensieve processtappen noodzakelijk zijn om tot het gewenste product te komen.

Hogedruk anaerobe gisting is een innovatieve technologie die ontworpen is voor gelijktijdige vergisting en opwaardering van biogas. Hogedruk anaerobe gisting maakt gebruik van de grote verschillen in oplosbaarheid tussen de bestanddelen van biogas, d.w.z. CH_4 en CO_2. Daardoor zal CH_4 na een drukverhoging overwegend in de gasfase blijven, terwijl de andere gassen in toenemende mate in de vloeistof zullen oplossen. Vanuit het perspectief van biogasproductie kan met de voorgestelde technologie een hoger CH_4-gehalte in de gasfase worden bereikt. Dit resulteert dan wel in een verhoogd opgelost CO_2-gehalte in het reactormedium. Op dit moment is er te weinig bekend over de invloed hiervan op de fermentatie. De beschikbare mechanistische verklaringen over de rol van verhoogde opgeloste CO_2 in het proces zijn speculatief, doordat er weinig experimenteel werk is verricht op hogedrukfermentatie met open culturen. Aangezien CO_2 een meervoudige rol speelt in biologische systemen, zou een toename van opgelost CO_2 een invloed kunnen hebben op de kinetische en energetische haalbaarheid van de metabolische routes in anaerobe gisting en fermentatie. Dit beïnvloed op zijn beurt weer de dynamiek van de microbiële gemeenschap, wat een belangrijke kennislacune vormt in dit vakgebied.

In dit proefschrift is gekeken naar de rol van de verhoogde partiële CO_2 spanning (pCO_2) in anaerobe processen. Als uitgangspunt is de hypothese gekozen dat door zijn complexe rol in biologische systemen, verhoogde pCO_2 zou kunnen worden benut om de productie van biogas en korte en middellange vetzuren doelbewust te sturen. **Hoofdstuk 1** omvat de achtergrond en probleemanalyse, een overzicht van relevante concepten om de werking bij verhoogde CO_2 te plaatsen in de context van hogedruk anaerobe gisting en fermentatie van organisch afval. Ook de afbakening van het onderzoek is gepresenteerd in dit hoofdstuk.

In de inhoudelijke hoofdstukken van dit proefschrift beginnen we me het onderzoeken van het effect van verhoogde pCO_2 op syntrofe microbiële omzettingen. **Hoofdstuk 2** gaat daarom in op de kinetische en thermodynamische analyse van de syntrofe conversie van gedissocieerd propion- en boterzuur. De resultaten toonden aan dat het verhogen van de pCO_2 druk van 0.3 naar 8.0 bar in reactoren op laboratoriumschaal leidde tot een afname van de maximale substraat omzettingssnelheid ($r_{s\max}$) voor beide substraten. Er wordt vervolgens voorgesteld dat deze kinetische beperkingen gekoppeld zijn aan een toename van de verandering van de Gibbs vrije energie ($\Delta G_{Overall}$). Dit leidt tot een herverdeling van de beschikbare biochemische energie binnen syntrofe microbiële partners. Desalniettemin konden deze kinetische en bio-energetische beperkingen maar de geobserveerde effecten maar gedeeltelijk verklaren. Her wordt vervolgens uit afgeleid dat het voorgestelde mechanisme aangevuld dient te worden met fysiologische beperkingen van de groei door een verhoogde zuurtegraad en remming door hogere concentraties van ongedissocieerde vluchtige vetzuren.

Een inherent probleem van hogedruk gisting en fermentatie is dat de waarneembare effecten moeilijk zijn toe te wijzen aan de verhoging van de totale operationele druk of juist aan de partiële dampspanning van gasvormige eind- en tussenproducten. Bovendien is de opgebouwde tolerantie tegen druk (piëzotolerantie) als gevolg van voorafgaande blootstelling aan andere fluctuerende omgevingscondities slechts in beperkte mate onderzocht. In **Hoofdstuk 3** onderzoeken we de respons van gedissocieerde vetzuurproductie als gevolg van blootstelling aan milde hydrostatische druk (MHD). Hierbij wordt er rekening gehouden met de oorspronkelijke omgevingstemperatuur en het zoutgehalte van de twee gekozen entstoffen: een microbiologisch actief sediment uit de Noordzee en een anaerobe cultuur uit een industriële vergister van afvalwater met een hoog zoutgehalte. Er is vastgesteld dat effecten van MHD op microbiële groei, kinetiek en gemeenschapsstructuur sterk temperatuurafhankelijk zijn. In tegenstelling tot lage en hoge temperaturen worden de biomassa-opbrengst en de ongedissocieerde vetzuurproductie niet beperkt door milde temperaturen in combinatie met MHD. Daarom wordt er gespeculeerd dat er kruistolerantie is opgetreden als gevolg van de incubatietemperatuur en halotolerantie. Bovendien is vastgesteld dat de temperatuur tijdens de verrijkingsperiode van invloed is op de structuur van de microbiële gemeenschap en dat er

slechts geringe verschillen worden waargenomen na blootstelling van de microbiële gemeenschap aan MHD.

Hoofdstuk 4 bouwt voort op het begrip van kruistolerantie uit hoofdstuk 3, en bestudeert van de effecten van verhoogde pCO_2 op de omzetting van complexere substraten. Hier wordt gerichte selectie, d.w.z. adaptieve laboratorium-evolutie (ALE), onder toenemende substraatbelasting voorgesteld als een strategie om de microbiële gemeenschap te herstructureren. Ook zou ALE een kruistolerantie kunnen induceren om de omzetting van glucose en glycerol onder verhoogde pCO_2 te verbeteren. Na het ALE proces vertoonde het geëvolueerde entstof verschillen in de verdeling van de koolstofflux bij verhoogde pCO_2: glucoseconversie correleerde met hogere cel dichtheid en hoger aantal levende cellen, terwijl glycerol leidde tot hoge propionaat productie, wat zich weerspiegelde in een verhoogde CH_4 opbrengst. De hogere CH_4 opbrengst in het geëvolueerde entstof werd toegeschreven aan adaptie op cel niveau en aan de herstructurering van de microbiële gemeenschap. De geëvolueerde gemeenschap wordt gekenmerkt door een verhoogde aanwezigheid van *Methanosaeta* en syntrofe propionaat oxiderende bacteriën (SPOB). Bij de SPOB was het *Smithella* genus overheersend, vooral na het gebruik van glycerol als substraat.

In de loop van deze studie werd vastgesteld dat de microbiële gemeenschap kan worden geherstructureerd door te sturen op operationele omstandigheden, bv. aanpassing van de atmosferische biomassa aan stijgende substraat/biomassa-verhoudingen (S/X) ratio. Dit bleek daarbovenop gunstig te zijn voor de CH_4-productie onder verhoogde pCO_2. Daarom was het noodzakelijk de interactie van verhoogde pCO_2 met andere operationele omstandigheden te bestuderen. **Hoofdstuk 5** onderzocht of interactie-effecten tussen substraattype, hoge S/X ratio en aanwezigheid van externe elektronendonor (ongedissocieerd mierenzuur) het mogelijke sturende effect van pCO_2 zouden kunnen beïnvloeden. De hypothese was dat met deze strategie konden we de CH_4-productie beperken en tegelijk de productie van vetzuren bevorderen. De resultaten toonden aan dat het interactie-effect tussen hoge substraatconcentratie (verhoging van de S/X ratio) en verhoogde pCO_2, bij aanwezigheid van ongedissocieerd mierenzuur als extra elektrondonor, significant was om verschillen in de verhouding tussen metabolieten en opgebouwde celmassa te verklaren. Het productspectrum werd beïnvloed door de samenstelling van de microbiële gemeenschap, die op zijn beurt werd beïnvloed door de interactie van pCO_2 met externe elektronendonor. Ook bleek de interactie van pCO_2 met een externe elektronendonor noodzakelijk te zijn voor de productie van barnsteenzuur.

Tot slot worden in **Hoofdstuk 6** de meest relevante resultaten uit dit proefschrift met elkaar in verband gebracht en uitvoerig besproken. De vooruitzichten voor toekomstig onderzoek naar hogedruk anaerobe gisting en fermentatie worden gepresenteerd in combinatie met de verwachte rol van verhoogde pCO_2 in de context van negatieve-emissietechnologie.

Resumen

Los procesos anaerobios, como la digestión anaerobia (DA) y la fermentación de cultivos mixtos (FeCM), son tecnologías importantes en el contexto de la bioeconomía, ya que pueden utilizarse para convertir materias primas (biomasa de desecho) en portadores gaseosos de energía y productos químicos, teóricamente sin utilizar ninguna fuente de energía adicional. La DA es un proceso de bioconversión en varias fases que persigue la estabilización de la materia orgánica y cuyo producto final, el biogás, puede utilizarse como fuente de energía. Por otro lado, la FeCM emplea cultivos mixtos abiertos, en condiciones no esterilizadas para producir carboxilatos, es decir, ácidos orgánicos de cadena corta y media, que servirán como bloques de construcción química tras un posterior procesamiento.

Las limitaciones de la producción de biogás están relacionadas con el bajo contenido de CH_4 (≈50-60%), la presencia de impurezas (como el H_2S) y una presión final inadecuada para la conexión directa a las redes nacionales. Por ello, en los últimos años, el tema de la mejora del biogás para convertirlo en biometano (es decir, CH_4>90%) ha cobrado impulso y se han propuesto alternativas in situ y ex situ con diferencias en cuanto a la viabilidad financiera y técnica, así como al contenido final de CH_4 alcanzado. Mientras que para la producción de carboxilatos, las principales limitaciones están asociadas a la selectividad del proceso, la presencia de contaminantes traza y las concentraciones demasiado bajas en el líquido de fermentación para su utilización directa, lo que induce a la necesidad de un procesamiento posterior caracterizado por un alto consumo energético.

La digestión anaeróbica de alta presión (DAAP) es una tecnología innovadora diseñada para la llevar a cabo de manera simultánea el proceso de DA y mejora del biogás. La DAAP aprovecha las grandes diferencias de solubilidad entre los componentes del biogás, es decir, el CH_4 y el CO_2. En consecuencia, el CH_4 permanecerá predominantemente en la fase gaseosa tras un aumento de presión, mientras que los gases ionizables como el CO_2 y el H_2S se disolverán cada vez más en el líquido. Así, desde la perspectiva de la producción de biogás, la tecnología propuesta consigue un mayor contenido de CH_4 en la fase gaseosa a costa de un aumento de los niveles de CO_2 disuelto. Sin embargo, no se ha abordado adecuadamente el rendimiento general del proceso bajo una pCO_2 elevada. Las explicaciones mecanísticas sobre el papel del aumento del CO_2 disuelto en el proceso de fermentación siguen siendo especulativas, en parte debido a la escasa cantidad de trabajos experimentales publicados sobre la DA y fermentación a alta presión con cultivos mixtos. Dado que el CO_2 ejerce múltiples funciones en los sistemas biológicos, el aumento del CO_2 disuelto podría afectar a la viabilidad cinética y energética de la cadena de reacción en la DA y la FeCM, así como a la dinámica de la comunidad microbiana. Estos efectos constituyen una notoria laguna de conocimiento que requiere atención urgente.

En esta tesis se examina el papel de la elevada presión parcial de CO_2 (pCO_2) en los procesos anaerobios, partiendo de la premisa de que, debido a su complejo papel en los sistemas biológicos, la elevada pCO_2 podría ser aprovechada para orientar de forma deliberada la producción de biogás o carboxilatos. En el **Capítulo 1** se describen los antecedentes y el análisis del problema y se ofrece una visión general de los conceptos relevantes para el funcionamiento en condiciones de elevada pCO_2 en el contexto de la DAAP y la FeCM a alta presión, así como también el alcance de la investigación.

En los capítulos de contenido de esta tesis, comenzamos examinando el efecto de la elevada pCO_2 en las conversiones sintróficas. El **Capítulo 2** presenta un análisis cinético y termodinámico de la conversión sintrófica de propionato y butirato. Los resultados muestran que el aumento de la pCO_2 de 0.3 a 8.0 bar en reactores discontinuos a escala de laboratorio disminuyó la tasa máxima de utilización del sustrato ($r_{s\max}$) para ambas oxidaciones sintróficas. Es así que se propone que estas limitaciones cinéticas están relacionadas con un aumento del cambio de energía libre de Gibbs ($\Delta G_{Overall}$), lo que conduce a una redistribución de la energía bioquímica disponible entre los asociados sintróficos. Sin embargo, estas limitaciones cinéticas y bioenergéticas ayudan a explicar los efectos observados en las conversiones sintróficas bajo elevada pCO_2 sólo hasta un cierto punto. Por tanto, se plantea la incorporación de limitaciones fisiológicas al crecimiento microbiano debido a procesos de acidificación y la inhibición resultante de un incremento en las concentraciones de ácidos grasos volátiles no disociados como partes complementarias del mecanismo explicativo inicialmente propuesto.

Una cuestión latente en el funcionamiento a alta presión es la incertidumbre de que los efectos observables puedan atribuirse a un aumento de la presión operativa total o a modificaciones de las presiones parciales de los componentes en la fase gaseosa. Además, la posibilidad de que la biomasa desarrolle una tolerancia a la presión (piezotolerancia) debido a la exposición previa a otras fuentes de estrés ambiental se ha abordado de forma limitada. Por ello en el **Capítulo 3**, se investiga la producción de carboxilatos y la respuesta-de-estrés a la presión hidrostática moderada (PHM), considerando la temperatura de incubación y la halotolerancia de inóculos proveniente de un sedimento marino (ISM) y de un digestor anaerobio (IDA). Se estableció que los efectos de la PHM en el crecimiento microbiano, la actividad y la estructura de la comunidad dependen considerablemente de la temperatura. A diferencia de las bajas y altas temperaturas, las temperaturas moderadas en concomitancia con la PHM no limitaron el rendimiento de la biomasa ni la producción de carboxilatos. Por tanto, se propone un efecto de resistencia cruzada entre la temperatura de incubación y la halotolerancia. Además, se determinó que la temperatura afecta a la estructura de la comunidad microbiana durante el periodo de enriquecimiento, y sólo se observaron diferencias menores tras la posterior exposición del microbioma a PHM.

El **Capítulo 4** hace uso del entendimiento ganado acerca de los efectos de resistencia cruzada (capítulo 3) y pasa a estudiar los efectos de la pCO_2 elevada en la conversión de sustratos más complejos. Aquí se propone la selección direccional, es decir, un proceso de **e**volución **a**daptativa a nivel de **l**aboratorio (EAL), bajo una carga creciente de sustrato, como estrategia para reestructurar la comunidad microbiana e inducir mecanismos de protección cruzada que permitan la conversión de glucosa y glicerol bajo una elevada pCO_2. Tras el proceso de EAL, el inóculo evolucionado mostró diferencias en la distribución del flujo de carbono bajo elevada pCO_2. La conversión de glucosa se correlacionó con una mayor densidad y viabilidad celular, mientras que la conversión de glicerol condujo a una alta producción de propionato, cuya reanudada conversión reflejó en un mayor rendimiento de CH_4. El alto rendimiento de CH_4 en el inóculo evolucionado se atribuyó a la adaptación de la biomasa y a una restructuración de la comunidad microbiana que se volvió más resiliente. La comunidad evolucionada se caracterizó por una mayor abundancia de miembros del género *Methanosaeta* y de bacterias sintróficas oxidadoras de propionato (SPOB) asociadas al género *Smithella*, especialmente tras utilizar glicerol como sustrato.

A lo largo de este estudio, se estableció que la comunidad microbiana puede ser reestructurada por las condiciones operacionales, por ejemplo, en el caso de la adaptación de la biomasa al aumento de la carga orgánica en condiciones atmosféricas. Esta adaptación resultó beneficiosa para la producción de CH_4 bajo una elevada pCO_2 (capítulo 4). Por tanto, resultó imperativo estudiar la interacción de la elevada pCO_2 con otras condiciones operacionales. En el **Capítulo 5** se investigó si los efectos de la interacción entre el tipo de sustrato, una alta relación sustrato/biomasa (S/X) y la presencia de un donador externo de electrones (formato) podían influir en el posible efecto direccionador de la pCO_2. Se planteó la hipótesis de que con esta estrategia se podría limitar la producción de CH_4 mientras se promovía la producción de carboxilatos. Los resultados evidenciaron que el efecto de interacción entre una alta concentración de sustrato (para aumentar la relación S/X) y una elevada pCO_2 era significativo para explicar las diferencias en la predominancia de metabolitos y la densidad celular, mientras que se garantice la presencia de formato como donador adicional de electrones. Además, el espectro de producto se vio influenciado por la composición de la comunidad microbiana, que a su vez fue modificada por la interacción de la pCO_2 y la presencia de formato como donador adicional de electrones. Este último efecto de interacción también mostró significancia estadística para explicar las diferencias en la producción de succinato.

Por último, en el C**apítulo 6**, se interrelacionan y discuten exhaustivamente los resultados más relevantes asociados a los capítulos de esta tesis. Además, se presentan las perspectivas de la investigación en DAAP y FeCM a alta presión junto con el rol previsto para la elevada pCO_2 en el contexto de las tecnologías de emisiones negativas.

Nomenclature

Abbreviations

AA	absolute abundance
ABE	acetone-butanol-ethanol
AC	atmospheric control
AcM	aceticlastic methanogenesis
AD	anaerobic digestion
ADI	anaerobic digestion inoculum
AHPD	autogenerative high pressure anaerobic digestion
ALE	adaptive laboratory evolution
AnMBR	anaerobic membrane bioreactor
ANC	acid neutralizing capacity
CCA	canonical correspondence analysis
CD	cell density
C-mol	carbon mole (mol)
COD	chemical oxygen demand
CSTR	continuous stirred tank reactor
DAF	dissolved air flotation
DGGE	denaturation gradient gel electrophoresis
DIC	dissolved inorganic carbon
DIET	direct interspecies electron transfer
EGSB	expanded granular sludge bed reactor
EMC	engineered microbial communities
EPS	extracellular polymeric substances
FSC-H	forward scatter height
FCM	flow cytometry measurement
FW	food waste
GC	gas chromatography
HA	homoacetogenesis
HAc	undissociated acetic acid
HBu	undissociated butyric acid
HPr	undissociated propionic acid
HHP	high hydrostatic pressure
HP	hydrostatic pressure
HPAD	high pressure anaerobic digestion
HP-MCF	high pressure mixed culture fermentation
HRT	hydraulic retention time
HyM	hydrogenotrophic methanogenesis
IC	ion chromatography
IEA	International Energy Association
LC	liquid chromatography
LCV	lower calorific value
MBB	moving bed biofilm
MCF	mixed culture fermentation
MHP	mild hydrostatic pressure
MP	microbial protein
MSI	marine sediment inoculum

NAD	Nicotinamide adenine dinucleotide
NADH	Nicotinamide adenine dinucleotide + hydrogen
NGS	Next generation sequencing
NMC	natural microbial communities
NMDS	Non-metric multidimensional scaling
OAA	oxaloacetate
OLR	organic loading rate
OTU	operational taxonomic unit
PBS	phosphate-buffered saline
PBB	purple phototrophic bacteria
PCR	polymerase chain reaction
PEP	phosphoenolpyruvate
PERMANOVA	Permutation analysis of variance
PHA	polyhydroxyalkanoate
PTS	phosphotransferase transport system
RA	relative abundance
RID	refractive index detector
SAO	syntrophic acetate oxidation
SBO	syntrophic butyrate oxidation
sCOD	soluble chemical oxygen demand
SMP	soluble microbial products
SMPR	specific methane production rate
SMY	specific methane yield
SPO	syntrophic propionate oxidation
SPOB	syntrophic propionate oxidation bacteria
SRB	sulfate reducing bacteria
SRT	solids retention time
SSC-H	side scatter height
TAN	total ammonium nitrogen
TCA	Tricarboxylic acid cycle
tCOD	total chemical oxygen demand
TOC	total organic carbon
TP	total phosphorous
TS	total solids
TSS	total suspended solids
UASB	up-flow anaerobic sludge blanket reactor
VFA	volatile fatty acids
VS	volatile solids
VSS	volatile suspended solids
WLP	Wood–Ljungdahl pathway

Symbols

$[C_{gas}]$	Dissolved gas concentration in the liquid	(mol L^{-1})
K_H	Henry's constant	(mol L^{-1} bar^{-1})
P_{gas}	Gas partial pressure	(bar)
K	Equilibrium constant	h^{-1}
$\Delta V^{\neq}$	Reaction activation volume	cm^3 mol^{-1}
R	Universal gas constant	m^3 Pa K^{-1} mol^{-1}

T	Temperature	K
y	Substrate concentration in the modified Gompertz equation	(mg L^{-1})
λ	Lag phase in the modified Gompertz equation	(day)
$r_{s\max}$	Maximum substrate utilization rate in the modified Gompertz equation	(mg L^{-1} day^{-1})
A	the maximum substrate concentration	(mg L^{-1})
t	Time in the modified Gompertz equation	(days)
ΔG_R^0	Gibbs free energy change for reaction R at standard temperature and pressure	(kJ mol^{-1})
ΔG_R^{01}	Gibbs free energy change for reaction R corrected by biological pH reference value (pH=7)	(kJ mol^{-1})
ΔG_R^1	Gibbs free energy change for reaction R corrected by actual operational conditions	(kJ mol^{-1})
$\Delta G_{Overall}$	Gibbs free energy change for the syntrophic reaction corrected by actual operational conditions	(kJ mol^{-1})
ΔG_{Pr-Ox}	Gibbs free energy change for propionate oxidation corrected by actual operational conditions	(kJ mol^{-1})
ΔG_{Bu-Ox}	Gibbs free energy change for butyrate oxidation corrected by actual operational conditions	(kJ mol^{-1})
ΔG_{AcM}	Gibbs free energy change for aceticlastic methanogenesis corrected by actual operational conditions	(kJ mol^{-1})
ΔG_{HyM}	Gibbs free energy change for hydrogenotrophic methanogenesis corrected by actual operational conditions	(kJ mol^{-1})
rs	Spearman's correlation coefficient	
ΔG_{cat}^{01}	Gibbs energy change for catabolism corrected for biological pH=7	(J/ reaction)
ΔG_{Tr-HA}	Gibbs energy change for active transport acid molecule (HA) through the membrane	(kJ $mmol^{-1}$)
m	Gibbs energy change for maintenance	(J d^{-1})
m_G	Gibbs energy coefficient for maintenance purposes	(kJ C-mol^{-1} X h^{-1})
m_{tot}	Overall maintenance	(C-mol substrate C-mol X^{-1} h^{-1})
$Y_{X/S}$	Biomass yield on substrate	(C-mol X mol $glucose^{-1}$)
μ	growth rate	(h^{-1})
μ_{max}	maximal growth rate	(h^{-1})
μ_{net}	net growth rate	(h^{-1})
q_s	overall substrate conversion flux	(mol substrate mol-X^{-1} h^{-1})
X	biomass	(mol)
ΔV	change in reaction volume	(cm^3 mol^{-1})

1

CHAPTER 1
INTRODUCTION

This chapter is partially based on:

Ceron-Chafla, P., De Vrieze, J., Rabaey, K., van Lier, J. B., & Lindeboom, R. E. F. Potentials and limitations of elevated pCO_2 as steering parameter in anaerobic processes. Submitted to Biotechnology for Biofuels and Bioproducts.

Ceron-Chafla, P., García-Timermans, C., Vrieze, J., Ganigué, R., Boon, N., Rabaey, K., Lier, J.B., Lindeboom, R.E.F., 2022. Pre-incubation conditions determine the fermentation pattern and microbial community structure in fermenters at mild hydrostatic pressure. Biotechnol. Bioeng. 1–16.

Ceron-Chafla, P., Chang, Y., Rabaey, K., van Lier, J. B., & Lindeboom, R. E. F. (2021). Directional Selection of Microbial Community Reduces Propionate Accumulation in Glycerol and Glucose Anaerobic Bioconversion Under Elevated pCO_2. Frontiers in Microbiology, 12(June), 1583.

Ceron-Chafla, P., Kleerebezem, R., Rabaey, K., van Lier, J.B., & Lindeboom, R. E. F (2020). Direct and Indirect Effects of Increased CO_2 Partial Pressure on the Bioenergetics of Syntrophic Propionate and Butyrate Conversion. Environmental Science & Technology, 54(19), 12583–12592.

1.1 Background and problem analysis

The pursuit of carbon neutrality is a pressing issue in our society (Bataille et al., 2018). Thus, technological developments for capture, sequestration, and utilization of CO_2 toward value addition are on the rise (Shi et al., 2015). CO_2, as the most oxidized form of carbon, plays an essential role in numerous natural processes. For example, atmospheric CO_2 reacts with the Earth's crust during the denominated weathering process (Schlesinger, 2005) and changes in atmospheric CO_2 concentrations are regulated via the ocean carbonate system (Falkowski et al., 2000). Deep ocean carbon storage after sedimentation processes and terrestrial and marine primary production (*e.g.,* via phytoplankton and plants) are important natural CO_2 sinks (Schweitzer et al., 2021). On the other hand, inside the global carbon cycle, CO_2 emissions result from respiration and decay processes of macro and microorganisms, volcanic emissions, forest fires and "anthropogenic" processes such as land-use change and fossil fuels combustion (Friedlingstein et al., 2020; Post et al., 1990). Understanding the intricate relationship of CO_2 with life could be invaluable from the perspective of achieving a balance between anthropogenic CO_2 production and consumption and the essential ecosystem services that CO_2 provides.

The spectrum of possible CO_2 utilization/valorization alternatives extends beyond primary biomass production via photosynthetic processes, since CO_2 exerts multiple roles in biological systems: electron acceptor, carbon source, intermediate and end-product of biochemical reactions, and contributor to the aquatic buffer system via the carbonate equilibrium (Bhatia et al., 2019; Connell et al., 2013; Lindeboom et al., 2016; Mikkelsen et al., 2010). The possibility of microbial CO_2 fixation in bioprocesses and transformation into value-added commodities looks promising for balancing anthropogenic CO_2 emissions when comparing energy requirements for catalyst-based CO_2 transformation in chemical and biological routes (Jajesniak et al., 2014). Nonetheless, bottlenecks such as feasibility, productivity and economic aspects need to be overcome before a mainstream implementation is achieved (Kondaveeti et al., 2020). Bioelectrochemical conversion processes for formate production, acetate and medium-chain alcohols from CO_2 are currently gaining momentum (Christodoulou et al., 2017). The more traditional CO_2 assimilation using algae and photosynthetic bacteria is being scaled up and is becoming important inside circularity approaches to diversify biofuel production, livestock feed and fertilizers (Lam and Lee, 2012). Syngas (*i.e.,* mixture of CO, CO_2 and H_2) fermentation to value-added organic products, such as acetate and ethanol, is also a process of interest. Direct utilization of CO_2 and H_2 by methanogens in the anaerobic digestion (AD) process is possible, even under extreme pressure and temperature conditions (Mauerhofer et al., 2021; Rittmann et al., 2015).

At atmospheric pressure, AD is an organic matter stabilizing multi-step process whose final output, *i.e.,* biogas, can be used as an energy source (Appels et al., 2011; Kleerebezem and van Loosdrecht, 2007; Mao et al., 2015; Van Lier et al., 2008). AD is a very well-established and robust technology (Appels et al., 2011), with a wide range of applications from sanitation (Kujawa-Roeleveld and Zeeman, 2006; Lohri et al., 2014) to bioenergy purposes (Mao et al., 2015; Weiland, 2010). However, some drawbacks of AD applied to sludge and slurry digestion are associated with the relatively low CH_4 content (≈55-65%) of the biogas due to the oxidation state of the substrate, impurities (H_2S) and unsuitable final pressure. These drawbacks do not allow direct biogas recovery for injection into regional natural gas grids or biogas usage in other high-value applications such as vehicle fuel (Fu et al., 2021).

Anaerobic microbiomes are versatile, diverse and resilient (De Vrieze et al., 2017), with fermenting capabilities widely distributed in various natural and "engineered" habitats such as marine environments, high salinity soils and sediments, the mammalian rumen and anaerobic digesters (Holtzapple et al., 2022). The diverse range of biocatalysts, *i.e.,* anaerobic microbes, the presence of a high fraction of readily fermentable carbon in waste feedstock (Kleerebezem et al., 2015), as well as the demands for more sustainable and market-appealing chemical building blocks (Angenent and Kleerebezem, 2011), has motivated the revision of biogas as the ultimate product of the anaerobic conversion of (waste) biomass. The reasons mentioned above have paved the way for the emergence of the "carboxylate platform" as an alternative for biofuel production, under the condition of inhibited methanogenesis (Agler et al., 2011; Holtzapple and Granda, 2009; Stamatopoulou et al., 2020).

Financial attractiveness in producing high-value end products (biopolymers) from a selective carboxylate production process instead of complete AD has also motivated research on the carboxylate platform. Kleerebezem et al. (2015) highlighted considerable differences in the value that could be added by high COD-wastewater treatment (8 g L^{-1}) when targeting methane production with an end-product price (2015 price level) of 0.4 euro kg^{-1} or polyhydroxyalkanoates (PHA) at 2.0 euro kg^{-1}. However, the prices of energy commodities are highly volatile and are influenced by external factors (geopolitics, natural disasters, climate change) (Ji and Fan, 2012). For example, the average Dutch gas price has almost triplicated in the winter of 2021/2022 compared to the same period in 2020 (CBS, 2022); thus, prices do not constitute a reliable and fair metric for comparison of the process output. Moreover, economic diversification with more than one economic output (*e.g.,* carboxylates and biogas) from anaerobic processes in the framework of resource recovery from waste streams presents itself as a more sustainable alternative to reduce vulnerability, when facing a fast-changing economy. In this line, rather than focusing on prices, other authors have also pointed out the benefit of focusing on more complex, high value-added end-products in the context of market supply potential for "water resource factories" (Kehrein et al., 2020; Puyol et al., 2017b) and

biorefineries, the latter aiming for fuel and chemical production from biomass feedstock via integration of diverse conversion technologies (Brehmer et al., 2009; Cherubini, 2010).

Since one of the limitations of traditional AD applied to waste treatment is the low methane content, higher operational pressures constitute a suitable alternative to increase it, due to the large differences in solubility between biogas constituents. Considering Henry's law

$$[C_{gas}] = K_H * P_{gas} \quad (1\text{-}1)$$

which describes partitioning in the gas and liquid phase depending on partial pressures, CH_4 is less soluble (k_H= 0.0014 mol L^{-1} bar^{-1}) than ionizable gases such as CO_2 (k_H= 0.033 mol L^{-1} bar^{-1}), H_2S (k_H= 0.100 mol L^{-1} bar^{-1}) and NH_3 (k_H= 59 mol L^{-1} bar^{-1}) (Sander, 2015) at a temperature of 25°C. Thus, subsequent to a pressure increase, CH_4 will predominantly remain in the gas phase, whereas the other ionizable gases will increasingly dissolve in the liquid. The pressure can be externally supplied or autogenerated due to the microbial activity in digesters equipped with a pressure valve for biogas release. Autogenerative High-Pressure Digestion (AHPD) is a novel concept proposed by Lindeboom et al. (2011) to improve the CH_4 content (>90%) and biogas pressure, in-situ, in a single step, avoiding costly post-treatment operations.

A limitedly studied outcome of AHPD concerns the increased levels of dissolved CO_2 and its effects on the overall performance of the high-pressure system beyond accumulating acidity (Lindeboom et al., 2013a). Limited attention has been paid to its possible impact on metabolic conversion routes, degradation rates and microbial community dynamics. Increased accumulation of short and medium-chain fatty acids such as propionate and valerate has been observed in high-pressure AD studies. Acid accumulation in the investigations by Lindeboom et al. (2013a, 2016) was attributed, to a certain extent, to accumulating partial pressure of CO_2 (pCO_2) in the pressure reactor and increased cation requirement to achieve CO_2 sequestration. In the case of Lemmer et al. (2017), acid accumulation was reported but not explicitly addressed. Hence, it is evident that mechanistic explanations are lacking for the proposed inhibitory effects of increasing dissolved CO_2 due to elevated headspace pressure in the reactor.

Furthermore, resulting changes in the microbial community dynamics, pathways up-or down-regulation, possible pressure-induced alterations of the enzymatic activity and inhibitory/stimulatory thresholds for the activity of open cultures have not been adequately addressed in pressurized AD. Hence, a comprehensive mechanistic explanation for carboxylates accumulation at high pressure is required if further process exploitation is intended. New studies focusing on the effect of elevated pCO_2 in pressurized AD or fermentation could reveal how this parameter could be used to influence process selectivity. Either alone or intertwined with other operational conditions, *e.g.,* substrate type, the substrate

to biomass ratio and additional electron donors, elevated pCO_2 could allow operational steering between biogas and carboxylates production in the same reactor.

1.2 Effects of high hydrostatic pressure vs elevated partial pressure of CO_2 (pCO_2)

1.2.1 Bioprocess operation at high and moderate hydrostatic pressure

Hydrostatic pressure (HP) exerts unique effects on essential properties of biological systems such as cell structure and physiology, physical and chemical properties of the surrounding environment, and metabolic activity (Aertsen et al., 2009; Dong and Jiang, 2016; Qiao et al., 2016). Traditionally, high-pressure treatment (250-700 MPa) has been used in food processing for microbial inactivation of food-borne pathogens or enzyme stabilization as an alternative to thermal processing (Bertucco and Spilimbergo, 2001; Patterson and Linton, 2008). However, the potential of sub-lethal pressure levels (< 50 MPa) to trigger specific physiologic and metabolic responses that could be of interest for applications in environmental biotechnology has not been sufficiently exploited (Ferreira et al., 2019; Mota et al., 2018, 2017).

Moderate HP has been evaluated to optimize fermentation and biopolymer production. As some of the main advantages, results have shown modifications in the product spectrum (Bothun et al., 2004), faster fermentation rates in ethanol fermentation (Picard et al., 2007) and higher polymer content with adjusted density and composition in biopolymer production (Mota et al., 2019). Concomitantly, drawbacks such as a lowered catabolic conversion capacity and biomass growth (Iwahashi et al., 2005; Molina-Höppner et al., 2003; Mota et al., 2015; Tholosan et al., 1999), as well as increased maintenance requirements (Mota et al., 2018; Wemekamp-Kamphuis et al., 2002) also have been identified, but without detailed mechanistic explanations for their occurrence. Overall, HP-operation bottlenecks will depend upon the specific response of the involved microorganisms to pressure, *i.e.,* piezotolerance (Bothun et al., 2004).

Piezotolerance is the ability to grow when exposed to elevated HP. It is widely spread from subsurface ecosystems such as the deep sea (Canganella and Wiegel, 2011; Tamburini et al., 2013) to shallow surface waters and coastal sediments (Jebbar et al., 2015; Marietou and Bartlett, 2014; Vossmeyer et al., 2012). Piezotolerance has also been evidenced in industrial strains, namely *Lactobacillus* and *Clostridium* spp. (Pavlovic et al., 2008; Vanlint et al., 2011). Considering the pressure levels where microorganisms could have an optimal growth rate, they can be classified as piezophilic (>50 MPa), piezo-tolerant (up to 50 MPa) and piezo-sensitive (low pressures). If piezotolerant organisms are exposed to a continuous high-pressure

environment, they could develop adaptations to these conditions and grow at an optimum rate through modifications in their enzymatic complexes (Abe and Horikoshi, 2001; Mota et al., 2017). Moreover, previous exposure to sources of environmental stress could also trigger piezotolerance to a different extent, depending on the nature of the interaction among stressors, namely high/low temperature, pH and high salinity (Aertsen et al., 2009).

1.2.2 Cross-resistance effects to increase microbial piezotolerance

Cross-resistance results from pre-incubation under other environmental stress conditions, *e.g.,* temperature variation, non-neutral pH, and salinity extremes (Abe, 2007). In natural habitats, cross-resistance develops from the exposure to local-scale environmental gradients occurring due to tidal, seasonal and depth variations (Johnson et al., 2009; Tholosan et al., 1999). There is increasing evidence that microbial piezotolerance is related to halotolerance and thermotolerance (Booker et al., 2019; Harrison et al., 2013). Halotolerance adaptations at the cell level (Figure 1-1) are interlinked with piezotolerance (Booker et al., 2019, 2017). Among adaptations relevant to survival under elevated pressure, membrane configuration and composition, synthesis of compatible solutes (Martin et al., 2002; Oren, 2011), cytoplasmatic accumulation of salts (Kish et al., 2012), changes in the central carbon metabolism and production of extracellular polymeric substances (EPS) have been described in literature. Particularly, microbial biofilms have been highlighted as the "protective clothing" allowing microorganisms to thrive in microbiomes from extreme environments (Yin et al., 2019).

Concerning temperature, cold exposure decreases the cell membrane fluidity and alters its lipid composition (Macdonald, 1984), which is an analogous effect to HP exposure. Conversely, high temperature increases fluidity; hence it might counteract the effects of high HP on the membrane (Fichtel et al., 2015; Winter and Jeworrek, 2009). Thermal stress triggers the synthesis of heat and cold shock proteins, which is also upregulated in the stress response under HP (Wemekamp-Kamphuis et al., 2002). The growth rate of non-adapted microorganisms can be affected by high HP and low temperature due to physiological and kinetic constraints (Jebbar et al., 2015). However, previous work shows that declining growth rates in *Halomonas spp.* after exposure to 0.1-35 MPa at 2°C improved when the medium total salt concentration was adjusted to 11% because of antagonistic effects of osmotic stress and HP in protein production and spatial configuration of the membrane (Kaye and Baross, 2004).

Microorganisms from ecosystems with limited substrate availability, such as marine sediments (Chapter 3), are already adapted to survive with limited energy at low growth rates (Lipson, 2015). In these natural habitats, microorganisms allocate higher energy for maintenance purposes compared to reactor-adapted microorganisms, which could be a strategy that allow them to thrive under several environmental stress conditions (Bonk et al., 2019).

1.2.3 Bioprocesses at high and moderate pCO_2

Supercritical CO_2, whose critical point occurs at 31.1 °C and 7.38 MPa, has been used in the food industry because of the inactivation effect on microorganisms and enzymes associated with food spoilage (Manzocco et al., 2017). In particular, bacteriostatic effects of high pCO_2 applied for sterilization occur at 4-30 MPa and 20-50°C. The bacteriostatic action leads to cytoplasm acidification, cell rupture, and the inactivation of key enzymes and transport proteins (Manzocco et al., 2017; Spilimbergo and Bertucco, 2003; Yu and Chen, 2019). Even though the technology is widely used, the exact mechanisms for the inactivation are not entirely elucidated.

The effects of elevated pCO_2 at the cell viability level can be attributed to the detrimental effect of increased H_2CO_3* concentrations on cell membrane permeability. Leakage of internal components, structural modifications, and internal acidification are part of the explanatory mechanisms (Garcia-Gonzalez et al., 2010; Wu et al., 2007). In bioreactors with a pressurized headspace, the effects of elevated pCO_2 differ from inert gases, such as N_2, which do not severely compromise cell viability (Wu et al., 2007). Considerably higher pressures of N_2 are required to achieve the same inactivation levels as with elevated pCO_2 (Aertsen et al., 2009).

The detrimental effects of increased dissolved CO_2 concentrations on cell membranes depend on localized conditions. Some microbial species have acid tolerance mechanisms involving enzymatic systems carrying out neutralization reactions, proton pumps and modifications in the cell membrane (Guan and Liu, 2020). Consequently, they can counteract ramping H^+ concentrations due to $H_2CO_3^*$ intracellular dissociation. Some authors observed during sterilization experiments that a reduction in water activity in the liquid medium decreases CO_2 dissolution, thus diminishing its intracellular diffusion (Chen et al., 2017; Kumagai et al., 1997). In other cases, microorganisms induce the synthesis of compounds acting as compatible solutes, such as glutamate, which help tackle changes in osmolarity and CO_2 toxicity (Oger and Jebbar, 2010; Park et al., 2020). Additionally, the presence of fats in the medium affects the porosity and structure of the cell wall or membranes, thus limiting CO_2 penetration (Lin et al., 1994).

The impact of "moderate" pCO_2 from 0.1 up to 10 bar is less comprehensively described in the literature and is mainly attributed to a decreased intracellular pH (Watanabe et al., 2007). However, pH reduction by itself does not explain reduced microbial activity, as shown in the case of denitrifying bacteria after exposure to dissolved CO_2 concentrations up to 30 000 ppm (Wan et al., 2016). Here, the authors provided experimental evidence that elevated pCO_2 caused direct inhibition of the carbon metabolism, electron transport chain, enzymatic activity and substrate consumption. Furthermore, these effects occurred at the expense of providing an

increased buffer concentration to prevent a pH drop, evidencing that pH effects are only one aspect of the inhibitory mechanism of moderate pCO_2 (Wan et al., 2018, 2016).

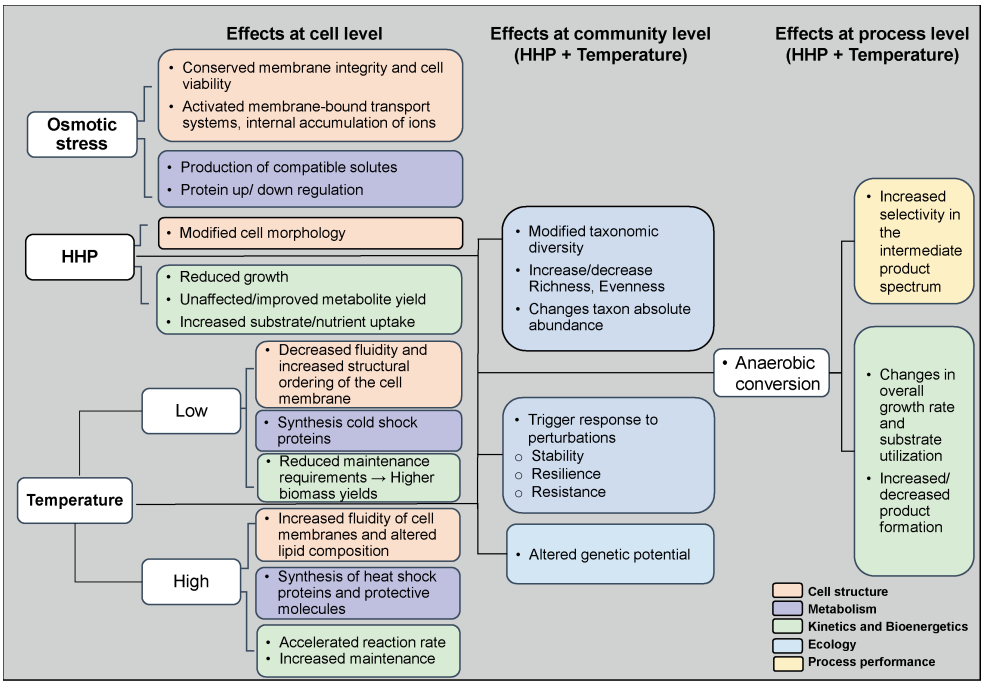

Figure 1-1: Scheme summarizing the effects of high hydrostatic pressure (HHP), osmotic stress and temperature at the cell, community, and process level. Effects are colour-coded and distributed according to target: cell structure (orange), metabolism (purple), kinetics and bioenergetics (green), ecology (blue) and process performance (yellow).

1.2.4 High hydrostatic pressure and elevated pCO_2: effects on enzymatic activity

High HP pressure effects on enzymatic activity have not been extensively described as in the case of other operational parameters such as temperature (Coquelle et al., 2007) and pH (C. Li et al., 2018). However, high HP (<200 MPa) affects chemical equilibria and reaction feasibility, depending on the partial molar volumes of products and reactants, as described by the Eyring equation (1-2), where K is the equilibrium reaction constant (h^{-1}), R is the universal gas constant (8.314 m^3 Pa K^{-1} mol^{-1}), T represents the temperature (K) and $\Delta V^{\neq}$ is the activation volume (cm^3 mol^{-1}) (Eyring, 1935; Martinez-Monteagudo and Saldaña, 2014).

$$\left(\frac{\partial \ln K}{\partial P}\right)_T = -\frac{\Delta V^{\neq}}{RT} = \frac{-\left(\Delta V_{products}{}^{\neq} - \Delta V_{reactants}{}^{\neq}\right)}{RT} \quad (1\text{-}2)$$

In consequence, positive activation volumes are inhibited by HP, whereas reactions with negative volumes are enhanced (Bruins et al., 2006; Low and Somero, 1975). Furthermore, depending on the nature of the enzyme, limited, stabilized, or even enhanced activity can result from exposure to high HP, as in the case of some hydrolases, transferases and oxidoreductases (Eisenmenger and Reyes-De-Corcuera, 2009).

High-pressure CO_2 exerts a specific influence on physicochemical properties of enzymes, *e.g.,* the secondary structure, and decreases activity due to lowered intracellular pH (Ishikawa et al., 1996; Manzocco et al., 2016). Further, increasing the availability of intracellular CO_2 inactivates specific critical enzymes involved in glycolysis, transport of amino acids and ions, and proton translocation due to structural modification and effects on internal electrostatic forces (Dixon and Kell, 1989; Hong and Pyun, 1999). Ultimately, the exposure to supercritical levels of CO_2 could lead to enzyme inactivation as a result of irreversible intracellular pH drop (Chen et al., 1992). On the other hand, the enzymatic activity could be upregulated or downregulated due to the internal availability of CO_2. In the case of PEP carboxykinase (Song et al., 2007), pyruvate carboxylase (Boock et al., 2019; Parizzi et al., 2012), which are important enzymes for glycolysis and the TCA cycle, incrementing CO_2 availability in a non-biocidal range correlates with enhanced activity. Conversely, the decreased activity because of exposure to high pCO_2 is still not clearly understood. It has been suggested that the release of intracellular components, due to cell membrane disruptions, contributed to explaining the lowered in-vivo activity of enzymes, such as alkaline phosphatase and ATPase (Bertoloni et al., 2006) on top of the acidification effect, due to lowered pH.

1.2.5 High hydrostatic pressure and elevated pCO_2: impact in microbial community dynamics

At the community level, significant changes in structure have been observed when both low temperature and high HP (4˚C, 22 MPa) have been applied to mesophilic oil-degrading marine sediments (Figure 1-1) (Fasca et al., 2018). Other studies reported that during simultaneous application of high HP and temperature, *e.g.,* in marine sediment degrading hydrocarbons at 30 MPa and 5 or 20°C, temperature has a more pronounced modifier effect on the structure and taxonomic diversity than pressure (Perez Calderon et al., 2019). In studies on the degradation of organic matter in sinking marine particles, incubation under increasing HP (0.1 to 40 MPa) at 13˚C has shown to decrease the absolute abundance of archaea, generating a community predominantly dominated by bacteria (90%) of the phylum Gammaproteobacteria (Tamburini et al., 2009b). However, other studies have reported roughly equivalent relative abundances of archaea and bacteria in warmer and more oligotrophic environments and, in particular, have

identified a sustained abundance of phyla Euryarchaeota (≈10%), which includes methanogenic microorganisms (Tamburini et al., 2009a). Bacterial phyla such as Proteobacteria, Bacteroidetes, Actinobacteria and Firmicutes became predominant when samples from coastal sediments and surface marine water were incubated at high HP (Marietou and Bartlett, 2014; Perez Calderon et al., 2019).

Elevated pCO_2 has also shown effects at the ecological level in anaerobic microbial communities. The overall response to high CO_2 concentrations, in terms of structure and taxonomic diversity, included a decrease in richness and lowered diversity, dependent on the actual prevailing pH (Fazi et al., 2019; Gulliver et al., 2014). Moreover, shifts in predominant bacterial and archaeal groups, *e.g.,* acetogens and hydrogenotrophic methanogens, have been observed since CO_2 is a reactant in these biochemical reactions; therefore, it could selectively enhance metabolic pathways fixing CO_2 (Gulliver et al., 2014; Yu and Chen, 2019). However, recent studies have pointed out that microbial community dynamics is not an isolated effect of exposure to elevated pCO_2, but results from its interaction with other operational conditions, in particular the absence or presence of additional electron donors, which strongly modifies microbial community structure and functionality (Baleeiro et al., 2021; Hu et al., 2010). Thus, it is foreseen that the elevated pCO_2 under varying operational conditions may influence metabolic activity, community structure and, likely, the overall process performance.

1.3 Anaerobic processes at atmospheric pressure

1.3.1 Role of CO_2 in anaerobic digestion AD

After the disintegration and enzymatic dissolution of complex organic matter, four stages within the AD process can be identified: a) hydrolysis of complex substrates; b) acidogenesis of hydrolysis products into carboxylates, alcohols, hydrogen and CO_2; c) acetogenesis, characterized by the production of acetate, H_2 and CO_2 from acidogenic compounds and d) methanogenesis, by which the acetogenic products are converted into methane (CH_4) by aceticlastic or hydrogenotrophic methanogenic archaea (Figure 1-2). CO_2 is produced and consumed in different stages of the AD process, owing to its multiple roles in the various biochemical pathways. Hence, it is anticipated that CO_2 availability should play an important role in AD biochemistry (Xu et al., 2021). In particular, increasing CO_2 concentrations could stimulate the selection of CO_2 fixation traits in the microbial community (Lemaire et al., 2020) and concomitantly improve the reaction feasibility of biochemical reactions capturing CO_2 (Figure 1-3A).

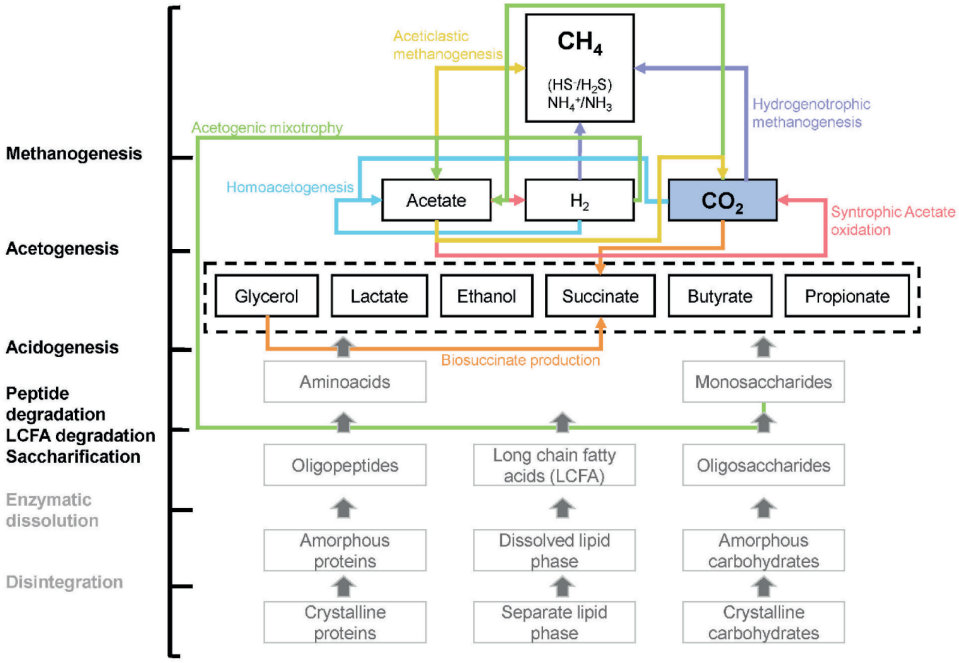

Figure 1-2: Schematic overview of the anaerobic digestion (AD) process. Biochemical reactions where CO_2 is produced or consumed are indicated with coloured arrows. Figure adapted from Lindeboom (2014).

If enough reducing equivalents are present, the main mechanisms likely enabling CO_2 fixation in AD systems correspond to, *e.g.,* the Wolfe cycle for hydrogenotrophic methanogenesis (Rouviere and Wolfe, 1988; Thauer, 2012). In this cycle, CO_2 reduction is carried out by archaeal orders such as Methanobacteriales, Methanococcales, Methanocellales and Methanomicrobiales (Conrad, 2020; Mand and Metcalf, 2019). CO_2 can also be fixed via the Wood-Ljungdahl pathway (WLP) for homoacetogenesis (Demirel and Scherer, 2008; Ragsdale and Pierce, 2008), carried out by acetogenic bacteria such as *Acetobacterium* and *Clostridium* spp. (Xu et al., 2021). Another process to consider is the coupling of glycolysis and WLP in acetogenic mixotrophy (Fast et al., 2015; Jones et al., 2016; Maru et al., 2018). Here, heterotrophic and autotrophic metabolism co-occur because external CO_2 can be fixed into acetyl-CoA and eventually converted into acetate due to the availability of reducing equivalents from heterotrophic carbohydrate conversion. Acetate can be further converted via chain elongation if lactate or ethanol are present (Angenent et al., 2016; Coma et al., 2016) or taken up by acetotrophic methanogens. Depending on the established microbial community and provided substrate, bio-succinate production could also enable CO_2 fixation to some extent (Ferreira et al., 2020; Lindeboom et al., 2014).

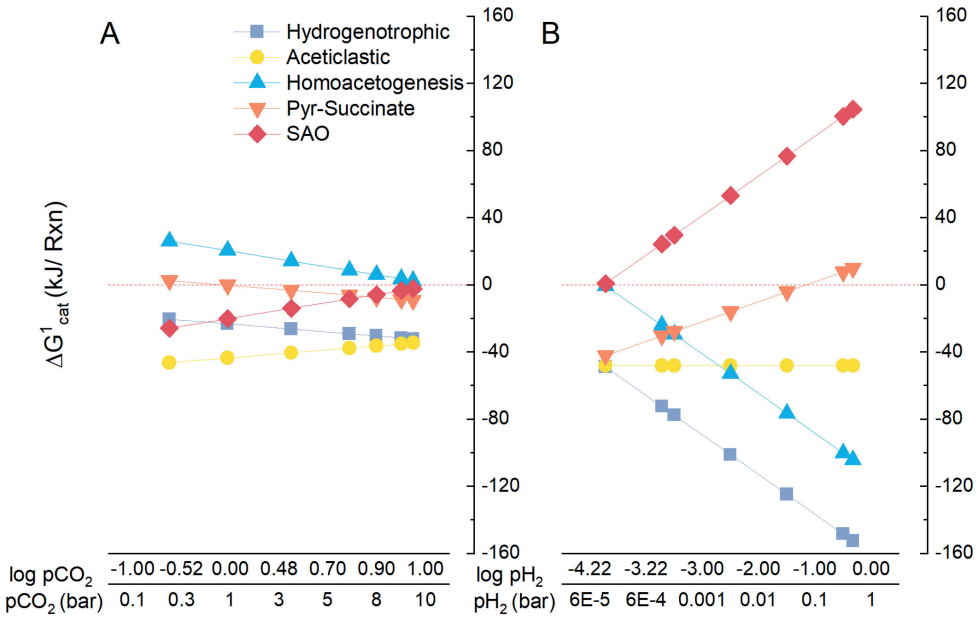

Figure 1-3: Impact of elevated partial pressure of A) carbon dioxide (pCO_2) and B) hydrogen (pH_2) on the Gibbs free energy change (ΔG_{cat}^1) of selected biochemical reactions in anaerobic digestion, calculated at pH=7.5. Abbreviations: Syntrophic Acetate Oxidation (SAO), Pyruvate (Pyr).

Recent studies concerning "CO_2 enrichment" of digesters have shown that while accompanied by stoichiometric H_2 provision (4:1 H_2:CO_2) or formate, CH_4 production is enhanced due to promoted hydrogenotrophic methanogenesis (Xu et al., 2019; Zabranska and Pokorna, 2018). As well, if the ratio of electron donor - CO_2 differs (*e.g.,* 2:1) and in turn modifies the composition of the microbial community, exogenous CO_2 could be indirectly converted to CH_4 via homoacetogenesis coupled to aceticlastic methanogenesis (Bajón Fernández et al., 2019; Pan et al., 2021). This mechanism has been proposed to explain the increased CH_4 production after CO_2 direct injection in a) single-phase laboratory digesters and b) pilot-scale digester treating food waste. These systems exhibited higher specific methane production (SMPR – m^3 CH_4 kg VS_{fed}^{-1} d^{-1}) than controls without direct CO_2 injection (Bajón Fernández et al., 2015, 2014), with reducing equivalents for CO_2 reduction most likely coming from enhanced H_2 production from food waste fermentation.

High H_2 yields have been reported when food waste is used as substrate in fermentative hydrogen production at pH values between 5.0-6.3 (Ghimire et al., 2015; Han and Shin, 2004) and also at increasing organic loading rate (OLR) of easily degradable substrates, such as carbohydrates in food waste (Kraemer and Bagley, 2007). H_2 production occurs via proton

reduction with the electron carrier ferredoxin (Fd_{red}), a reaction that is thermodynamically enhanced by low pH (Lee and Rittmann, 2009). CO_2 dissolution, in the absence of additional buffering capacity, will cause a pH drop due to the formation of H_2CO_3*. Thus, a pH drop may have enhanced acidogenesis from food waste, particularly of butyrate and acetate, whose presence correlates with high H_2 yields at low pH (H. S. Lee et al., 2008). In turn, high H_2 concentrations could promote the presence of homoacetogens, characterized by higher threshold concentrations than hydrogenotrophic methanogens (350-700 nM vs 30-75 nM) (Cord-Ruwisch et al., 1988). Moreover, a liquid phase enriched with CO_2, where its biocidal effects are evident in the absence of community priming, *i.e.,* adaptation to extreme conditions (Rillig et al., 2015; Sarvenoei et al., 2018), could have led to enhanced availability of additional electron donor from increased cell lysis. Homoacetogenesis + aceticlastic methanogenesis could be seen as a suitable alternative for CH_4 production under conditions of elevated pCO_2 when modification of process conditions (low pH, high OLR) impact the intrinsic formation of reducing equivalents and ultimately pH_2, as recently reported by (Muntau et al., 2021) in continuous digesters subjected to CO_2 enrichment.

Increased CO_2 concentrations in poorly buffered systems could further lower the pH than an eventual drop associated with carboxylates production. CO_2 and its distribution towards different species in solution (H_2CO_3*, HCO_3^- and CO_3^{2-}) modify the carbonate equilibrium and concomitantly the pH of the AD reactor. Fluctuations in operational pH could negatively impact microbial physiology and enzymatic activity (Merkel and Krauth, 1999). Methanogenic archaea have an optimal level of performance at pH between 6.8-7.4 (Mao et al., 2015); thus, they are susceptible to pH variations outside of this range. At high CO_2 levels, without increasing the acid-neutralizing capacity (ANC) of the system, an indirect, pH-dependant shift in product spectrum from CH_4 towards carboxylates has been observed (Lindeboom et al., 2016). If pH continues to drop, eventually, H_2 could become a predominant product (Dareioti et al., 2014). On the other hand, if the system is buffered and circumneutral pH values are established, H_2 production faces thermodynamic limitations (H. S. Lee et al., 2008). In that case, reducing equivalents from the fermentation could capture the extra available CO_2 via homoacetogenesis (Zhou et al., 2017).

1.3.2 Role of high and moderate pCO_2 in AD

Research on the impact of high pCO_2 on AD is limited to observations relevant to oil reservoirs. Operational conditions of 50 bar pressure, 10% pCO_2 and temperature of 55°C resulted in a shift from syntrophic acetate oxidation (SAO) to aceticlastic methanogenesis (Mayumi et al., 2013). On the other hand, the usage of supercritical CO_2, in a separate pre-treatment of lignocellulosic material denominated "CO_2 explosion" (Park et al., 2001; Zheng et al., 1998), has shown to be beneficial for enzymatic hydrolysis. Increased yields of total reducing sugars

when employing, for example, agave and sugar cane bagasse (Benazzi et al., 2013; Navarro et al., 2021), corn stover (Van Walsum and Shi, 2004) and starch (Miyazawa and Funazukuri, 2005), have been observed. However, moderate conditions in terms of total operational pressure and pCO_2, at the mesophilic range, do not evidence enhancing effects for hydrolysis rates (Lindeboom et al., 2014).

The particular effects of moderate pCO_2 (<10 bar) in single-stage AD have not been thoroughly elucidated. The work of Hansson and Molin (1981) studied the effects of pCO_2 until 1 bar in the overall AD process and concluded that there is an inhibitory effect of increased pCO_2 in fermentative and acetogenic bacteria. Uncoupled acidogenesis and acetogenesis translated into slower glucose and propionate degradation rates. In the case of butyrate, whose catabolism does not produce CO_2, degradation rates remained practically unchanged. These authors also established an inhibition effect on acetate utilization by methanogens at 1 bar pCO_2, which reflected in a 20-30% reduction in the CH_4 yield (Goran Hansson and Molin, 1981). Lindeboom et al. (2016) also observed a decline in the propionate oxidation rate at 5 bar pCO_2. As part of the explanatory mechanism, an acidification process and reversible toxicity linked to carbamate formation were proposed. Both processes occur due to increased aqueous CO_2 concentration ($H_2CO_3^*$) resulting from enhanced CO_2 dissolution in the liquid medium. Nonetheless, additional effects of elevated pCO_2, *e.g.,* on syntrophic conversions occurring in AD, may also be explained by more detailed analysis of bioenergetic, kinetic, and physiological effects, which have not been addressed in the current body of literature.

1.4 Mixed culture fermentation at atmospheric pressure

The carboxylate platform proposes the use of methanogenic-arrested biomass[1] for the conversion of low-value, carbon-rich feedstocks into a mixture of monocarboxylic acids, with carbon atoms varying from C1-C8 (Agler et al., 2011; Holtzapple et al., 2022; Holtzapple and Granda, 2009; Kleerebezem et al., 2015; Wu et al., 2021). The carboxylate mixture could subsequently undergo downstream processing with technologies such as nanofiltration, liquid/liquid extraction and anion exchange to directly recover the carboxylates (Agler et al., 2011; Kleerebezem et al., 2015). Additionally, the carboxylate mixture could undergo a secondary fermentation to medium-chain fatty acids (Leng et al., 2017; Stamatopoulou et al., 2020), alcohols or be used for electrosynthesis employing bio-electrochemical systems (Liu et al., 2017).

Contrastingly to single-stage AD targeting biogas production, where the accumulation of intermediates such as propionate and butyrate is a symptom of reactor malfunctioning (L. Dong

[1] Biomass with inhibited methanogenic consortium

et al., 2019), high carboxylate productivity and yield are intended in mixed culture fermentation. Some approaches proposed in the literature to favour carboxylates production rely on taking advantage of the dissimilarities between the bio-conversion rates of acidogenic, acetogenic and methanogenic microorganisms (Hickey and Switzenbaum, 1991). Hence, substrate overload (Amorim et al., 2018) and promoting disparities in the proportionality of syntrophic microorganisms by modifying operational conditions (Li et al., 2016; McMahon et al., 2004; Town and Dumonceaux, 2016) could be applied as selection pressures to favour carboxylate production.

The bottlenecks that currently constrain the advancement and scale-up of the mixed culture fermentation process inside a biorefinery concept are associated with low productivity (expressed as mg kg broth^{-1} day^{-1}), selectivity (composition of the product profile) as well as the costs and energy intensity for the downstream processing (Agler et al., 2011; Arslan et al., 2016). On the other hand, promising alternatives for mixed culture fermentation rely on the operation under extreme conditions, *e.g.,* salinity, high/low pH, elevated pressure with resilient microbial communities from highly fluctuating habitats (rumen, marine environments and the deep sea, oil wells, sediments) (Holtzapple et al., 2022).

1.5 Steering product formation in mixed culture fermentation

1.5.1 Role of environmental parameters, process conditions and elevated pCO_2

The trophic diversity and numerous interspecies interactions in anaerobic microbiomes enable the utilization of complex compounds as feedstock inside biorefinery applications (Agler et al., 2011; Braz et al., 2019; Marshall et al., 2013). In this way, complete mineralization of the organic matter to CH_4 and CO_2 in AD or intermediate production of carboxylates under conditions of inhibited methanogenesis in mixed culture fermentation can be achieved.

The intrinsic diversity of anaerobic communities is also a challenge for process selectivity, which fundamentally relies on modifying environmental conditions (Angenent and Wrenn, 2008; Kleerebezem and van Loosdrecht, 2007; Rodríguez et al., 2006). Several parameters and process conditions, either alone or as part of designed operational strategies, have shown a steering effect in mixed culture fermentation (Arslan et al., 2016). Substrate characteristics such as concentration in the range of 5-40 g COD L^{-1} to avoid inhibition and achieve product yields between 10-60%, presence of digestible lignocellulosic biomass, and adequate C/N ratio play a significant role in carboxylates production rate and product spectrum. Moreover, a low concentration of long-chain fatty acids and moderate concentrations of typical cations and

transition metals could significantly affect product yield and productivity (Coma et al., 2016; Hoelzle et al., 2021; Holtzapple et al., 2022; Jankowska et al., 2017).

Among conventionally manipulated operational parameters to influence the product profile, pH (Tamis et al., 2015; Temudo et al., 2007; Zoetemeyer et al., 1982) and temperature (M. Lee et al., 2008; Zhuo et al., 2012) can be mentioned. The hydrolysis rate is regulated by pH, with mildly acidic values favouring its rate (Jankowska et al., 2017). Depending on the nature of the substrate, carboxylates production can be favoured at pH values around 6.0 or more alkaline levels (9.5-10.0) in the case of municipal or solid food waste (Cheah et al., 2019). The product spectrum can also be strongly defined by pH and its influence on microbial community dynamics: higher butyrate fractions have been observed at pH lower than 5.5, whereas pH around 6.5 was associated with an elevated fraction in the case of propionate (Min et al., 2005). Temperature affects microbial growth, biochemical production rates, enzyme activity and affinity; however, a clear effect of temperature on the product spectrum is not evident when considering the current literature (Arslan et al., 2016; Holtzapple et al., 2022).

On the other hand, reactor configuration and operation (Dai et al., 2017; Khan et al., 2016) could also influence carboxylates formation and product spectrum. Studies report that in-situ product removal enhanced product yield in batch mixed culture fermentation (De Sitter et al., 2018). As well biomass retention via, *e.g.,* anaerobic membrane bioreactors (AnMBR) and continuous operation (Fernando-Foncillas and Varrone, 2021) have shown a positive effect on carboxylates production (Wu et al., 2021). Increasing the organic loading rate (OLR) under a threshold value that prevents instabilities due to system overload has also been reported as a possible modifier of productivity and product profile (Jiang et al., 2013; Lim et al., 2008). Literature also suggests that headspace composition can alter product spectrum due to the gas partial pressure (*e.g.,* pCO_2, pH_2) effects on metabolic pathways (Arslan et al., 2013, 2012; Darvekar et al., 2019; De Kok et al., 2013). Despite the changes mentioned above in process parameters and operational conditions, strategies for steering toward carboxylates production in high-pressure mixed culture fermentation are lacking (Lindeboom et al., 2011). In such an operational strategy, partial pressures of biogas components, *e.g.,* CO_2, may play a prominent role in product selectivity and pathway steering (Arslan et al., 2012; Bothun et al., 2004; Lindeboom et al., 2016).

CO_2 availability can steer fermentation pathways because of a tuning effect in the activity of enzymes carrying out carboxylation and decarboxylation reactions. Among those enzymes, PEP carboxykinase, pyruvate carboxylase, and oxaloacetate decarboxylase can be mentioned (Amulya and Mohan, 2019; Sawers and Clark, 2004; Song et al., 2007). Reactions for carbon fixation and release are highly relevant for the anaerobic breakdown of substrates that share most of the glycolytic pathway, such as glucose and glycerol (Saint-Amans et al., 2001) (Figure

1-4). In this pathway, the carbon and electrons distribution towards the reductive or the oxidative branch occurs at the phosphoenolpyruvate (PEP) - pyruvate - oxaloacetate (OAA) node. This allocation occurs in response to cultivation conditions and encompasses CO_2 fixation and release (Sauer and Eikmanns, 2005). Concomitant to elevated pCO_2, the type of substrate and OLR could be highly determinant of the product spectrum, biomass yields and selected microbial community in the anaerobic bioconversion.

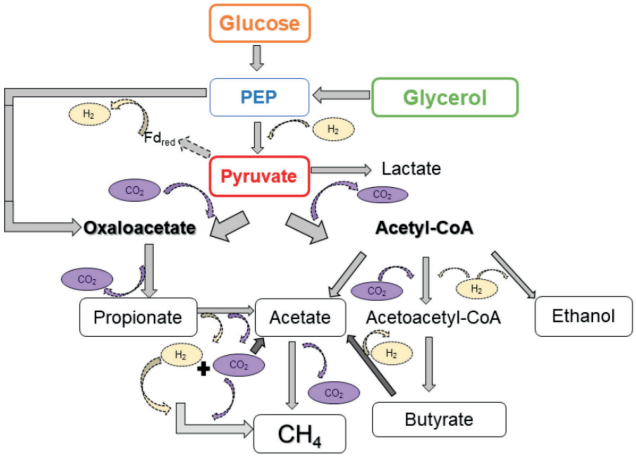

Figure 1-4: Simplified pathway representation for the anaerobic conversion of glucose and glycerol in undefined mixed cultures. As a generalization, reducing equivalents are represented as H_2. PEP- Phosphoenolpyruvate. Figure adapted from (Agler et al., 2011; Ammar et al., 2014; Zhu et al., 2009).

1.5.2 Role of bioenergetics and microbial community dynamics

The AD process relies on syntrophy to overcome thermodynamic limitations for converting intermediate compounds, such as propionate and butyrate, with clear relevance for the scope of this thesis. The accumulation of these intermediates correlates with reactor disturbance due to increased organic loading rate, pH changes, and unpaired acidogenesis and methanogenesis (Henze, 2008). Since these conversions operate close to the thermodynamic equilibrium, subtle variations in substrate/product concentrations and environmental conditions can modify the actual Gibbs free energy change ($\Delta G_R^{'}$) of a specific pathway (Heijnen and Kleerebezem, 2010). A detailed bioenergetics analysis under real operational conditions in digesters and fermenters, as the one carried out in this research (Chapters 2 and 3), constitutes a valuable predictive and explanatory tool inside strategies aiming to steer product formation and prevent process instabilities (González-Cabaleiro et al., 2013; Xiao et al., 2020). On the one hand,

under the premise that microbial metabolism will proceed towards the pathway that maximizes energy harvest, bioenergetic analysis could explain pathway dominance at a particular set of environmental conditions (González-Cabaleiro et al., 2015). On the other hand, since the feasibility of the biochemical reactions is subjected to thermodynamic constraints, fluctuating operational conditions can exacerbate those limitations (Oren, 2011) and the abundance and interactions of syntrophic partners.

Inhibition of syntrophic interactions has been mostly attributed to the high partial pressure of hydrogen (pH_2). Values lower than 2.6 and 74 Pa of pH_2 are required for syntrophic oxidation of propionate and butyrate to overcome the thermodynamic barrier of -20 kJ mol^{-1}, respectively (Zabranska and Pokorna, 2018). This value is considered the smallest energy quantum required to sustain life (Kleerebezem and Stams, 2000; Leng et al., 2018; Schink, 1997). However, as seen in Figure 1-3A, increasing pCO_2 levels might also redefine reaction feasibility. Studies performing bioenergetic simulations of methanogenesis occurring in subsurface environments destined for geological carbon storage (Jin and Kirk, 2016) have shown different outcomes on the ΔG_R^1 of intermediate reactions due to elevated CO_2. The energetic feasibility of substrate oxidation and aceticlastic methanogenic conversions decreased, whereas the contrary occurred for hydrogenotrophic methanogenesis (Jin and Kirk, 2016; Kirk, 2011).

Bioprocess operation under environmental stress conditions, such as elevated pressure, could increase the energy requirements for maintenance (m_G) due to the activation of stress response mechanisms such as the synthesis of cold and shock proteins and EPS production (Danevčič and Stopar, 2011; Gustafsson et al., 1993). Moreover, since anaerobic process are characterized by limited energy availability, an increase in m_G due to moderate stress conditions could push for a decoupling between catabolism and anabolism to satisfy increasing maintenance requirements at the expense of biomass synthesis.

Due to an apparent thermodynamic control exerted by pCO_2, specific bacterial metabolisms may be promoted or inhibited, supporting a potential steering role of elevated CO_2 in AD (Jin and Bethke, 2007). Lindeboom et al. (2016) indicated a negligible effect of elevated pCO_2 (5 bar) in the overall thermodynamics of syntrophic propionate oxidation. However, under simultaneously changing pCO_2 and pH_2, a new "niche" for reaction feasibility could develop. Under this particular set of conditions, the conversion of other intermediates such as butyrate and acetate may also be amended, highlighting the importance of bioenergetic analysis in anaerobic processes.

A strong dependence on the thermodynamic feasibility of biochemical reactions and community structure in the AD or fermentation system can be speculated due to the importance of syntrophic interactions (Hao et al., 2016; Nobu et al., 2020). Hence, quantifying phylogenetic diversity could also help formulate mechanistic explanations and hypotheses

associated with pathway steering (Nakasaki et al., 2020; Treu et al., 2018). One of the most commonly used procedures for phylogenetic diversity quantification in anaerobic microbiomes is Next Generation Sequencing (NGS), with high-throughput techniques such as gene amplicon sequencing in the Illumina platform emerging as a popular and affordable choice in the field of environmental microbiology (Dumbrell et al., 2016; Vanwonterghem et al., 2014).

The usage of NGS techniques has proven to be relevant in studies to evaluate the effects of environmental stressors on the community structure (De Vrieze et al., 2015b; Li et al., 2015; S. Wang et al., 2017; Ziganshin et al., 2013) and to elaborate hypotheses about microorganism associations in identified metabolic networks for anaerobic digesters and fermenters (B. Liu et al., 2020). However, despite its usefulness and increasing popularity, care should be taken with the outcome of the bioinformatics analysis associated with the amplicon sequencing data, since results reliability can be influenced by the choice of primers and the number of hypervariable regions selected for the analysis (Campanaro et al., 2018). Moreover, under the well-known premise in microbial ecology that "presence does not imply activity" (De Vrieze et al., 2016), conjectures about metabolic functionality in AD and mixed culture fermentation would remain highly speculative. Multivariate statistical tools that correlate environmental parameters and sequencing data give insight into the physiological potential but need further confirmation using complementary techniques such as metagenomics and proteomics (Regueiro et al., 2012; Vanwonterghem et al., 2014). These limitations and intrinsic biases limit the conclusions that can be withdrawn from these analyses to a set of general trends and further limit the comparability of different studies at the laboratory and full-scale operation.

1.6 High-pressure operation in AD and mixed culture fermentation

The composition of biogas under atmospheric conditions is majorly defined by the average carbon oxidation state in the converted substrate. In general terms, dealing with organic wastes, CH_4 commonly corresponds to 50-70%, CO_2 accounts for 30-50% and other gases such as NH_3, H_2S, and H_2 are present in low concentrations (van Lier et al., 2020). The range of biogas applications can be widened and its economic value incremented when a higher "lower calorific value" (LCV) is achieved by removing CO_2 and impurities. Hence, upgrading to biomethane, *i.e.,* biogas with CH_4 content >95% and an LCV of 36 MJ m^{-3} (Fu et al., 2021; IEA, 2020), is required and can be achieved by implementing several physicochemical and biological alternatives, with different commercial readiness and costs (Angelidaki et al., 2018; Fu et al., 2021; Rotunno et al., 2017). Physicochemical upgrading includes processes such as physical absorption with water scrubbing systems or organic solvents (Bauer et al., 2013), chemical absorption using amine/aqueous alkaline salt solutions (Adnan et al., 2019), pressure swing adsorption (Augelletti et al., 2017) and separation using polymeric membranes (Díaz et al.,

2015). These processes operate at moderate pressures between 3-10 bar, increase the CH_4 content to 96-99% and deliver upgraded biogas at pressures of around 1.3-10 bar, which are compatible with natural gas requirements (Angelidaki et al., 2018). Biological upgrading enhances hydrogenotrophic activity by increasing hydrogen availability at in-situ (Zhu et al., 2020) or ex-situ conditions (Kougias et al., 2017).

AHPD is also considered an in-situ biogas upgrading process. AHPD avoids external pressurization necessary for the physicochemical biogas upgrading process by letting the pressure build-up due to the increased concentration of gaseous end-products, originating from microbial activity, while operating a digester with a closed release valve (Lindeboom et al., 2011). By this pressure increase, AHPD takes advantage of the differences in solubility predicted by Henry's law among the main biogas components leading to a gas phase enriched in CH_4 (See Background and problem analysis). Furthermore, if hydrogen is externally added as in biological biogas upgrading, the pressure built up in AHPD can increase the driving force for mass transfer (Díaz et al., 2020). Methane production can be further improved at elevated pressure due to enhanced H_2 and CO_2 transfer to the liquid being beneficial for hydrogenotrophic methanogenesis or homoacetogenesis coupled to aceticlastic methanogenesis.

Moreover, operating bioreactors at high pressure might become a suitable alternative to steer product formation in mixed culture fermentation due to the modulatory effect of pressure on reaction rates depending upon activation volumes (Morild, 1981). In addition, pressure combined with other process conditions can trigger cross-resistance effects leading to increased microbial "fitness" under environmental stress conditions (Goel et al., 2012). Furthermore, by modifying the headspace composition and gas partial pressures, with associated kinetic and thermodynamic effects, pressure can have an effect on metabolic pathway regulation, allowing for increased selectivity in metabolite production (Arslan et al., 2012).

A summary of recent and relevant studies concerning high-pressure AD (including particular applications for biogas upgrading) and high pressure mixed and single culture fermentation under anaerobic conditions is presented in Table 1-1 and Table 1-2. The selected body of literature reflects knowledge gaps in the application of high pressure to AD and mixed culture fermentation. Among them, a possible piezotolerance of microorganisms from genera frequently identified in anaerobic reactors has been limitedly addressed. This limits the conclusions that can be withdrawn from microbial community dynamics studies under high pressure. Moreover, hardware and setup configuration issues are usually not reported in detail in the materials and methods sections of the below mentioned studies, which limits the reproducibility of the high-pressure research. In terms of employed substrates, more research

is needed employing complex rather than well-defined substrates to address inhibition effects by the interaction of pressure with other inhibitory compounds.

Table 1-1: Recent literature regarding the use of pressure technology to improve CH_4 content in AD systems

System	Operational conditions	Pressure	Methane content	Reference
Fed-batch reactors with different working volumes (0.6, 1.7 and 13.5 L)	T=30°C Substrate= 1-14 g COD L^{-1}	0.3-9.0 MPa	89-96%	(Lindeboom et al., 2011)
Fed-batch reactor for sodium acetate /acetic acid conversion	T=30°C Substrate = 50 mM Buffered and non-buffered system	0.1-2.1 MPa	>80% (pH ~5-6) >95% (pH~7)	(Lindeboom et al., 2012)
Fed-batch reactor treating VFA mixture (acetate, propionate, butyrate)	T=30°C Substrate = 1-10 g COD L^{-1}	0.1-2.0 MPa	>94%	(Lindeboom et al., 2013a)
Fed-batch reactor for glucose conversion + silicate minerals for CO_2 sequestration	T=30°C Substrate = 0-10 g COD- Glucose L^{-1}	0.1-1.0 MPa	75-88%	(Lindeboom et al., 2013b)
Fed-batch reactor for sodium acetate, glucose, and propionate conversion	T=30°C	0.1-2.0 MPa	75-86%	(Lindeboom et al., 2016)
Three acidogenesis-leach-bed-reactors and one pressure-resistant anaerobic filter	T=37°C OLR= 5.1 g COD L^{-1} d^{-1} No pH adjustment (pH~ 6.5-7.2)	0.1-0.9 MPa	66-75%	(Chen et al., 2014a)
Six acidogenesis-leach-bed-reactors and one pressurized anaerobic filter treating maize silage	T=55°C OLR=5-17.5 g COD L^{-1} d^{-1} No pH adjustment	0.15-0.9 MPa	66-75%	(Chen et al., 2014b)
Two-stage anaerobic digestion (leach-bed reactors (6) + pressurized anaerobic filter) treating maize silage or mixture grass+ maize silage	T=55°C (leach bed) 37°C (methane reactors) OLR= 5 g COD L^{-1} d^{-1} No pH adjustment	0.1-0.9 MPa	87%	(Lemmer et al., 2015a)
Two stage anaerobic digestion (leach-bed reactors (6) + pressurized anaerobic filter) + water scrubbing treating maize silage	OLR= 5 g COD L^{-1} d^{-1} Recirculation ratio 5.9 T=37°C	0.1-0.9 MPa	75-87%	(Lemmer et al., 2015b)
Batch reactors treating mixture grass + maize silage	Substrate= 8.8 g COD L^{-1} T=37°C	1-3 MPa	22-39% (diluted because of N_2 in headspace)	(Lemmer et al., 2017)

Two-phase pressurized biofilm anaerobic reactor	T=37°C OLR = 3.1 g COD L^{-1} d^{-1} No pH adjustment HRT= 7 days	1.7 MPa	90.8%	(Li et al., 2017)
Two-stage system treating grass + maize silage	T=55°C (leach bed) at atmospheric pressure and T=37°C (methane reactor) HRT= 4 days OLR= 4-4.5 g COD L^{-1} d^{-1} No pH adjustment	1.0-5.0 MPa	79-91%	(Merkle et al., 2017b)
Batch reactors treating hydrolysate mixture from maize silage + grass	T=37°C	0.1-10 MPa	Specific methane yield (SMY) 230-244 L kg^{-1} COD_{input}	(Merkle et al., 2017a)
CSTR treating waste activated sludge	HRT= 12 days T=37°C No pH control	0.1-0.6 MPa	81%	(Latif et al., 2018)
Two-stage system + micro-filtration unit treating maize and grass silage	T=37°C HRT=1.5 days No pH control OLR=4.5 kg m^{-3} day^{-1}	0.1-0.25 MPa	93%	(Bär et al., 2018)
High alkalinity synthetic wastewater	T=37°C Alkalinity between 14.4-18.6 g L^{-1} as $CaCO_3$ Substrate = 5.6 to 11.2 g COD in reactor as acetate or glucose	≈0.1 MPa	88% vs 52.4% in atmopsheric control	(Zhao et al., 2020)
CSTR (3L) treating food waste (FW) + H_2 injection	Substrate = 200 g COD L^{-1} H_2 injection= 0-0.25 L H_2/g $COD_{FW.fed}$ T=37°C OLR= 2.7-3.1 g COD L^{-1} day^{-1} No pH adjustment	0.1-0.7 MPa w/o H_2 injection 0.5 MPa + H_2 injection	77% CH_4 >90% CH_4	(Kim et al., 2021)
Fed-batch thermophilic electromethanogenic system	Inoculum from oilfield formation water Substrate= Sodium acetate (1.6 g L^{-1}) T= 55°C	5 MPa and 700 mV	91% CH_4	(Kobayashi et al., 2017)
Other applications				
Trickle-bed reactors for biomethanation	H_2:CO_2 ratio= 4 Retention time = 1.6-9.8 h	0.1-0.9 MPa	64-87%	(Ullrich et al., 2018)
Semi-continuous reactor treating mixed sludge for direct biomethanation	T=35°C H_2 flow rate= 0.45-0.64 NL $L_{recirculation}^{-1}$ day^{-1}	0.2-0.3 MPa	69-93%	(Díaz et al., 2020)

Table 1-2: Relevant literature regarding the use of pressure technology to improve mixed and single culture anaerobic fermentation

System	Operational conditions	Pressure	Fermentation performance (productivity and product spectrum)	Microbial community	Reference
Mixed culture fermentation					
Batch experiments in stainless steel CSTR to evaluate mixed culture homoacetogenesis	T=25°C $NaHCO_3$= 3.4 g L^{-1} as dissolved inorganic C-source Initial pH=8.5	pH_2=0.1-2.5 MPa (pH_2 hydrogen partial pressure)	Highest concentration of total carboxylates (3.55 g L^{-1}) at 1.5 MPa Acetate at pH_2 ≤ 1.5 MPa. Minor amounts of propionate and valerate at pH_2 ≥1.5 MPa	Dominance of Pseudomonadaceae and Clostridiaceae	(Sivalingam et al., 2021)
High-pressure syngas fermentation reactor combined with moving bed biofilm (MBB) carriers	T= Ambient Agitation = 200 rpm	pH_2=1.5 MPa	48 % enhancement in acetate synthesis rate (37.4 mmol L^{-1} day^{-1}) at 1.5 MPa + MBB reactor		(Sivalingam and Dinamarca, 2021)
Batch high pressure dark fermentation	T= 37°C pH= 8.0 Agitation = 100 rpm	pH_2= 0.1-1 MPa	Total carboxylates concentration (3.5–3.7 g COD L^{-1}) Lowest acetate/butyrate ratio (0.44-0.54) and highest lactate proportion (11-24%) at pH_2 = 0.3-1 MPa	Higher abundance of Lactococcus (20.1%), Enterococcus (18.3%), and Pediococcus (11.8%) and decreased abundance of *Clostridium spp*.	(Lee et al., 2018)
Autogenerated high pressure anaerobic digestion	T= 30°C Buffer= 150 meq $NaHCO_3$ L^{-1} Substrate= Glucose (14.4 g COD $reactor^{-1}$)	0.10-1.06 MPa (autogenera-ted) pCO_2= 0.00-0.5 MPa	Propionate accumulation at 0.50 MPa, 90% reduction in specific propionate conversion rate (from 30.3 to 2.2 mg g^{-1} VS_{added} day^{-1})	Archaea: *Methanosaeta concilii*, *Methanobacterium formicicum* and *Mtb. beijingense* Bacteria: Kosmotoga-like (31%), Propioniferax-like (25%) and Treponema- like (12%)	(Lindeboom et al., 2016)

Pure culture fermentation					
Stirred batch reactors inoculated with *Clostridium ljungdahlii*	T= 37°C Substrate = glucose (5 g L^{-1}) pH= 5.9	0.1-0.7 MPa Gas mixture (53.3% vol H_2 and 26.7% vol CO_2)	4 g L^{-1} of total products consisting of 82.7 % formic acid, 15.6 % acetic acid, and 1.7 % ethanol		(Oswald et al., 2018)
Syngas fermentation *Clostridium ljungdahlii*	T= 37°C pH= 5.9 Agitation= 757 rpm	0.4-0.7 MPa	Acetate concentration decreased by 85%. Formate as the main product of H_2/CO_2 fermentation (2-98 mmol L^{-1})		(Stoll et al., 2018)
Fed-batch glycerol fermentation with *Citrobacter amalonaticus*	pH=7.0 Substrate = Glycerol	pCO_2=0.06-0.2 bar	Succinate concentration of 14.86 gL^{-1} was achieved, productivity of 0.36 $gL^{-1}h^{-1}$ and yield of 52.10%		(Amulya et al., 2020)
Glycerol/glucose batch fermentation with *Lactobacillus reuteri*	T= 37°C	0.1-25 MPa	1,3 propanediol titer increased 15% relative to control at 0.1 MPa. Decreased production of ethanol and lactate		(Mota et al., 2018)
Batch tests with genetically modified *Escherichia coli K12*	T= 37°C pH > 6.8 (8.0) Agitation= 500 rpm	0.1-1 MPa (H_2:CO_2 mixture 1:1)	Max. 0.5 mol formate L^{-1} and 0.12 mmol formate mg^{-1} total cell protein at 1 MPa		(Roger et al., 2018)
Batch fermentation with *Clostridium* sp.	T= 37°C pH= 5.5 Agitation= 500 rpm Substrate= Glucose (60 g L^{-1})	pH_2=0.112 MPa by H_2 recirculation	Butanol concentration, productivity and yield of 21.1 g L^{-1}, 1.25 g L^{-1} h^{-1}, and 0.8 mol butanol mol^{-1} glucose (combined with butyric acid addition)		(Cheng et al., 2012)
Lactic acid fermentation for yoghurt production	T=43°C pH=8.9 Reducing sugars=55 g L^{-1}	0.1-100 MPa	Lactic acid concentration at 5 MPa 2.5 g L^{-1} after 600 min (comparable to 0.1 MPa) Fermentation inhibition at 100 MPa	*Streptococcus thermophilus*, *Lactobacillus bulgaricus*, and *Bifidobacterium lactis*	(Mota et al., 2015)

1.6.1 Challenges and opportunities in HPAD and High-Pressure MCF

Some remarks can be made from the studies presented in Table 1-1 and Table 1-2 regarding the impact of pressure on the bioconversion processes. Firstly, a clear effect of high pressure on conversion rates is not evident. For example, Lindeboom et al. (2013a) observed a reduction in maximum conversion rates for acetate, propionate, and butyrate at a final pressure of 20 bar. In the first instance, those effects were attributed to cation requirement (ratio Na^{+}/K^{+}) to keep pH stable and HCO_3^- dissolved rather than to the accumulated pressure itself, end-product inhibition, or enhanced CO_2 dissolution. Lemmer et al. (2017) stated that performing high-pressure AD at 30 bar affected pH with a recorded reduction from 7.0 to 6.3. However, the pressure increment did not significantly influence organic degradation or CH4 yield despite the pH drop. Hence, more investigation is needed to elucidate how interactions between total operational pressure, pCO_2, pH and substrate type/concentration can inhibit the overall AD or mixed culture fermentation processes.

Secondly, the microbial community dynamics of high-pressure AD/ fermentation systems are not well understood. The response of the established community to synergistic interactions between pressure, pCO_2 and other operational parameters has been limitedly explored. For example, the role of the archaeal genus *Methanosaeta*, consistently present in anaerobic digesters under high pressure and high acetate levels, needs to be revisited (Lindeboom et al., 2016; Zhao et al., 2020). In anaerobic reactors operated at atmospheric conditions, a shift in the predominance of *Methanosaeta* to *Methanosarcina* has been observed under conditions of environmental stress and high acetate production (De Vrieze et al., 2012). However, *Methanosaeta* predominance at elevated pCO_2 in high-pressure AD/fermentation systems may be explained by moderately increased acetate availability due to enhanced homoacetogenic activity and a particular syntrophic relation with aceticlastic methanogens that remains to be confirmed. Nonetheless, the "homoacetogenesis-aceticlastic methanogenesis" hypothesis is supported by reports from metagenomics analysis of sediments from deep seabed petroleum seeps (3 km water depth) where genes associated with the Wood−Ljungdahl pathway have shown high relative abundances (X. Dong et al., 2019). Furthermore, other studies suggest an increase in aceticlastic methanogenesis with ocean depth (Heuer et al., 2009).

The stress-response at the microbial community level after perturbations, *i.e.,* high pressure and elevated pCO_2, needs to be researched to identify possibly detrimental effects in syntrophic interactions that could be correlated with shifts in the product spectrum (Shade et al., 2012). Microbial succession at the archaeal level also requires deeper investigation to find possible analogies with observations in AD under environmental stress (high TAN, low pH and high acetate concentrations). Under these conditions, a shift in the predominant archaeal genus from *Methanosaeta* toward *Methanosarcina* has been reported (De Vrieze et al., 2012). The effect

of high pressure as a selection parameter in AD/fermentation microbiomes needs to be further studied and possible cross-tolerance effects due to temperature, substrate, among others, need to be identified.

During long-term operation of high-pressure AD systems, Lindeboom et al. (2013a) and Lemmer et al. (2017) observed accumulation of carboxylates (propionic, valeric acid). The mechanisms underlying this accumulation need to be further explored to establish if this observation can be explained by a) "reversible CO_2 narcosis" of a part of the community or b) uncoupled acidogenesis – methanogenesis rates due to higher acid production but restrained consumption as a consequence of constrained syntrophy. If a cohabitation of the "biogas economy" and the "carboxylates economy" is envisioned, the selective production and accumulation of carboxylates, which could have been considered an "operational problem" in AD, may redeem itself into a "default operational advantage."

The role of designed operational strategies to steer product formation towards selective carboxylates production in emerging technologies, such as AHPD, has not been adequately addressed. Possible steering effects of headspace composition in AD could be magnified by applying elevated pressure (Lemmer et al., 2015a; Lindeboom et al., 2011). Moreover, inoculum selection and adaptation could play a significant role in these strategies. Previous studies have shown that the directional selection of microbial community through adaptive laboratory evolution (ALE) processes is highly effective in improving stress tolerance and selectively enhancing product formation by activating downregulated pathways (Dragosits and Mattanovich, 2013; Portnoy et al., 2011). In particular, ALE has shown to trigger the development of features such as acid resistance mechanisms (Kwon et al., 2011) and other physiological mechanisms to conserve cell membrane integrity. It needs to be corroborated if such insights could act as cross-protection mechanisms against stressful pCO_2 levels and improve metabolic activity. Moreover, it would be interesting to assess if this "ecological specialization" in environmental stress conditions could be conserved in the long term in mixed culture communities as observed in single-species cultures (Cooper and Lenski, 2000; Dragosits and Mattanovich, 2013).

1.7 Thesis scope and outline

This investigation aimed to expand the current knowledge regarding the role of elevated pCO_2 in high-pressure systems (AD and mixed culture fermentation) to unravel its potential as a steering parameter. The research project has been structured as follows:

Chapter 2 presents a detailed thermodynamic and kinetic study describing the direct and indirect influence of elevated pCO_2 in the syntrophic conversion of propionate and butyrate.

This analysis is complemented with experimental evidence from batch experiments under mesophilic conditions. An anaerobic inoculum from a membrane bioreactor (AnMBR) treating wastewater from the food and feed industry was selected for the experiments. This inoculum showed superior performance under elevated pressure than inocula from a UASB treating waste activated sludge from a municipal wastewater treatment plant in the Netherlands and another one treating the effluent from a sugar beet processing factory.

Chapter 3 aims to provide experimental evidence to differentiate the effects of mild hydrostatic pressure (MHP) from the ones of elevated pCO_2 studied in other chapters. Moreover, it deals with the importance of inoculum history and cross-tolerance effects associated with incubation temperature and intrinsic community halotolerance to improve carboxylate production under MHP.

Chapter 4 describes the approach of adaptive laboratory evolution (ALE) adapted from pure culture to open culture microbiology to promote alternative and more robust metabolic pathways under environmental stress conditions. In particular, the ALE strategy was selected to show that limited propionate oxidation under conditions of elevated pCO_2 can be overcome by selecting key and versatile microbial genera with better adaptations to environmental stressors.

Chapter 5 builds upon knowledge gained in the previous chapter and changes the lens through which elevated pCO_2 has been treated. Instead of ascribing effects only to the presence of elevated pCO_2, the perspective was widened to include the analysis of how interaction effects with operational conditions such as the provision of mixed substrate, a high substrate to biomass ratio (S/X), and presence of external electron donor (formate), could contribute to steering product formation in high pressure mixed culture fermentation. Concomitantly, changes in the microbiome were monitored to propose further correlations between community structure and shifts in product spectrum.

Finally, Chapter 6 highlights the main findings of this investigation and discusses them in an integrative manner to establish to what extent the knowledge regarding high-pressure AD and mixed culture fermentation has been expanded. It is envisioned that process development in high-pressure biotechnology could be carried out more comprehensively, bridging the gap between the microbiological component and process operation based on the main outcomes discussed throughout this document. Complementarily, some elaboration is made about the future perspectives of the emerging field of high-pressure biotechnology and the opportunities for enhancing carbon neutrality through anaerobic bioprocesses.

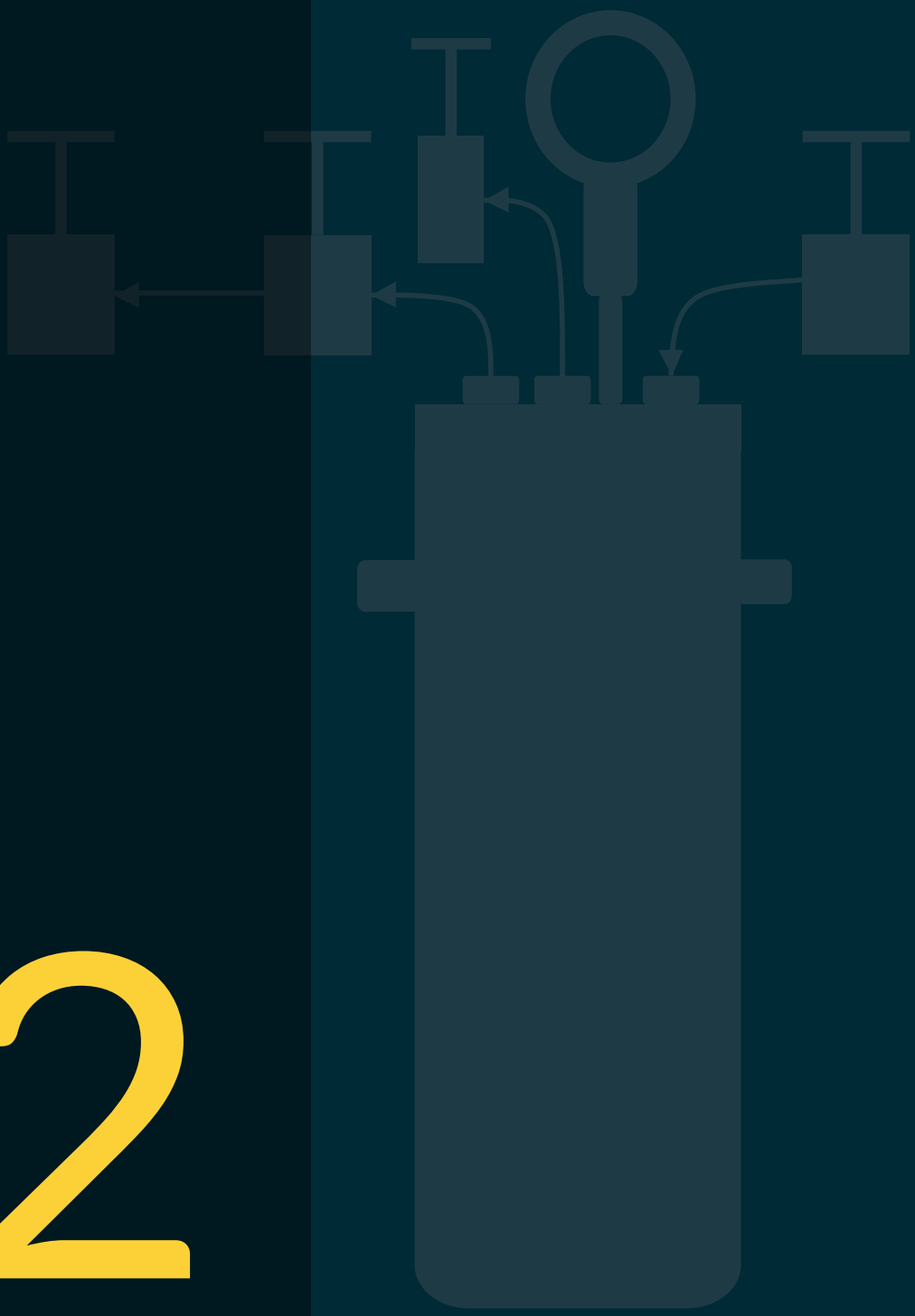

2

CHAPTER 2

EFFECTS OF INCREASED pCO_2 ON SYNTROPHIC CONVERSIONS

This chapter is based on:

Ceron-Chafla, P., Kleerebezem, R., Rabaey, K., B. van Lier, J., & Lindeboom, R. E. F (2020). Direct and Indirect Effects of Increased CO_2 Partial Pressure on the Bioenergetics of Syntrophic Propionate and Butyrate Conversion. Environmental Science & Technology, 54(19), 12583–12592. https://doi.org/10.1021/acs.est.0c02022

Abstract

Simultaneous digestion and in-situ biogas upgrading in high-pressure bioreactors will result in elevated CO_2 partial pressure (pCO_2). With the concomitant increase in dissolved CO_2, microbial conversion processes may be affected beyond the impact of increased acidity. Elevated pCO_2 was reported to affect the kinetics and thermodynamics of biochemical conversions since CO_2 is an intermediate and end-product of the digestion process and modifies the carbonate equilibrium. Our results showed that increasing pCO_2 from 0.3 to 8 bar in lab-scale batch reactors decreased the maximum substrate utilization rate ($r_{s\max}$) for both syntrophic propionate and butyrate oxidation. These kinetic limitations are linked to an increased overall Gibbs free energy change ($\Delta G_{Overall}$) and a potential biochemical energy redistribution among syntrophic partners, which showed interdependence with hydrogen partial pressure (pH_2). The bioenergetics analysis identified a moderate, direct impact of elevated pCO_2 on propionate oxidation and a pH-mediated effect on butyrate oxidation. These constraints, combined with physiological limitations on growth exerted by increased acidity and inhibition due to higher concentrations of undissociated volatile fatty acids, help to explain the observed phenomena. Overall, this investigation sheds light on the role of elevated pCO_2 in delicate biochemical syntrophic conversions by connecting kinetic, bioenergetic and physiological effects.

Keywords

Elevated CO_2 partial pressure, syntrophic oxidation, high-pressure anaerobic digestion, Gibbs free energy, carbonate equilibrium

2.1 Introduction

In this chapter the impact of elevated pCO_2 on the kinetics and bioenergetics of the syntrophic conversion of propionate and butyrate was studied. It is hypothesized that an increase in the overall available Gibbs free energy for substrate conversion, due to increased pCO_2, could provoke an unbalance in the energy share among syntrophic partners that might translate into kinetic limitations. A scenario analysis is proposed to understand the individual and combined effects of pCO_2 and pH in the bioenergetics of syntrophic conversions. Furthermore, the relationship between bioenergetic and kinetic data is evaluated through a correlation analysis aiming to provide insight into the system's response to changing available energy.

2.2 Materials and methods

2.2.1 Experimental setup and reactor operation

Five initial operational pCO_2, *i.e.,* 0.3, 1, 3, 5, 8 bar, were selected for the experimental treatments based on pH equilibrium calculations performed with the hydrogeochemical software PHREEQC (version 3, USGS). The application of an elevated buffer concentration of 100mM as HCO_3^- in the system, allowed to maintain circumneutral pH, despite the elevated pCO_2. Batch experiments at 0.3 and 1 bar were carried out at atmospheric pressure in 250 mL Schott bottles sealed with rubber stoppers. In parallel, the elevated pressure experiments were performed in 200 mL stainless steel pressure-resistant reactors (Nantong Vasia, China). The experiments were conducted at a liquid: gas ratio of 1.5:1 and inoculum: substrate ratio of 2:1 gCOD $gVSS^{-1}$. The liquid medium consisted of macronutrient and micronutrient stock solution (6 mL L^{-1} and 0.6 mL L^{-1}, respectively) prepared according to Lindeboom et al. (2011), plus 1 g COD L^{-1} of the substrates propionate or butyrate.

The headspace of bottles and reactors was replaced with N_2 gas (>99%) to ensure anaerobic conditions after filling. Then, the bottles were flushed with the corresponding gas mixture: 70:30% N_2: CO_2 for 0.3 bar pCO_2 or >99% CO_2 for 1 bar pCO_2. Elevated pressure reactors were subjected to three consecutive pressurization-release cycles to ensure complete N_2 replacement by CO_2 (>99%) at the intended pressure. Temperature and agitation speed were controlled using an incubator shaker (Innova® 44, Eppendorf, USA) set to 35±1°C and 110±10 rpm. Pressure was online-monitored using digital sensors (B+B Thermo-Techniek, Germany) and a microcontroller (Arduino Uno©, Italy). The experiments had a fixed duration of 14 days.

2.2.2 Inoculum selection

Preliminary batch experiments of propionate anaerobic conversion under 1 bar pCO_2 were conducted in triplicates using three mesophilic inocula collected from A) sludge digester treating excess sewage sludge, B) UASB reactor treating sugar beet wastewater and C) Anaerobic Membrane Bioreactor (AnMBR) treating food industry wastewater. The three inocula were characterized in terms of physicochemical parameters (Table 2-1). Anaerobic conversion of propionate was monitored for nine days for inocula A, B, C and the results are presented in Figure 2-1. Inoculum C showed the fastest propionate conversion. Inoculum B showed an unusually low level of activity and was discarded for additional testing. Propionate conversion by inoculum A seemed to be halted after two days of incubation, which hindered further assessment of conversion rates. The main differences between inoculum A and C, in terms of the physicochemical characteristics, were associated with the initial alkalinity as well as the NH_4^+ concentration (Table 2-1). Bacterial and archaeal communities differed among inoculum A and C, with the latter showing a higher abundance of uncultured microorganisms and hydrogenotrophic methanogens (Figure 2-2). This preliminary data led to the selection of C as the working inoculum for further experiments.

Table 2-1: Physicochemical characteristics of the three inocula initially selected for the study of propionate oxidation activity at pCO_2=1 bar. SD=Standard Deviation.

Parameter	Inoculum A	SD	Inoculum B	SD	Inoculum C	SD	Units
COD	34.63	0.19	38.99	2.33	22.22	0.52	g L^{-1}
sCOD	0.64	0.01	5.37	0.08	1.92	0.04	g L^{-1}
P	0.25	0.00	1.06	0.01	0.11	0.00	mg L^{-1}
N-total	1.93	0.03	2.08	0.08	ND	ND	mg L^{-1}
N-NH_4^+	1.08	8.66	0.93	0.01	0.11	0.00	mg L^{-1}
Alkalinity	120.10	0.01	182.22	0.52	36.29	0.50	meq L^{-1}
VSS	21.47	0.02	30.42	0.15	13.62	0.01	g L^{-1}
TSS	28.88	0.06	57.42	0.60	15.87	0.07	g L^{-1}
VSS/TSS	74.35		52.97		85.80		%
pH	7.10		7.25		7.30		-

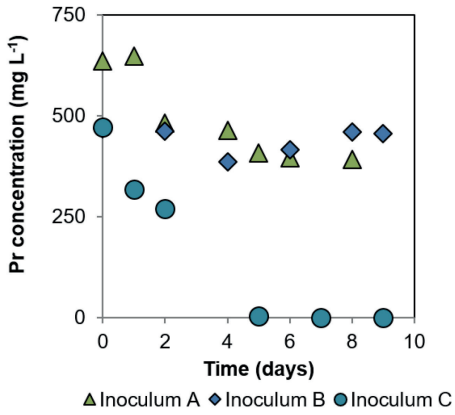

Figure 2-1: Evolution of propionate concentration (mg L^{-1}) for the experiments of anaerobic substrate oxidation under moderate pCO_2 (1 bar) using three different inocula (A, B and C).

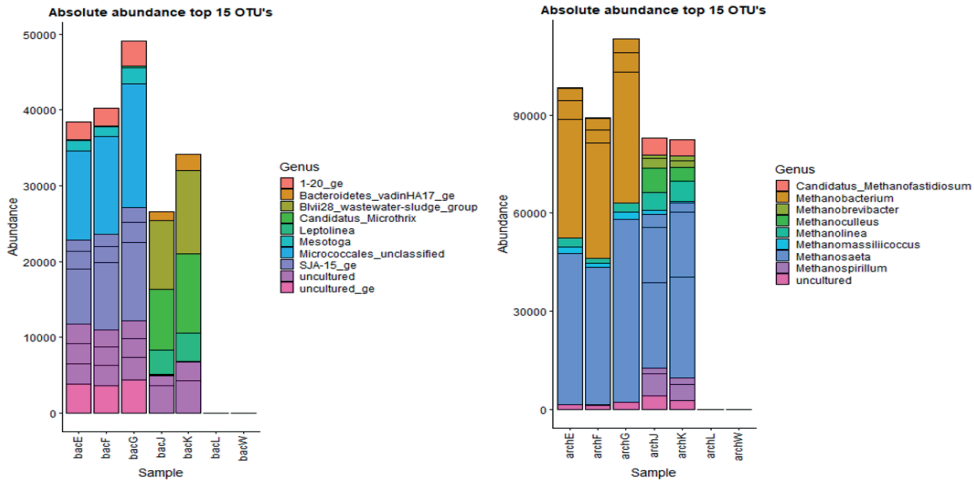

Figure 2-2: Absolute abundance of different genera for bacteria and archaea. Samples E, F and G correspond to starting inoculum C. Samples J and K correspond to starting inoculum A. Samples L and W correspond to negative controls.

2.2.3 Analyses

Experiments were carried out in a triplicate incubation; however, due to the small working volume of the reactors (200 mL), a sampling strategy for liquid and gas samples was designed

that enabled us to account for replicate variability, minimizing disturbance of the batch incubations (Table 2-2). Headspace composition and volatile fatty acids (VFAs) were analyzed using gas chromatographs (7890A GC system, Agilent Technologies, US). In the first one, gas samples (5 mL) taken twice per week at atmospheric pressure were measured via a thermal conductivity detector and directed through an HP-PLOT Molesieve GC column (30m length x 0.53mm inner diameter x 25µm film thickness). Helium was used as the carrier gas at a constant flow of 10 mL min^{-1}. The oven and detector were operated at 45°C and 200°C, respectively. In the second one, VFAs were determined according to Ghasimi et al. (2016). Total and soluble COD, Total Suspended Solids (TSS), Volatile Suspended Solids (VSS) and pH were measured at the beginning and end of the experiment according to Standard Methods (American Public Health Association, 2017).

Table 2-2: Sampling strategy for the triplicate incubation carried out for the experiments of syntrophic propionate and butyrate conversion under elevated pCO_2.

pCO_2 (bar)	**Propionate** Time (days)	Replicate	Liquid (1.5 mL)	Gas (5 mL)	**Butyrate** Time (days)	Replicate	Liquid (1.5 mL)	Gas (5 mL)
0.3, 1, 3, 5, 8	0, 10, 13	1	x	x	0, 5, 12	1	x	x
		2	x	x		2	x	x
		3	x	x		3	x	x
	Other	1	x		Other	1	x	
		2		x		2		x
		3	-	-		3	-	-

Microbial community analysis

DNA extraction

Biomass pellets stored at -80°C, were thawed and DNA was extracted according to the instructions included in the DNeasy Ultra- Clean Microbial kit (Qiagen, Germany). Quality and quantity of the obtained DNA were checked by means of Qubit 3.0 DNA detection (Qubit® dsDNA HS Assay Kit, Life Technologies, U.S).

Amplicon libraries construction

Library construction and sequencing were performed at the Roy J. Carver Biotechnology Center, University of Illinois at Urbana-Champaign. Their internal procedure summarizes as follows: Approximately 1ng of DNA was used for amplification with the bacterial 16S V3_F357_V4-R805 and archaeal 349F-806R primers in the Fluidigm Access Array. The

barcoded amplicons generated from each sample were harvested, transferred to a 96 well plate, quantified on a Qubit fluorometer (ThermoFisher, CA) and the average size of the amplicons was determined on a Fragment Analyzer (AATI, IA). All amplicons were pooled in equimolar concentration, size selected on a 2% agarose Ex-gel (Thermofisher) to remove primer dimers and extracted from the isolated gel slice with a Qiagen gel extraction kit (Qiagen). Cleaned size selected product was quantitated and run on a Fragment Analyzer again to confirm appropriate profile and for determination of average size. The pool was diluted to 5nM and further quantitated by qPCR on a CFX Connect Real-Time qPCR system (Biorad, Hercules, CA) for maximization of number of clusters in the flowcell.

Sequencing on Illumina MiSeq

The pool was denatured and spiked with 20% non-indexed PhiX V3 control library provided by Illumina and loaded onto the MiSeq V2 flowcell at a concentration of 8 pM for cluster formation and sequencing. The PhiX control library provides a balanced genome for calculation of matrix, phasing and prephasing, which are essential for accurate base-calling. The libraries were sequenced from both ends of the molecules to a total read length of 250nt from each end. The run generated .bcl files which were converted into demultiplexed fastq files using bcl2fastq 2.20 (Illumina, CA).

2.2.4 Estimation of kinetic parameters

The modified Gompertz equation (Do et al., 2008)

$$y = A * e^{\left[-e^{\frac{r_{smax} * e}{A} * (\lambda - t) + 1}\right]}, \quad (2\text{-}1)$$

where y represents the substrate concentration (mg L^{-1}), λ the lag phase (day), $r_{s\,max}$ the maximum substrate utilization rate (mg L^{-1} day^{-1}), A the maximum substrate concentration (mg L^{-1}) and t the time (days), was used to fit the data from the atmospheric and pressure experiments. The kinetic parameters were estimated using non-linear minimization methods from the package nlstools in R (v3. 6. 1) (2019).

2.2.5 Bioenergetic calculations

ΔG_R^1, the actual Gibbs free energy change for the reactions was calculated according to (Kleerebezem and Van Loosdrecht, 2010):

$$\Delta G_R^1 = \Delta G_R^{01} + RT\sum_{i=1}^{n} Y_{Si}^R \ln(a_{Si}), \quad (2\text{-}2)$$

where ΔG_R^{01} is the Gibbs free energy at pH 7 and 308.15 K, R the gas constant (8.31 J K^{-1} mol^{-1}), T the temperature in Kelvin, Y_{Si}^R the stoichiometric coefficient of compound i and a_{Si} the molar concentration of compound i. ΔG_R^{01} was corrected for temperature using the Gibbs-Helmholtz equation (Kleerebezem and Van Loosdrecht, 2010). The values at standard conditions, ΔG_R^0, were taken from Heijnen and Kleerebezem (2010).

2.2.6 Estimation of potential biochemical energy distribution in syntrophic oxidation of propionate and butyrate

The stoichiometry of the overall syntrophic reaction and the intermediate catabolic reactions is presented in Table 2-3. From the acetotrophic reactions, only aceticlastic methanogenesis (AcM) was included in the analysis since syntrophic acetate oxidation (SAO) was considered unlikely to occur under our experimental conditions and initial community composition (Figure 2-2). The stoichiometric coefficients of AcM and hydrogenotrophic methanogenesis (HyM) for each substrate correspond to the balance of the formed species during the oxidation (Schink, 1997). At the initially adjusted circumneutral pH, the dissolved inorganic carbon (DIC) corresponds to $H_2CO_3^*$ and HCO_3^-. $H_2CO_3^*$ can be expressed in terms of pCO_2 using Henry's law with its proportionality constant (k_H) corrected by temperature. The equations presented in Table 2-3 are deliberately written in terms of the H^+ concentrations and pCO_2 to illustrate the effect of these variables on the thermodynamic calculations.

ΔG_R^1 for the reactions presented in Table 2-3 can be affected by pCO_2, pH, or by a combined interaction. The nature of the effect will depend on the role of the parameter in the catabolic reaction, meaning it acts as a reagent, product, or is not directly involved. As well, the magnitude of the effect might be amplified due to an initially less negative ΔG_R^{01}. A scenario analysis was performed to understand the impact of changing pCO_2 and pH on the ΔG_R^1 of the overall and intermediate catabolic reactions. The resulting calculations, subsequently, were used to estimate the change in the potential biochemical energy share. A summary of input

parameters in each scenario (A, B and C) is presented in Table 2-4. The calculations were performed using a pH_2 value of $1x10^{-5}$ bar, typical for ADs (Patón and Rodríguez, 2019) and at which syntrophic reactions become thermodynamically feasible (Schink, 1997).

Table 2-3: Stoichiometry of the main sub-reactions related to syntrophic propionate and butyrate oxidation with their corresponding ΔG_R^{01} (kJ mol^{-1}) calculated at biochemical standard conditions of temperature= 298.15 K, concentration of aqueous reactants= 1 mol L^{-1}, pressure of gaseous reactants= 1 bar, and pH= 7.

Substrate	Reaction		ΔG_R^{01} (kJ mol^{-1})
Propionate	Overall	$C_3H_5O_2^- + H^+ + 0.5H_2O \longrightarrow 1.75CH_4 + 1.25CO_2$	-60.2
	Oxidation (Pr-Ox)	$C_3H_5O_2^- + 2H_2O \longrightarrow C_2H_3O_2^- + 3H_2 + CO_2$	+73.7
	Aceticlastic methanogenesis (AcM)	$C_2H_3O_2^- + H^+ \longrightarrow CH_4 + CO_2$	-35.8
	Hydrogenotrophic methanogenesis (HyM)	$3H_2 + 0.75CO_2 \longrightarrow 0.75CH_4 + 1.5H_2O$	-98.0
Butyrate	Overall	$C_4H_7O_2^- + H^+ + H_2O \longrightarrow 2.5CH_4 + 1.5CO_2$	-88.8
	Oxidation (Bu-Ox)	$C_4H_7O_2^- + 2H_2O \longrightarrow 2C_2H_3O_2^- + H^+ + 2H_2$	+48.2
	AcM	$2C_2H_3O_2^- + 2H^+ \longrightarrow 2CH_4 + 2CO_2$	-71.6
	HyM	$2H_2 + 0.5CO_2 \longrightarrow 0.5CH_4 + H_2O$	-65.4

Table 2-4: Summary of input parameters for the bioenergetics scenario analysis of syntrophic propionate and butyrate conversion. The initial concentrations of propionate, butyrate and acetate were fixed at 10, 7 and 0.1 mM, respectively. Temperature was fixed at mesophilic conditions, 308 K. The employed bicarbonate concentration corresponded to the initial amount of buffer supplied to the system, 100 mM as HCO_3^-. The initial partial pressure was selected at 0.001 bar for CH_4 and $1x10^{-5}$ bar for H_2.

Scenario	pCO_2 (bar)	pH	Scenario	pCO_2 (bar)	pH	Scenario	pCO_2 (bar)	pH
A	0.1	7.0	B	0.3	7.9	C	0.1	7.9
	1				6.9		1	6.9
	3				6.4		3	6.4
	5				6.2		5	6.2
	8				5.9		8	5.9
	10				5.8		10	5.8
	20				5.5		20	5.5

2.2.7 Statistical analysis

The Spearman's rank-order correlation coefficient (r_s) was calculated via the function *rcorr*() of the package "Hmisc" in R (v3.6.1) (R Core Team 2019, 2019), ordered using hierarchical clustering and plotted using the package "corrplot" (Wei and Simko, 2017).

2.3 Results and discussion

2.3.1 Effect of elevated pCO_2 on the anaerobic substrate conversion and metabolite production rate

Subplots A and C in Figure 2-3 show the decrease in substrate conversion rates in the experimental treatments at increased pCO_2 ranging from 0.3 to 8 bar during the 14 days. The reduction in $r_{s\,max}$ was further quantified using the process parameters extracted from the data-fitting to the modified Gompertz equation presented in Table 2-5. Data from the 8 bar pCO_2 experiment is not included since it was not possible to determine the kinetic parameters accurately. Increasing pCO_2 from 0.3 to 5 bar led to a 93% reduction in $r_{s\,max}$ for propionate, whereas for butyrate, the $r_{s\,max}$ dropped by 57%. The calculated specific $r_{s\,max}$ for propionate at 0.3 bar pCO_2 is already in the low-range of the values proposed in the literature: 150-292 mg Propionate g VSS^{-1} day^{-1}. In the case of butyrate, the specific $r_{s\,max}$ at 0.3 bar pCO_2 was one order of magnitude lower than the inferior boundary of the theoretical range: 3.9 to 10.9 g Butyrate g VSS^{-1} day^{-1} (Van Lier et al., 2008) For both cases, elevated pCO_2 resulted in a concomitantly increase in the lag phase (λ), which is likely associated with inadequate levels of adaptation to operational conditions. A considerable effect on the production and consumption of acetate was not evident in the propionate experiment; however, for butyrate, a decrease in acetate production occurred (Figure 2-3, B and D). Lower methane production was observed in the propionate experiment only at 8 bar pCO_2, while it appeared already at 5 bar pCO_2 for butyrate (Figure 2-4, A and B).

Hansson and Molin firstly reported the adverse effects of pCO_2 on the propionate and butyrate anaerobic conversion rate (Gora Hansson and Molin, 1981). These authors observed a decrease of 70% in the $r_{s\,max}$ in propionate degradation when increasing pCO_2 from 0.2 to 1 bar. The effect for butyrate was not significant, as opposed to our current work in which we identified an 18% reduction in $r_{s\,max}$ at a comparable pCO_2 increase. In a previously reported experiment, using suspended pressure-cultivated inoculum that originated from anaerobic granular sludge

degrading propionate (Lindeboom et al., 2016), it was shown that 5 bar pCO_2 caused a 93% reduction in the $r_{s\max}$. This value agrees with the calculations presented here (Table 2-5).

Table 2-5: Overview of the kinetic parameters estimated using the modified Gompertz equation for propionate and butyrate oxidation at the different conditions of initial pCO_2: 0.3, 1, 3, and 5 bar. The measured equilibrium pCO_2 and the calculated equilibrium pH are additionally provided.

Substrate	**Propionate**					**Butyrate**			
Parameter	Initial pCO_2 (bar)	0.3	1	3	5	0.3	1	3	5
	Eq. pCO_2 (bar)	0.3	1	1.5	2	0.3	1	1.5	2.0
	Eq. pH	7.4	6.9	6.4	6.2	7.4	6.9	6.4	6.2
A (mg L^{-1})		667.9 ***	681.8 ***	664.8 ***	587.5 **	516.2 ***	540.1 ***	465.9 ***	525.9 ***
$r_{s\max}$ **(mg L^{-1} day^{-1})**		223.9 ***	149.5 **	89.8 ***	14.4 ()	291.2 ( )	238.9 ***	216.9 *	126.6 **
λ **(day)**		3.3 ***	3.4 **	6.6 ***	4.7 ()	4.3 ***	4.8 ***	6.3 ***	7.3 ***
Specific $r_{s\max}$ (mg substrate g^{-1} VSS day^{-1})		117.2	78.3	46.9	7.5	138.7	113.8	103.3	60.3

Levels of significance of the parameters estimation: p-value ( ) < 0.1, * < 0.05, ** < 0.01 and *** < 0.001

2.3.2 Effects of elevated pCO_2 on the $\Delta G_{Overall}$ of syntrophic propionate and butyrate conversion and the intermediate biochemical reactions

Figure 2-5 shows the effect of pCO_2 on the overall available Gibbs free energy ($\Delta G_{Overall}$) during syntrophic propionate and butyrate conversion calculated using the actual concentrations of reactants during the atmospheric and pressure experiments and at pH_2= $1x10^{-5}$ bar.

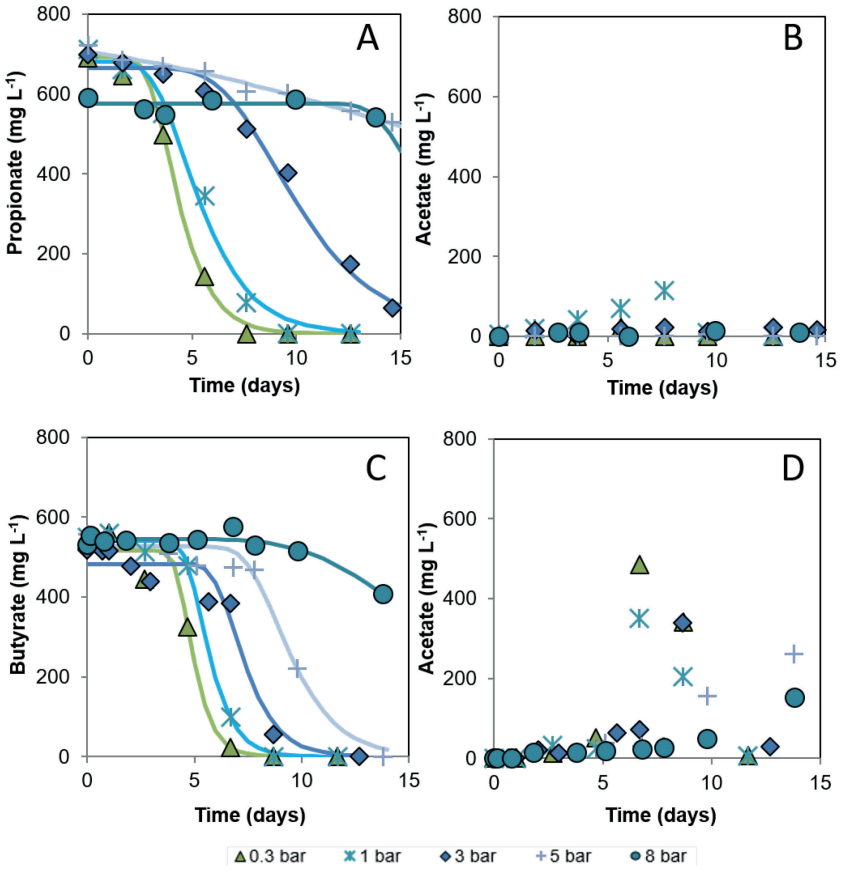

Figure 2-3: Evolution of substrate consumption and acetate production during mesophilic syntrophic substrate oxidation under 0. 3, 5 and 8 bar initial pCO_2. A) and B) correspond to the propionate and acetate concentration (mg L^{-1}) for the propionate experiment, respectively. The concentrations shown in time points 0, 10, 13 days represent the average of three sampled reactors with a relative standard deviation <16%. C) and D) correspond to the butyrate and acetate concentration (mg L^{-1}) for the butyrate experiment, respectively. The concentrations presented in time points 0, 5 and 12 days represent the average of three sampled reactors with a relative standard deviation <18%. Data points represent experimental data. Continuous lines correspond to the simulated data using the modified Gompertz equation, which significance levels are presented in Table 2-5.

Results showed a less steep increasing trend over time for $\Delta G_{Overall}$ from 1 bar pCO_2 onwards, indicating that the two syntrophic reactions became less energetically feasible due to decreased substrate consumption or product accumulation. At day 0, the $\Delta G_{Overall}$ at 0.3 bar pCO_2 for propionate oxidation was -85.0, compared to -145.0 kJ mol^{-1} for butyrate oxidation. At 8 bar pCO_2, the $\Delta G_{Overall}$ for propionate increased to -78.0 compared to -137.9 kJ mol^{-1} for butyrate.

The calculated dissimilarity in the $\Delta G_{Overall}$ of the reactions (≈40%) might have weakened the driving force to carry out propionate conversion at increased values of pCO_2 at atmospheric and pressurized conditions. This observation relates well with what Kleerebezem and Stams (2000) proposed in their metabolic network analysis of syntrophic butyrate conversion, where they highlighted the possibility of a lowered specific reaction rate as a function of increased Gibbs free energy change of the catabolic reaction.

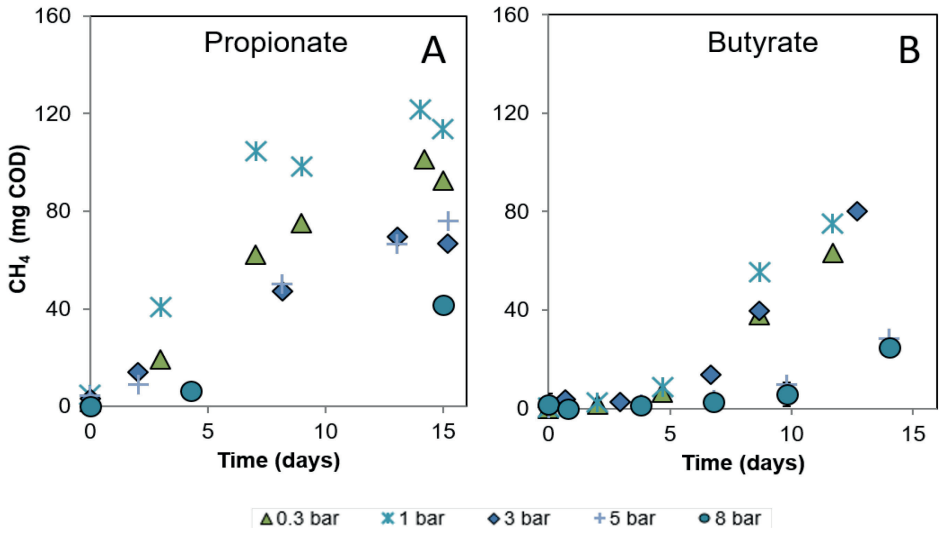

Figure 2-4: Evolution of daily methane production (mg COD) during mesophilic syntrophic substrate oxidation under 0.3, 1, 3, 5 and 8 bar initial pCO_2. Data points represent experimental data. A) Propionate experiment. Values presented in time points 0, 10, 13 days represent the average of three sampled reactors with a relative standard deviation <14%. B) Butyrate experiment. Values presented in time points 0, 5 and 12 days represent the average of three sampled reactors with a relative standard deviation <20%.

ΔG_R^1 responds to direct and indirect changes in biochemical reactions (Jin and Kirk, 2018a). A deliberate change in the concentration of one or more biochemical species is considered a direct intervention. A change in the concentration of the species induced by the modification of another operational parameter is an indirect intervention. The predominance of a direct or indirect effect of increased pCO_2 on the $\Delta G_{Overall}$ and intermediate biochemical reactions of syntrophic conversions has not been thoroughly elucidated in literature. We tried to gain further insight into the individual and combined effect of elevated pCO_2 and pH on the bioenergetics using scenario analysis. By such analysis, possible bioenergetic limitations caused by an increase in the $\Delta G_{Overall}$ value might be identified.

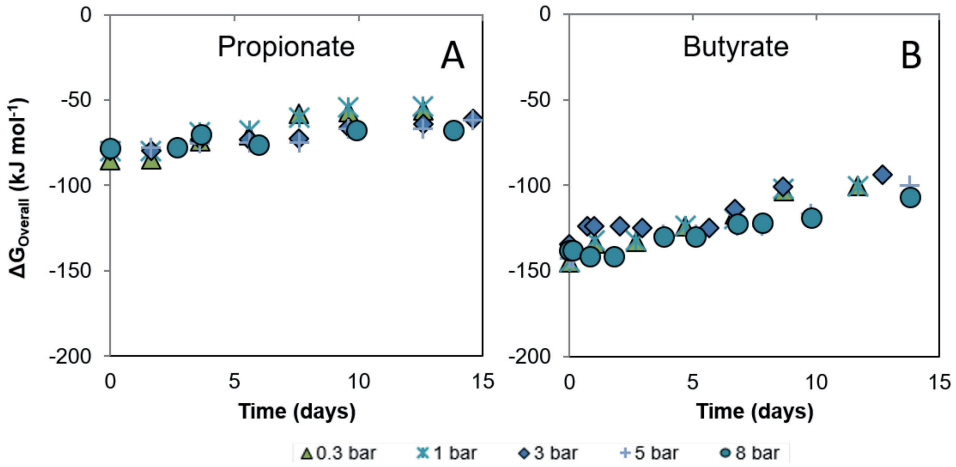

Figure 2-5: Change in the overall available Gibbs free energy ($\Delta G_{Overall}$) during mesophilic syntrophic A) propionate oxidation and B) butyrate oxidation at 0.3, 1, 3, 5 and 8 bar initial pCO_2 calculated with measured concentrations of reactants and products during the experimental period. Aqueous concentrations were used (in mol L^{-1}), the partial pressure of gases (in bar), T=35°C and a theoretical value of pH_2= $1x10^{-5}$ bar.

Figure 2-6 visualizes the change in ΔG_R^1 value when the parameters pCO_2 and pH are independently and concomitantly modified in syntrophic propionate and butyrate conversion. Lines represent the change in Gibbs free energy at increasing pCO_2 or decreasing pH for the intermediate biochemical reactions: substrate oxidation (ΔG_{Pr-Ox}, ΔG_{Bu-Ox}), AcM (ΔG_{AcM}), HyM (ΔG_{HyM}) and for the overall reaction ($\Delta G_{Overall}$). An increase in the $\Delta G_{Overall}$ in the subplots of Figure 2-6, means that less energy is available for all the sub-reactions, whereas a decrease implies that more energy is at hand. In scenario A, the $\Delta G_{Overall}$ for the syntrophic conversion of propionate and butyrate was calculated for an initial pCO_2 increasing from 0.1 to 20 bar, to amplify the effect of elevated pCO_2 in comparison to our experimental range (0.3 to 8 bar). An elevated pCO_2 of 20 bar increased the $\Delta G_{Overall}$ of propionate by 19% and butyrate by 15%, compared to 0.1 bar (A and D). In scenario B, $\Delta G_{Overall}$ was calculated using the corresponding equilibrium pH values at pCO_2 ranging between 0.1 and 20 bar and buffer concentration of 100 mM as HCO_3^-. A pH change from 7.9 to 5.5 caused the $\Delta G_{Overall}$ to decrease by 14% and 10% for propionate and butyrate, respectively (B and E). In scenario C, $\Delta G_{Overall}$ was calculated with pCO_2 of scenario A and the pH values of scenario B. Under these conditions, there is a marginal increase in $\Delta G_{Overall}$ for the conversion of both substrates (C and F).

Concerning the intermediate reactions at 20 bar pCO_2 in scenario A, ΔG_{Pr-Ox} increased by 44% and ΔG_{Bu-Ox} remained constant since CO_2 is not a reaction product. Regarding the methanogenic reactions, ΔG_{AcM} increased by 30%, whereas ΔG_{HyM} decreased by 40% for both substrates (A and D). The pH decrease to 5.5 in scenario B did not strongly affect the reactions where H^+ ions are not produced, *i.e.,* ΔG_{Pr-Ox} and ΔG_{HyM}. Contrastingly, ΔG_{Bu-Ox} increased by 32% and ΔG_{AcM} decreased by 27% and 28% for the propionate and butyrate-fed assays, suggesting enhanced energetical feasibility of this reaction (B and E). In scenario C, ΔG_{Pr-Ox} and ΔG_{Bu-Ox} changed analogously to scenario A. ΔG_{AcM} remained the same in the entire pCO_2 range, which could be attributed to the simultaneous variation of pCO_2 annihilating the pH effects on the bioenergetics. The behaviour of ΔG_{HyM} resembled scenario A due to the absent effect of H^+ production (C and F).

Scenario A highlighted the adverse effects of increased pCO_2 on the bioenergetics of syntrophic reactions. In this regard, Jin and Kirk (2016) postulated that increasing pCO_2 from 0 to 30 bar in simulated non-buffered and buffered aquifer systems made SAO and AcM less energetically feasible, whereas the contrary was calculated for HyM. Moreover, they proposed additional effects of elevated pCO_2 on biochemical reactions due to induced changes in aqueous speciation, ionic strength and in the reduction potential of redox couples such as H^+/H_2. Kato et al. (2014) found that increasing pCO_2 from 0 to 1 bar strongly suppressed syntrophic activity in a model bacterial consortium for SAO, including the bacterium *Thermacetogenium phaeum* and the archaea *Methanothermobacter thermautotrophicus* and *Methanosaeta thermophila*. They established a 91% reduction in the $r_{s\max}$ of acetate, coincidently occurring when ΔG_{Ac-Ox} became higher than -20 kJ mol^{-1}, which is considered the smallest quantum to sustain life (Schink, 1997). In our experiments, $r_{s\max}$ values decreased when pCO_2 increased from 0.3 to 8 bar and the most significant drop also occurred when, theoretically, ΔG_{Pr-Ox} was higher than -20 kJ mol^{-1} (Table 2-6).

Scenario B showed that decreasing pH modifies the bioenergetics of syntrophic propionate and butyrate conversion in a different direction than elevated pCO_2. Interestingly, pH can directly change the ΔG_R^1 when reactions produce or consume protons and indirectly as a result of modified chemical speciation (Bethke et al., 2011; Jin and Kirk, 2018a). From the bioenergetics point of view, proton (H^+) consuming reactions, namely syntrophic oxidation and AcM (Table 2-3), could be promoted when decreasing pH inside a physiologically reasonable range. The more negative $\Delta G_{Overall}$ value in this scenario indicates a potential increase in the driving force to carry out the syntrophic reaction. Nonetheless, this might be compromised by physiological limitations and enhanced toxicity effects (Ali et al., 2019) observed at decreased pH levels, particularly in the case of methanogenic populations (Mao et al., 2015). In consequence,

bioenergetics does not suffice to elucidate the detrimental effects observed in the syntrophic conversions if pH is considered as the main explanatory variable.

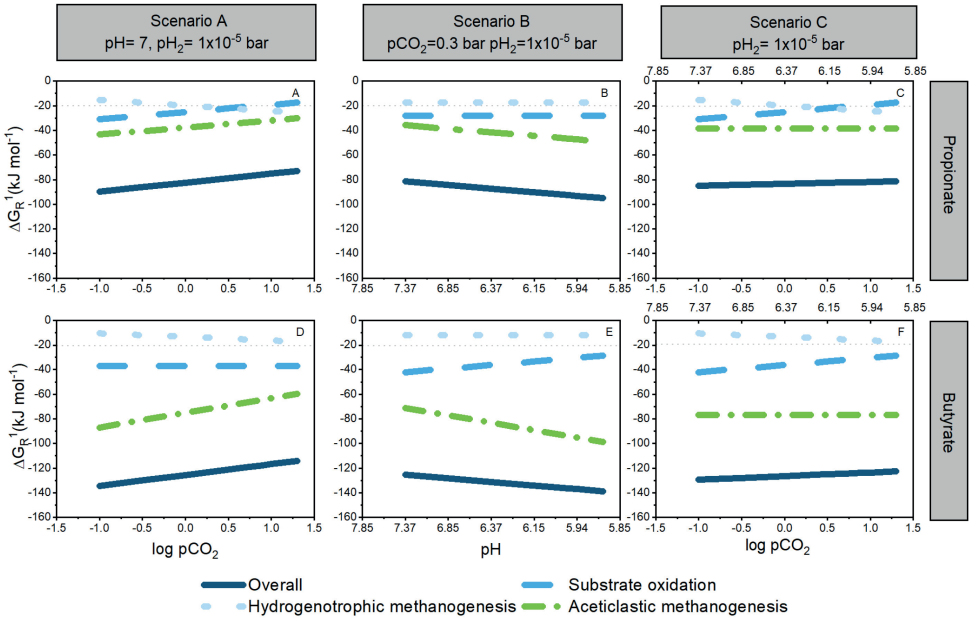

Figure 2-6: Effect of changing selected operational parameters in the ΔG_R^1 in the proposed scenarios for the syntrophic conversions. Scenario A – partial pressure of CO_2 (pCO_2) in propionate and butyrate conversion (A and D, respectively). Scenario B – pH in propionate and butyrate conversion (B and E, respectively). Scenario C - concomitant effect of pH and pCO_2 in propionate and butyrate conversion (C and F, respectively). Lines represent the ΔG_R^1 for the intermediate biochemical reactions: dotted-light blue (hydrogenotrophic methanogenesis - ΔG_{HyM}), dashed-blue (oxidation of propionate - ΔG_{Pr-Ox} or butyrate - ΔG_{Bu-Ox}), short-dash-dotted green (aceticlastic methanogenesis - ΔG_{AcM}), solid navy blue (overall reaction - $\Delta G_{Overall}$). The experimental conditions (pH, pCO_2 and pH_2) that remained fixed during the calculation are included for reference in the upper part of the subplots. Values are presented as log pCO_2 for data linearization purposes. Concentrations of liquid reactants (mol L^{-1}) and gases (bar) correspond to the initial experimental conditions at T=35°C presented in the heading of Table 2-4.

Table 2-6: $\Delta G_{\mathrm{Pr}-Ox}$ calculated for different pCO_2 used in Scenario A to evaluate the effect of increased pCO_2 in the thermodynamic feasibility of syntrophic conversion of propionate and butyrate

	pCO_2 (bar)	log pCO_2	$\Delta G_{\mathrm{Pr}-Ox}$ (kJ mol^{-1})
	0.10	-1.00	-31.0
Experimental range	0.30	-0.52	-28.2
	1.00	0.00	-25.1
	3.00	0.48	-22.3
	5.00	0.70	-21.0
	8.00	0.90	-19.8
	10.00	1.00	-19.2
	20.00	1.30	-17.4

2.3.3 Elevated pCO_2 as a biochemical steering parameter

The distribution of available biochemical energy between the syntrophic partners is expected to change due to the direct and indirect effects of increasing pCO_2 on ΔG_R^1 of the overall and intermediate reactions (Figure 2-7). In our results, the biochemical energy allocation is proposed under conditions of fixed pH_2. Under conditions of changing pH_2, pH and pCO_2 (Figure 2-8, scenarios D, D.1 and D.2), a new thermodynamic equilibrium will be established, which can further modify the biochemical energy distribution among partners in syntrophic propionate and butyrate conversion. Values of pH_2 lower than $6x10^{-4}$ bar will have a positive effect on reaction feasibility, whereas higher values will reduce the feasibility "niche". The impact of increasing pH_2 on the available Gibbs free energy has been previously discussed in the literature (De Kok et al., 2013); nevertheless, its interaction with increased pCO_2 and decreased pH, to the best of our knowledge, has not been thoroughly described.

A correlation analysis with hierarchical clustering of bioenergetic and experimental data was performed in order to verify whether the highlighted trends of the scenario analysis were still valid at a varying pH_2. (Figure 2-9). Two theoretical values were chosen: a typical value for ADs at which syntrophic reactions are thermodynamically feasible ($1x10^{-5}$ bar) (Patón and Rodríguez, 2019) and the lowest detection level of the used gas chromatograph ($6x10^{-4}$ bar).

A strong negative correlation was found between pCO_2 and $r_{s\,\max}$ (r_S=-0.82, $p<0.05$) for both propionate and butyrate. Concerning the Gibbs free energy change, a strong negative correlation was encountered only between ΔG_{Bu-Ox} and pH (r_S=-0.78, $p<0.05$). ΔG_{AcM} was strongly negatively correlated with ΔG_{HyM} (r_S=-0.87, $p<0.05$), evidencing the role of increasing pCO_2 and pH_2 in modulating the feasibility of methanogenic reactions.

2.3.4 Response of syntrophic anaerobic conversion at elevated pCO_2: possible physiological effects

This study highlighted a possible relation between bioenergetic limitations and the observed kinetic effects occurring due to increased pCO_2. However, additional limitations cannot be discarded. For example, in our experiments, the dissolution of CO_2 from the headspace could decrease pH levels, irrespective of the applied high buffer concentration (100 mM HCO_3^-). Changes in pH disrupt cell homeostasis and impose limitations for growth, maintenance, and metabolic activity. In particular, syntrophic butyrate oxidizers (SBO) and syntrophic propionate oxidizers (SPO) demonstrate moderate growth at a pH lower than 6.5 (Balk et al., 2008) and 6.0 (Li et al., 2012), respectively. The increased lag phases and limited conversion under elevated pCO_2 could then be explained by the combination of pH effects on, *e.g.*, ΔG_{Bu-Ox} and physiological limitations affecting SBO and SPO at a different extent.

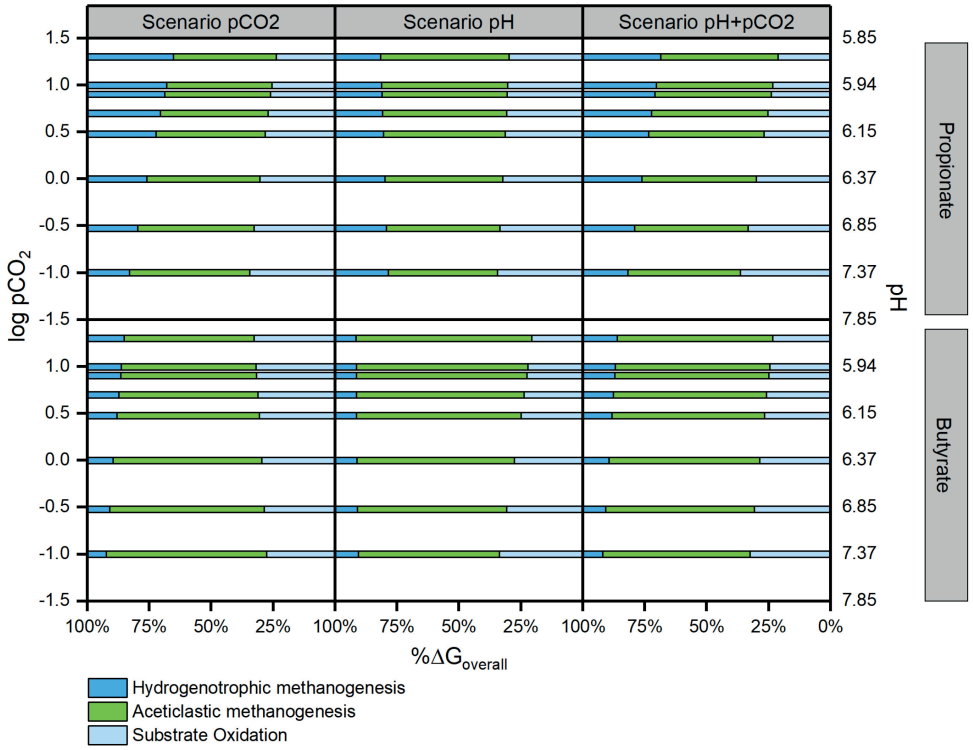

Figure 2-7: Theoretical share of $\Delta G_{Overall}$ for each of the proposed scenarios for the syntrophic conversion of propionate and butyrate. Scenario A – partial pressure of CO_2 (pCO_2) in propionate and butyrate conversion. Scenario B – pH. Scenario C - concomitant effect of pH and pCO_2. All the scenarios were calculated at T=35°C and pH_2= $1x10^{-5}$ bar.

As well, the acidification of the fermentation medium modifies the equilibrium between undissociated and dissociated forms of the VFAs (Xiao et al., 2016), further altering cell homeostasis. At the applied pCO_2 of 8 bar and resulting equilibrium pH of 5.9, the concentrations of undissociated propionic acid (HPr) were slightly above inhibitory levels, *i.e.,* 20 mg L^{-1} HPr (Maillacheruvu et al., 2013) (Table 2-7). The concentration of undissociated butyric acid (HBu) remained below 500 mg L^{-1} HBu (Monot et al., 1984), proposed in literature as inhibitory for growth in, *i.e., Clostridium acetobutylicum.* Acetic acid concentrations (HAc) remained below indicative inhibitory levels in methanogenesis (Xiao et al., 2013). However, the detrimental effects of elevated pCO_2 in our experimental treatments were already seen at 1 bar pCO_2. Consequently, increased undissociated VFAs concentrations do not explain the observed phenomena.

At elevated pCO_2, the equilibrium dissolved CO_2 concentration in the liquid medium increased from 320 to 8 620 mg L^{-1} (Table 2-7). These dissolved CO_2 concentrations are in line with values reported by Wan et al. (2016) (3 000 – 30 000 ppm), which negatively impacted the nitrogen removal efficiency due to increased membrane permeability, thus inhibiting electron transport and protein expression.

Furthermore, Salek et al. (2015) showed that there is at least one order of magnitude difference in the kinetically controlled rate of physical reactions such as CO_2 dissolution and biochemical reactions, such as production of VFA. This, in turn, may affect the concentration of the various species that are responsible for the reactions used in the thermodynamic calculations, leading to disparities in the calculated and observed bioenergetic effects at specific time points. More accurate pH_2 measurements in the low range, *e.g.,* $<6x10^{-4}$ bar, are required to further validate the occurrence of the postulated effects on the feasibility of syntrophic reactions due to concomitant variation of pH_2 and pH or pCO_2. The possible role of other electron shuttles, whose appearance is favoured by the presence of hydrogen and elevated pCO_2, particularly formate, needs to be further addressed (Oswald et al., 2018; Roger et al., 2018).

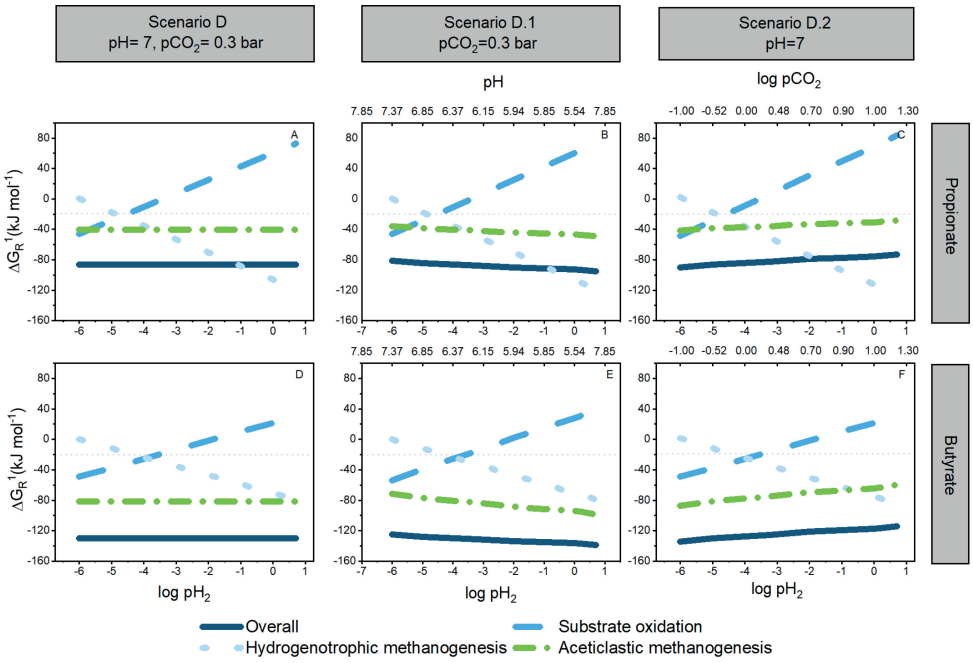

Figure 2-8: Effect of changing selected operational parameters in the $\Delta G_R^{\,1}$ in the proposed scenarios for the syntrophic conversions. Scenario D – partial pressure of H_2 (pH_2) in propionate and butyrate (A and D, respectively). Scenario D.1 – concomitant effect of pH and pH_2 in propionate and butyrate (B and E, respectively). Scenario D.2 - concomitant effect of pH_2 and pCO_2 in propionate and butyrate (C and F, respectively). Lines represent the $\Delta G_R^{\,1}$ for the intermediate biochemical reactions: dotted-purple (hydrogenotrophic methanogenesis - ΔG_{HyM}), dashed-orange (oxidation of propionate - $\Delta G_{\mathrm{Pr}-Ox}$ or butyrate - ΔG_{Bu-Ox}), short-dash-dotted green (aceticlastic methanogenesis - ΔG_{AcM}), solid black (overall reaction - $\Delta G_{Overall}$). The experimental conditions (pH, pCO_2 and pH_2) that remained fixed during the calculation are included for reference in the upper part of the subplots. Values are presented as log pCO_2, log pH_2 for data linearization. Concentrations of liquid reactants (mol L^{-1}) and gases (bar) correspond to the initial experimental conditions at T=35°C presented in the heading of Table 2-4.

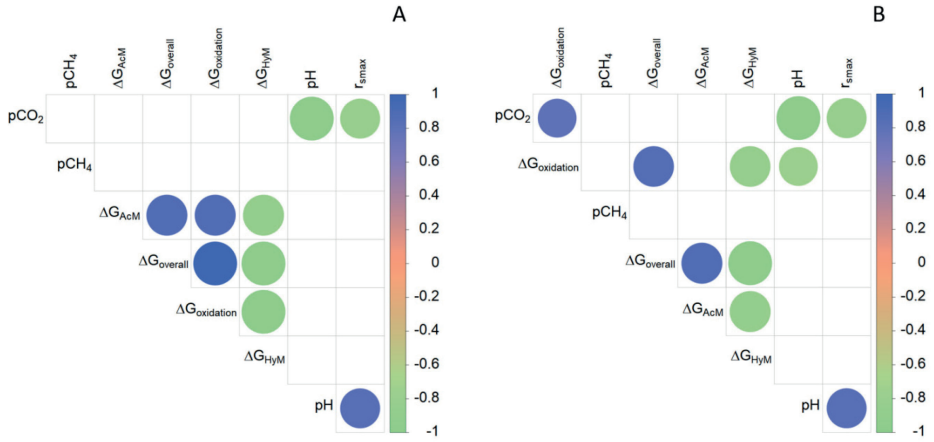

Figure 2-9: Correlogram for the measured and calculated data from the experiments of syntrophic propionate (A) and butyrate (B) conversion under conditions of elevated pCO_2. The correlation was calculated using the Spearman correlation coefficient (r_S) and ordered through hierarchical clustering. Circles with increased diameter represent a stronger correlation. According to the scale included to the right of the figure, values closer to 1 (in blue) represent a significant positive correlation, whereas values closer to -1 (in green) represent a significant negative correlation. Abbreviations correspond to the overall Gibbs free energy (Gibbs_Ov), the sub-reactions (Substrate oxidation: Gibbs_Ox, Acetoclastic methanogenesis: Gibbs_AcM, Hydrogenotrophic methanogenesis: Gibbs_HyM) and to the maximal substrate utilization rate ($r_{s\,\max}$).

Table 2-7: Calculation of the dissolved CO_2, undissociated acid concentrations corresponding to the experimental conditions of this study

Initial pressure (bar)					**0.3**	**1**	**3**	**5**	**8**
Eq. pCO_2 (bar)					0.3	1	1.3	2	3.5
$CO_{2(aq)}$ (g L^{-1})					0.3	1.1	3.8	5.4	8.6
HCO_3^- (g L^{-1})					6.1	6.1	6.1	6.1	6.1
Eq. pH					7.4	6.9	6.8	6.6	6.3
Compound	Exp. Initial Concentration (M)	Exp. Concentration (gCOD L^{-1})	pKa (35°C)	Undisso-ciated specie	Concentration range in the experiments (mg L^{-1})				
Acetate	0.02	1.0	4.76	HAc	26.9 - 45.1				
Propionate	0.01	1.1	4.89	HPr	2.3 - 27.3				
Butyrate	0.01	1.2	4.81	HBu	1.6 - 18.9				

*Undissociated acids calculated using carbonate equilibrium constant $k_1 = 5.54 \times 10^{-7}$ corrected by temperature (35°C), Henry's equilibrium constant $k_H = 0.0245$ mol L^{-1} bar^{-1} corrected by temperature (35°C).

2.4 Conclusions

Elevated pCO_2 influences the kinetics and bioenergetics of the syntrophic conversion of propionate and butyrate. Based on this study, we propose that kinetic effects might appear as an evident sign of thermodynamic limitations, which is different for each compound. From detailed bioenergetic calculations, it was concluded that pCO_2 increases the ΔG_{Pr-Ox}, induces pH changes that make ΔG_{Bu-Ox} more positive and increases the $\Delta G_{Overall}$ of the syntrophic conversion. The more positive $\Delta G_{Overall}$ at elevated pCO_2 likely induces a redistribution of the available biochemical energy among the syntrophic partners that, if unbalanced, will translate into kinetic constraints. However, the here discussed biochemical energy limitations could not fully explain the strong kinetic effects in the system at increasing pCO_2. Presumably, the overall effects resulted from the concomitant impact of reduced thermodynamic feasibility, physiological effects associated with a lowered pH, and a minor detrimental impact of increased concentrations of undissociated VFAs. The observed kinetic and bioenergetic aftermath of elevated pCO_2 exposure might confer potential for steering metabolic pathways, if limitations are overcome. Furthermore, the use of energy-rich substrates such as sugars, proteins or lipids, could minimize the physiological impact of lowered pH and relieve bioenergetic limitations. Under such conditions, the steering potential of elevated pCO_2 on biochemical pathways in mixed culture anaerobic conversions could be unravelled.

3

CHAPTER 3

EFFECT OF PRE-INCUBATION CONDITIONS IN FERMENTERS AT MILD HYDROSTATIC PRESSURE

This chapter is based on:

Ceron-Chafla, P., García-Timermans, C., de Vrieze, J., Ganigué, R., Boon, N., Rabaey, K., van Lier, J.B., Lindeboom, R.E.F., 2022. Pre-incubation conditions determine the fermentation pattern and microbial community structure in fermenters at mild hydrostatic pressure. Biotechnol. Bioeng. 1–16. https://doi.org/10.1002/bit.28085

Abstract

Fermentation at elevated hydrostatic pressure is a novel strategy targeting product selectivity. However, the role of inoculum history and cross-resistance, *i.e.,* acquired tolerance from incubation under distinctive environmental stress, remains unclear in high-pressure operation. In our here presented work, we studied fermentation and microbial community responses of halotolerant marine sediment inoculum (MSI) and anaerobic digester inoculum (ADI), pre-incubated in serum bottles at different temperatures and subsequently exposed to mild hydrostatic pressure (MHP <10 MPa) in stainless steel reactors. Results showed that MHP effects on microbial growth, activity and community structure were strongly temperature-dependent. At moderate temperature (20°C), biomass yield and fermentation were not limited by MHP; suggesting a cross-resistance effect from incubation temperature and halotolerance. Low temperatures (10°C) and MHP imposed kinetic and bioenergetic limitations, constraining growth and product formation. Fermentation remained favourable in MSI at 28°C and ADI at 37°C, despite reduced biomass yield resulting from maintenance and decay proportionally increasing with temperature. Microbial community structure was modified by temperature during the enrichment, and slight differences observed after MHP-exposure did not compromise functionality. Results showed that the relation incubation temperature – halotolerance proved to be a modifier of microbial responses to MHP and could be potentially exploited in fermentations to modulate product/biomass ratio.

Keywords

Anaerobic fermentation, halotolerance, mild hydrostatic pressure, piezotolerance, psychrotolerance.

3.1 Introduction

Operation at elevated hydrostatic pressure (HP) has been evaluated to optimize fermentation processes and biopolymer production. HP conditions induce synthesis of stress metabolites with industrial relevance, such as trehalose and glutathione (Dong and Jiang, 2016). Elevated HP also steers the fermentation product spectrum towards alternative value-added products, *e.g.,* ethanol (Bothun et al., 2004). Concerning biopolymer production, HP increases the intracellular polymer content with adjusted density and composition (Mota et al., 2019). Lowered biomass productivity and growth (Iwahashi et al., 2005; Molina-Höppner et al., 2003; Mota et al., 2015; Tholosan et al., 1999), as well as increased microbial maintenance requirements (Mota et al., 2018; Wemekamp-Kamphuis et al., 2002) have been identified as drawbacks but without detailed mechanistic explanations for their occurrence. HP-operation bottlenecks depend on the specific response of the involved microorganisms to elevated HP, *i.e.,* whether or not the biomass shows piezotolerance (Bothun et al., 2004), which constitutes a defining feature to promote the usage of this technology.

Piezotolerance refers to the ability of microorganisms to grow when exposed to elevated HP and is widely spread in subsurface ecosystems like the deep sea (Canganella and Wiegel, 2011; Tamburini et al., 2013). It is also encountered in shallow surface waters and coastal sediments (Jebbar et al., 2015; Marietou and Bartlett, 2014; Vossmeyer et al., 2012), as well as in specific industrial strains (Pavlovic et al., 2008; Vanlint et al., 2011). In particular, *Lactobacillus* and *Clostridium* spp. have shown piezotolerance after short-term treatments with HP (7 to 50 MPa), or it was attributed to developed cross-resistance (Mota et al., 2013).

Cross-resistance refers to the microbial capacity to resist negative impacts of environmental stress potentially resulting from a) pre-incubation under other environmental stress conditions, *e.g.,* low to high temperature variation, non-neutral pH, water activity and salinity extremes; b) differences in the growth stage of microbial cells and c) starvation effects (Abe, 2007; Gao et al., 2021; Lanciotti et al., 1996; Scheyhing et al., 2004). In natural habitats, cross-resistance develops from the exposure to local-scale environmental gradients occurring due to tidal, seasonal and depth variations (Johnson et al., 2009; Tholosan et al., 1999). The stress-response associated with cross-resistance effects comprises adaptations at the cellular level, such as accumulation of compatible solutes and salts, protein synthesis and reorganization of cell membrane lipids (Kish et al., 2012). As well, it includes the modulation of metabolic pathways and growth rates (Gao et al., 2021) and, ultimately, the modification of microbial community functionality and composition due to differences in stress tolerance, energy investment and exacerbated competition between microbial species (Rillig et al., 2015).

Enhancing product selectivity and overall process productivity by carrying out mixed culture fermentation at sub-lethal or mild hydrostatic pressure (MHP < 10 MPa) has been limitedly explored in the field of high pressure biotechnology (section 1.2). Moreover, in the context of high pressure application in anaerobic processes is important to differentiate effects associated with exposure to MHP (this chapter) and with changes in gas partial pressures, particularly CO_2, occurring from headspace pressurization (chapters 2, 4 and 5). In this study, we investigated whether the combination of inoculum halotolerance - temperature adaptation can trigger cross-resistance mechanisms to MHP, leading to enhanced/sustained carboxylate production under environmental stress. Fermentation experiments at MHP with two halotolerant inocula adapted to different operational temperatures were conducted to test our cross-resistance hypothesis. In alignment with the mentioned links between temperature and HP, adjusting operational temperature might be a viable operational process strategy to improve process performance under HP (Lopes et al., 2019). Metabolic energy analysis was performed to identify energy limitations as part of the explanatory mechanism for reduced biomass/ product yields and changes in product spectrum. Finally, these results are discussed concerning their influence on process efficacy and resilience.

3.2 Materials and Methods

3.2.1 Enrichment

Two anaerobic inocula without prior exposure to MHP were used in the experiments. Marine sediment inoculum (MSI) was enriched from a manually homogenized mixture of three sediment samples obtained from a subtidal mud accumulation site located approximately 5 km offshore from Oostende (51°16.30N, 2°54.30E, West-Flanders, Belgium) at an average water depth of 12 m (HP of 0.12 MPa) (van de Velde et al., 2016). Mesophilic anaerobic digestion inoculum (ADI) was enriched from a sample of a full-scale up-flow anaerobic sludge blanket (UASB) reactor of 5.5 m height (HP of maximally 0.05 MPa at the bottom of the reactor), treating saline wastewater from a petrochemical industry. The physicochemical characterization of both inocula is presented in Table 3-1.

The medium described in Table 3-2 with adjusted salinity and glucose as substrate (2.45 g COD L^{-1}) was used to enrich MSI and ADI for 27 days, with enrichment cycles lasting 5-7 days. MSI enrichment experiments were carried out at 10 and 20˚C (MSI-10, MSI-20). These temperatures are comparable to the seasonal environmental regime of the site of sediment collection. An additional experiment was conducted at 28˚C (MSI-28), a temperature close to the typical range for anaerobic carboxylates production (Arslan et al., 2016; Infantes et al., 2011) and in the upper range for growth of psychrotolerant marine bacteria (Groudieva et al.,

2003). ADI enrichment was carried out at the operational temperature of the UASB of origin, *i.e.,* 37˚C (ADI-37). Initial MSI inoculation was done from re-suspended sediment to final volatile solids (VS) concentration of 1.4 mg VS mL^{-1} in serum bottles, prepared according to Table 3-2. In parallel, ADI was first diluted with marine medium to the same initial VS concentration as MSI and added to prepared serum bottles. Effective volume reached 45 mL after inoculation and the liquid to gas ratio was kept at 1.7: 1.0.

Table 3-1: Physicochemical characterization of marine sediment inoculum (MSI) and anaerobic digester inocum (ADI).

Parameter	Marine Sediment Inoculum (MSI)*	Anaerobic Digester Inoculum (ADI)
Total Solids (%)	47.53 ± 1.1	6.07 ± 0.09
Volatile Solids (%)	10.50 ± 0.39	45.79 ± 1.13
Total COD (g L^{-1})	0.43 ± 0.12	64.32 ± 11.89
Alkalinity (g HCO_3^- L^{-1})	15.36 ± 0.39	19.49 ± 1.31
Conductivity (mS cm^{-1})	19.74	1400
Temperature natural/adapted habitat (°C)	9	37
pH	8.77	7.37

*The sampling campaign was carried out in March 2019. After collection, the sediment samples were stored in vacuum-sealed containers and kept for two months at 5°C before utilization.

An in-house developed flush system was used to exchange the headspace of the serum bottles with a mixture of N_2: CO_2 (90:10). On average, 20 cycles per bottle were applied to guarantee anaerobic conditions after inoculation and set an initial overpressure of 0.005 ± 0.001 MPa. Enrichment cycles were concluded when recovered COD-glucose into carboxylates corresponded to ≥ 70%. Afterwards, 5 mL non-pooled transfers (*i.e.,* replicates were not combined) to fresh anaerobic saline medium were carried out. All the experimental treatments were carried out in triplicates plus a negative control without substrate. Serum bottles were shaken at 120 rpm in orbital shakers.

3.2.2 Mild hydrostatic pressure (MHP) experiments

A non-pooled transfer from each biological replicate and negative control of the last cycle of the MSI and ADI enrichment was performed to sterile 5 mL syringes, previously flushed with N_2: CO_2 (90:10) (Figure 3-1). The same liquid to gas ratio as in the serum bottles was kept. After inoculation and medium addition, syringes were closed using two-way valves and positioned inside six high-pressure stainless-steel reactors (Parr, USA) filled with deionized water. Due to reactor availability, MHP experiments at different temperatures were carried out in a sequential incubation. The increment of hydrostatic pressure to 5 and 8 MPa, to achieve CO_2 partial pressures comparable to our previous work (Ceron-Chafla et al., 2020, 2021), was done by pumping distilled water inside the reactors using a manual hydraulic pump. One

syringe from each replicate and negative control of the enrichment was incubated in parallel under atmospheric conditions (AC) at a pressure of 0.1 MPa (Figure 3-1). Experiments lasted between 8-12 days depending on each pressure, temperature and inoculum tested. On the final day, reactors were depressurized through liquid release. Syringes were left to stabilize to atmospheric pressure (0.1 MPa) for 30 min. Afterwards, total liquid content was recovered and distributed as follows: a) carboxylates determination, b) DNA extraction from biomass pellet to be stored at -20°C and c) flow cytometry measurement (FCM) from samples fixed with 1% glutaraldehyde.

Table 3-2: Description of fermentation medium and additional solutions used in the enrichment and mild hydrostatic pressure (MHP) experiments of glucose anaerobic conversion at 5 and 8 MPa with marine sediment (MSI) and anaerobic digester (ADI) inocula

Saline medium[a]	**Tungstate and selenite solution**	**Alkaline earth metals solution**	**Trace elements solution**	**Growth factors and vitamins solution**	**Substrate**	**Reducing agent**
Seawater composition Millero et al. (2008) Medium recipe proposed by Patil et al. (2015)	Na_2WO_4• 2 H_2O (4 mg L^{-1}) Na_2SeO_3• 5 H_2O (3 mg L^{-1}) NaOH (0.5 g L^{-1})	$MgCl_2$• 6 H_2O (11 g L^{-1}) $CaCl_2$ • 2 H_2O (1.6 g L^{-1}) $SrCl_2$ • 6 H_2O (0.03 g L^{-1})	Prepared according to Patil et al. (2015)		Glucose concentrated solution (103 g L^{-1}), sterilized and added to a final concentration of 2.45 g COD[b] L^{-1}	1 mL filter-sterilized Na_2S solution (final concentration 0.08 g L^{-1})
Total volume 36 mL bottle^{-1}	1 mL L^{-1} saline medium	2 mL bottle^{-1}	0.1 mL bottle^{-1}	0.1 mL bottle^{-1}	1 mL bottle^{-1}	1 mL bottle^{-1}

[a]Sulfate (SO_4^{2-}) was deliberately not added to the medium in order to limit the sulfate reducing activity of sulfate reducing bacteria (SRB) present in the inoculum
[b]COD: Chemical Oxygen Demand

3.2.3 Analyses

Flow Cytometry Measurements

Collected samples were fixed using 25% glutaraldehyde solution (final concentration 1% v/v) and marine medium. Prior FCM, fixed samples were sonicated for three minutes using a sonication bath (Elma, Germany) at controlled temperature (20° C). Based on an internal preliminary study to establish the effect of the sonication time on the measured cell density for marine sediment samples (Figure 3-2), three minutes were selected as treatment time. This

sonication time is a conservative estimate also based in previous analyses of other marine sediment samples (unpublished results and not part of this thesis) and the visualization of agglomerate disruption via fluorescence microscopy (Zeiss Axioskop microscope, Oberkochen, Germany). After sonication, the samples were vortexed for approximately 30 seconds to ensure detachment. Next, they were filtered using 20 µm falcon, sterile, syringe-type filters (BD, San Jose, USA).

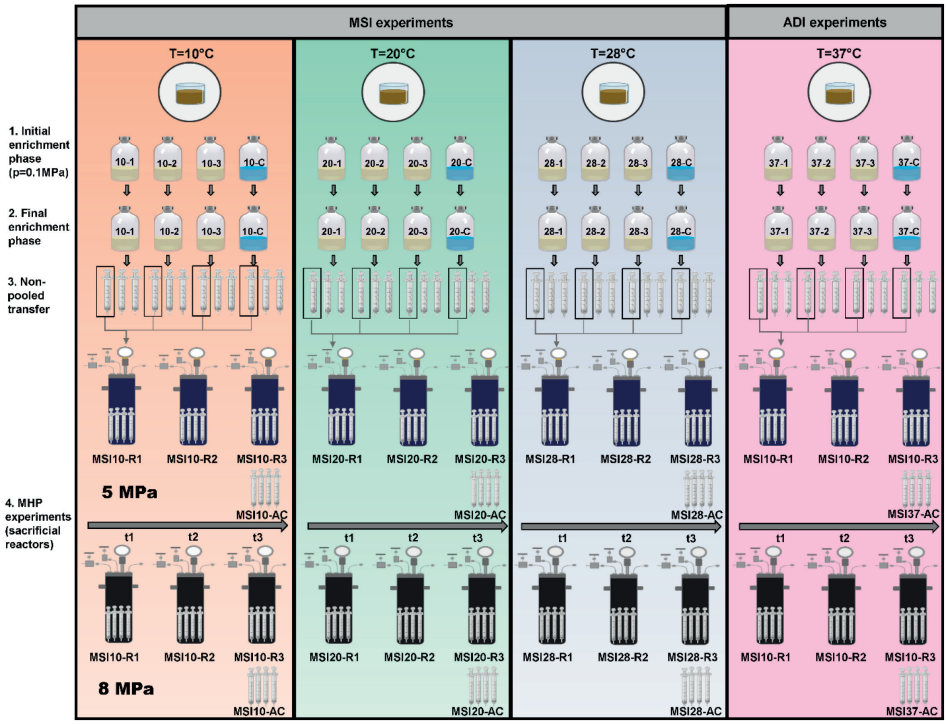

Figure 3-1: Experimental design applied for the inoculum enrichment at atmospheric pressure and the non-pooled biomass transfer for the glucose conversion experiments at mild hydrostatic pressure (MHP) of 5 and 8 MPa. Experiments with marine sediment inoculum - MSI were carried out at 10, 20, 28˚C and the experiments with anaerobic digestion inoculum - ADI at 37 ˚C. For all the experiments, triplicate incubation syringes (biological replicates) plus a negative control without substrate were placed inside the pressure reactors. The time points where samples from sacrificial pressure reactors were recovered are represented by t1, t2 and t3.

Pre-treated samples were once more vortexed at the same speed for 30 seconds, diluted (x100 or x1000 depending on their density) with filtered marine medium (0.22 µm) and placed in 96-well plates. The Accuri C6+ was checked daily using CS&T RUO beads (BD Biosciences, Belgium) and for every acquisition, the stability of FL1 over time was monitored. The channels forward scatter height (FSC-H), side scatter height (SSC-H), and fluorescence intensity

(FL1-H, FL3-H) were used for data analysis. The flow cytometry data were imported in R (v3.3.2) using the flowCore package (v1.40.3) (62). The Phenoflow package (v1.1.1.) was used to assess the phenotypic structure of the bacterial communities, and to calculate the total cell density (Props et al., 2016).

After pre-treatment, cells were counted using flow cytometry. Diluted samples (x 1 000) were stained with SYBR Green I and incubated at 37°C for 13 min following the protocol of van Nevel et al. (2013) and immediately analyzed in an Accuri C6+ flow cytometer (BD Biosciences, Belgium). The Accuri C6+ was equipped with four fluorescence detectors (530/30 nm, 585/40 nm, >670 nm and 675/25 nm), two scatter detectors and a 20-mW 488-nm laser, and was operated with Milli-Q (Merck Millipore, Belgium) as sheath fluid.

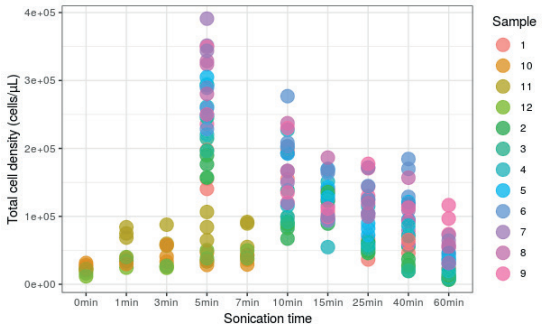

Figure 3-2: Effect of high-range and low-range sonication time in measured cell density for the triplicate incubations during the first cycle of enrichment at atmospheric pressure. Samples correspond to marine sediment inoculum (MSI) at 10°C (samples 1, 2, 3, 10), 20°C (samples 4, 5, 6, 11) and 28°C (samples 7, 8, 9, 12).

Microbial community analysis

The DNA extraction was carried out according to the protocol of Vilchez-Vargas et al. (2013). Agarose gel electrophoresis and PCR analysis were used to determine the quality of DNA extracts. The PCR was carried out using the bacterial primers 341F and 785Rmod following an in-house PCR protocol (Boon et al., 2002). After quality validation, DNA extracts were sent to LGC genomics GmbH (Berlin, Germany) for amplicon sequencing of the bacterial community through the 16S rRNA gene V3-V4 hypervariable region on the Illumina MiSeq platform. After processing the amplicon sequencing data, a table was generated with the relative abundances of the different OTUs and their taxonomic assignment of each sample. Next, absolute abundances were estimated based on the FCM data according to Props et al. (2017) and statistically analyzed.

Amplicon sequencing

The forward primer 341F 5'- NNNNNNNNNTCCTACGGGNGGCWGCAG and reverse primer 785R 5'- NNNNNNNNNNTGACTACHVGGGTATCTAAKCC (Klindworth et al., 2013) were used. The PCR mix included 1 µl of DNA extract, 15 pmol of both primers in 20 µL volume of MyTaq buffer containing 1.5 units MyTaq DNA polymerase (Bioline) and 2 µl of BioStabII PCR Enhancer (Sigma). For each sample, the forward and reverse primers had the same unique 10-nt barcode sequence. The PCR contained 30 cycles with 2 min 96°C predenaturation; 96°C for 15 s, 50°C for 30 s, 70°C for 90 s.

The DNA concentration of the amplicons was determined by gel electrophoresis. Next, 20 ng amplicon DNA of each sample was pooled for up to 48 samples carrying different barcodes. The amplicon pools were purified with one volume AMPure XP beads (Agencourt, US) to remove primer dimer and other small mispriming products, followed by an additional purification on MinElute columns (Qiagen, The Netherlands). Finally, 100 ng of each purified amplicon pool DNA was used to construct Illumina libraries using adaptor ligation using the Ovation Rapid DR Multiplex System 1-96 (NuGEN, US). Illumina libraries were pooled and size selected by preparative gel electrophoresis.

Data Processing

The Mothur software package (v.1.42.3), and guidelines developed by Schloss et al. (2009) were used to process the raw Illumina data on a GNU/Linux 3.16.0-46-generic x86_64 system. The forward and reverse reads were assembled into contigs by a heuristic approach, taking the Phred quality scores into account. Ambiguous contigs or with unsatisfying overlap were removed, and the remaining sequences were aligned to the mothur formatted silva seed v132 database. Those sequences not aligning within the region targeted by the primer set or sequences with homopolymer stretches with a length > 12 bp were removed. The sequences were pre-clustered, allowing mismatch for every 100 bp of sequence. Chimeric sequences were removed with VSEARCH (v2.13.0) (Rognes et al., 2016). Classification of the sequences was carried out by a naïve Bayesian classifier (Wang et al., 2007), with an 85% cut-off for the pseudobootstrap confidence score. Taxa that were annotated as Chloroplast, Mitochondria, unknown, Archaea or Eukarya at the kingdom level, which are due to a specific amplification, were excluded. Sequences were clustered into operational taxonomic units (OTUs) with average linkage, and at a 97% sequence identity, using the OptiClust method (Westcott and Schloss, 2017). Representative sequences were picked for each OTU as the most abundant sequence within that OTU.

Statistical Analysis

Statistical analyses from microbial community analysis data were carried out in R version 3.6.1 (http://www.r-project.org) (R Core Team 2019, 2019). The R packages vegan (Oksanen et al., 2016) and phyloseq (McMurdie and Holmes, 2013) were used for bacterial community analysis.

The non-metric multidimensional scaling (NMDS) plots, based on the bacterial amplicon data, were constructed using the Bray-Curtis (1957) distance measure. Significant differences ($p < 0.05$) in microbial community composition between the different inocula, temperatures or pressures were identified employing pair-wise Permutational ANOVA (PERMANOVA) with Bonferroni correction, using the *adonis* function (vegan). The PERMANOVA method was also used to evaluate the significance ($p < 0.05$) of the relation of lactate, formate, acetate, propionate and butyrate with community structure, and their effect was visualized via canonical correspondence analysis (CCA) plotting. Significant differences in cell numbers and residual VFA concentrations associated with pressure and temperature in the different inocula groups were identified through non-parametric Kruskal-Wallis H test. Order-based Hill's numbers were used to evaluate the α-diversity. These Hill's numbers represent richness (number of OTUs, H_0), the exponential of the Shannon diversity index (H_1) and the Inverse Simpson index (H_2) (Hill, 1973).

Chemical Analyses

The chemical oxygen demand (COD), volatile solids (VS) and pH were measured according to Standard Methods (American Public Health Association, 2017), whereby alkalinity measurements used an automatic titration unit (Metrohm, Switzerland). Electroconductivity was measured using an electroconductivity meter (C833 Consort, Turnhout, Belgium). Organic acids (lactate, formate, acetate, propionate and butyrate) were measured using ion chromatography (Metrohm 930 Compact IC Flex, Herisau, Switzerland) and a Metrosep Organic acid 250/7.8 column coupled to a Metrosep Organic acids Guard/4.6 column using 0.001 M H_2SO_4 as eluent. The lower detection limit was 1 mg L^{-1} for all the acids.

Bioenergetics calculation

The catabolic Gibbs free energy change (ΔG_{cat}^{01}) is the amount of Gibbs free energy from a redox reaction between an electron donor and acceptor (Heijnen and Kleerebezem, 2010). We calculated ΔG_{cat}^{01} based on the final product spectrum of each temperature-adapted treatment

at 5, 8 MPa and AC (Table 3-3). Based on each ΔG_{cat}^{01}, a) the energy requirements for maintenance (m – J d^{-1}) to sustain the initial biomass in the inoculum and b) the "theoretical" biomass (X) yield ($Y_{X/S}$) on the substrate were estimated. The stoichiometry of catabolic reactions was proposed for the different pressure-temperature-inoculum incubations. These equations were constructed based on the final soluble COD distribution in the MSI and ADI experiments at 5 and 8 MPa and atmospheric controls.

We followed an adapted procedure based on the work of Lee et al. (2008) and Heijnen and Kleerebezem (2010). The metabolite proportions calculated based on the final measured COD were used for the construction of a combined electron acceptor equation for the catabolism. The proposed equations required additional inspection for element and charge balance since COD balances from the experiments were not closed. The effects of temperature variation, MHP exposure, and pH were incorporated in the calculation of the Gibbs free energy for catabolism (ΔG_{cat}^{01}, kJ mol glucose^{-1}). ΔG_{cat}^{01} was used to calculate the catabolic flux for maintenance purposes (m, mol glucose C-mol biomass^{-1} h^{-1}).

Overall Growth Reaction

Based on the final product composition of the different experimental treatments for anaerobic glucose conversion at 5 MPa, 8 MPa and their respective controls, the proportion of each metabolite was calculated on a COD basis and employed to construct a mixed electron acceptor equation for the catabolic reaction (Lee and Rittmann, 2009).

Glucose was used as the carbon and energy source for defining the anabolic equation. The metabolism was calculated via the coupling of catabolic and anabolic equations using the energy dissipation approach proposed by Heijnen and Kleerebezem (2010). From the different metabolic equations of the inoculum-temperature-pressure groups, the biomass yield on substrate ($Y_{X/S}$) was calculated. Due to the employed biomass composition for the calculations ($CH_{1.8}O_{0.5}N_{0.2}$), the metabolic equations express the Gibbs free energy per C-mol of biomass.

Correction by non-standard conditions (Temperature, pH and hydrostatic pressure)

Gibbs free energy values for the catabolic, anabolic and metabolic equation were corrected for the different incubation temperatures using the Gibbs-Helmholtz equation. Additionally, correction due to higher hydrostatic pressure was also applied, according to Mayumi et al. (2013). Finally, the obtained Gibbs free energy values were corrected for pH measured after decompression.

Maintenance energy

The Gibbs free energy requirements for maintenance (*m*) were computed according to Tijhuis et al. (1993) and were corrected for the different temperatures using the Gibbs-Helmholtz equation (Kleerebezem and Van Loosdrecht, 2010). This value was converted to units of kJ C mol^{-1} employing the conversion procedure described in the normalization section. The Gibbs free energy for maintenance per cell was multiplied by the final measured number of cells in each experimental treatment.

Normalization

Gibbs free energy values for the catabolic, anabolic and metabolic equation and maintenance were expressed on a per-cell basis. For this, the final cell concentration in cells mL^{-1} was converted to C-mol using theoretical values for the biovolume and carbon content per cell of anaerobic bacteria, according to Fry (1990).

Table 3-3: Catabolic reaction stoichiometric coefficients calculated based on the final product spectrum measured at the end of the experiments of glucose anaerobic conversion at 5 and 8 MPa using marine sediment inoculum (MSI) at 10, 20 and 28°C, an anaerobic digester inoculum at 37°C

Inoculum	**Marine Sediment (MSI)**												**Anaerobic Digester (ADI)**			
P (MPa)	5	0.1	8	0.1	5	0.1	8	0.1	8	0.1	5	0.1	8	0.1	5	0.1
T(°C)	20	20	20	20	10	10	10	10	28	28	28	28	37	37	37	37
Glucose	-1.00	-1.00	-1.00	-1.00	-1.00	-1.00	-1.00	-1.00	-1.00	-1.00	-1.00	-1.00	-1.00	-1.00	-1.00	-1.00
Formate	0.00	0.00	0.00	0.01	0.55	0.44	0.22	0.31	0.00	0.00	0.00	0.00	0.00	0.00	0.00	0.17
Lactate	0.00	0.00	0.00	0.00	0.03	0.10	0.51	1.11	0.00	0.00	0.00	0.00	0.03	0.04	0.28	0.15
Butyrate	0.01	0.01	0.01	0.01	0.00	0.01	0.00	0.00	0.02	0.01	0.02	0.02	0.01	0.00	0.00	0.00
Propionate	0.70	0.91	0.66	1.20	0.53	0.44	0.00	0.01	0.91	0.72	1.11	0.96	0.60	0.30	0.61	0.60
Acetate	1.37	1.44	0.87	1.72	0.86	0.85	0.14	0.34	1.50	1.78	1.33	1.52	1.32	1.75	0.95	1.56
CO_2	1.13	0.37	2.26	-1.11	2.03	2.21	3.95	1.67	0.22	0.25	-0.06	0.02	1.44	1.44	1.43	0.46
Hydrogen	1.55	-0.18	3.85	0.00	4.07	4.40	8.13	3.64	-0.50	-0.24	-1.27	-1.00	2.26	2.57	2.25	0.48
Water	-0.41	0.55	-1.59	2.31	-2.04	-2.20	-4.16	-1.97	0.72	0.49	1.21	0.96	-0.82	-1.13	-0.82	-0.02
Proton	2.07	2.34	1.54	-3.90	1.97	1.84	0.83	1.76	2.42	2.51	2.46	2.58	1.95	2.12	1.84	2.48
ΔG_{cat}[1]	-277.02	-319.45	-219.29	-112.50	-188.07	-178.19	-60.12	-144.51	-330.90	-325.26	-349.52	-344.97	-270.06	-263.57	-255.33	-299.79

3.3 Results

3.3.1 Effects of MHP exposure on cell density of temperature adapted enrichments

As a proxy for biomass growth, cell density was monitored via FCM, simultaneously with carboxylates production. The absolute change in cell density in temperature incubations and AC (Figure 3-3) was calculated by subtracting endogenous decay estimated from controls without substrate. A decreasing trend in the final cell density is observed in most cases except for condition MSI-20, where the absolute change is positive over time and higher than the absolute maximum change observed during the enrichment (Figure 3-3B). The most negative absolute change was assessed for MSI-28 (Figure 3-3C) and in particular for ADI-37 (Figure 3-3D).

Differences in the absolute cell density change were evaluated by the non-parametric Kruskal-Wallis H test using temperature and MHP as grouping variables. In experiments with MSI at 5, 8 MPa and the AC, significant differences in cell density absolute change were found considering incubation temperature as determining parameter ($p=0.0002$). Differences evaluated with MHP as determining parameter were non-significant ($p=0.09$). Post-hoc tests revealed that MSI-20 was significantly different from MSI-28 and MSI-10 ($p=0.0002$ and 0.005, respectively). There were no significant differences ($p=0.26$) ascribed to MHP exposure for the case of ADI-37 .

3.3.2 Effects of MHP exposure on the final product spectrum of temperature adapted enrichments

The product spectrum (expressed in mg COD L^{-1}) in the glucose conversion experiments at 5 and 8 MPa using temperature-adapted halotolerant enrichments is presented in Figure 3-4. Measurements were performed at three time points for pressurized incubations and the end-point for AC. Product spectrum in all incubations is consistent with glucose primary fermentation to lactate and secondary fermentation to propionate and acetate. A similar composition was observed during the enrichment at different temperatures (See Appendix). The statistical analysis (Kruskal-Wallis) showed that there were significant differences in lactate ($p=0.001$), as well as propionate and formate concentrations ($p<0.001$) of MSI incubations at the three different temperatures. In addition, significant differences in acetate concentrations were found when MSI incubations were analyzed in function of temperature ($p<0.001$) or applied MHP ($p=0.01$).

Regarding carboxylates production for ADI-37 incubated at different MHPs, significant differences were only found for acetate (p=0.009) and to a lesser degree for propionate (p=0.08). The fraction of initial COD recovered as soluble products is presented in the different subplots as dotted coloured lines. For incubations MSI-10 and MSI-20 at 8 MPa, a notable reduction in the percentage of COD recovered as soluble products was observed compared to the AC (Figure 3-4 A and B). COD recovery was almost identical for all tested conditions in MSI-28 (Figure 3-4 C). Similarly, just a slight decrease in COD recovery was determined for ADI-37 (Figure 3-4 D).

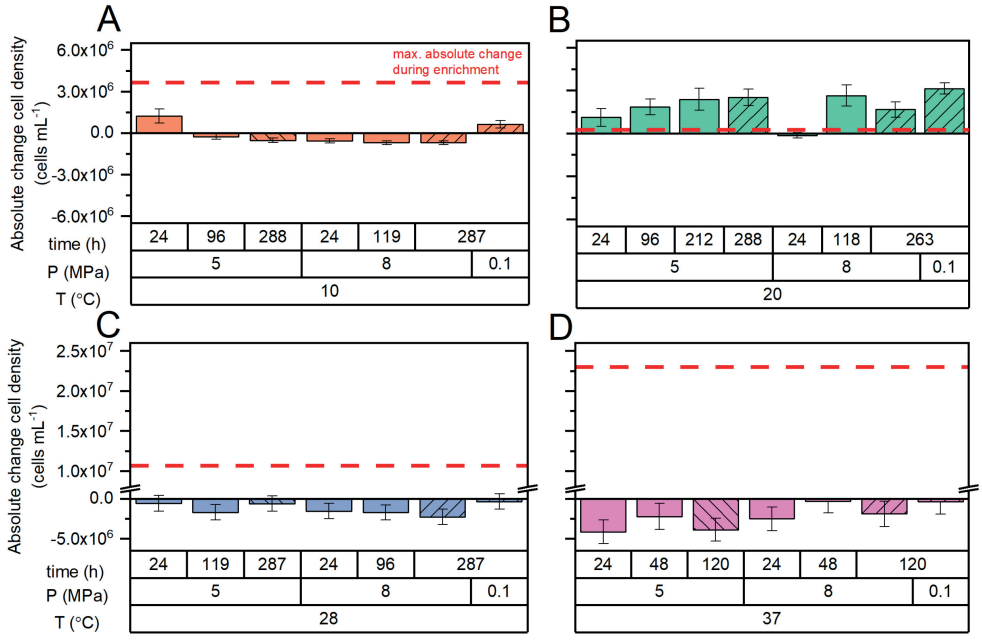

Figure 3-3: Absolute change in the final cell concentration in the marine sediment inoculum (MSI) at 10°C A), 20°C B) and 28°C C) and in the anaerobic digester inoculum (ADI) at 37°C D) along the incubation at MHP of 5 and 8 MPa. The atmospheric control (0.1 MPa) was measured only at the end of the incubation. Bars represent the average of three biological replicates in pressure treatments and six replicates in the atmospheric controls. Bars with stripped pattern differentiate the final time point for each experiment. Error bars correspond to the standard deviation. Dotted red line corresponds to the maximal absolute change in cell density measured during the enrichment before MHP incubation.

3.3.3 Effects at the community level: taxonomic diversity and community structure

The MSI inoculum replicates presented distinctive differences in absolute and relative abundance of the top 13 OTUs (Figure 3-5, Figure 3-6) despite the initial homogenization. Absolute abundances in MHP treatments were impacted by the exposure to 5 and 8 MPa. In MSI-10, the exposure to 5 MPa resulted in a generalized, but statistically non-significant decrease in the average absolute abundance of genera such as *Marinifiilum*, *Dethiosulfatibacter* and *Psychromonas* compared to the AC. The abundance of fermentative bacteria was negatively impacted by MHP of 8 MPa, which led to the predominance of *Trichococcus*. For MSI-20, the exposure to 5 MPa caused a distinct increase in the average absolute abundance of genera *Psychromonas*, *Marinifillum* and a decrease in *Trichococcus* and *Dethiosulfatibacter* (p=0.05). At 8 MPa, the average absolute abundance of identified genera decreased except for *Desulfomicrobium* (Figure 3-5A). In MSI-28, the average absolute abundance of *Trichococcus* (p=0.04) increased after exposure to 5 MPa. However, the absolute abundances of sulfate-reducing bacteria (SRB) genera, namely *Dethiosulfatibacter* and *Desulfomicrobium* (p=0.05) decreased. The exposure to 8 MPa decreased absolute abundances of predominant fermentative genera, excluding *Ilyobacter,* which became the main fermenter (Figure 3-5A). For ADI-37 , average absolute numbers of *Ercell*a, *Proteiniphilum*, *Desulfomicrobium* (p=0.05)*, Halolactibacillus* and *Dethiosulfovibrio* also decreased after exposure to 5 and 8 MPa compared to AC (Figure 3-5B).

Significant differences in MSI richness (H_0, p=0.006) were found in function of incubation temperature rather than MHP (Figure 3-7). Conversely, when analyzed as a function of MHP exposure, H_0 in the ADI experiments was significantly different (p=0.020). In terms of β-diversity, we found significant differences in community structure when incubation temperature was the grouping variable (p=0.001, Figure 3-8 A). However, when grouped by MHP, differences were non-significant (p=0.84, Figure 3-8 B). Additionally, significant differences in community structure were identified as a function of formate (p=0.0136), propionate (p=0.0001) and butyrate (p=0.013) concentrations (Figure 3-9).

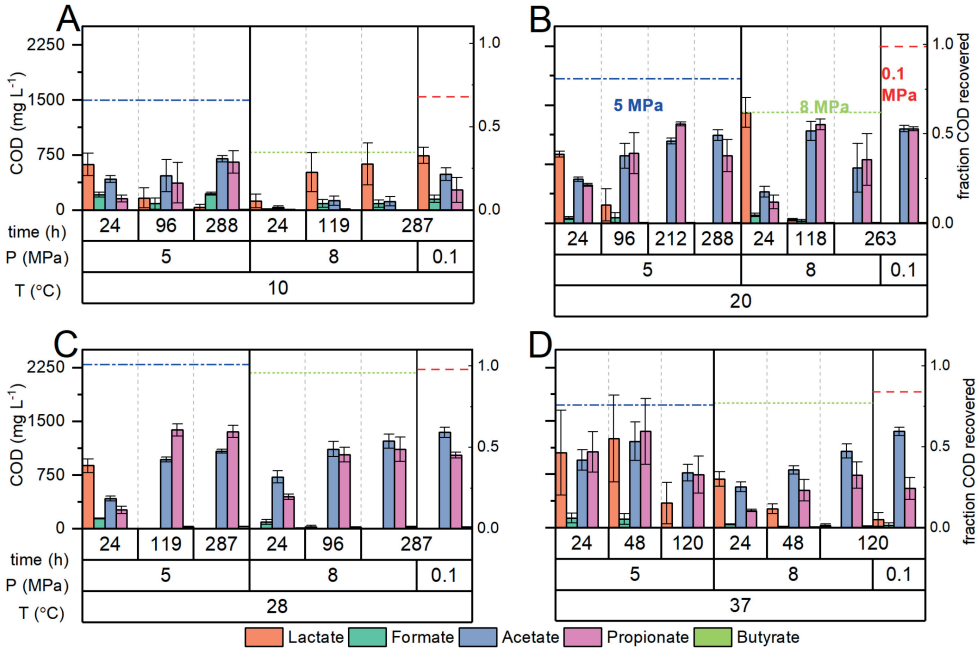

Figure 3-4: Product spectrum (in mg COD L^{-1}) at three selected time points during anaerobic glucose conversion by temperature adapted halotolerant enrichments. The marine sediment inoculum (MSI) was evaluated at 10°C A), 20°C B) and 28°C C) and the anaerobic digester inoculum (ADI) at 37°C D). The pressure of atmospheric controls was 0.1 MPa (included in the subplots as reference) and the hydrostatic pressures were 5 and 8 MPa. Bars represent the average of three biological replicates in pressure treatments and six replicates in the atmospheric controls. Error bars correspond to the standard deviation. Dotted lines represent the average fraction of COD recovered with glucose as feed in the atmospheric controls (red) and in the experiments at 5 MPa (blue) and 8 MPa (green).

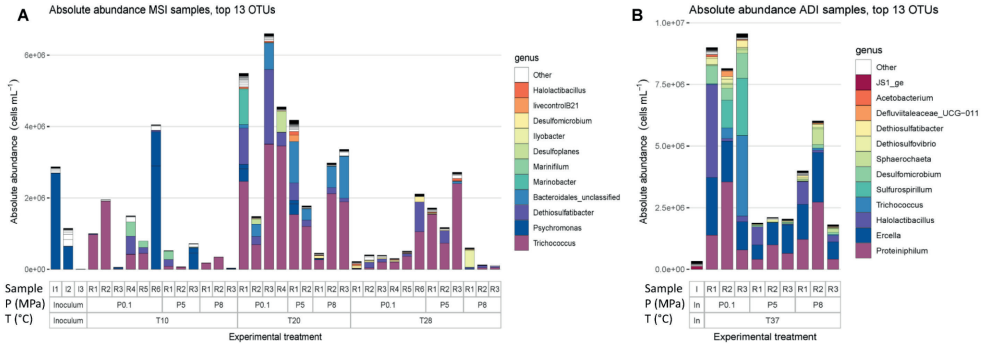

Figure 3-5: Absolute abundances of bacterial top 13 OTUs in the different experimental treatments and calculated based on flow cytometry (FCM) data. Columns represent biological replicates for the atmospheric controls (0.1 MPa) and the mild hydrostatic pressure (MHP) experiments at 5 and 8 MPa. A) Marine sediment inoculum - MSI experiments for different temperatures (10, 20 and 28 C°) - MHP combinations. B) Anaerobic digester inoculum - ADI experiments at 37°C and different MHP.

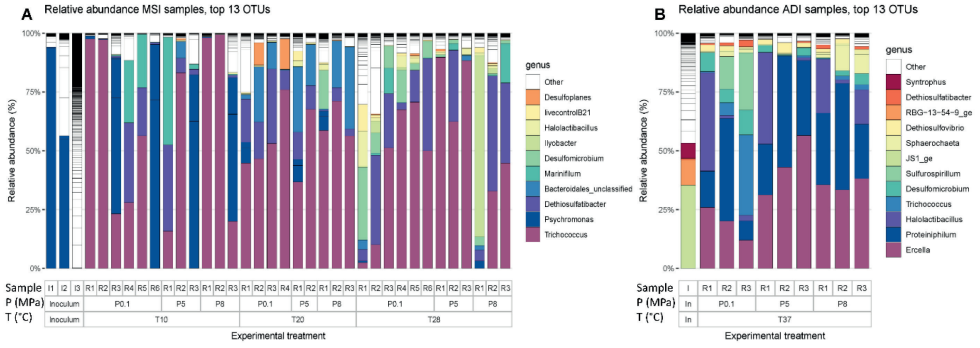

Figure 3-6: Relative abundances of bacterial top 13 OTUs in the different experimental treatments and calculated based on flow cytometry (FCM) data. Columns represent biological replicates for the atmospheric controls (0.1 MPa) and the mild hydrostatic pressure (MHP) experiments at 5 and 8 MPa. A) Marine sediment inoculum - MSI experiments for different temperatures (10, 20 and 28 C°) - MHP combinations. B) Anaerobic digester inoculum - ADI experiments at 37°C and different MHP.

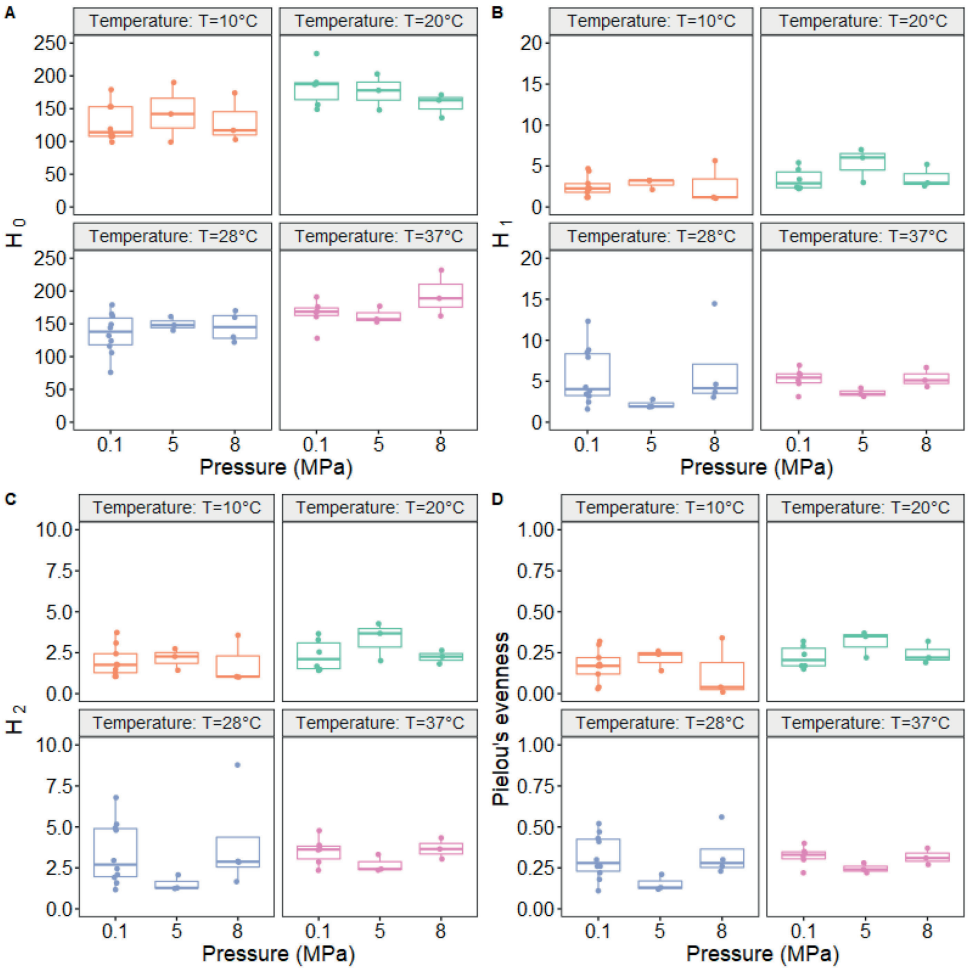

Figure 3-7: Alpha diversity indices for marine sediment inoculum (MSI) at 10, 20 and 28°C and the anaerobic digester inoculum (ADI) at 37°C after exposure to mild hydrostatic pressure (MHP) of 5 and 8 MPa. Atmospheric controls at 0.1 MPa are included as references. A) Richness - H0, B) Exponential of the Shannon diversity index - H1, C) Inverse Simpson index - H2 and D) Pielou's evenness

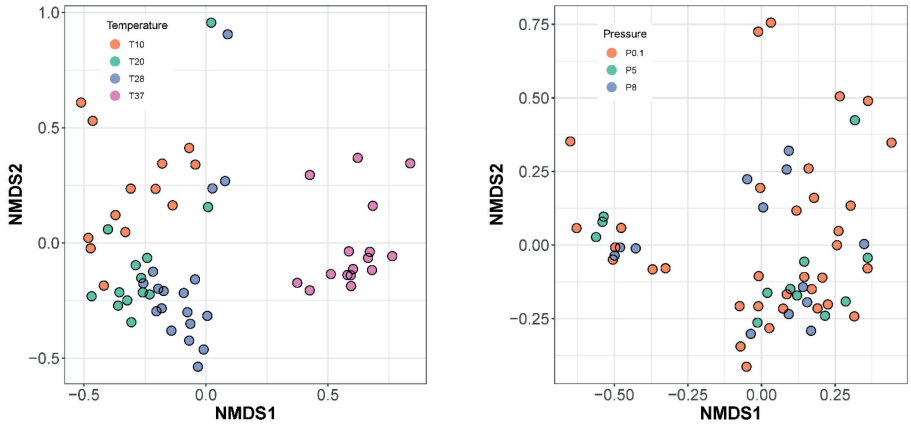

Figure 3-8: Non-metric distance scaling (NMDS) analysis of the Bray-Curtis dissimilarity index of the bacterial community at OTU level for the marine sediment inoculum (MSI) anaerobic digester inoculum (ADI) considering A) Temperature of 10°C, 20°C and 28°C and 37°C as well as B) Hydrostatic pressure of 0.1, 5 and 8 MPa

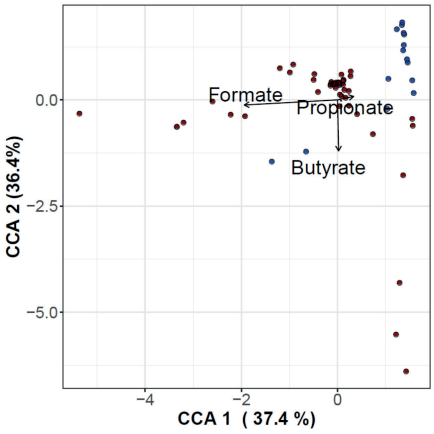

Figure 3-9: Canonical correspondence analysis (CCA) of the bacterial community of the marine sediment inoculum - MSI and the anaerobic digester inoculum - ADI samples at the OTU level. PERMANOVA was carried out to evaluate the relation between the concentrations of lactate, formate, acetate, propionate and butyrate and community composition. Arrows represent significant correlations ($p<0.01$)

3.3.4 Metabolic energy analysis

Figure 3-10A summarizes the ΔG_{cat}^{01} for each incubation condition at MHP and its corresponding AC. The lowest values for ΔG_{cat}^{01} were found for MSI-10 and MSI-20 at 8 MPa. A low ΔG_{cat}^{01} indicates a low ATP yield, considering an energy requirement of +31.8 kJ mol^{-1} ATP based on the hydrolysis of acetyl coenzyme-A (Thauer et al., 1977). $Y_{X/S}$ showed a decreasing trend with increasing MHP (Figure 3-10 D), particularly for MSI-10 and MSI-20. Notably, only for MSI-10 at 8 MPa, the calculated *m* was higher than the value for AC (Figure 3-10 B).

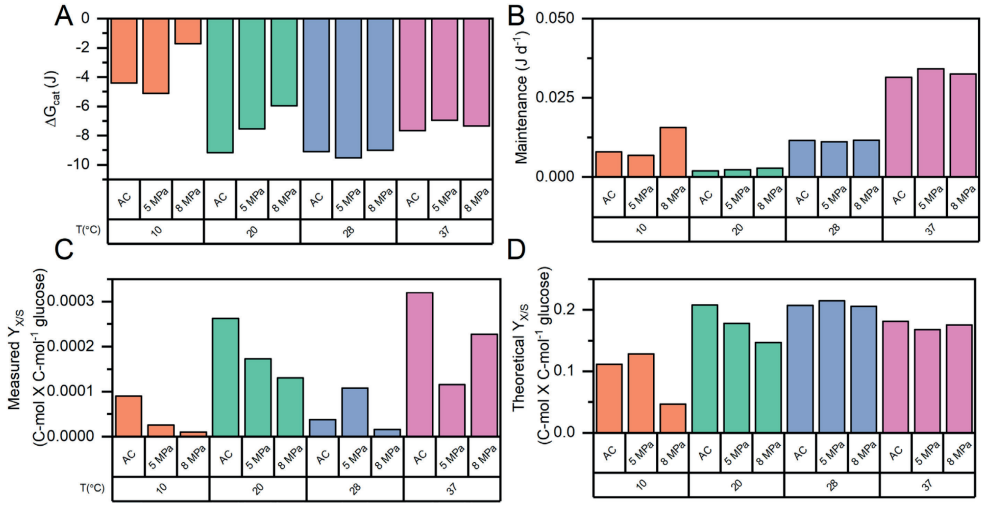

Figure 3-10: A) Gibbs free energy available to carry out catabolism (ΔG_{cat}^{01}) for each temperature incubation at 0.1 MPa (atmospheric control – AC) and mild hydrostatic pressure (MHP) of 5 and 8 MPa. B) Gibbs free energy requirements for maintenance (*m*) to sustain the initial biomass density used to inoculate AC and the pressurized treatments. C) Measured biomass yield ($Y_{X/S}$) based on cell numbers converted to units of C-mol biomass. D) Theoretical biomass yield calculated based on proposed stoichiometries for the different incubations. Each subplot has a different scale and units for visualization purposes. Data correspond to the marine sediment inoculum (MSI) at 10, 20 and 28°C and the anaerobic digester inoculum (ADI) at 37°C.

Slight differences were observed in ΔG_{cat}^{01}, *m* and $Y_{X/S}$ for incubations MSI-28 and ADI-37 at 5 and 8 MPa in reference to the AC (Figure 3-10). However, following their dependency on temperature, calculated values for maintenance coefficients (m_G) were 6.0 and 13.4 kJ mol^{-1} X

h^{-1} at 28 and 37°C, respectively. At low (10°C) and moderate (20°C) temperatures, m_G decreased to 1.0 and 2.8 kJ C-mol^{-1} X h^{-1}, respectively. Despite these differences, calculations showed that maintaining initial cell density in all treatments for the entire experiment duration would have required less than 3% of the initially available glucose biochemical energy.

Results showed differences of three orders of magnitude in the theoretical $Y_{X/S}$ and those estimated from the conversion of cell numbers to C-mol biomass (Figure 3-10 C and D). This large discrepancy is attributed to using theoretical approximations for cell volume that might not reflect HP effects on cell morphology (Molina-Höppner et al., 2003). Thus, the theoretical and estimated $Y_{X/S}$ values are not directly comparable but provide insight into the effects of temperature, the composition of the product spectrum, and MHP on $Y_{X/S}$.

3.4 Discussion

3.4.1 Biomass yield and fermentative activity are modulated by interaction effects of incubation temperature and MHP

MSI-20 was the only condition where growth, expressed as a positive absolute change in cell density, occurred after MHP incubation (Figure 3-3). Therefore, we hypothesized that observed growth in MSI-20 at MHP could be attributed to a cross-resistance effect originating from adaptation to moderate temperature and salinity. This hypothesis aligns with a previously reported analogous stress response to low temperature and HP (Abe, 2007). However, this cross-resistance effect positively impacting cell densities was not evident in conditions MSI-10, MSI-28 and ADI-37 at 5 and 8 MPa.

In MSI-10 the incubation temperature was lower than the presumed optimum for psychrotolerant growth ($T_{opt} \approx 20$°C); thus, declining growth rates (μ) were expected following the Arrhenius equation (Infantes et al., 2012). Literature has revisited the relationship between μ, maintenance (m) and $Y_{X/S}$, indicating that it is more complex than suggested by previous models ("Herbert model", "Pirt model") (Wang and Post, 2012) and dependent on growth conditions (Bonk et al., 2019; Lipson, 2015). In slow-growing microorganisms, *e.g.,* psychrotolerant/psychrophilic microorganisms, a "growth rate-yield tradeoff" has been observed at T< T_{opt}, leading to high $Y_{X/S}$ at low temperatures (Nedwell and Rutter, 1994). Holding onto this premise, an increase in cell density in MSI-10 could have been anticipated. However, the lowest ΔG_{cat}^{01} values were calculated for MSI-10 (Figure 3-10A); thus, limited growth might have resulted from energetic constraints. Furthermore, if protective mechanisms linked to low temperature and piezotolerance were upregulated, such as synthesis of cold shock proteins and extracellular polymeric substances (EPS), it would have come at a high energy

cost, further limiting growth: 0.39 mmol ATP/ g protein and 12.8 mmol ATP/ g polysaccharide (Kim and Gadd, 2008). Thus, considering that some energy is also dissipated during anabolism, the generated catabolic energy may only have sufficed to produce cryoprotective structures such as EPS, but not for synthesis of complex cellular components enabling growth (Nichols et al., 2005).

The hypothesis concerning EPS production aligns well with some investigations in marine microorganisms (Decho and Gutierrez, 2017). EPS synthesis is considered a survival strategy to counteract low temperatures and/ or saline conditions (Aslam et al., 2012). Previous work indicates that at high glucose concentrations (Decho, 1990), increased salinity, low/ moderate temperatures (15-25°C), and fluctuating nutrient availability, bacterial EPS production is favoured (Degeest et al., 2001). Also, enhanced EPS production has been observed at temperatures lower than T_{opt} in both psychrophilic (Nichols et al., 2005) and mesophilic organisms (Degeest et al., 2001). EPS formation cannot be discarded in all the other treatments, since visual inspection of the bottom of the syringes after reactor depressurization indicated biomass agglomeration. However, it is recommended to follow up our current work with future HP fermentation experiments, using larger sample volumes that enable an in-depth quantification of EPS concentrations.

In terms of fermentative activity, in MSI-10 and MSI-20 incubations at 5 and 8 MPa, differences were observed regarding the COD recovered as measured soluble products compared to their respective AC (Figure 3-4, A and B). These differences might be partially explained due to the effect of incubation temperature on process kinetics exacerbated as MHP increased. According to the Arrhenius equation, decreasing temperatures exponentially decrease biochemical reaction rates and may compromise enzymatically driven processes (Arnosti et al., 1998). Similar to temperature, also pressure has an exponential relation to the reaction rate constant, in co-dependence of the reaction activation volume according to Equation (3-1) (Morild, 1981; Somero, 1990):

$$k_p = k_0 e^{\frac{-P\Delta V^{\neq}}{RT}}, \tag{3-1}$$

where k_p (h^{-1}) is the rate constant at pressure P (atm), k_0 is the rate constant at atmospheric pressure (h^{-1}), $\Delta V^{\neq}$ is the activation volume, R the universal gas constant (L atm K^{-1} mol^{-1}) and T the reaction temperature (K). From Equation (3-1) follows that HP decreases the rate of reactions with positive $\Delta V^{\neq}$. Glycolytic enzymes such as glyceraldehyde-phosphate-dehydrogenase ($\Delta V^{\neq}$= +60 cm^3 mol^{-1}), pyruvate kinase ($\Delta V^{\neq}$= +11 to +26 cm^3 mol^{-1}) have positive $\Delta V^{\neq}$; thus, their activity could be compromised by MHP regardless of low-temperature adaptations (Morild, 1981). Consequently, they could become a bottleneck for glucose

conversion at low temperatures and MHP, explaining the dissimilarities in the recovered COD between MHP treatments and AC in MSI-10 and MSI-20.

We were not able to collect sufficient data points for adequate calculation of production and consumption rates due to sampling constraints associated with the reactor configuration. However, evaluation of the individual metabolite concentration per cell over time pinpointed a "slowing down" of intermediates consumption. As an example, reduced lactate consumption in MSI-10 at 8 MPa is noticeable and could have hindered subsequent fermentation (Figure 3-12). This observation is in alignment with previous enzymatic studies, which suggested that HP and low temperatures significantly decrease lactate dehydrogenase activity, an enzyme that reversibly catalyzes pyruvate to lactate conversion (Gillen, 1971).

	MSI			ADI	MHP (MPa)	MSI			ADI
	10	20	28	37		10	20	28	37
Parameter	T(°C)					T(°C) + MHP (MPa)			
Predicted Growth temperature	$T<T_{opt}$	$T\approx T_{opt}$	$T>T_{opt}$	$T\approx T_{opt}$					
μ (h^{-1})					↓				
q_s (C-mol S/ C-mol X/ h)					↑				
Yield $Y_{X/S}$ (C-mol X / C-mol S)					↓				
Manteinance m_D (C-mol S/ C-mol X/ h)					↑				
Decay (k_d) (day^{-1})					↑				
ΔG_{cat} (kJ/mol S)					depends on the rxn activation volume				

Figure 3-11: Graphical summary of foreseen effects of incubation temperature (T) (left) and T + mild hydrostatic pressure (MHP) (right) on kinetic and bioenergetic parameters. Columns correspond to the experimental treatments with marine sediment inoculum (MSI) at 10, 20 and 28°C and anaerobic digester inoculum (ADI) at 37°C. Coloured blue bars represent a qualitative indication of the expected range for the parameter (one=low, two=moderate, three=high, four=highest). Upward green arrows in MHP column indicate an incremental effect, whereas downward red arrows indicate a detrimental effect.

Another limitation on substrate and intermediates conversion at low temperatures, *e.g.,* in MSI-10, might have come from energy requirements in transmembrane transport. Rodriguez et al. (2006) proposed that more energy is required for the active transport of organic acids when extracellular concentrations increase, as foreseen in batch fermentations (Table 3-4). Additionally, since increased pressure enhances acid dissociation due to negative $\Delta V^{\ddagger}$ (Low

and Somero, 1975), more energy would have been required for proton (H^+) transport to keep homeostasis, further limiting energy allocation to anabolic processes.

The combined effect of moderately high temperature and MHP was detrimental for biomass yield in MSI-28 and ADI-37 incubations at 5 and 8 MPa (Figure 3-3, B and C); however, it did not severely compromise carboxylates production (Figure 3-4, C and D). Hence, our experimental observations suggest that limited growth with conserved metabolic activity resulted from an increased susceptibility to MHP due to prolonged exposure to moderately high temperatures. Studies with pure cultures of psychrotolerant *Listeria monocytogenes* and *Yarrowia lipolytica* incubated at high HP have shown that increasing incubation temperature coincided with intensified pressure susceptibility and ultimately reflected in higher microbial inactivation (death) rates (Lanciotti et al., 1996). This observation aligns well with the cell density results of incubations MSI-28 (compared to MSI-20 and MSI-10) and ADI-37 (Figure 3-3). The same study reported that inactivation of mesophilic *E. coli* was comparable to psychrotolerant strains at 20°C but showed an increasing trend in the interval 20-35°C (Lanciotti et al., 1996). Consequently, literature suggests a relatively strong effect of MHP on $Y_{X/S}$ for mesophilic microorganisms, which may explain the observed high negative absolute change in cell density in ADI-37 (Figure 3-3D).

It is known that microbial μ exponentially increases with temperature within a certain span. For psychrotolerant microorganisms, temperatures higher than T_{opt} (T>20°C *e.g.,* MSI-28) are associated with a decreasing μ (Bakermans and Nealson, 2004; Kaye and Baross, 2004; Knoblauch and Jorgensen, 1999). Consequently, an increased $Y_{X/S}$ could have been foreseen on the grounds of the "growth rate-yield trade-off" theory. However, prolonged exposure to moderate high temperatures resulted in increased substrate turnover to fulfill the higher maintenance (*m*) requirements due to a) the Arrhenius dependency of *m* on temperature (Figure 3-10B) and b) the proposed increased susceptibility to MHP after prolonged exposure to moderate high temperature. Hence, despite more favourable bioenergetics in MSI-28 than in MSI-20 and MSI-10 (Figure 3-10A), energy was deviated from growth ($Y_{X/S}$) to satisfy increasing *m* requirements. Moreover, low-temperature stress response shares commonalities with the one triggered by MHP attributable to similar effects at the cell membrane level (Allen and Bartlett, 2000). Hence, it is reasonable to suspect that relevant enzymatic machinery already in place was upregulated in microorganisms from MSI-10 and MSI-20 incubations, implying that a smaller fraction of the energy budget was allocated for *m* (Figure 3-10). Pressure and temperature fluctuation responses are not entirely equal; thus, particular mechanisms triggered by MHP could have still occurred. For example, the synthesis of heat shock proteins (Welch et al., 1993) is likely to occur in psychrotolerant organisms at temperatures from 28°C onwards (Potier et al., 1990), implying energy deviation for other anabolic processes than growth in MSI-28.

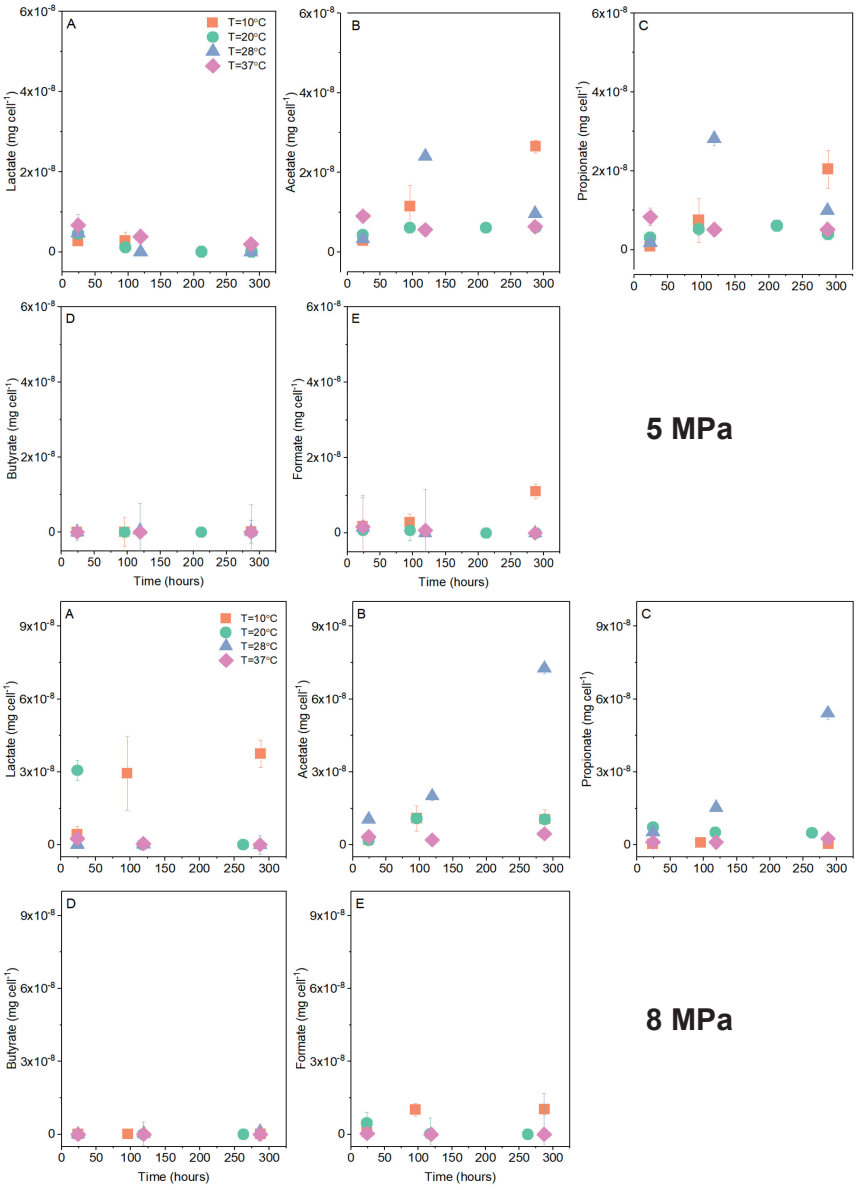

Figure 3-12: VFA and organic acids per cell calculated for the experiment of anaerobic glucose conversion at mild hydrostatic pressure (MHP) of 5 and 8 MPa. Data represent measured concentrations, on a per-cell basis for the marine sediment inoculum (MSI) at 10, 20 and 28°C and for the anaerobic digester inoculum (ADI) at 37°C.

The exclusively temperature-dependent *m* calculations presented here should be used as a first approximation since only the major and not all carbon and energy-deriving processes have been considered. If proton leakage, cell death, intracellular carbon storage, membrane fluidity conservation and pathway shifts (van Bodegom, 2007) would have been included, higher overall maintenance (m_{tot}) and a further constrained μ and $Y_{X/S}$ would have been obtained. These requirements constitute part of the initial halotolerance and a postulated temperature-MHP adaptation. Hence, carbon and energy derivation towards *m* likely have occurred under all experimental conditions (Schimel et al., 2015) but may have been overlooked due to process complexity and methodological simplifications.

A higher μ was expected for ADI-37 since it was incubated at T≈T_{opt} (Figure 3-11) and due to differences in the order of magnitude of mesophilic and psychrotolerant μ in microorganisms grown under laboratory conditions (Nedwell and Rutter, 1994). A higher decay rate (k_d) and *m* requirements (Figure 3-10B) were anticipated for this treatment due to temperature dependence of k_d, *m* and μ (Biselli et al., 2020); thus, a lower μ_{net} ascribed to temperature effects in ADI-37 when compared to MSI-28 could be reasonably expected. Moreover, in ADI-37 additional stress response mechanisms needed to be fully upregulated to counteract MHP effects on susceptible biomass resulting from prolonged exposure to moderate high temperature. Moreover, prolonged incubation could have triggered the utilization of biomass to satisfy increasing m_{tot} requirements when carbon was less available (Bradley et al., 2018). If unsaturated lipids would have been produced to safeguard membrane fluidity, it would have come at the price of diverting energy from growth to maintenance (Casadei et al., 2002; Kaneko et al., 2000). Lipid synthesis is a less energy-intensive process (0.015 mmol ATP/ g lipid) (Kim and Gadd, 2008) in comparison to the synthesis of proteins and carbohydrates, which could also have been part of the general microbial stress response in ADI-37 (Gross and Watson, 1996).

Table 3-4: Gibbs energy change for active transport of acid molecule (HA) through the cell membrane $\Delta G_{Tr\text{-}HA}$ (kJ $mmol^{-1}$) for different organic acids measured in the glucose experiments at mild hydrostatic pressure (MHP) using marine sediment inoculum – MSI and anaerobic digester inoculum – ADI at different temperatures

	Extracellular concentration (mM)	Intracellular concentration (mM)[a]	$\Delta G_{Tr\text{-}HA}$ (10°C)	$\Delta G_{Tr\text{-}HA}$ (20°C)	$\Delta G_{Tr\text{-}HA}$ (28°C)	$\Delta G_{Tr\text{-}HA}$ (37°C)
Lactic acid	15.11	10	2.74	2.78	2.86	2.95
		5	19.34	19.68	20.22	20.82
Propionic acid	18.9	10	15.38	15.64	16.07	16.55
		5	31.98	32.54	33.42	34.42
Acetic acid	24.20	10	9.57	9.74	10.00	10.30
		5	26.18	26.63	27.36	28.17

[a] Intracellular concentration taken from Rodriguez et al. (2006)

3.4.2 Product spectrum is defined by inoculum enrichment strategy and minorly impacted by the interaction temperature - MHP

Our results showed that the enrichment strategy predominantly impacted the product spectrum (See Appendix), while both incubation temperature and MHP played a minor and indirect role (Figure 3-4). High substrate concentration, high biomass load, complex medium, and sequencing batch incubations can be considered the process parameters with the most substantial influence on the product spectrum. Rombouts et al. (2020) and Hoelzle et al. (2021) have proposed that complex medium and high glucose concentrations favour lactate production over butyrate, propionate and acetate, which are typically observed in mixed culture conversions at low substrate concentration and even occurring at elevated operational pressure (Ceron-Chafla et al., 2021).

We did not observe significant differences in the product spectrum of the different incubations due to MHP. However, other studies highlighted deviations in product formation after the exposure to higher HP (30-35 MPa) and associated this phenomenon with changes in the central carbon metabolism (Booker et al., 2019; Scoma et al., 2019). Their results showed that propionate and butyrate were formed to dispose of reducing equivalents under limited hydrogen production. A declined hydrogen production is expected when the lactate pathway is favoured (Ghimire et al., 2015) and could also result from the hindered hydrogenase activity by elevated HP (Booker et al., 2019). Consequently, the favoured disposal of reducing equivalents in the form of propionate/ butyrate and formate production to act as "aqueous electron carrier" are reasonable outputs of MHP incubations. However, formate production is not an exclusive outcome of combined incubation temperature and MHP. Previous studies reported formate as an alternative electron sink to H_2 in, *e.g.,* glucose conversion carried out at pH > 6 (Temudo et al., 2007) and during shock loads of substrate at circumneutral pH (Voolapalli and Stuckey, 1999). Moreover, formate production may also be a characteristic fermentation pathway in organisms from temperate marine sediments, as postulated by previous work (Kondo et al., 1993).

3.4.3 Understanding the interaction effects of MHP and temperature on microbial community composition

The taxonomic diversity changed in response to substrate concentration and incubation temperature after the enrichment (See Appendix). Due to insufficient homogenization in the MSI samples, replicate 3 was different in composition and abundance from the other inoculum replicates. These differences in composition remained observable in the experiments at mild selective pressure, *i.e.,* low temperature and MHP (Figure 3-5). Under an apparently stronger

"selective pressure", *i.e.,* moderate-high temperature and MHP, the inoculum variability effect was no longer observed and changes in absolute abundance due to temperature and MHP became more evident and reproducible as in other studies dealing with environmental disturbance effects in community structure (Pagaling et al., 2014). After MHP-exposure, specific genera lost their predominance or became absent, but fermentative activity was conserved. At 10 and 20°C in MSI, a minor decrease in absolute abundance was identified in groups with recognized fermenting metabolism such as *Marinifilum*, *Psychromonas*, *Halilactibacillus* and *Trichococcus* after MHP was applied. This was also the case for some of the identified SRB, *i.e., Dethiosulfatibacter and Desulfomicrobium* (Figure 3-5A). Piezotolerant/ piezophilic strains were previously identified in coastal marine sediments with no apparent exposure to significant pressure gradients (Marietou and Bartlett, 2014; Tamburini et al., 2009b). Most of those microorganisms additionally have a psychrotolerant nature with T_{opt} between 10-20°C (Fu et al., 2018; Xu et al., 2003), supporting the previously described link between low/moderate temperature adaptation and pressure resistance.

In MSI-28, general multitrophic microorganisms belonging to the genera *Trichococcus* and *Ilyobacter,* as well as *Proteiniphilum* and *Ercella*, in ADI-37 showed some degree of tolerance to MHP (Figure 3-5, A and B). So far, proven piezotolerance in these genera has not been reported. Nonetheless, piezotolerant/piezophilic strains in marine sediments (Bhattarai et al., 2018; Fasca et al., 2018; Wannicke et al., 2015) and high-pressure anaerobic digesters (Lindeboom et al., 2016) belong to the phyla Firmicutes and Bacteroidetes, which comprise the genera mentioned above. Innate adaptations in these species might allow a certain degree of piezotolerance. Microorganisms from the genus *Trichococcus* (Pikuta and Hoover, 2014) and *Ilyobacter* (Schink, 1984) produce mucopolysaccharides for adaptation to low temperatures, which might confer adaptability to more extreme conditions such as MHP (Yin et al., 2019). An increase in the proportion of unsaturated fatty acids (UFAs) is a mechanism to safeguard membrane fluidity via homeo-viscous adaptation (Wang et al., 2014). Members of the genus *Ercella* (van Gelder et al., 2014) and *Proteiniphillum* (Wang et al., 2014) are characterized by a high content of UFAs and ante-iso-branched fatty acids in their cell membranes. This innate feature could counteract the reduced fluidity caused by increased MHP.

3.4.4 Extrapolation of cross-resistance effects towards the process level

The use of stress conditions such as MHP to promote new products synthesis and bioprocess selectivity, while limiting biomass growth, has gained interest in latest years (Mota et al., 2017). However, microbial resilience is still a bottleneck in operation under environmental stressors such as MHP (Lopes et al., 2019). Inoculum history, thermal adaptation and halotolerance could promote cross-resistance effects, which can be further exploited depending

on desired process outcome. In yield-dependent processes, *e.g.,* biopolymer production, whose properties seem interestingly modified by MHP, operation at mild temperature could be advisable to obtain a balanced biomass-product output. If the microbial community is already temperature-adapted, the predominance of product-accumulating organisms should not be compromised by MHP exposure. On the other hand, if excess biomass growth needs to be controlled, operation at MHP in combination with increased temperature, high organic loading rate, and rich medium could promote uncoupling of catabolism and anabolism. As indicated by our experimental results, this could occur without the abundance of key genera being jeopardized.

3.5 Conclusions

Effects of an environmental stressor (MHP) on metabolic activity and community structure could be modulated by cross-resistance effects associated with incubation temperature and halotolerance. At mild temperatures, an apparent cross-resistance effect balanced growth and fermentation under MHP. At low temperatures and MHP, compromised growth and carboxylates production resulted from bioenergetic and kinetic constraints. High temperature positively impacted carboxylates production and combined with MHP, further limited biomass yield due to high maintenance requirements and decay. Fermentative activity was conserved despite absolute abundances of predominant groups in MSI, being compromised by temperature and, to a minor extent, MHP. Community composition in mesophilic ADI also underwent slight modifications after MHP exposure. We anticipate that fermentation resilience to environmental stress relies on understanding how cross-resistance effects at the physiological level could influence microbial community composition and, ultimately, process yield.

Appendix: Enrichment of halotolerant mixed microbial culture: product spectrum and microbial community dynamics

After the final cycle of enrichment, inocula MSI and ADI showed differences in the final product spectrum, cell numbers and community diversity. Regarding the measured metabolites as soluble COD, MSI-28 showed a balanced production: 54% of the soluble COD corresponded to acetate and 45% to propionate. In MSI-20, there was a marginal increase in propionate production compared to acetate: 53 vs 47%. For MSI-10, the product spectrum was composed of acetate, formate and lactate: 45, 29 and 14%, respectively. ADI-37 showed a product spectrum also dominated by acetate and propionate: 56 vs 41%, respectively. The achieved cell density at the end of the enrichment is presented in Figure 3-13.

Changes were observed in the predominant OTUs identified in MSI and ADI samples after the enrichment at atmospheric conditions. *Psychromonas* was replaced as the main fermentative genus in the original MSI sample by *Marinifilum, Psychromonas, Halolactibacillus, Trichococcus* at 10, 20 and 28°C and *Ilyobacter,* only at 28°C. Two genera associated with SRB, namely *Dethiosulfatibacter* and *Desulfomicrobium,* were further identified. In the case of ADI, the transition occurred from genera such as JS1 and RBG-13-54-9 to fermentative halotolerant, neutrophilic bacteria such as *Proteiniphillium, Ercella, Halolactibacillus* and the SRB *Dethiosulfovibrio* and *Desulfomicrobium*.

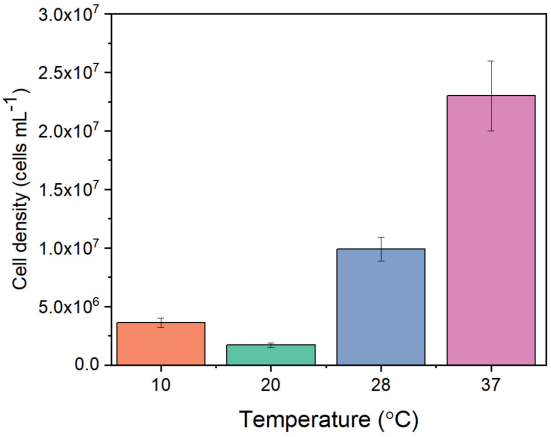

Figure 3-13: Cell density measured by flow cytometry (FCM) at the end of the first cycle of the enrichment for the marine sediment inoculum (MSI) at incubation temperatures of 10°C, 20°C and 28°C and the anaerobic digester inoculum (ADI) at 37°C.

4

CHAPTER 4

DIRECTIONAL SELECTION OF MICROBIAL COMMUNITY IN MIXED CULTURE FERMENTATIONS UNDER ELEVATED pCO_2

This chapter is an adapted version of:

Ceron-Chafla, P., Chang, Y., Rabaey, K., van Lier, J. B., & Lindeboom, R. E. F. (2021). Directional Selection of Microbial Community Reduces Propionate Accumulation in Glycerol and Glucose Anaerobic Bioconversion Under Elevated pCO_2. Frontiers in Microbiology, 12(June), 1583. https://doi.org/10.3389/fmicb.2021.675763

Abstract

Volatile fatty acid (VFA) accumulation is a sign of digester perturbation. Previous work showed the thermodynamic limitations of hydrogen and CO_2 in syntrophic propionate oxidation under elevated partial pressure of CO_2 (pCO_2). Here we study the effect of directional selection under increasing substrate load as a strategy to restructure the microbial community and induce cross-resistance mechanisms to improve glucose and glycerol conversion performance under elevated pCO_2. After an adaptive laboratory evolution (ALE) process, viable cell density increased and predominant microbial groups were modified: an increase in *Methanosaeta* and syntrophic propionate oxidizing bacteria (SPOB) associated with the *Smithella* genus was found with glycerol as the substrate. A modest increase in SPOB along with a shift in the predominance of *Methanobacterium* towards *Methanosaeta* was observed with glucose as the substrate. The evolved inoculum showed affected diversity within archaeal spp. under 5 bar initial pCO_2; however, higher CH_4 yield resulted from enhanced propionate conversion linked to the community shifts and biomass adaptation during the ALE process. Moreover, the evolved inoculum attained increased cell viability with glucose and a marginal decrease with glycerol as the substrate. Results showed differences in terms of carbon flux distribution using the evolved inoculum under elevated pCO_2: glucose conversion resulted in a higher cell density and viability, whereas glycerol conversion led to higher propionate production, whose enabled conversion reflected in increased CH_4 yield. Our results highlight that limited propionate conversion at elevated pCO_2 resulted from decreased cell viability and low abundance of syntrophic partners. This limitation can be mitigated by promoting alternative and more resilient SPOB and building up biomass adaptation to environmental conditions via directional selection of microbial community.

Keywords

High-pressure anaerobic digestion, Elevated CO_2 partial pressure, Syntrophic propionate oxidation, *Smithella*, Adaptive laboratory evolution.

4.1 Introduction

In this work, we applied a directional selection process based on increasing substrate load to restructure the microbial community and activate cross-protection mechanisms to enhance the anaerobic conversion of glucose and glycerol under elevated pCO_2. As a negative control, we investigated the effect of elevated pCO_2 on the original inoculum. We expected differences in the product spectrum as a result of the dissimilar substrate oxidation state and increased pCO_2 favoring propionate production. Nonetheless, further propionate oxidation (Pr-Ox) would be limited due to thermodynamic constraints on syntrophic Pr-Ox in relation to interspecies hydrogen transfer (Stams et al., 1998). Further constraints will be established due to the negative effects of elevated pCO_2 on cell viability and relative abundance of methanogens and syntrophic propionate oxidation bacteria (SPOB) in the original inoculum. The evolved inoculum would feature enhanced cell viability, a higher proportion of fermenters and more resilient SPOB and methanogenic groups. These factors could help to circumvent thermodynamic and performance limitations present in the original inoculum, thereby enabling propionate conversion under elevated pCO_2.

4.2 Materials and Methods

4.2.1 Inoculum

Flocculent anaerobic sludge from an anaerobic membrane bioreactor (AnMBR) treating wastewater from a chocolate and pet food industry was used as the starting inoculum. Measured physicochemical parameters are presented in Table 4-1.

4.2.2 Reactor set-up and operation

Batch experiments with original inoculum were conducted at four different pCO_2, namely 0.3, 3, 5, 8 bar initial pressures. Schott bottles with a working volume of 250 mL, air-tight sealed with rubber stoppers were used for the experiments at atmospheric conditions, *i.e.,* 0.3 bar pCO_2. The employed gas to liquid ratio was 2:3. Stainless steel reactors working in a pressure range of 1 - 600 bar (Nantong Vasia, China) were used for the experiments at moderately elevated pressure, *i.e.,* 3, 5 and 8 bar. These reactors are fitted with gas and liquid sampling ports in the head, as well as a glycerin manometer. The working liquid volume, in this case, was 120 mL, and the same gas to liquid ratio as before was kept. Reactors were inoculated with 2 g VSS L^{-1}. The liquid medium added to each reactor contained 1 g glucose or glycerol as COD L^{-1}, macronutrients, micronutrients, both prepared according to García Rea et al. (2020)

and buffer solution (100 mM as HCO_3^-). The initial pH of all the reactors was not adjusted and values were in the range 7.5 – 8.0.

Table 4-1: Physicochemical characterization of the original anaerobic inoculum used for the experiments of glucose and glycerol conversion under elevated pCO_2 and evolved inoculum after adaptive laboratory evolution (ALE) using glucose and glycerol (1 g COD L^{-1}) at T= 35˚C, initial pCO_2= 0.3 bar and pH in the range 7.5-8.0

Parameter	Unit	Original inoculum Mean ± SD (n=3)	Glucose-evolved inoculum Mean ± SD (n=3)	Glycerol-evolved inoculum Mean ± SD (n=3)
TCOD	mg L^{-1}	22 200 ± 1000	3 500 ± 550	6 800 ± 650
SCOD	mg L^{-1}	1 900 ± 400	678 ± 65	162 ± 4
TOC	mg L^{-1}	7 700 ± 800	681 ± 6	705 ± 3
TSS	g L^{-1}	15.9 ± 0.5	3.5± 0.1	6.0 ± 0.1
VSS	g L^{-1}	13.6 ± 0.1	2.9 ± 0.3	4.9 ± 0.1
VSS/TSS	%	86	81	82
NH_4-N	mg L^{-1}	107 ± 2	269 ± 22	281 ± 7
TP	mg L^{-1}	112 ± 1	17 ± 2	28 ± 1
pH	-	7.3	7.2	7.2

After filling and closure, atmospheric reactors were flushed for two minutes with 100% N_2 and sequentially with N_2: CO_2, 70:30%. Pressure reactors were initially flushed with the same gas mixture as the atmospheric reactors and afterwards, consecutive pressurization-release cycles with >99% CO_2 were applied to ensure initial headspace composition. Reactors were operated for approximately 10 days, kept at 35°C and continuously shaken at 110 rpm. All the experimental treatments were conducted in triplicates. Pressurized controls with only nitrogen in the headspace were additionally included. To diminish sampling interference during the experiment, we applied the same sampling strategy as previously described (Ceron-Chafla et al., 2020). A graphical description of the experimental design is presented in Figure 4-1.

4.2.3 Directional selection of microbial community via adaptive laboratory evolution (ALE) with increased glucose and glycerol load

The total length of the atmospheric ALE process was 61 days, divided into four cycles with duration as follows: the two first cycles lasted seven days, which corresponded to complete substrate conversion for initial atmospheric experiments at 0.3 bar pCO_2. However, due to the limited growth and conversion of intermediates identified after the second cycle, it was decided to perform the third and fourth cycles at 0.3 bar pCO_2 for 21 and 26 days, respectively, to achieve complete conversion. Schott bottles with a working volume of 2000 mL were used for

the ALE incubation. After every cycle, 240 mL were removed, replaced by fresh medium and the bottles were flushed with N_2: CO_2, 70:30%. The substrate concentration in the medium refreshing solution was fixed for all the cycles at 1 g COD L^{-1} glucose or glycerol. It should be noted that owing to the serial dilution procedure, biomass was exposed to a deliberately increased substrate load per cycle. The evolved inoculum was harvested after the fourth cycle, employing low-speed centrifugation and resuspension with macro and micronutrient solution. After this, the obtained biomass was characterized in terms of physicochemical parameters (Table 4-1) and used to inoculate pressure reactors at 5 bar pCO_2 and controls at 5 bar pN_2 to evaluate anaerobic conversion performance of evolved microbial biomass at a higher Food to Mass ratio (F:M ratio) (phase 3 Figure 4-1). The pressurized experiments with evolved inoculum lasted approximately 10 days.

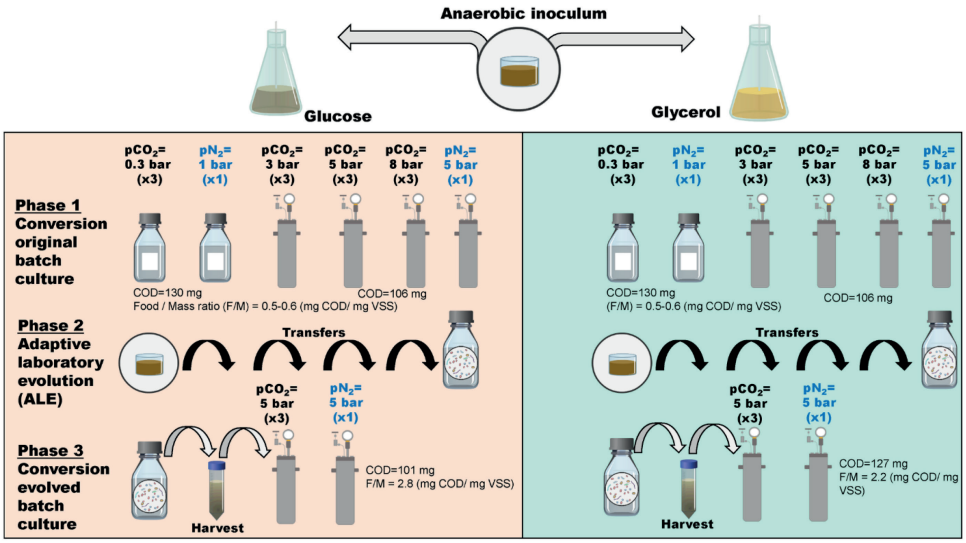

Figure 4-1: Graphical summary of experimental conditions for the anaerobic conversion experiments at elevated pCO_2 using glucose and glycerol as substrates. Experiments are organized according to substrate and inoculum conditions.

4.2.4 Microbial community analysis

Biomass samples stored at -80°C from the endpoint of the batch experiments were used to evaluate Microbial community dynamics. After thawing, DNA was extracted according to the instructions included in the DNeasy UltraClean Microbial Kit (Qiagen, Germany). The quality and quantity of the obtained DNA were checked through Qubit 3.0 DNA detection (Qubit®

dsDNA HS Assay Kit, Life Technologies, U.S). Library construction and sequencing by the Illumina platform were conducted by Novogene (Hong Kong).

Internal protocol for Illumina sequencing Novogene

During the amplification, DNA concentration and purity were first monitored on 1% agarose gels and diluted to 1ng/μL by sterile water. Then, 16S rRNA genes of distinct regions (16S V3-V4) were amplified with the specific primer (e.g. 16S V4: 515F-806R). The choice of two primer pairs for the bacteria and archeae domain targeting different variable regions has been reported in literature as a proven approach to screen a relative diverse community at the expense of limitations in taxonomic assignment at the species level (Bonk et al., 2018; Campanaro et al., 2018; Caporaso et al., 2011). The chosen PCR products, between 400 to 450 bp, were mixed in equidensity ratios. Then, the mixture PCR products were purified with Qiagen Gel Extraction Kit (Qiagen, Germany). The libraries of the samples, generated with NEBNext® UltraTM DNA Library Prep Kit for Illumina and quantified via Qubit and Q-PCR, were analyzed by the Illumina platform.

Paired-end reads were assigned to samples based on their unique barcode and truncated by cutting off the barcode and primer sequence. Paired-end reads were merged by FLASH (Magoc et al., 2011), and quality filtering on the raw tags was performed under specific filtering conditions to obtain the high-quality clean tags (Bokulich et al., 2013) with the Qiime quality-controlled process (Caporaso et al., 2010). The effective tags were obtained after comparison with UCHIME algorithm (Edgar et al., 2011) the reference database, to detect chimera sequences and subsequent removal of those.

Sequences analysis was performed by Uparse software (Edgar, 2013), using all the effective tags. Sequences with ≥97% similarity were assigned to the same operational taxonomic units (OTUs). The representative sequence for each OTU was screened for further annotation. For each representative sequence, Mothur software was performed against the SSUrRNA database of SILVA Database (Wang et al., 2007) for species annotation at each taxonomic rank (Threshold:0.8~1) (Quast et al., 2012) (kingdom, phylum, class, order, family, genus, species). To get the phylogenetic relationship of all OTUs representative sequences, the MUSCLE algorithm (Edgar, 2004) was applied to compare multiple sequences. OTUs abundance information was normalized using a standard of sequence number corresponding to the sample with the least sequences.

4.2.5 Analyses

Secondary metabolites in the liquid medium (acetate, propionate, butyrate and valerate) were measured by gas chromatography (7890A GC; Agilent Technologies, US) according to the method described by Muñoz Sierra et al. (2020). The gas composition of samples stabilized at atmospheric conditions was determined via gas chromatography (7890A GC; Agilent Technologies, US) using a thermal conductivity detector operated at 200°C and oven temperature ramping from 40 to 100°C. The system operated with two columns: an HP-PLOT Molesieve GC Column 30 m x 0.53 mm x 25.00 µm and an HP-PLOT U GC Column, 30 m, 0.53 mm, 20.00 µm (Agilent Technologies, US). The carrier gas was helium at a constant flow rate of 10 mL min^{-1}.

Total cell numbers and live/dead cells were assessed by flow cytometry (BD Accuri® C6, BD Biosciences, Belgium) using Milli-Q as sheath fluid. Before measurement, samples were pre-treated as follows: First, samples were diluted (x 500) with 0.22-µm filtered phosphate-buffered-saline (PBS) solution. Diluted samples were sonicated in 3 cycles of 45 seconds at 100 W and the amplitude at 50%. Subsequently, samples were diluted (x 500) and filtered at 22 µm. Immediately after the pre-treatment, the samples were stained with 5% SYBR® Green I or SYBR® Green I combined with propidium iodide (Invitrogen) and incubated at 37°C for 10 min. pH, total and soluble COD, TSS and VSS, ammonium and total phosphorus were measured according to standard methods (American Public Health Association, 2017).

4.2.6 Statistical Analyses

Statistical analyses were carried out in R version 3.6.1 (2019). After processing the amplicon sequencing data, a table was generated with relative abundances of the different OTUs and their taxonomic assignment of each sample. Normalization of the samples was carried out based on the flow cytometry data (Props et al., 2017). The R packages vegan (Oksanen et al., 2016) and phyloseq (McMurdie and Holmes, 2013) were used for community analysis. Significant differences ($p < 0.05$) in microbial community composition were identified employing pair-wise Permutational ANOVA (PERMANOVA) with Bonferroni correction using the *adonis* function included in the vegan package.

The order-based Hill's numbers were used to evaluate the alpha diversity in terms of richness (number of OTUs, H_0), the exponential of the Shannon diversity index (H_1) and the Inverse Simpson index (H_2) (Hill, 1973). Beta diversity was evaluated via the Bray-Curtis distance measure (Bray and Curtis, 1957). Spearman's correlation analysis was performed using the function *cor.test* ().

4.3 Results

The main results of the glucose and glycerol conversion experiments at elevated pCO_2 using the evolved and original inoculum are summarized in Table 4-2. Observations are categorized in terms of cell viability, microbial community and product spectrum and explained in detail in the following sections.

4.3.1 Effect of ALE strategy on glucose conversion under elevated pCO_2

Cell viability

Original inoculum

The total and viable cell density of the starting inoculum is presented in Figure 4-2A. During the experiments of glucose conversion at pCO_2 of 0.3 bar using this inoculum, there was a negligible reduction in the final viable cell density, expressed as percentage change, after 10 days (Figure 4-2B). However, at moderately high pressures, *i.e.,* 3, 5 and 8 bar initial pCO_2, the treatments showed a more substantial decrease of approximately 66% in viable cell density for the same period (Figure 4-2B). It should be noted that nitrogen controls at 5 bar showed a comparable decrease of 73% in viable cell density.

Evolved inoculum

Total and viable cell density increased in comparison to the original inoculum after the ALE cycle using glucose as a substrate. In particular, there was a 2.2-fold increase in viable cell density in comparison to the original inoculum (Figure 4-2A). After the exposure to 5 bar pCO_2, the viable cell density of the evolved inoculum showed an increase of 163% compared to the original inoculum. Nitrogen controls at 5 bar presented a smaller increase of 67% in viable cell density after 10 days (Figure 4-2B).

Table 4-2: Summary of the observed effects of the adaptive laboratory evolution (ALE) strategy in the performance of anaerobic conversion of glucose and glycerol under 5 bar pCO_2

	Glucose		Glycerol	
	Original 5 bar initial pCO_2	Evolved	Original	Evolved
Cell density	Decrease in final total and viable cell density.	Increase in final total and viable cell density.	Increase in final total and viable cell density.	Moderate decrease in final cell density and comparable viable cell density between start and endpoint.
Microbial community	Low relative abundance (RA) (<1%) of syntrophic groups. Higher RA of *Methanosaeta* compared to *Methanobacterium.*	Increased RA of *Smithella* and *Syntrophobacter* (8%). Slight increase in RA of *Methanosaeta* compared to *Methanobacterium.*	Higher RA of *Methanosaeta* compared to *Methanobacterium* than in glucose treatments.	Highest RA of Smithella and Syntrophobacter (18%) RA of *Methanosaeta* and *Methanobacterium* comparable to upper limit in original inoculum treatments.
Product spectrum and productivity	Propionate accumulation. Higher acetate and butyrate concentration than under atmospheric conditions. Low CH_4 production.	Propionate conversion. Higher CH_4 production than using original inoculum.	Propionate accumulation, despicable butyrate production. Lower CH_4 production compared to glucose.	Propionate conversion. Higher CH_4 production than original inoculum treatment and glucose treatment.

Microbial community

Original inoculum

The proportion of bacteria and archaea, based on the total number of processed reads, corresponded to 79% and 21%, respectively, in the original inoculum. The bacterial community of the original inoculum was majorly composed of the phyla Chloroflexi (52%), Actinobacteriota (22%), Firmicutes (10%) and Proteobacteria (5%). In terms of the relative abundance of the bacterial community at the genus level, there were a representative proportion of *SJA-15_ge* (35%) and *unclassified Micrococcales* (19%) (Figure 4-3A). The proportion of genera associated with syntrophic propionate oxidation, namely *Smithella,* was low (<1%). The archaeal community was mainly composed of members of the aceticlastic genus *Methanosaeta* (68%) and the hydrogenotrophic genus *Methanobacterium* (31%) (Figure 4-3B).

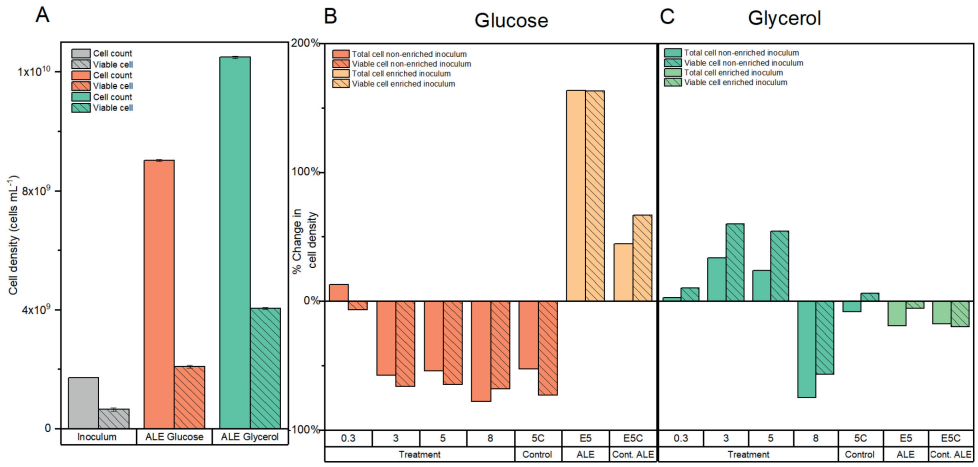

Figure 4-2: (A) Total and viable cell density for the original and evolved inoculum with glucose and glycerol. Percentage of change of total and viable cell density for the (B) glucose and (C) glycerol conversion experiments at different initial pCO_2 in the headspace (0.3, 3, 5 and 8 bar) using original inoculum and at 5 bar initial pCO_2 using evolved inoculum. Pressure controls with N_2 headspace for the original and evolved inoculum at 5 bar (5C and E5C in the graphs) are included for reference.

In the experiments at 3, 5 and 8 bars initial pCO_2, bacterial genera from the class Anaerolineae: *SJA-15_ge* (38-45%), *unclassified Micrococcales* (11-16%) were predominant (Figure 4-3A). The relative abundance of syntrophic groups remained low (<1%). The proportion of total archaea was below 45% in all treatments. Additionally, Figure 4-3B suggests a contrasting relationship in the relative abundance of *Methanobacterium* and *Methanosaeta* in the treatments when compared to the original inoculum.

Evolved inoculum

After the ALE cycles, the proportion of bacteria and archaea was 70 and 30%, respectively. The directional selection of microbial community favoured the relative abundance of bacterial phyla Actinobacteria, increasing its abundance to 48% and decreased the proportion of Chloroflexi to 20% of total bacterial reads for this inoculum. At the genus level, the relative abundance of *unclassified Micrococcales* and *SJA-15_ge* corresponded to 44% and 12%, respectively (Figure 4-3A). *Smithella* increased to 4% of the total bacterial reads. At the archaeal level, the proportions of the two methanogenic genera *Methanosaeta* and *Methanobacterium* corresponded to 68 and 31% of the archaeal reads, respectively (Figure 4-3B).

For the experiments at 5 bars initial pCO_2 with evolved inoculum, at the genus level, *unclassified Micrococcales* remained predominant (28%), as well as *SJA-15_ge* (15%) (Figure 4-3A). Under the imposed experimental conditions, the abundance of syntrophic groups, *e.g., Smithella* (Figure 4-3A) and *Syntrophobacter*, cumulatively increased to 8% of the total bacterial reads. The proportion of total archaea after exposure to pCO_2 corresponded to 39% of the total reads. The relative abundance of *Methanosaeta* increased to 77%, whereas *Methanobacterium* remained around 22% of total processed archaeal reads (Figure 4-3B).

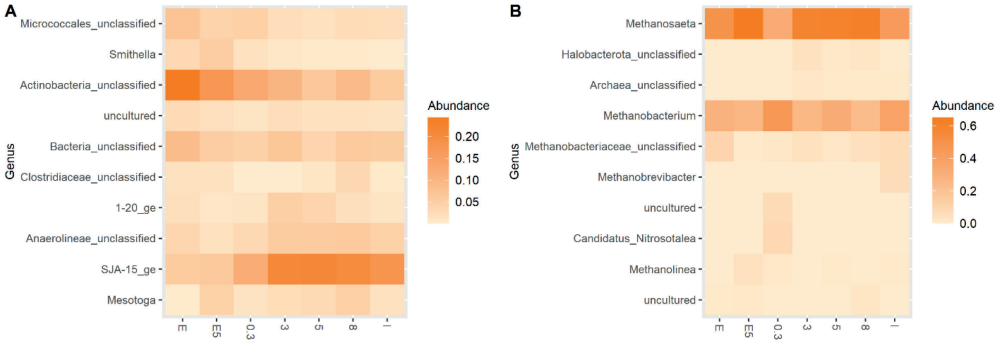

Figure 4-3: Heatmap presenting the relative abundance of (A) Bacterial community and (B) Archaeal community at the genus level. Experimental treatments correspond to glucose conversion at elevated pCO_2 using original (0.3, 3, 5 and 8 bar) and evolved inoculum (5 bar – E5). I corresponds to the original inoculum and E to the evolved inoculum. Pressure corresponds to initial values before equilibrium.

Product spectrum during glucose consumption

Original inoculum

The product spectrum of the anaerobic conversion of glucose under different initial pCO_2 levels was mainly composed of propionate, acetate, butyrate and CH_4. Propionate production was predominant under initial pCO_2 of 0.3 bar, reaching 399 mg COD - Pr L^{-1}, which in terms of the mass balance corresponded to 44% of the initial COD (Figure 4-4A). In the experiments at 3, 5 and 8 bar pCO_2, propionate production peaked at approximately 407±32 mg COD - Pr L^{-1}, which accounted for 38% of the initial COD. Small discrepancies in the total amount being fed to atmospheric and pressure reactors were experienced since the effective volume differed among reactors to keep the liquid to gas ratio comparable. Acetate and butyrate amounts were higher at initial pCO_2 of 8 bar compared to atmospheric conditions, whereas at 3 and 5 bar, a

noteworthy accumulation of these metabolites was not detected (Figure 4-4D, B and C). Propionate conversion was hindered by elevated pCO_2 and in consequence, decreased CH_4 production was observed in the treatments at high initial pCO_2. The experiments at 3, 5 and 8 bar pCO_2 resulted in an average 30% decrease in the final amount of COD-CH_4 produced in comparison to the atmospheric control at 0.3 bar pCO_2 evaluated after 10 days (Figure 4-4 A, B, C and D).

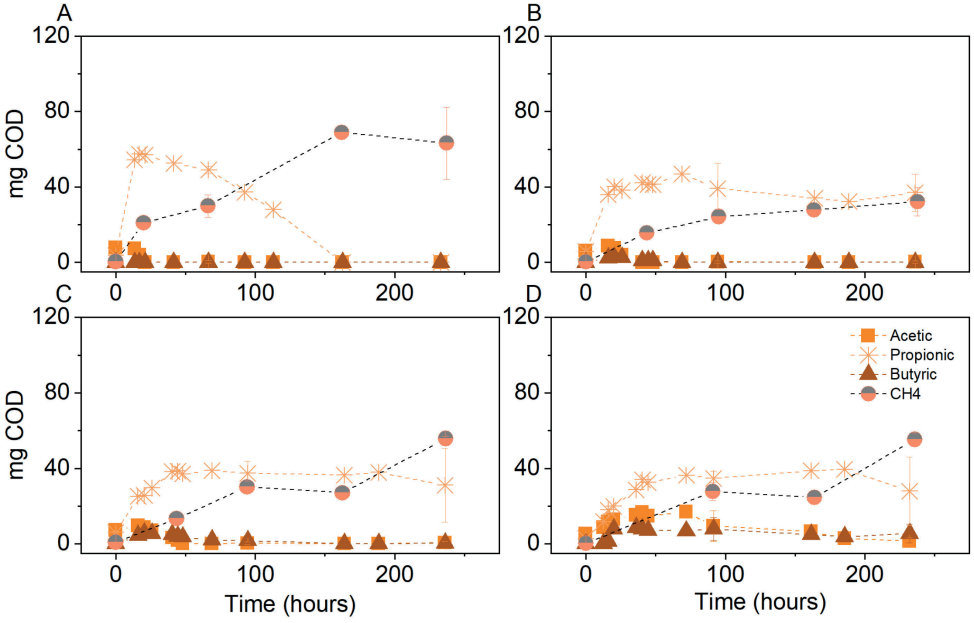

Figure 4-4: Volatile fatty acid (VFA) and CH_4 production (mg COD) over time for the glucose conversion experiments using original inoculum at initial pCO_2 of (A) 0.3 bar (B) 3 bar (C) 5 bar and (D) 8 bar. Pressure corresponds to initial values before equilibrium. Data points represent experimental data. Bars represent the standard deviation of three biological replicates measured at the beginning, middle and end of the experiment.

Evolved inoculum

Figure 4-5A shows the composition of the product spectrum in the experiments with evolved inoculum, which remained similar to the experiments with original inoculum; however, less accumulation of intermediates, particularly propionate, was detected. Propionate production peaked after 92 hours (Figure 4-6), and it was no longer detected at significant amounts at the end of the experiment (Table 4-3). A preliminary 33% decrease in the final COD-CH_4 was calculated when comparing to the treatment at the same pCO_2, *i.e.,* 5 bars, using the original inoculum (Figure 4-4C).

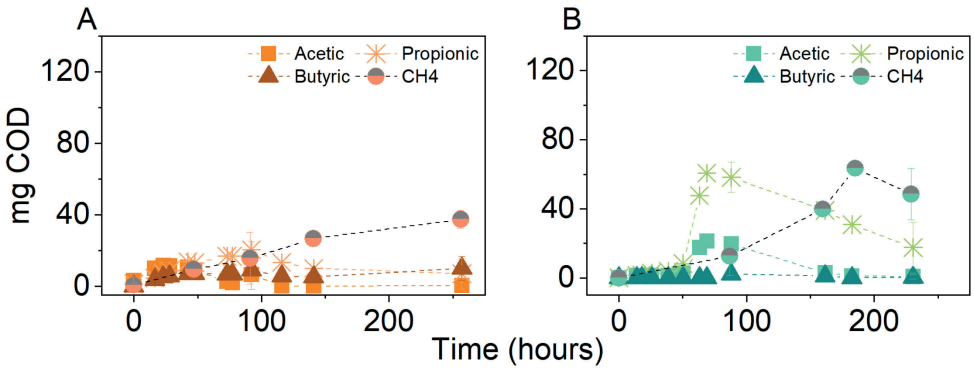

Figure 4-5: Volatile fatty acid (VFA) and CH_4 production (mg COD) over time for (A) glucose and (B) glycerol conversion experiments at elevated pCO_2 using evolved inoculum at 5 bar initial pCO_2. Pressure corresponds to initial values before equilibrium. Data points represent experimental data. Bars represent the standard deviation of three biological replicates measured at the beginning, middle and end of the experiment.

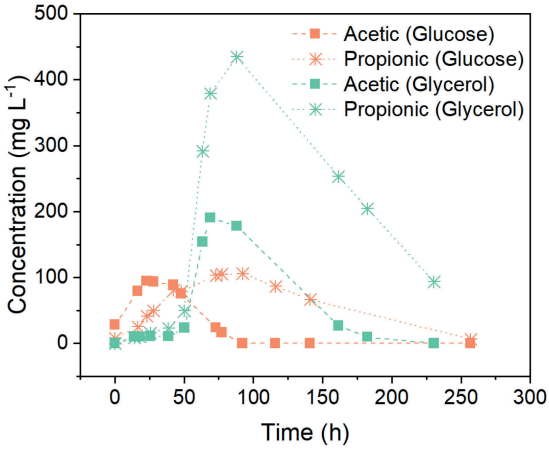

Figure 4-6: Measured acetate and propionate concentrations (mg/L) during the experiments with the evolved inoculum at 5 bar pCO_2 using glucose and glycerol as substrates

Table 4-3: COD balance calculated for each experimental condition for glucose and glycerol conversion under elevated pCO_2 with original anaerobic inoculum and evolved inoculum. pH value measured after reactor depressurization is additionally provided.

Substrate	pCO_2/ pN_2 (bar)	Acetate (mg COD)	Propionate (mg COD)	Butyrate (mg COD)	Others (mg COD)	CH_4 (mg COD)	Biomass (mg COD)	Total (mg COD)	Initial substrate (mg COD)	pH
Glucose	0.3 (n=3)	ND	ND	ND	ND	63.2±19	33.2	96.4	130	7.2
	3 (n=3)	0.3±0.1	36.9±10	ND	1.06	32.2±8	62.4	132.9	106	6.9
	5 (n=3)	ND	40.6±5	0.43±0.1	2.37±0.6	55.8±1	81.2	180.3	106	6.6
	8 (n=3)	1.9±0.2	36.9±3	7.24±4	4.07±0.1	55.3±4	47.1	152.4	106	6.6
	5CN* (n=1)	1.9	2.44	ND	0.67	120	59.8	184.6	106	6.7
Glycerol	0.3 (n=3)	0.4±0.1	ND	ND	ND	81.6±2	66.1	148.1	130	7.2
	3 (n=3)	0.4±0.1	59.8±2	ND	2.1±0.2	22.3±1	26.9	111.5	106	6.6
	5 (n=3)	0.7±0.3	66.5±6	ND	2.3±0.3	21.8±5	27.6	118.8	106	6.5
	8 (n=3)	5.9±0.5	68.8±4	1.6±0.8	2.9±0.1	31.1	31.1	127.4	106	6.6
	5CN (n=1)	1.4	2.5	ND	ND	94.9	15.4	114.2	106	7.6
Glucose (ALE)**	E5 (n=3)	0.4±0.1	7.0±0.8	9.9±0.7	3.1±0.5	37.5±5	20.0	77.9	101	6.4
	E5CN (n=1)	ND	ND	ND	ND	51.6	6.4	58.1	101	7.5
Glycerol (ALE)	E5 (n=3)	0.7±0.1	17.6±1.5	0.3±0.1	0.8±0.1	48.5±15	26.7	94.6	127	6.5
	E5CN (n=1)	1.05±0.5	ND	ND	1.03±0.4	87.9	20.9	110.8	127	7.6

*CN: Control Nitrogen, **ALE: Adaptive laboratory evolution, *** ND: Not detected

4.3.2 Effect of ALE strategy on glycerol conversion under elevated pCO_2

Cell viability

Original inoculum

In the experiments of glycerol conversion at elevated pCO_2 using the starting inoculum at 0.3 bar pCO_2, there was a negligible 10% increase in final viable cell density compared to initial conditions. However, at initial pCO_2 of 3, 5 and 8 bar there was an increase of approximately 50% for the two lowest pressures and a comparable percentage decrease for the highest pCO_2. Nitrogen controls at 5 bar did not present a considerable change in viable cell density, just accounting for a 6% increase (Figure 4-2C).

Evolved inoculum

After the ALE process with increasing glycerol load, there was a 5.2-fold increase in viable cell density in comparison to the original inoculum and a 0.9-fold increase compared to the ALE with glucose as substrate (Figure 4-2, A and B). After exposure to 5 bar pCO_2, the evolved inoculum showed a negligible 5% decrease in viable cell density. Nitrogen controls at 5 bar showed a 20% decrease compared to the initial conditions after 10 days (Figure 4-2C).

Microbial community

Original inoculum

In the experiments with the original inoculum at 3, 5 and 8 bar initial pCO_2, results showed a predominance of bacterial genus *SJA-15_ge*, whose relative abundance calculated based on processed reads varied between 34-42%, and other genera, such as *Clostridium_sensu_stricto_12* (8-12%), as well as *unclassified Micrococcales* and *Mesotoga* with relative abundances <14% (Figure 4-7A). The relative abundance of SPOB remained low (<1%) in all cases. There was a descending trend regarding the changes in the proportion of total archaea for the high pCO_2 experiments using the original inoculum: for experiments at 3, 5 and 8 bar pCO_2, the archaeal presence corresponded to 35, 22 and 18% of the total number of processed reads, respectively. *Methanosaeta* had the highest relative abundance at the genus level, varying between 58 and 82%, while *Methanobacterium* ranged between 17-41% of total processed archaeal reads (Figure 4-7B).

Evolved inoculum

After ALE with glycerol, the proportion of Bacteria and Archaea corresponded to 81 and 19% of processed reads, respectively. The bacterial community composition was dominated by phyla Chloroflexi (35%), Actinobacteriota (19%), Desulfobacterota (14%), and Synergistota (14%). At the genus level, *SJA-15* (27%), *unclassified Micrococcales* (17%), *Smithella* (13%) and *Thermovirga* (11%) showed the highest relative abundances (Figure 4-7A). The archaeal community was majorly composed of genera *Methanosaeta* and *Methanobacterium* at a corresponding relative abundance of 76 and 22% (Figure 4-7B).

For the experiments at 5 bar pCO_2 with evolved inoculum, the relative abundance of *SJA-15_ge* decreased to 19% and *Clostridium_sensu_stricto_12* (21%) was predominant. At this condition, the relative abundance of syntrophic groups, *e.g., Smithella* (Figure 4-7A) and *Syntrophobacter,* cumulatively increased to 18%. The proportion of total archaea, in this case, showed an increase to 35% of total processed reads. In terms of community composition, it differed from the glucose experiments: a slightly higher proportion of *Methanosaeta* (89%) was observed, whereas *Methanobacterium* represented 10% of processed archaeal reads (Figure 4-7B).

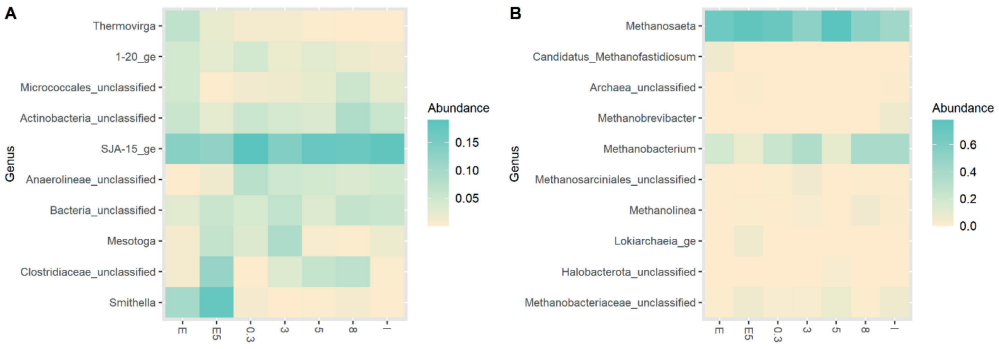

Figure 4-7: Heatmap presenting the relative abundance of (A) Bacterial community and (B) Archaeal community at the genus level. Experimental treatments correspond to glycerol conversion at elevated pCO_2 using original (0.3, 3, 5 and 8 bar) and evolved inoculum (5 bar – E5). I corresponds to the original inoculum and E to the evolved inoculum. Pressure corresponds to initial values before equilibrium.

Changes in microbial community structure due to exposure to glycerol and glucose and elevated pCO_2

A basic analysis of alpha diversity via calculation of the Hill numbers showed an overall decrease in the richness (H_0) of the bacterial community associated with the directional selection process at increasing substrate concentrations, which seemed to be more noticeable in the case of glycerol compared to glucose (Figure 4-8). The inoculum condition (original vs evolved) only exposed significant differences in terms of the bacterial community structure for the case of richness, H_0 ($p=0.032$), when all treatments were analyzed together. In the case of Pielou's evenness, significant differences were explained by the type of substrate ($p=0.044$) and not by elevated pCO_2.

Beta diversity analysis via calculation of the Bray Curtis distance measures revealed significant differences in the community at the highest taxonomic level (Kingdom) because of exposure to elevated pCO_2 ($p=0.01$ and $p=0.04$, respectively). The inoculum condition was significant only to explain the variability of the bacterial community ($p=0.07$) among all experimental treatments.

Product spectrum

Original inoculum

The glycerol anaerobic conversion experiments showed a similar final product spectrum to glucose in terms of VFA. The difference was observed in the overall production: propionate in each condition of glycerol fermentation was around two times higher than during glucose fermentation and butyrate production was, on average, four times lower. Under atmospheric conditions, propionate production reached 600 mg COD – Pr L^{-1} at 0.3 bar pCO_2. In terms of the mass balance, this accounts for 67% of the initial COD (Figure 4-9A). In the elevated pCO_2 experiments, the propionate concentration reached its plateau around 647 ± 41 mg COD – Pr L^{-1}, corresponding in mass to 57-66% of the initial COD input. Similar to the glucose experiments, propionate conversion was seemingly affected by elevated pCO_2 leading to its accumulation after approximately 70 hours and until the end of the experimental period (Figure 4-9 B, C and D). Consequently, CH_4 production was majorly impacted in the glycerol treatments at elevated pCO_2. On average, methane production was lowered by 69%, compared to the atmospheric control at 0.3 bar pCO_2. CH_4 production in the pressurized treatments was, on average, 48% lower in the case of glycerol compared to glucose.

Evolved inoculum

In the case of glycerol conversion at 5 bar pCO_2 using evolved inoculum, propionate peaked after 69 hours (Figure 4-6) and decreased until complete conversion was observed by the end of the experiment (Figure 4-5B). An increment of 55% in final CH_4 production was achieved when compared to the treatments at the same pCO_2 using the original inoculum (Figure 4-9C). Contrary to what was observed with the original inoculum experiments, CH_4 production from glycerol with evolved inoculum was 23% higher than from glucose at 5 bar pCO_2.

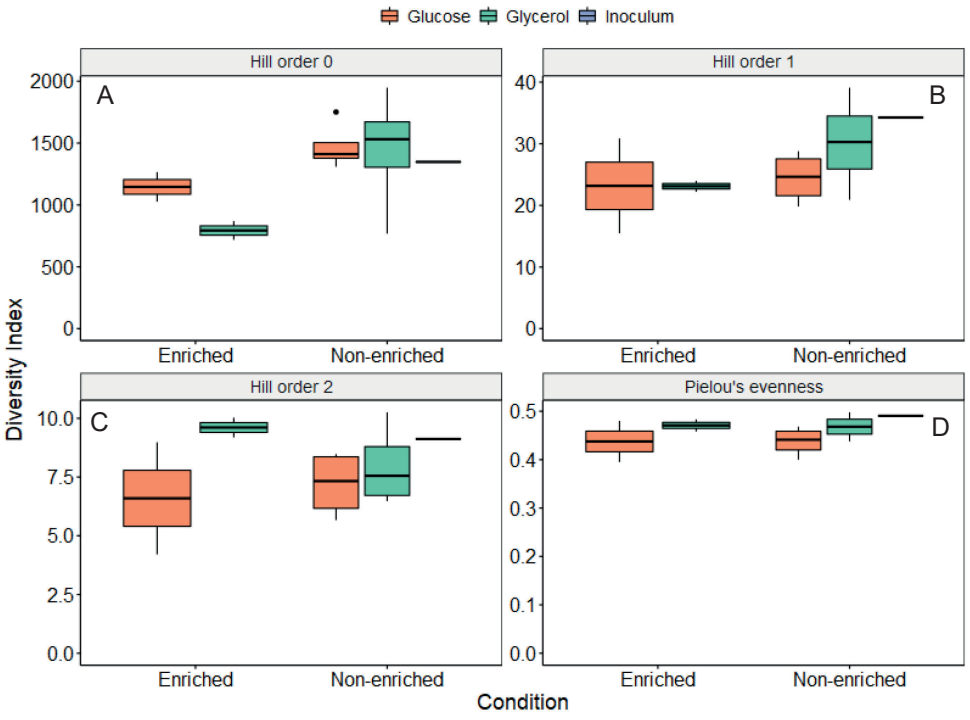

Figure 4-8: Boxplots of the alpha diversity index (A) Richness - H_0, (B) Exponential of the Shannon diversity index - H_1, (C) Inverse Simpson index - H_2 and (D) Pielou's evenness calculated for the experiments of glucose and glycerol anaerobic conversion under elevated pCO_2 using original and evolved inoculum.

4.3.3 Evaluation of CH_4 yield of glucose and glycerol conversion under elevated pCO_2 using evolved inoculum

The processed sequencing data were used to estimate the proportions of bacteria and archaea in the incubations at atmospheric and pressurized conditions with glucose and glycerol. These proportions, together with the results of FCM analysis, were used to estimate the theoretical CH_4 yield in ng of COD per viable archaeal cell for the experimental treatments (Figure 4-10). Based on these results, we calculated that in the 5 bar pCO_2 experiment using evolved inoculum, the CH_4 yield per viable archaeal cell was approximately 2.6 and 4.4 times higher compared to the same condition using the original inoculum for glucose and glycerol, respectively. When comparing glucose and glycerol incubations with evolved inoculum and 5 bar pCO_2, the CH_4 yield per cell in the incubation with glycerol was slightly higher than with glucose (1.3 times), which contrasts with the results of the original inoculum. In all cases, elevated pCO_2 treatments evidenced lower CH_4 yield than pN_2 controls. The increased CH_4 production is likely associated with changes in total archaeal proportion, resulting from the directional microbial community selection process.

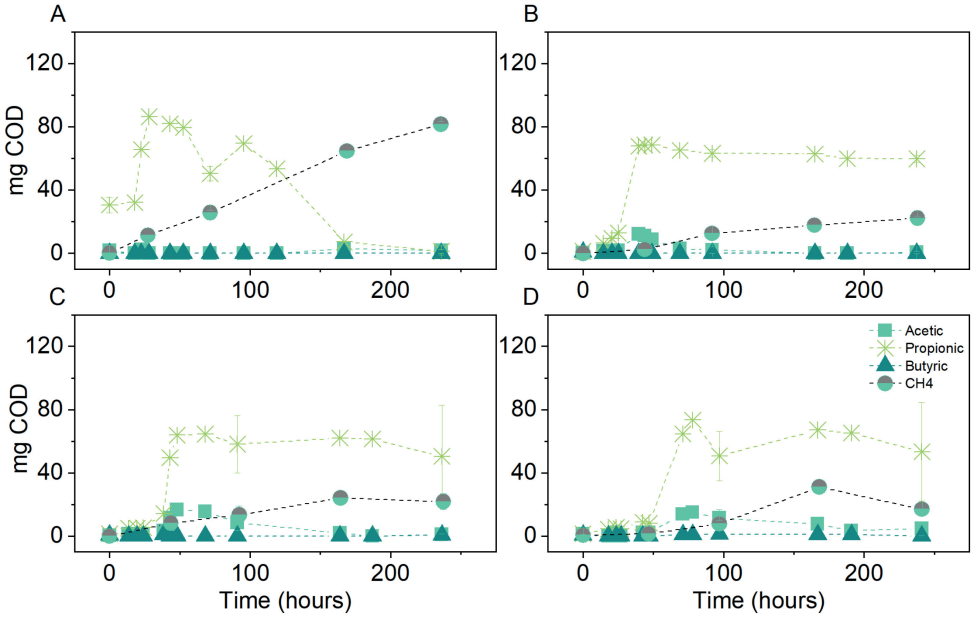

Figure 4-9: Volatile fatty acid (VFA) and CH_4 production (mg COD) over time for the glycerol conversion experiments using original inoculum at initial pCO_2 of (A) 0.3 bar (B) 3 bar (C) 5 bar and (D) 8 bar. Pressure corresponds to initial values before equilibrium. Data points represent experimental data. Bars represent the standard deviation of three biological replicates measured at the beginning, middle and end of the experiment.

Furthermore, enhanced product formation is remarkable since an elevated pCO_2 of 5 bar seemed to constrain cell growth in the case of the glycerol evolved inoculum (Figure 4-2C), but not for glucose (Figure 4-2B). This might suggest the development of different stress-response strategies to elevated pCO_2 depending on the type of substrate and selected microbial community. Moreover, the relative abundance of *Smithella* + *Syntrophobacter* is 2.3 times higher in glycerol than glucose evolved inoculum (Figure 4-7A and Figure 4-3A), which in turn might help to explain higher CH_4 production due to community and pathway selection despite limited growth. It is postulated that due to the ALE process, a higher F:M ratio employed during the elevated pCO_2 experiments with evolved inoculum did not constrain bioconversion activity. The F:M ratio was 4-5 times higher in elevated pCO_2 experiments with evolved inoculum (phase 3, Figure 4-1) compared to original inoculum (phase 1, Figure 4-1). However, due to the differences in viable cell concentration, the substrate loads (calculated as mg COD per viable cell), were actually 10 and 3 times higher compared to the ones using original inoculum for glucose and glycerol, respectively. These differences at the "biomass" and "cell" level could have caused additional inhibition of the biochemical activity of the evolved inoculum; however, results indicate that the ALE process selected for more resilient microorganisms able to cope with the imposed conditions.

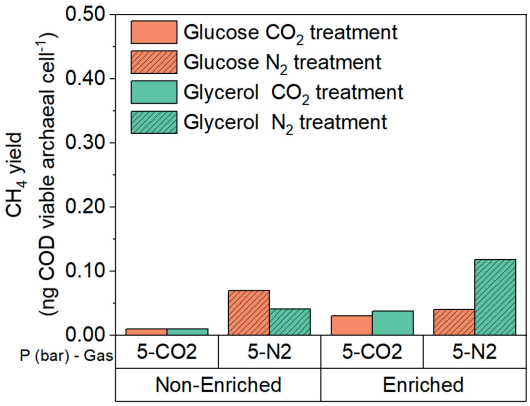

Figure 4-10: CH_4 yield normalized by the viable archaeal cell density at the end of the experiment for the glucose and glycerol conversion experiments at elevated pCO_2 using original inoculum and evolved inoculum at 5 bar. Pressure corresponds to initial values before equilibrium. Nitrogen controls (5 bar) are included as a reference.

4.4 Discussion

From the directional selection of microbial community via ALE, the three main achievements were: i) an increase in the overall total and viable cell density, ii) a higher proportion of archaea compared to the original inoculum for glucose and iii) a larger proportion of SPOB for both substrates (Table 4-2). These achievements provide a reasonable explanation for enabling propionate conversion and consequently improving CH_4 production under elevated pCO_2.

The ALE process could have contributed to the development of protective mechanisms associated with the conservation of cell membrane integrity. It is known that changes in environmental conditions, such as temperature and osmotic pressure, trigger modifications in the structure and fluidity of cell membranes (Beney and Gervais, 2001). Bacteria and Archaea differ in the chemical composition of their membrane lipids (Albers and Meyer, 2011), which confers them a distinctive degree of protection towards changes in total pressure and pCO_2. If membrane fluidity and permeability are being compromised, both groups of microorganisms are capable of adjusting their lipid composition to control ion leakage (Van De Vossenberg et al., 2000). However, previous works suggest that the lipid core of bacterial membranes can adjust itself better to regulate membrane fluidity (Siliakus et al., 2017). This adaptation might confer a survival advantage to bacterial spp. under conditions compromising membrane fluidity and, in turn, intracellular fluxes, such as the exposure to elevated pCO_2.

According to Wu et al. (2007), the application of high-pressure CO_2, *i.e.,* >20 bar, has shown a strong bactericidal effect in cultures of the model organism *E.coli*. The mechanisms contributing to the bactericidal effect included: i) compromised membrane integrity due to facilitated intracellular diffusion of increased H_2CO_3*, ii) drainage of internal cell components such as DNA, and cations as K^+, Na^+ that are linked to a more permeable membrane, and iii) possible internal acidification jeopardizing enzymatic activity as a consequence of a surpassed cytoplasmic buffering capacity (Yao et al., 2014). In our experiments, final pH measurements after decompression (Table 4-3) did not show dramatic differences at the studied pCO_2 levels because of elevated buffer concentration. It should be realized that the external pH only partly determines cytoplasmic pH, which depends on the physiological features of each microorganism and the internal buffer capacity of the cell. The latter could be compromised by additional neutralization requirements to keep pH homeostasis when H_2CO_3* dissociation occurs in the cytoplasm (Slonczewski et al., 2009). Thus, some degree of cytoplasmic acidification cannot be discarded compromising cell growth in the case of glucose experiments with original inoculum (Figure 4-2B) and inhibition of microbial activity leading to intermediate propionate accumulation at elevated pCO_2 for both substrates with the inoculum before the ALE process (Figure 4-4 and Figure 4-9)

It can be hypothesized that the increased load of an acidifying substrate, such as glucose, in every ALE cycle will lead to the development of protective measures against accumulating acidity, which could help to minimize effects on cell membrane integrity by elevated pCO_2 (Sun et al., 2005) and could help to explain the increase in cell viability after ALE with glucose (Figure 4-2B). The noticeable positive effects of using glycerol as the substrate on cell viability (Figure 4-2C) could be attributed to several factors. Firstly, changes in the medium viscosity can affect the diffusion rate of CO_2 and could lead to lower microbial inactivation rates by high-pressure CO_2. A similar observation previously has been reported for a growth medium with increased fat content (Lin et al., 1994). Secondly, researchers recently described that compatible solutes can also act as piezolytes to increase tolerance to pressure exposure (Martin et al., 2002; Scoma and Boon, 2016). Since glycerol can also act as a compatible solute, it might as well confer a temporary piezotolerance depending on its specific uptake and conversion rate. Thirdly, because of its non-ionic nature, glycerol may reduce water activity (a_w) in the medium, which in turn could contribute to lower microbial inactivation rates by high-pressure CO_2 as a result of decreased H_2CO_3* formation and a stabilization effect on membrane proteins (Kish et al., 2012; Wu et al., 2007). Regarding the effects of substrate concentration on the a_w in the experimental treatments, theoretical calculations performed in the hydrogeochemical software Phreeqc® indeed showed that glycerol lowered the water activity compared to glucose but at elevated substrate concentrations (Table 4-5). At the applied low substrate concentrations of 5 and 9 mM for glycerol and glucose, respectively, it is questionable whether changes in a_w would have significantly impacted cell viability in our experiments. Nonetheless, the observed differences in cell viability between glycerol and glucose treatments with the original inoculum (Figure 4-2), where a higher biomass concentration was applied, might suggest the occurrence of CO_2 diffusion limitation associated with the presence of glycerol in the medium.

Table 4-4: Proposed stoichiometries of the glucose and glycerol anaerobic conversion when propionate is oxidized via the methyl malonyl-CoA and the dismutation pathway (*Smithella*) in the case of glucose and glycerol

Reaction	Stoichiometry
	Methyl malonyl-CoA pathway
Glucose fermentation	$2C_6H_{12}O_6 \rightleftarrows 2C_3H_5O_2^- + C_2H_4O^- + 0.50C_4H_7O_3^- + 2CO_2 + H_2 + H_2O$
Propionate oxidation	$2C_3H_5O_2^- + 2H_2O \rightleftarrows 2C_2H_4O^- + 6H_2 + 2CO_2$
Butyrate oxidation	$0.5C_4H_7O_3^- + H_2O \rightleftarrows C_2H_4O^- + H_2 + H^+$
Aceticlastic methanogenesis	$4C_2H_4O^- + 4H^+ \rightleftarrows 4CH_4 + 4CO_2$
Hydrogenotrophic methanogenesis	$8H_2 + 2CO_2 \rightleftarrows 2CH_4 + 2H_2O$
Glucose (syntrophic conversions)	$2C_6H_{12}O_6 \rightleftarrows 6CH_4 + 4CO_2 + H^+$

Dismutation pathway	
Glucose fermentation	$C_6H_{12}O_6 \rightleftarrows C_3H_5O_2^- + C_2H_4O^- + CO_2 + H_2$
Propionate oxidation	$C_3H_5O_2^- + H_2O \rightleftarrows 0.5C_2H_4O^- + 0.5C_4H_7O_3^-$
Butyrate oxidation	$0.5C_4H_7O_3^- + H_2O \rightleftarrows C_2H_4O^- + H_2 + H^+$
Aceticlastic methanogenesis	$2.5C_2H_4O^- + 2.5H^+ \rightleftarrows 2.5CH_4 + 2.5CO_2$
Hydrogenotrophic methanogenesis	$2H_2 + 0.5CO_2 \rightleftarrows CH_4 + H_2O$
Glucose (syntrophic conversions)	$C_6H_{12}O_6 \rightleftarrows 3.5CH_4 + 3CO_2$
Methyl malonyl-CoA pathway	
Glycerol fermentation	$C_3H_8O_3 \rightleftarrows C_3H_5O_2^- + H_2O$
Propionate oxidation	$C_3H_5O_2^- + 2H_2O \rightleftarrows C_2H_4O^- + 3H_2 + CO_2$
Aceticlastic methanogenesis	$C_2H_4O^- + H^+ \rightleftarrows CH_4 + CO_2$
Hydrogenotrophic methanogenesis	$3H_2 + 0.75CO_2 \rightleftarrows 0.75CH_4 + 1.5H_2O$
Glycerol (syntrophic conversions)	$C_3H_8O_3 + H^+ \rightleftarrows 1.75CH_4 + 1.25CO_2$
Dismutation pathway	
Glycerol fermentation	$2C_3H_8O_3 \rightleftarrows 2C_3H_5O_2^- + 2H_2O$
Propionate oxidation	$2C_3H_5O_2^- \rightleftarrows C_2H_4O^- + C_4H_7O_3^-$
Butyrate oxidation	$C_4H_7O_3^- \rightleftarrows 2C_2H_4O^- + 2H_2 + 2H^+$
Aceticlastic methanogenesis	$3C_2H_4O^- + 3H^+ \rightleftarrows 3CH_4 + 3CO_2$
Hydrogenotrophic methanogenesis	$2H_2 + 0.50CO_2 \rightleftarrows CH_4 + H_2O$
Glycerol (syntrophic conversions)	$2C_3H_8O_3 \rightleftarrows 4CH_4 + 2.5CO_2$

The detrimental effects of high pCO_2 cannot be solely attributed to a pressure effect. A comparable loss of viability as the one observed at elevated pCO_2 has up till now only been achieved at hydrostatic pressures higher than 100 MPa (Pagán and Mackey, 2000). When using a non-reactive gas such as N_2, strong biocidal effects have not been observed even if the pH is significantly lowered to emulate pH levels due to CO_2 dissolution (Wu et al., 2007). However, we observed a detrimental effect of pressurized N_2 on the cell viability of evolved inoculum with glycerol (Figure 4-2C) which suggests a negative effect of headspace pressure at low biomass concentration. Moreover, an increased amount of non-viable cells following pressurized conditions can also be explained by reactor depressurization. It has been shown

that pressure release, even if performed gradually, can increase the amount of permeabilized cells (Park and Clark, 2002), thus, compromising their viability. Further investigations are needed to thoroughly quantify possible decompression effects on cell viability and metabolic activity when using reactive and inert gases such as CO_2 and N_2.

Table 4-5: Effect of substrate concentration in the water activity of the liquid medium employed in the experiments of anaerobic conversion of glucose and glycerol under elevated pCO_2

Component			Water activity (a_w)	Volume atm reactor (mL)	Volume pressure reactor (mL)	Remarks
Anaerobic sludge			0.992	20	14	(Agoda-Tandjawa et al., 2013) Solids content in the sludge ≈1.5% w/w
Concentrated Macronutrients and micronutrients solution			0.870	0.90	0.72	Calculated in PhreeqC based on the composition indicated by Garcia-Rea et al., (2020)
Substrate solution + 100 mM HCO_3^-				130	106	Experiments (this work)
			a_w	a_w atm. reactor	a_w pressure reactor	a_w is calculated from an approximation based on Raoult's law (Parkhurst and Appelo, 1999)
Glucose Concentration (mM)	0		1	0.998	0.997	Calculated in PhreeqC
	50		1.00	0.994	0.993	
	100		0.99	0.994	0.993	
	1000		0.97	0.977	0.978	
	2500		0.92	0.925	0.933	
Glycerol Concentration (mM)	0		1	0.998	0.997	Calculated in PhreeqC
	100		0.99	0.994	0.993	
	200		0.99	0.992	0.991	
	2000		0.96	0.960	0.963	
	5000		0.86	0.876	0.890	
	Pr (mM)	Ac (mM)				
VFA mixture (Propionate - Pr + Acetate - Ac)	0	0	1	0.998	0.998	Calculated in PhreeqC
	100	50	1.00	0.994	0.995	
	200	100	0.99	0.992	0.992	
	1000	500	0.97	0.972	0.972	
	5000	2500	0.74	0.771	0.767	

At high propionate concentrations and low pH, a microbial community shift towards increased proportions of hydrogenotrophic methanogens has been evidenced, which contributes to maintaining a low partial pressure of hydrogen (pH_2) to enable propionate oxidation under syntrophic conditions (Han et al., 2020; Y. Li et al., 2018). Apparently, low pH_2 conditions

favour the production of H_2 instead of NADH from the oxidation of reduced ferredoxin (Fd_{red}) (H. S. Lee et al., 2008). Furthermore, at low pH_2, hydrogenotrophic methanogenesis has been described as kinetically (Liu et al., 2016) and thermodynamically more feasible than homoacetogenesis at increasing pCO_2 (Figure 4-11). This would imply that, in principle, we should have observed an increased proportion of hydrogenotrophic methanogens in the glucose experiments. However, this occurred only in the treatment with the original inoculum at the lowest pCO_2 of 0.3 bar (Figure 4-3B). Zhang et al. (2011) described a possible detrimental effect of elevated CO_2 concentration on the transcription levels of functional [FeFe] hydrogenases of the moderate thermophile *Thermoanaerobacterium thermosaccharolyticum W16*. The reduction in the ratio mRNA expression to 16S DNA gene depended on the type of substrate employed, glucose or xylose, and varied between 66-98% (Zhang et al., 2011). Considering this as a plausible hypothesis, H_2 production might have been hindered in our elevated pCO_2 experiments, leaving the production of reduced compounds as the main route for NADH consumption.

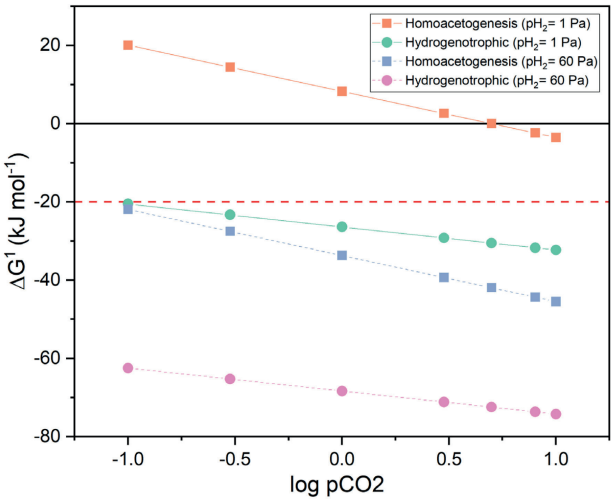

Figure 4-11: Effect of increasing the partial pressure of carbon dioxide in the thermodynamic feasibility of homoacetogenesis and hydrogenotrophic methanogenesis under conditions of low and high partial pressure of hydrogen (pH_2).

The biochemical pathways of anaerobic conversion of glucose and glycerol share phosphoenolpyruvate (PEP) and pyruvate as central intermediates (Zhang et al., 2015). Pathway steering towards particular electron sinks such as propionate will depend on the environmental conditions and type of microorganism (Figure 1-4). Under the assumption of CO_2 fixation, the carboxylation from PEP or pyruvate to oxaloacetate (OAA), which is subsequently further reduced to fumarate, is favoured at the reductive branch of the PEP-

pyruvate-OAA node (Sauer and Eikmanns, 2005; Stams and Plugge, 2009). Without the presence of sufficient reducing equivalents, a presumed CO_2 fixation will have a more limited impact on the production of more reduced compounds during glucose fermentation.

It should be realized that, compared to glucose, the metabolism of glycerol requires balancing double the amount of reducing equivalents per mole of pyruvate or PEP produced. Under limited hydrogen production, NADH will act as electron carrier, channelling the reducing equivalents towards products such as propionate, whose formation stoichiometrically consumes the NADH from glycerol conversion (Zhang et al., 2015). Concomitantly, acetate production from the acetyl-CoA pathway is downregulated to limit reductive stress due to presence of excess NADH (Doi and Ikegami, 2014). Propionate production from pyruvate in glucose metabolism requires an additional electron donor or extra NADH input. Thus, the simultaneous production of a more oxidized compound, namely acetate, helps to satisfy the redox balance. However, this will occur at the expense of a decreased propionate yield, due to diverged carbon flux (Zhang et al., 2015), helping to explain the differences in propionate levels between the used substrates (Figure 4-4, Figure 4-5 and Figure 4-9). Increased propionate production could also be attributed to enhanced enzymatic activities as a result of the substrate choice for the ALE cycles. The activity of pyruvate carboxylase and succinyl CoA: propionyl CoA transferase, both enzymes with a significant role in propionate production, has been enhanced in cultures of *Propionibacterium acidipropionici* using glycerol as the substrate (Zhang et al., 2016). Conversely, this was not observed by these authors when the culture was grown using glucose as the sole carbon and energy source.

The premise of compromised hydrogenase activity because of elevated CO_2 concentrations could help to explain the decreased proportions of hydrogenotrophic methanogens, particularly in the treatments with glucose. The enhancement of a propionate oxidation pathway where thermodynamic limitations associated with interspecies H_2 transfer play a less significant role, *i.e.,* the dismutation pathway, is supported by several factors. Among them, the considerable increase in the relative abundance of the *Smithella* genus in all treatments following the ALE process (Figure 4-3A and Figure 4-7A) and the initially high proportion of *Methanosaeta* in the original inoculum (Figure 4-7B) can be mentioned. Moreover, the reduced H_2 production when using glycerol as the substrate according to stoichiometry, and a plausible detrimental effect of pCO_2 on hydrogenase activity could have influenced pathway predominance. Members of the genus *Smithella* are metabolically active in a broader range of propionate concentrations (Ariesyady et al., 2007), low HRT (Ban et al., 2015) and acidic pH (Y. Li et al., 2018) than members of the genus *Syntrophobacter*. The conditions imposed during the directional selection, *i.e.,* serial transfers to fresh medium, exposed the microorganisms to increased substrate loadings per cell. This possibly contributed to the enrichment of this genus, particularly in the glycerol experiments at 5 bar pCO_2 using evolved inoculum (Figure 4-7A).

Additionally, if thermodynamic feasibility is considered, the dismutation pathway, *i.e.* propionate conversion to butyrate and acetate, is less sensitive to the effects of increasing pH_2 and pCO_2 than the methyl malonyl-CoA pathway, where propionate is converted to acetate and H_2, which undergo further conversion by methanogenic bacteria (Dolfing, 2013) (Figure 4-12). For further reference, we have summarized the stoichiometries of possible metabolic pathways for the anaerobic conversion of glucose and glycerol, including either the dismutation or the methyl malonyl-CoA pathways (Table 4-4).

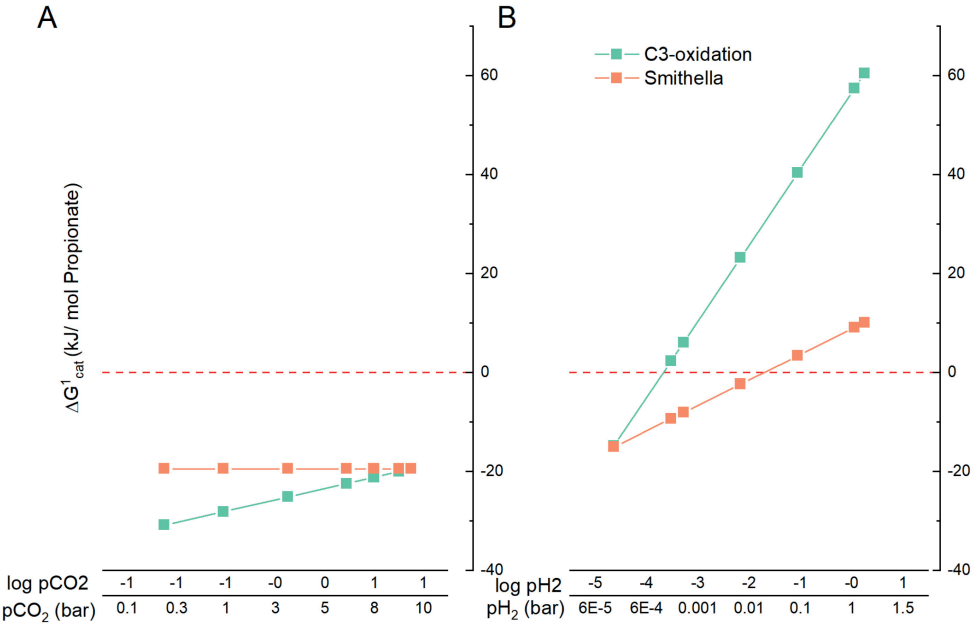

Figure 4-12: Effect of increasing the partial pressure of carbon dioxide (pCO_2) (A) and the partial pressure of hydrogen (pH_2) in the thermodynamic feasibility of propionate oxidation via the methyl malonyl Co-A pathway (C3-oxidation in green) and the *Smithella* (dismutation) pathway (in orange)

It is postulated that the occurrence of the *Smithella* pathway in the incubation with both substrates relates well with enhanced CH_4 yield and might ameliorate end-product inhibition due to elevated pCO_2 in the case of glucose (Table 4-4). Moreover, less CO_2 is being produced in the glycerol treatments either by methyl-malonyl-CoA pathway or by the dismutation pathway from *Smithella* (Table 4-4). Theoretically, this could enable a substantial CO_2 fixation via the oxaloacetate route (Figure 1-4) and enhanced propionate production if enough reducing equivalents are available. Regulation of the redox balance could be achieved in this pathway by the consumption of reducing equivalents in the intermediate steps, forming malate and

succinate. Due to these two reasons, moderately high pCO_2 levels have likely affected glycerol conversion to a lesser extent.

The here presented higher CH_4 yields at 5 bar pCO_2 using evolved inoculum have to be interpreted with caution since significant differences were found in the initial viable cell density of treatments with evolved and original inoculum ($p=0.004$) as a consequence of the higher microbial F:M ratio imposed to keep the experimental liquid volume comparable in all treatments. The observed lower initial cell density in the experiments with evolved inoculum is attributed to the followed harvesting and resuspension procedure for biomass recovery. These initial differences did not necessarily lead to statistically significant higher proportions of viable biomass ($p=0.43$) at the end of the experiments using original inoculum; thus, comparisons in terms of active biomass are fairly reasonable. The CH_4 yield calculated per viable cell showed that the methanogenic activity under elevated pCO_2 was moderately enhanced due to the directional selection process and might be indicative of microbial community resilience to elevated pCO_2. It was not possible to extrapolate these yields in terms of VSS concentration since this parameter only showed a moderate positive correlation with the log-transformed viable cell density data ($r_s=0.65$, $p=0.005$) (Figure 4-13) and did not constitute a good proxy for microbial biomass in the experiments here presented. We would not have been able to evidence subtle changes in total cell density and cell viability compromising overall metabolic activity by only relying on this measurement, since it includes dead/non-viable cells and extracellular compounds besides the active biomass (Foladori et al., 2010).

At the microbial ecology level, high CO_2 concentrations shift the community structure and reduce the taxonomic diversity in different environmental systems (Yu and Chen, 2019), with effects beyond acidification (Gulliver et al., 2014). In our experiments, the directional selection process, prior exposure to elevated pCO_2, proved to be preponderant for changes in community structure (Hill number 0 – Richness Figure 4-8) and overall diversity (Figure 4-3 and Figure 4-7), which can benefit reactor start-up. Changes in alpha diversity could be linked to a community reorganization as a consequence of the selection pressure (increased substrate load) or an applied disturbance, namely the elevated pCO_2 (Werner et al., 2011). In our experiments, as expected, microbial community richness decreased due to the ALE process, but carboxylates production was not compromised. Fermentative activity tends to be conserved even if decreased richness is observed, most likely due to the resilience of this process to stress conditions (Mota et al., 2017). However, conservation of functionality features of the evolved community and its prevalence as the core microbiome in long-term AD-operation will depend on process operation and control (Tonanzi et al., 2018). Concerning the archaeal community structure, CO_2 enrichment in anaerobic digesters at atmospheric conditions can modify the ratio aceticlastic: hydrogenotrophic methanogens favouring the abundance of *Methanosaeta* (Bajón

Fernández et al., 2019). This finding is in alignment with the observations here described and the study by Lindeboom et al. (2016), where a high relative abundance of *Methanosaeta* is reported at increased pCO_2 levels during high-pressure AD.

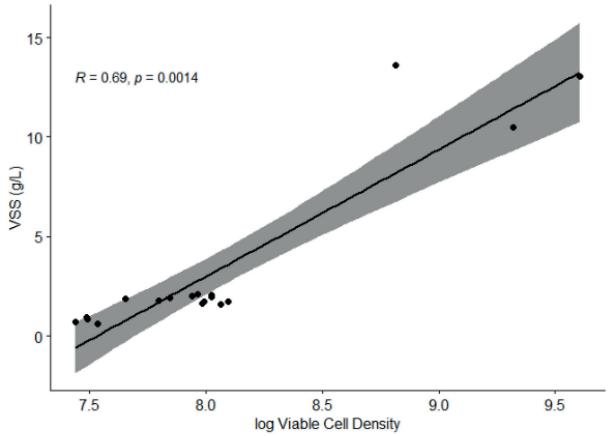

Figure 4-13: Scatter plot showing the correlation between the log-transformed viable cell density and the VSS concentration measured at the end of each experimental treatment and for the original inoculum and the evolved inoculum with glucose and glycerol.

Our observations associated with changes in structure and diversity are only indicative of the effects of elevated CO_2 in fermentative and methanogenic communities and their syntrophic interactions at the bioreactor level, because of the short duration of our experiments. Further support for these conclusions needs to come from longer incubations under pressurized CO_2 conditions with different types of inocula. Longer incubations leading to increased growth of adapted biomass could enable a more accurate quantification with standard methods (VSS). If a more thorough characterization of the biomass at cell level in terms of average cell dimension and biovolume would be performed, it could permit a better correlation between VSS and FCM results. Similar to previous work, a correlation between protein measurements following the Lowry method and VSS could also provide additional characterization (Lindeboom et al., 2018).

Moreover, if these incubations are monitored with online pH, pressure measurements and intensive sampling for microbial community dynamics, a clearer correlation could be obtained between changes in the community and operational variables modified by the pressurized operation. But, even then, the accounted effects might depend on specific system characteristics and operational strategy. Observations of natural soil communities exposed to elevated atmospheric pCO_2 show that there is not a common agreement over the effects on the microbial ecology. Recent studies have reported either no significant changes (Ahrendt et al., 2014; Bruce

et al., 2000) or major shifts in the microbial community (Šibanc et al., 2014; Xu et al., 2013). These shifts include, for example, the predominance of acid-resistant groups such as *Chloroflexi* and *Firmicutes* or acetogenic spore-forming *Clostridia* (Conrad, 2020), which agrees with the results here reported (Figure 4-3 and Figure 4-7). From these investigations, it can be deduced that other environmental factors such as temperature, pH, nutrient availability as well as CO_2 final concentration and exposure time, will determine the overall fate of the microbial community after exposure to elevated pCO_2.

4.5 Conclusions

A microbial community directional selection strategy was employed in this study to overcome limited syntrophic propionate oxidation in glucose and glycerol anaerobic conversions under elevated pCO_2. The pressurized incubations using evolved inoculum showed a dissimilarly enhanced final cell viability, with a stronger positive effect of the adaptive laboratory evolution in cell viability of glucose incubations. Our results suggest that directional selection of microbial community with increased substrate load per cell triggered mechanisms to preserve cell viability. Moreover, it increased the proportions and enhanced the metabolic activity of microorganisms resilient to increasing propionate concentrations, such as SPOB and the interrelated methanogenic community. The increased abundance of the genus *Smithella* accompanied by higher proportions of *Methanosaeta* after incubation with glycerol proved to be beneficial for propionate conversion at elevated pCO_2. The highest CH_4 yield per cell at conditions of elevated pCO_2 was observed in the glycerol experiments, which was attributed to enhanced propionate formation, as a way to incorporate CO_2 and maintain the redox balance via metabolic regulation. Overall, using an evolved inoculum with higher viable cell density and restructured community with a predominance of key microbial groups proved to be a right course of action into surmounting reduced metabolic performance associated with elevated pCO_2.

5

CHAPTER 5

POTENTIAL AND LIMITATIONS OF ELEVATED pCO_2 AS STEERING PARAMETER IN ANAEROBIC PROCESS

This chapter was submitted to Biotechnology for Biofuels and Bioproducts (April 2022) as:

Ceron-Chafla, P., De Vrieze, J., Rabaey, K., van Lier, J. B., & Lindeboom, R. E. F. Potentials and limitations of elevated pCO_2 as steering parameter inanaerobic processes.

Abstract

Elevated CO_2 partial pressure (pCO_2) has been proposed as a potential steering parameter for selective carboxylate production in mixed culture fermentation, since intermediate product spectrum and production rates, as well as microbial community dynamics, are anticipated to be (in)directly influenced by elevated pCO_2. It remains unclear how pCO_2 interacts with other operational conditions, namely substrate specificity, substrate to biomass (S/X) ratio and the presence of an additional electron donor, and what effect pCO_2 has on the composition of fermentation products. Here, we investigated possible steering effects of elevated pCO_2 combined with (1) mixed substrate (glycerol/glucose) provision, (2) subsequent increments in substrate concentration to increase the S/X ratio and (3) formate as an additional electron donor.

Metabolite predominance, *e.g.,* propionate vs butyrate/acetate, and cell density, depended on interaction effects between pCO_2 - S/X ratio and pCO_2 - formate. Individual substrate consumption rates were negatively impacted by the interaction effect between pCO_2 - S/X ratio and were not re-established after lowering the S/X ratio and adding formate. The product spectrum was influenced by the microbial community composition, which in turn was modified by substrate type and the interaction effect between pCO_2 - formate. High propionate and butyrate levels strongly correlated with Negativicutes and Clostridia predominance. After subsequent pressurized fermentation phases, the interaction effect between pCO_2 - formate enabled a shift from propionate towards succinate production when mixed substrate was provided.

Overall, interaction effects between elevated pCO_2, substrate specificity, high S/X ratio and availability of reducing equivalents from formate, rather than an isolated pCO_2 effect, modified the proportionality of propionate, butyrate and acetate in pressurized mixed substrate fermentations at the expense of reduced consumption rates and increased lag-phases. The interaction effect elevated pCO_2 – formate, due to the availability of extra reducing equivalents and likely enhanced carbon fixating activity, was beneficial for succinate production and biomass growth with a glycerol/glucose mixture as substrate.

Keywords

Elevated pCO_2, high-pressure anaerobic digestion, Veillonellaceae, carboxylates, succinate

5.1 Introduction

The emergence of the biorefinery concept, in which fuel and chemicals production from (waste) biomass feedstock are envisioned (Cherubini, 2010), has become a strong driver for product spectrum diversification in anaerobic processes. Consequently, it has motivated the inclusion of carboxylates production, such as propionate and butyrate, in addition to biogas from anaerobic digestion (AD), as (bio)products of interest (Agler et al., 2011; Braz et al., 2019; Marshall et al., 2013). Anaerobic processes using complex substrates rely on trophic diversity and interspecies interactions to carry out the required bioconversions; thus, the formation of specific intermediates and final products in open microbiomes depends on prevailing operational conditions (Angenent and Wrenn, 2008; Kleerebezem and van Loosdrecht, 2007; Rodríguez et al., 2006). Due to the interconnection between operational conditions, the intermediate products profile, microbial community and productivity/selectivity, management strategies have been proposed to boost performance by manipulating process parameters (operational-based strategy) and through biomass acclimation and bioaugmentation (microbial-based strategy) (Carballa et al., 2015).

Changes in substrate concentration (Coma et al., 2016; Hoelzle et al., 2021; Jankowska et al., 2017), pH (Tamis et al., 2015; Temudo et al., 2007; Zoetemeyer et al., 1982) and temperature (M. Lee et al., 2008; Zhuo et al., 2012) are known to influence the profile of intermediate products. Reactor operation (Dai et al., 2017; Khan et al., 2016), substrate to biomass (S/X) ratio (Jiang et al., 2013; Lim et al., 2008), and headspace composition (Arslan et al., 2013, 2012; De Kok et al., 2013) can also modify the intermediate product spectrum. However, thus far, strategies for the selective production of specific carboxylates as intermediate products are lacking. High-Pressure Anaerobic Digestion (HPAD) is considered an innovative technology with potential for direct biogas upgrading (Lindeboom et al., 2011). In an HPAD reactor, the partial pressure of biogas components, *i.e.,* CO_2, may play a role in pathway steering and selectivity in intermediate product formation (Bothun et al., 2004; Lindeboom et al., 2016).

An increased CO_2 partial pressure (pCO_2) in HPAD reactors may result from an autogenerated build-up in operational pressure (Lindeboom et al., 2016). Previous work showed that bioprocesses operating at high pCO_2 experienced toxicity and acidification effects (Lindeboom et al., 2016). Additionally, high pCO_2 impaired substrate transport over the microbial cell membrane due to a decreased membrane potential (Wan et al., 2018) and imposed kinetic, bio-energetic and physiological limitations (Chapter 2). Lindeboom et al. (2016), using a pressure-adapted inoculum, observed that low methane production rates and propionate accumulation correlated with increasing pCO_2, constituting pioneering evidence of a potential steering role of elevated pCO_2 in HPAD. Intermediate product formation does not only depend on the (re-)distribution of organic carbon from the original substrate and the possible role of pCO_2 on

the thermodynamics of (de)carboxylation reactions, but also on the availability of reducing equivalents and the ratio $NADH/NAD^+$ (Berríos-Rivera et al., 2002; Girbal and Soucaille, 1994).

At the macro-process level, changes in the degree of reduction of the employed substrate (Saint-Amans et al., 2001; Vasconcelos et al., 1994), high S/X ratio or provision of an additional electron donor (Hakobyan et al., 2018) can be applied to alter availability and reducing equivalents flux. However, an increasing S/X ratio could cause inhibition of non-adapted biomass and hinder bioconversions due to kinetic limitations in the production and utilization of intermediates (Mösche and Jördening, 1999). Biomass adaptation at increasing substrate concentrations and substrate specificity has been pivotal in selecting a microbial community that is more resilient to the detrimental effects of elevated pCO_2 (Chapter 4) and most likely also to fluctuations in the S/X ratio.

Under the premise that microbial resiliency is attained, elevated pCO_2 could play a role in steering metabolic pathways because of its tuning effect in enzyme activities related to (de)carboxylation of intermediates (Amulya and Mohan, 2019; Sawers and Clark, 2004; Song et al., 2007). These reactions are relevant for the breakdown of substrates sharing the glycolytic pathway, *e.g.,* glucose and glycerol, where carbon atoms and electrons are distributed towards the reductive (propionate) or oxidative (acetate) branch of the pathway in response to growth conditions (Sauer and Eikmanns, 2005). Elevated pCO_2 could also modify the intermediate product spectrum via autotrophic CO_2 fixation. Acetogenic bacteria such as *Clostridium* spp., which are crucial in anaerobic microbiomes, can fix CO_2 into acetyl-CoA via the Wood–Ljungdahl pathway (WLP), provided the availability of reducing equivalents (Ragsdale and Pierce, 2008). Mixotrophic acetogenic metabolism, *i.e.,* simultaneous heterotrophic and autotrophic growth with high acetate production (Fast et al., 2015; Jones et al., 2016; Maru et al., 2018), can be enhanced if sugars and CO_2 are present. Moreover, increasing acetate concentrations can favour chain elongation processes with lactate or ethanol (Angenent et al., 2016; Coma et al., 2016) as long as acetotrophic methanogenic activity is constrained by, *e.g.,* too low or too high pH or inoculum pre-treatment (Wainaina et al., 2019).

Elevated pCO_2 could also cause shifts in the microbial community structure, indirectly impacting the intermediate product spectrum. As an environmental driver, elevated pCO_2 could select carbon fixation traits leading to a predominance of specific acetogens, such as *Clostridium* spp (Heffernan et al., 2020). Combined pCO_2-pH effects may favour the predominance of acid-resistant groups from the phyla Chloroflexi and Firmicutes (Conrad, 2020). Depending on the electron transfer mediator (H_2, formate), elevated pCO_2 may also restructure the methanogenic community (Oppermann et al., 2010). In addition, the interplay of pCO_2 and substrate concentration impacting the S/X ratio could modify syntrophic

interactions (Ziels et al., 2019), and may cause metabolic uncoupling (Li et al., 2016), potentially affecting the intermediate product spectrum.

Overall, there is ample evidence that elevated pCO_2 influences anaerobic processes in multiple ways. However, the role of pCO_2 is insufficiently understood to use it as a steering parameter for specific carboxylate production in HPAD. For instance, it remains unclear how elevated pCO_2 could interact with process conditions to ultimately select for a particular carboxylate, *e.g.,* propionate. In this chapter, the interaction of elevated pCO_2 with the provision of mixed substrate (glycerol/glucose), high substrate concentration increasing the S/X ratio and the presence of an additional electron donor (formate) was studied. The mixed substrate was provided on the grounds of substrate divergence to propionate production (glycerol) and ATP provision to satisfy maintenance and growth requirements (glucose) (Liu et al., 2011; Wang and Yang, 2013). A high S/X ratio was imposed as a selection mechanism to favour fermentative and suppress methanogenic activity due to metabolic uncoupling. Finally, we assessed the effects of formate addition, concomitant to elevated pCO_2, to stimulate carbon fixating activity and the formation of reduced intermediates due to the increased availability of reducing equivalents.

5.2 Materials and Methods

5.2.1 Inoculum

Flocculent anaerobic sludge was obtained from an anaerobic membrane bioreactor (AnMBR), treating wastewater from a food and feed industry, as reported in Chapter 4. The physicochemical characteristics of the inoculum are presented in Table 5-1. The inoculum was stored for one month at 5.6°C. After that, biomass was acclimated to 35°C and concomitantly activated with 50 mg L^{-1} substrate (glucose) for 24 hours before starting the experiments.

5.2.2 Mixed substrate conversion under elevated pCO_2

Sequential batch experiments were carried out to investigate the effect of mixed substrate on carboxylates production under elevated pCO_2 (5 bar). This operational pressure was selected as a boundary condition between extended lag phases and noticeable CO_2 effects on substrate conversion based on previous work (Chapters 2 and 4). Pressurized stainless steel reactors (200 mL) (Nantong Vasia, China) were employed for the batch incubations. The liquid medium (120 mL), added to each reactor, consisted of substrate, macro and micronutrients solution prepared according to García-Rea et al. (2020) and buffer solution at a concentration of 150 mM as

HCO_3^- to keep pH around 7.5. Concentrations and molar ratios between glycerol and glucose in the feeding solution varied in the different experiments, as explained in Table 5-2.

Experiment I: Determination of the reference substrate conversion rate under elevated pCO_2

This experiment was conducted to estimate the conversion rates of glycerol, glucose and the mixture (1:1 molar ratio) at 5 bar pCO_2. We used the activated and acclimated inoculum described in section 1.2.1 and the operational conditions described in Table 5-2.

Table 5-1: Physicochemical characterization of anaerobic inoculum used in experiment I and as starting inoculum in experiment II. Average and standard deviations were calculated from technical replicates (n=3).

Parameter	Unit	Mean ± SD
Total Chemical Oxygen Demand (TCOD)	g L^{-1}	30.7±0.2
Soluble COD (SCOD)	mg L^{-1}	275±1.2
Total Suspended Solids (TSS)	g L^{-1}	15.7±0.3
Volatile Suspended Solids (VSS)	g L^{-1}	15.2±0.1
VSS/TSS	%	95±2
Ammonium (NH_4-N)	mg L^{-1}	21.7±0.2
Total Phosporous (TP)	mg L^{-1}	49.8±3.8
pH	-	7.3

Table 5-2: Overview of dual substrate conversion experiments under elevated partial pressure of carbon dioxide (pCO_2).

Experiment	Description	Conditions			
		Duration (hours)	pCO_2 (bar)	Biomass (g VSS L^{-1})	COD reactor[a] (g L^{-1})
I	Reference conversion rate of glucose, glycerol and 1:1 dual substrate mixture under elevated pCO_2	7	5	4.4	3.7
II-A	Dual substrate effect on carboxylates production under elevated pCO_2 (1:1 molar ratio)	0-216	5	4.4	5
II-B	Effect of increasing substrate concentration on carboxylates production under elevated pCO_2	216-376	5	2.1	10
II-C	Dual substrate effect on carboxylates production under elevated pCO_2 (1:1 molar ratio) + ext. electron donor (formate – 5 mM)	376-596	5	2.0	5

[a] COD reactor corresponds to the intended concentration after feeding concentrated substrate solution to each reactor as described in the Materials and Methods

Experiment II: Mixed substrate (glycerol and glucose) conversion under elevated pCO_2

This experiment consisted of three sequential phases (II-A, II-B and II-C) with varying operational conditions under elevated pCO_2 to monitor shifts in product spectrum and community structure. Experiments corresponding to the main condition of interest, mixed substrate of glycerol and glucose (GG_CO2), were carried out in triplicates. Three single controls were included for individual glycerol and glucose conversion at 5 bar pCO_2 (GLY_CO2, GLU_CO2) and conditions of pressurized headspace with a non-reactive gas, *i.e.,* 5 bar using nitrogen (GG_N2). Due to limited reactor availability, controls were carried out in parallel as single reactors. This approach was chosen to avoid differences in the characteristics of the starting inoculum between the main condition and controls if otherwise decided to carry out triplicate controls as temporal sequential batches. Stainless steel reactors were inoculated with activated/acclimated inoculum (section 5.3.1), incubated at 35°C and continuously shaken at 110 rpm. Samples (2 mL liquid and 10 mL gas) were taken trice per day (first two days), twice per day (subsequent days) and once per day (last 3-4 days) to measure substrate conversion and formation of liquid and gaseous products in each phase. From liquid samples collected at the initial (t= 0 hours) and the endpoint of each phase, 250 µL were fixed with glutaraldehyde (1% v/v) and stored at 5°C for total cell determination by flow cytometry.

Phase II-A: Mixed substrate conversion

Operational conditions and experiment duration are reported in Table 5-2. Macro and micronutrients were proportionally dosed according to the increase in initial COD to prevent nutrient limitations. Buffer solution (150 mM as HCO_3^-) was provided in the feeding solution. Reactor headspace was adjusted to 5 bar pCO_2 following the methodology described in Chapter 2 and let equilibrate with the liquid phase for 2 hours. The experiment was terminated after complete substrate depletion and >70% soluble COD was recovered in liquid and gaseous products.

Phase II-B: Effect of high substrate concentration to increase S/X ratio

After the final liquid and gas sampling in experiment II-A, 20 mL were removed from all reactors via the liquid sampling port and replaced by fresh medium (40 mL in total) to start phase II-B at a moderate volumetric exchange ratio of 33%. Fresh medium for reactors GG_CO2 consisted of a concentrated solution to achieve substrate concentrations indicated in Table 5-2. Macro and micronutrients were proportionally dosed. The fresh medium was injected into the pressurized reactors employing a pressure-resistant, stainless steel, double-ended liquid sampling vessel with an effective volume of 100 mL (Swagelok, US). One side of the vessel was connected to a >99% compressed CO_2 bottle, set at 2 bar overpressure from the manometer reading. The other side was connected to one of the liquid sampling ports of

the pressure reactors controlled by a stainless-steel needle valve. Pressure deviations occurred after liquid extraction and new medium injection; thus, before restarting the experiment, headspace pressure was adjusted to 5 bar total pressure with >99% CO_2 or N_2. After one hour stabilization period, gas samples (10 mL) were taken to determine the initial gas composition. Experiment II-B was finalized after complete substrate depletion (10 days comparable with phase II-A), corresponding to a COD-recovery >50% in gaseous and liquid products.

Phase II-C: Effect of external electron donor (formate)

This experiment was initiated after final liquid and gas sampling in phase II-B. Reactor feeding and re-pressurization were carried out as previously described and under the operational conditions mentioned in Table 5-2. Additionally, formate (5 mM) was added to the concentrated feeding solution to evaluate the effect of additional electron donor in the product spectrum under elevated pCO_2.

5.2.3 Analyses

Physicochemical Analyses

Secondary metabolites, *i.e.,* acetate, propionate, butyrate and valerate were measured from filtered (0.45 μm) liquid samples by gas chromatography (7890A GC, Agilent Technologies, US) according to Muñoz Sierra et al. (2020). The detection limits for these compounds were 12, 16, 18 and 23 mg L^{-1}, respectively. The method and device settings also allowed alcohol determination (ethanol, propanol, butanol); however, amounts in our samples were below the detection limits (5, 2.5 and 2.5 mg L^{-1}, respectively). Glucose, glycerol, formate, succinate and lactate were measured in filtered (0.45 μm), acidified samples by high-performance liquid chromatography (LC-20AT; Shimadzu, Japan) using an Aminex HPX-87H (300 x 7.8 mm) column with sulphuric acid (5 mM) as eluent. Operational conditions were as follows: flow rate of 0.5 mL min^{-1}, RID-20A detector at 50°C for glucose and glycerol determination and SPD-20A detector at 40°C with wavelength at 210 nm for organic acids. According to prepared calibration curves, the detection limits were 50 mg L^{-1} for organic acids, glucose, and glycerol. Gas samples (10 mL) were measured by gas chromatography (7890A GC, Agilent Technologies, US) as described in Chapter 4. The pH, total and soluble COD, TSS and VSS, ammonium and total phosphorus were measured according to standard methods (American Public Health Association, 2017).

Total cell numbers

Total cell numbers were assessed by flow cytometry (AttuneTM NxT 2019; InvitrogenTM - ThermoFisher SCIENTIFIC, US) using Mili-Q as sheath fluid. Pre-treatment started with fixed samples vortexed and diluted (1:10) with 0.20-µm filtered phosphate-buffered-saline (PBS) solution. Next, diluted samples were sonicated (100 W) for 3 minutes at room temperature, vortexed, filtered at 20 µm with falcon, sterile, syringe-type filters (BD BIOSCIENCES, US) and serially diluted (1:1000). After pre-treatment, samples were placed in 96-well plates, stained with 5% SYBR® Green I (InvitrogenTM - ThermoFisher SCIENTIFIC, US) and incubated at 37°C for 20 min. The AttuneTM NxT 2019 was used in the BRxx configuration with two lasers: 480 nm and 635 nm. The channel used during the measurements corresponded to BL1 (530/30).

Microbial community analysis and statistical processing

Liquid samples (1.5 mL) were centrifuged at 12,298 RCF for 2 minutes and obtained biomass pellets were collected and stored at -80°C. According to the DNeasy UltraClean Microbial Kit (Qiagen, Germany). The DNA quality and quantity were controlled using Qubit® 3.0 DNA detection (Qubit dsDNA HS Assay Kit, Life Technologies, United States). Library construction, sequencing in the Illumina platform and preliminary data processing were done according to the internal protocol from Novogene (Hong Kong), as indicated in Chapter 4. Statistical analyses from microbial community data were carried out in R version 3.6.1 (http://www.r-project.org) (R Core Team 2019, 2019). Canonical correspondence analysis (CCA) was performed in R software (2019), employing the function *cca* from the vegan package (Oksanen et al., 2016). The CCA was selected for the analysis since it effectively assesses how environmental factors or process conditions (pCO_2, carboxylates concentration, formate) affect the microbial community structure (Ma et al., 2017). The significance of the ordination based on the selected environmental constraints and of the canonical axes was tested via permutation analysis (*anova.cca*). As a measurement of alpha diversity, community richness was calculated based on the total number of taxa after singleton removal, using the function *estimate_richness()* from the phyloseq package (McMurdie and Holmes, 2013). Significant differences ($p<0.05$) in beta diversity, calculated using the Bray-curtis distance measure (Bray and Curtis, 1957), were identified employing pair-wise Permutational ANOVA (PERMANOVA) using the *adonis* function (vegan). Spearman's correlation analyses were carried out using the function *cor.test ()*. Non-parametric analysis of variance was performed using the Kruskal-Wallis test for paired samples. Additionally, the variance in carboxylates concentration (acetate, propionate, butyrate), succinate concentration and cell density due to the main effects and interactions of three independent factors, *e.g.,* process conditions as gas

pressure, substrate concentration and additional electron donor was analyzed with the R package ARTool (Align-and-rank data for non-parametric factorial ANOVA) (Kay et al., 2021).

Estimation of substrate conversion rates

The application "Simple fit" from OriginPro (2019) was used to adjust non-linear or linear models to describe substrate conversion. Logistic models and linear regression have been previously reported in the literature as good approximations to describe soluble substrate utilization in AD (Coelho et al., 2020; Mawson et al., 1991). Simple linear regression and the logistic model were employed to fit the data in experiment I, whereas only the logistic model proved adequate to fit the data in experiment II.

The logistic model equation (Eq. 5-1) corresponds to

$$y = \frac{a}{(1+\exp(-k(x-x_C)))}, \tag{5-1}$$

where y represents the substrate concentration, a the maximal initial substrate concentration (mg L^{-1}), k is the logistic model constant comparable to the consumption rate (h^{-1}), x corresponds to time (h), and x_c is the time point where the sigmoid changes its curvature.

5.2.4 Calculations

Bioenergetics

Thermodynamic calculations were developed according to Heijnen and Kleerebezem (2010) (Chapter 2) to establish the energy feasibility of biochemical reactions possibly occurring in the pressurized experiments. Substrate and product concentrations corresponded to the physiological range (1mM) and corrections were applied only for mesophilic temperature (35°C) and initial pH (7.5).

Reactor pH under elevated pCO_2 and concentration of undissociated carboxylic acids

Due to limitations in the employed experimental set-up, the pH could not be continuously registered during the pressurized experiments. Therefore, we estimated the lowest equilibrium pH possibly achieved in the system after the equilibration of CO_2 concentrations between the headspace and the liquid medium based on Henry's law (Eq. 5-2) and the Henderson-Hasselbalch equation (Eq. 5-3). This pH value was used to calculate the expected undissociated carboxylic acid concentrations throughout experiment II based on the GC measurements for

acetate, propionate and butyrate. Equilibrium constants (k_H, K_a) were corrected for mesophilic temperature (35°C). The pKa values for acetic, propionic and butyric were obtained from Xiao et al. (2016) and for H_2CO_3* from Stumm and Morgan (1996). For the Spearman correlation analysis, the total concentration of undissociated acids was expressed in acetic acid equivalents (mg L^{-1}) according to the method described by Fu and Holtzapple (2010).

$$H_2CO_3^* = p_{CO_2} * K_H \quad (5\text{-}2)$$

$$pH = pK_a + log\frac{[A^-]}{[HA]} \quad (5\text{-}3)$$

5.3 Results

5.3.1 Mixed substrate conversion in batch operation under elevated pCO_2

End of Phase (EoP) product spectrum

In phase II-A, COD was converted to lactate (28-33%) during the first 21 hours in all treatments and controls except for GLY_CO2 (<1%). Intermediate succinate and formate represented less than 2% of the COD fed in all cases, except for GG_N2 (5%) (Figure 5-2B). After 209 hours, the EoP product spectrum for GG_CO2 was composed of propionate (30±5%), butyrate (22±4%) and acetate (3±1%) (Figure 5-1, expressed in mg COD). The EoP product spectrum in GG_N2 showed similarities with GG_CO2, except for a low butyrate contribution (3%) (Figure 5-1). In the case of GLY_CO2, the EoP product spectrum was dominated by propionate (62%), with a small acetate proportion (3%) (Figure 5-1); whereas GLU_CO2 showed a high proportion of butyrate (29%) and a lower proportion of propionate (13%) and acetate (4%) (Figure 5-2D). Biomass decay, calculated as the difference between initial and final VSS concentrations, occurred in all treatments during phase II-A (Figure 5-1). Regarding the EoP gaseous products, in GG_CO2, approximately 19±3% of the COD-fed accounted as CH_4. In GG_N2, COD-CH_4 corresponded to 32% of COD-fed, and for GLY_CO2 and GLU_CO2 accounted for 5 and 18%, respectively.

Increased substrate concentrations during phase II-B did not cause important changes in the EoP product spectrum in GG_CO2. After correcting for carried-over concentration from phase II-A, EoP product spectrum was composed of propionate (24±2%), butyrate (2±0%) and acetate (2±0%) (Figure 5-1). In the control GG_N2, it was composed of propionate (17%) and acetate (1%), while butyrate was not detected (Figure 5-1). In GLY_CO2, COD was primarily transformed to propionate (43%), whereas in GLU_CO2, to a mixture of butyrate (35%), propionate (6%) and acetate (1%) (Figure 5-1). The CH_4 production accounted for 15±2%, 2

and 17% of the COD-fed in the case of GG_CO2, GLY_CO2 and GLU_CO2, respectively. The control GG_N2 showed a decrease in the recovery of COD as CH_4 (only 15%).

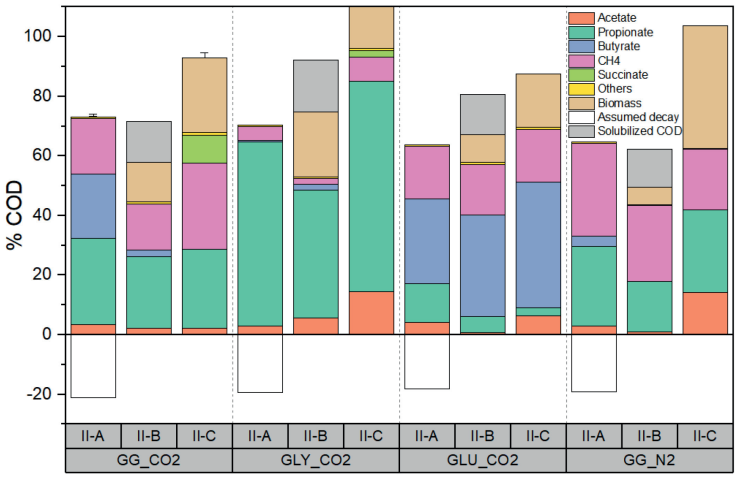

Figure 5-1: End of phase (EoP) product spectrum expressed as percentage of the COD fed in phases II-A, II-B and II-C in Experiment II. Data is presented for the mixed substrate treatments (GG_CO2) at 5 bar pCO_2, mix substrate control at 5 bar pN2 (GG_N2) and single substrate controls (glucose GLU_CO2 and glycerol GLY_CO2) at 5 bar pCO_2.

Noteworthy differences were observed in the EoP product spectrum after adding formate and reducing the substrate concentration to reduce the S/X ratio in phase II-C. An increase in succinate production (10±2% from COD fed) was detected in GG_CO2 (Figure 5-1). Succinate accumulated until the end of phase II-C after 214 hours. Lactate (8±2%) was detected in the first 16 hours and further converted to carboxylates (Figure 5-2). The EoP product spectrum in GG_CO2 included propionate (27±7%) and acetate (2±0.4%), while no butyrate was detected (Figure 5-1). The control GG_N2 did not show the same trend regarding lactate and succinate. Initially, 18% of the COD was directed to lactate and only 2% to succinate (Figure 5-2). By the end of phase II-C, both metabolites were not detected. The EoP product spectrum in GG_N2 was composed of propionate (28%), acetate (14%) but no additional butyrate. GLY_CO2 showed a COD recovery of 112% after discounting for carried over COD from phase II-B (Table 5-3) and its EoP product spectrum included propionate (85%) and acetate (17%). In the control GLU_CO2, the EoP product spectrum corresponded to butyrate (42%), propionate (3%) and acetate (6%). An increase in acetate was observed in all conditions, except for GG_CO2, which showed acetate levels comparable to phases II-A and II-B (Figure 5-1). CH_4

in GG_CO2 accounted for 29±10% of the COD-fed. In reactors GLY_CO2, GLU_CO2 and GG_N2, CH_4 production accounted for 10, 18 and 20% of the COD fed, respectively.

In GG_CO2 treatments, high propionate production was hypothesized as an effect of mixed substrate and elevated pCO_2 during experiment II; however, there were no significant differences ($p=0.32$) in propionate concentrations between GG_CO2 and GG_N2 (paired samples Wilcoxson test). In contrast, butyrate concentrations were significantly different ($p<0.0001$) in all phases of experiment II. The Aligned Rank Transform test was used to evaluate if independent factors, *e.g.,* process conditions or their interaction effects were significant to explain the differences in carboxylate concentrations and cell density in experiment II. When analyzing pCO_2 as the main effect, this factor was non-significant for carboxylates and succinate production, as evidenced by the p-values (Table 5-4). In contrast, the interaction effect between pCO_2 and process conditions was significant to explain differences in propionate and butyrate production (pCO_2 - substrate concentration) and succinate production (pCO_2 - additional electron donor) (Table 5-4).

Cell density

During phase II-A, a decrease in total cell density of 42±14, 49 and 57% was established for GG_CO2, GLY_CO2 and GG_N2, respectively, whereas GLU_CO2 showed a moderate increase (25%) (Figure 5-3). In phase II-B, the measured cell density was corrected for dilution, due to medium refreshing. A steep decrease of 70±8% in cell density was observed in GG_CO2, compared to initial values. A similar sharp decrease was registered in reactors GLY_CO2 and GLU_CO2, corresponding to 91 and 76%, respectively. Conversely, GG_N2 showed a slight reduction (7%).

Table 5-3: The COD balance for the different cycles in fed-batch experiments with dual substrate (GG_CO_2) at 5 bar pCO_2, control at 5 bar pN_2 (GG_N2) and individual substrate controls with only glucose (GLU_CO_2) or glycerol (GLY_CO_2). The standard deviation of three biological replicates is included only in the case of GG_CO_2 treatments.

Sample	Phase	Acetate (mg COD)	Propionate (mg COD)	Butyrate (mg COD)	CH_4 (mg COD)	Succinate (mg COD)	Others (mg COD)	Biomass[a] (mg COD)	Total (mg COD)	COD fed (mg)	Recovered fraction from COD substrate[b]	Recovered fraction from COD substrate (included solubilized COD)[c]	COD fed + carry over from previous phase (mg)
GG_CO2 (n=3)	II-A	25.26± 8.6	221.18± 31.3	163.86±3 1.3	142.80± 23.9	0.00± 0.0	3.31± 3.1	0.00±0.0	556.41± 56.7	762±28	0.73± 0.1	0.73± 0.1	779.21± 26.9
	II-B	20.57± 2.9	224.44± 32.9	20.11± 59.9	144.51± 16.2	0.00± 0.0	7.06± 2.3	123.92± 45.2	540.60± 88.6	935±143	0.58± 0.1	0.71± 0.1	1150.08± 78.6
	II-C	12.26± 2.4	155.70± 41.5	0.00± 0.0	169.66± 70.7	55.20± 6.4	5.50± 2.7	147.11± 42.0	545.43± 142.9	586±40	0.93± 0.3	0.93± 0.3	1032.26± 65.3
GLY_CO2 (n=1)	II-A	24.39	497.24	4.53	36.86	0.00	3.36	0.00	566.38	806	0.70	0.70	814.03
	II-B	40.18	310.46	14.02	13.88	0.00	3.44	158.36	540.34	722	0.75	0.92	1226.81
	II-C	84.02	410.60	0.00	47.28	13.53	2.92	94.42	652.79	582	1.12	1.12	1129.64
GLU_CO2 (n=1)	II-A	29.89	94.19	206.14	126.83	0.00	4.83	0.00	461.89	724	0.64	0.64	745.14
	II-B	6.44	41.18	261.65	128.86	0.00	5.97	71.45	515.56	768	0.67	0.81	1098.94
	II-C	36.91	16.00	244.83	101.94	0.00	4.79	103.14	507.60	581	0.87	0.87	1071.78
GG_N2 (n=1)	II-A	20.38	191.72	23.73	222.17	0.00	3.34	0.00	461.34	713	0.65	0.65	728.69
	II-B	9.14	145.75	0.00	219.17	0.00	2.57	50.69	427.32	862	0.50	0.62	1216.32
	II-C	87.79	171.39	0.00	124.81	0.00	2.57	253.33	639.89	617	1.04	1.04	846.69

[a] Biomass was calculated as the difference between initial and final VSS concentration in each phase and converted to COD using a conversion factor of 1.42 g COD/g VSS

[b] This fraction corresponds to the COD recovered as end of phase (EoP) products considering only the soluble COD from the substrate

[c] This fraction corresponds to the COD recovered as end of phase (EoP) products considering that a theoretical 80% of the COD from decay in phase II-A became solubilized into phase II-B

d This fraction corresponds to the COD recovered as end of phase (EoP) products considering COD from substrate and carried over carboxylates / organic acids from the immediate previous phase

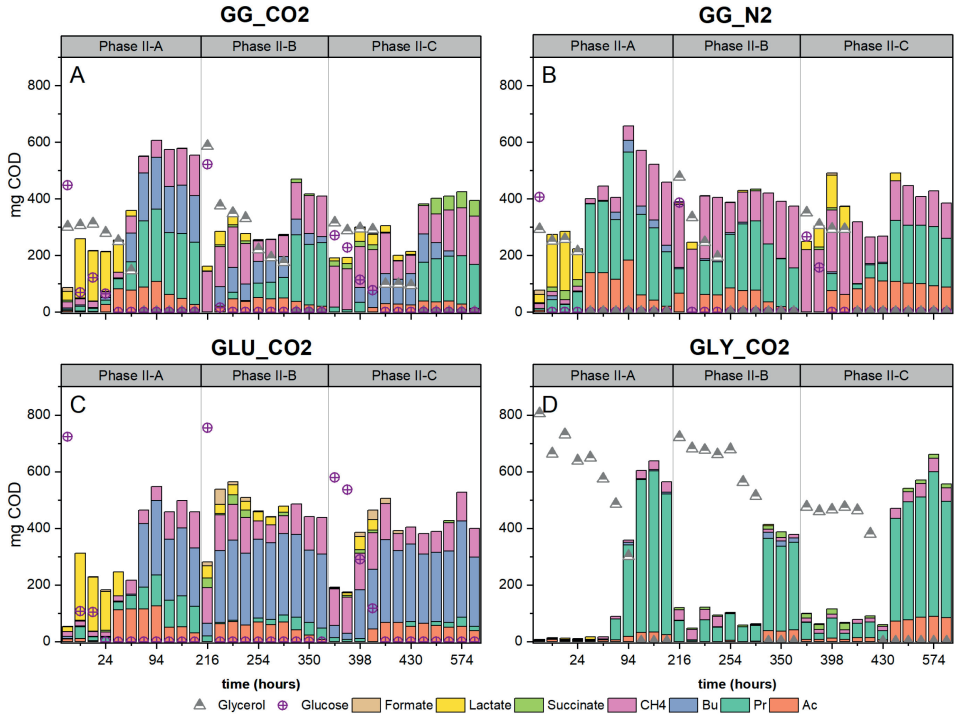

Figure 5-2: Product spectrum over time in the different phases (II-A, II-B and II-C) of Experiment II. Data is presented for mixed substrate treatments at 5 bar pCO_2 (GG_CO2) (A), mixed substrate control at 5 bar pN_2 (GG_N2) (B) and single substrate controls (glucose GLU_CO2 and glycerol GLY_CO2) (C and D). Abbreviations correspond to methane (CH_4), butyrate (Bu), propionate (Pr) and acetate (Ac).

Table 5-4: Summary of Aligned Rank Transform test for the main and interaction effects of elevated partial pressure of CO_2 (pCO_2) or N_2 (pN_2), substrate concentration and addition of external electron donor (formate) in carboxylates production and cell density during Experiment II.

Independent Factor		*pCO_2*		*Substrate concentration (S/X ratio)*	*pCO_2*		*External electron acceptor*
Interaction			**pCO_2:Substrate concentration**			**pCO_2:External electron acceptor**	
Dependent variable	Propionate (mg COD L^{-1})	0.81	0.94	****	0.78	0.07	0.59
	Butyrate (mg COD L^{-1})	0.37	****	****	0.62	0.11	0.76
	Acetate (mg COD L^{-1})	0.25	0.31	0.13	0.31	0.43	0.36
	Succinate (mg COD L^{-1})	0.22	0.18	0.67	0.26	****	****
	Cell density (cells mL^{-1})	0.77	0.09	*	0.87	0.75	****

Significance level *p<0.05,**p<0.01,***p<0.001, ****p<0.0001

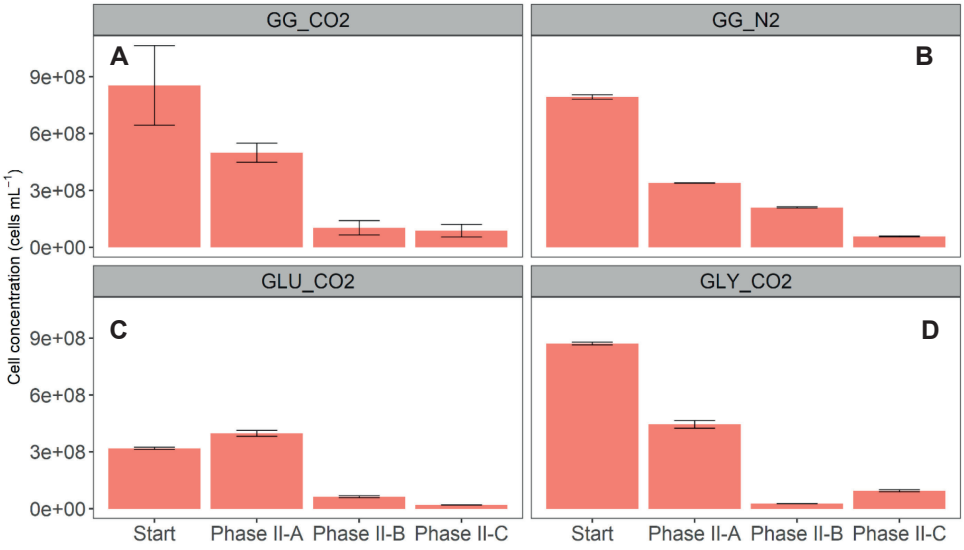

Figure 5-3: Total cell density per sub-experiment for treatment with dual substrate glycerol-glucose (GG_CO_2) at 5 bar carbon dioxide partial pressure (pCO_2), control at 5 bar nitrogen partial pressure (pN_2) (GG_N2) and controls for conversion of individual substrate as glucose (GLU_CO_2) and glycerol (GLY_CO_2) at 5 bar pCO_2.

The cell density was positively affected by formate addition and reduction in substrate concentration to lower the S/X ratio in phase II-C, with the final biomass in GG_CO2 increasing by 28±5%. In GLY_CO2, there was an even more predominant positive effect, since cell density experienced a five-fold increase compared to the initial concentration (Figure 5-3D). However, this effect did not appear in GLU_CO2, where a substantial decrease in cell density was assessed, *i.e.,* 53%. A similar observation was registered for control GG_N2, where the cell density decreased by 59%, higher than values observed in phase II-B.

Cell densities were significantly different between the start and end points of phase II-A (p=0.0008), II-B (p=0.0003) and II-C (p=0.00001). The Aligned Rank Transform test showed that substrate concentration and addition of external electron donor were the main effects explaining the differences in cell density, whereas pCO_2 did not. However, the interaction effects pCO_2 - substrate concentration and pCO_2 - additional electron donor were significant to explain differences in cell densities in experiment II (Table 5-4).

Substrate conversion rate

In experiment I, the reference substrate conversion rate under the provision of single or mixed substrate at 5 bar pCO_2 was determined using the activated inoculum without previous exposure to pressurized conditions. The logistic model, used to describe glucose conversion, showed three times faster glucose conversion at lower initial concentrations in the mixed substrate treatment than the single substrate (Figure 5-4A, Table 5-5). Conversely, the linear regression model showed that glycerol conversion was 1.6 times higher in the only glycerol condition than in the mixed substrate treatment (Figure 5-4B, Table 5-5).

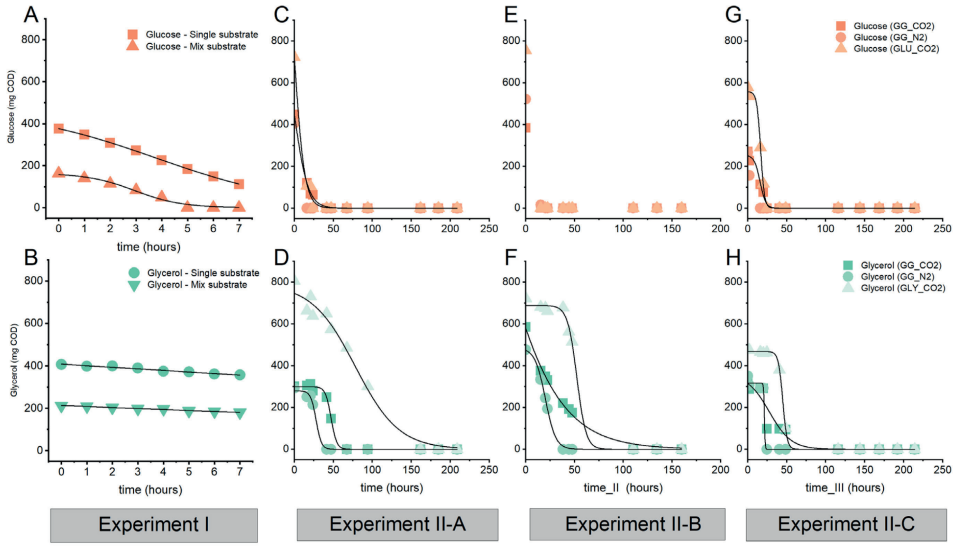

Figure 5-4: Glucose (A) and Glycerol (B) conversion in single and mixed substrate treatments during Experiment I at 5 bar pCO_2. Glucose and glycerol conversion in phases II-A (C and D), II-B (E and F) and II-C (G and H) during Experiment II. Experimental data is presented as discrete symbols for mix substrate treatments (GG_CO2) at 5 bar pCO_2, mix substrate control at 5 bar pN_2 (GG_N2) and single substrate controls (glucose GLU_CO2 and glycerol GLY_CO2). Modelled data according to the description provided in Table 5.3 is presented as a continuous black line. Substrate is expressed in mg COD after volume correction due to liquid sampling in the reactors during each phase.

In phase II-A of experiment II, the logistic model provided a good approximation (adjusted R^2 > 0.98) to describe substrate conversion in all cases, except for glucose conversion in GG_N2. The experimental data corresponding to GG_N2 are presented in Figure 5-4 (subplots C, E and G), but rates were not calculated due to the limited number of useful data to describe the curve shape in the interval 0-50 hours. Rates of glucose conversion were comparable between GG_CO2 and GLU_CO2 (Table 5-5). Glycerol conversion was similar between GG_CO2 and

GG_N2, representing an eightfold increase compared to GLY_CO2 (Table 5-5). It is worth mentioning that GLY_CO2 started with a higher substrate concentration due to a technical failure in feeding preparation, but as evidenced in Figure 5-2, complete substrate depletion was achieved after 160 hours. Moreover, since the standard deviation in COD fed during phase II-A was lower than 10%, reasonable comparisons between treatments and controls can be performed.

Table 5-5: Estimated glucose and glycerol conversion rates calculated with the logistic model (in h^{-1}) and simple linear regression (in mg substrate h^{-1}) for a) treatments with single and mixed substrate in Experiment I and b) single substrate controls at 5 bar pCO_2 (glucose GLU_CO2 and glycerol GLY_CO2), mix substrate control at 5 bar pN_2 (GG_N2) and treatments with mix substrate at 5 bar pCO_2 (GG_CO2) in Experiment II.

Experiment	Treatment	Phase	Model	Glucose conversion rate + (adjusted R^2)	Glycerol conversion rate + (adjusted R^2)	Rate Units
I	Single substrate - Glucose		Logistic	-0.36*** (0.95)		k (h^{-1})
	Single substrate – Glycerol		Linear regression		-7.4*** (0.96)	(mg Glycerol h^{-1})
	Mix substrate		Logistic + linear regression	-1.10*** (0.95)	-4.7*** (0.99)	k (h^{-1}) (mg Glycerol h^{-1})
II	Single substrate - Glucose (GLU_CO2)	II-A	Logistic	-0.15** (0.99)		k (h^{-1})
		II-B		NA		
		II-C		-0.41*** (0.99)		
	Single substrate – Glycerol (GLY_CO2)	II-A			-0.04*** (0.98)	
		II-B			-0.21** (0.99)	
		II-C			-0.36*** (0.99)	
	Mixed substrate (GG_CO2)	II-A		-0.12*** (0.99)	-0.27*** (0.99)	
		II-B		NA	-0.03*** (0.99)	
		II-C		-0.27** (0.98)	-0.07* (0.89)	
	Mixed substrate (GG_N2)	II-A		NA	-0.29** (0.99)	
		II-B		NA	-0.19*** (0.99)	
		II-C		NA	-1.95* (0.99)	

Significance level *p<0.05,**p<0.01,***p<0.001
NA: Not available

During phase II-B, glucose conversion occurred faster than in II-A, with glucose being not detectable after 20 hours in all cases (Figure 5-4E). Consequently, accurate rate estimation was not possible because of the limited useful data points. Glycerol conversion rate in GG_CO2 was lower than in GG_N2 (Table 5-5). Conversely, rates in GLY_CO2 and GG_N2 were comparable but differentiated by a noticeable lag phase approximately corresponding to 50 hours (Table 5-5).

In phase II-C, the reduction in substrate concentration and adding 5 mM formate were beneficial to achieve a faster substrate conversion. Although the glucose conversion rate in GG_CO2 was lower than GLU_CO2, both rates were higher than in phase II-A but still with a noteworthy lag phase approximately corresponding to 20 hours. Glycerol conversion rates also improved; for example, in GG_CO2, the rate was faster than in phase II-B, but remained lower than the calculated value in II-A (Table 5-5). In GG_N2 and GLY_CO2, the glycerol conversion rates were faster than in phases II-B and II-A (Table 5-5).

5.3.2 Microbial community dynamics

During experiment II, the effect of sequential changes in operational conditions on microbial community structure and its relation with shifts in product spectrum under elevated pCO_2 was examined. Microbial community analysis resulted in an average of 140,365 ± 6,153 total reads per sample and 2230 OTUs in total. After singleton removal, OTUs were reduced to 1935. Bacteria and Archaea corresponded to 80% and 20% of total processed reads in the original inoculum. The bacterial community in the inoculum was composed of Anaerolineae (77%), Actinobacteria (6%) and Clostridia (5%) at the class level. The archaeal community in the inoculum primarily included Methanomicrobia (81%) and Methanobacteria (19%). Changes in the relative abundance of Bacteria and Archaea during phases II-A, II-B and II-C are presented in Table 5-6.

Table 5-6: Relative abundance of total Bacteria and Archaea for the different experimental conditions in Experiment II. Values for treatment GG_CO_2 correspond to the average of (n=3) biological replicates

Condition	**GG_CO_2**			**GG_N2**			**GLY_CO_2**			**GLU_CO_2**		
Experiment	II-A	II-B	II-C	II-A	II-B	II-C	II-A	II-B	II-C	II-A	II-B	II-C
Archaea (%)	5.5±1.3	18.1±1.4	20.3±2.3	3.8	19.3	9.7	14.1	8.8	18.2	16.0	13.9	23.2
Bacteria (%)	94.5±1.2	81.9±1.4	79.7±0.0	96.1	80.7	90.3	85.9	91.2	81.8	84.0	86.1	76.8

In phase II-A, the bacterial community of GG_CO2 was mainly composed of class Anaerolineae (35±8%), Negativicutes (family Veillonellaceae) (27±20%), Clostridia (19±16%) and Thermotogae (6±0%). GG_N2 included Clostridia (42%), Anaerolineae (37%) and Thermotogae (7%). GLY_CO2 comprised Negativicutes (37%), Anaerolineae (32%) and Clostridia (13%). GLU_CO2 showed a predominance of Anaerolineae (51%), Clostridia (28%) and Actinobacteria (8%) (Figure 5-5A). In phase II-B, Anaerolineae became predominant in GG_CO2 (62±1%), being followed by Actinobacteria (11±1%) and Clostridia (12±2%). GG_N2 showed an almost complete predominance of Anaerolineae (72%). The major classes in GLY_CO2 corresponded to Anaerolineae (51%), Negativicutes (27%) and in GLU_CO2 to Anaerolineae (69%), Clostridia (11%) and Actinobacteria (9%) (Figure 5-5A). Noticeable changes in the community were observed in phase II-C: GG_CO2 still showed Anaerolineae predominance (50±6%), but the abundance of Clostridia (20±14%) and Negativicutes (11±9%) increased. Synergistia (6±4%) also showed higher abundance than phases II-A and II-B. In GG_N2, Clostridia (52%) and Anaerolineae (37%) were predominant and Synergistia exhibited low abundance (2%). Clostridia (36%) dominated in GLY_CO2, followed closely by Anaerolineae (27%), Negativicutes (23%) and Synergistia corresponded to 4%. In GLU_CO2, bacterial community composition resembled phase II-A: Anaerolinea (54%), Clostridia (32%), but Synergistia accounted for 5% (Figure 5-5A)

The dominant classes in the archaeal community were Methanomicrobia and Methanobacteria, with fluctuating abundances throughout experiment II. After phase II-A, Methanomicrobia and Methanobacteria accounted for 76±4% and 23±4% in GG_CO2. In GG_N2, their abundances were 66 and 32%, respectively. In GLY_CO2 and GLU_CO2, abundances were similar: 59% vs. 41% (Figure 5-5B). In phase II-B, abundances remained comparable to phase II-A for GG_CO2, GLY_CO2 and GLU_CO2. However, GG_N2 showed an increased abundance of Methanomicrobia (80%) (Figure 5-5B). In phase II-C, some slight changes in the abundance were observed. Methanomicrobia corresponded to 76±1% and Methanobacteria to 23±1% in GG_CO2. Relative abundances of both families in GG_N2, GLU_CO2 and GLY_CO2, corresponded to 73-27%, 67-32% and 72-28%, respectively (Figure 5-5B) The trends in group predominance in the bacterial and archaeal communities were also validated by absolute taxon abundance with flow cytometry data according to Props et al. (2017) to highlight the effect of changes in cell density during experiment II (Figure 5-6).

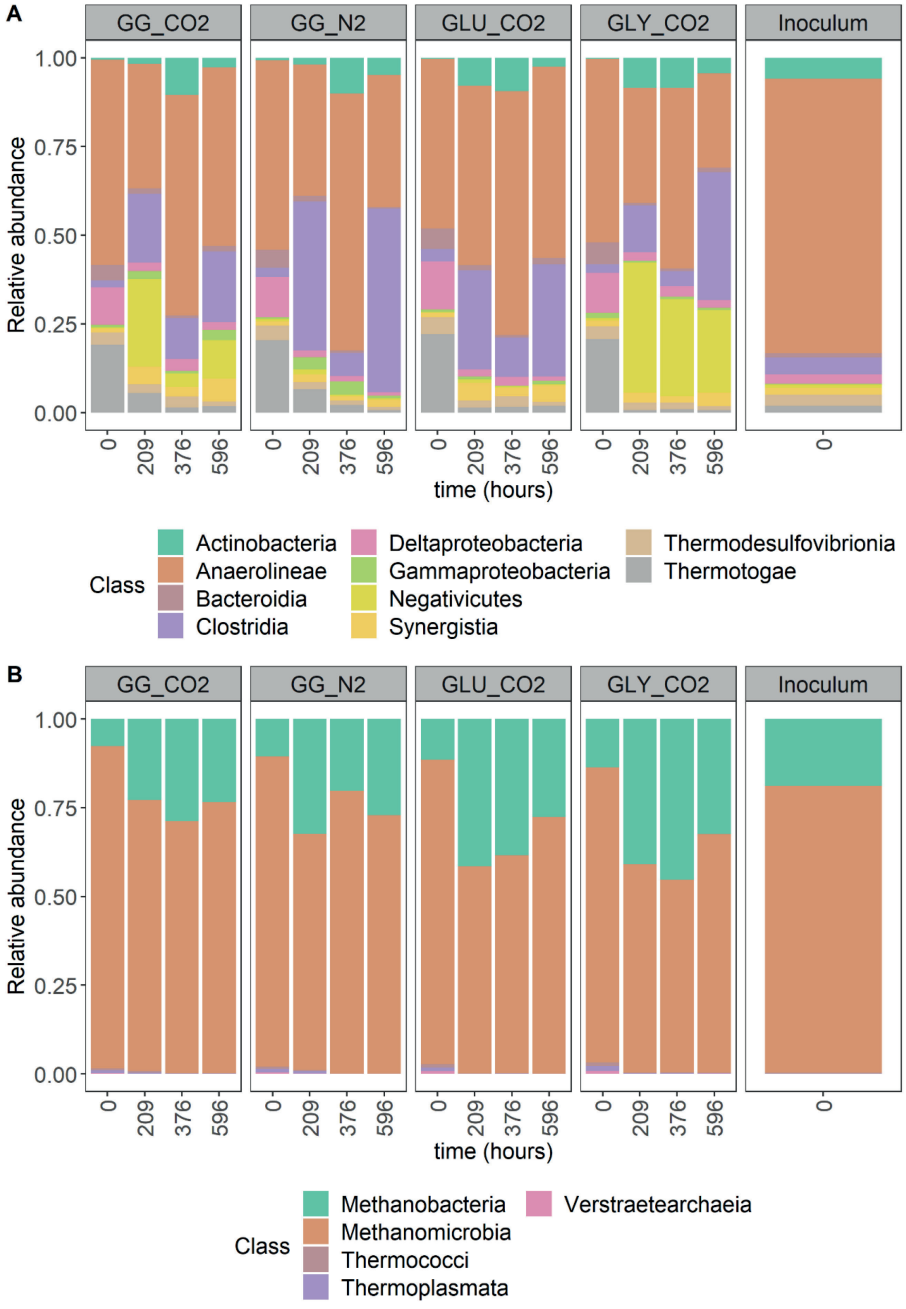

Figure 5-5: Relative abundances of the top 10 most abundant classes across all samples in A) bacterial community and the top 5 most abundant classes in B) archaeal community. The horizontal axis includes the time points where samples were taken and that correspond to the start of experiment II and the end of phase II-A (209 hours), II-B (376 hours) and II-C (596 hours).

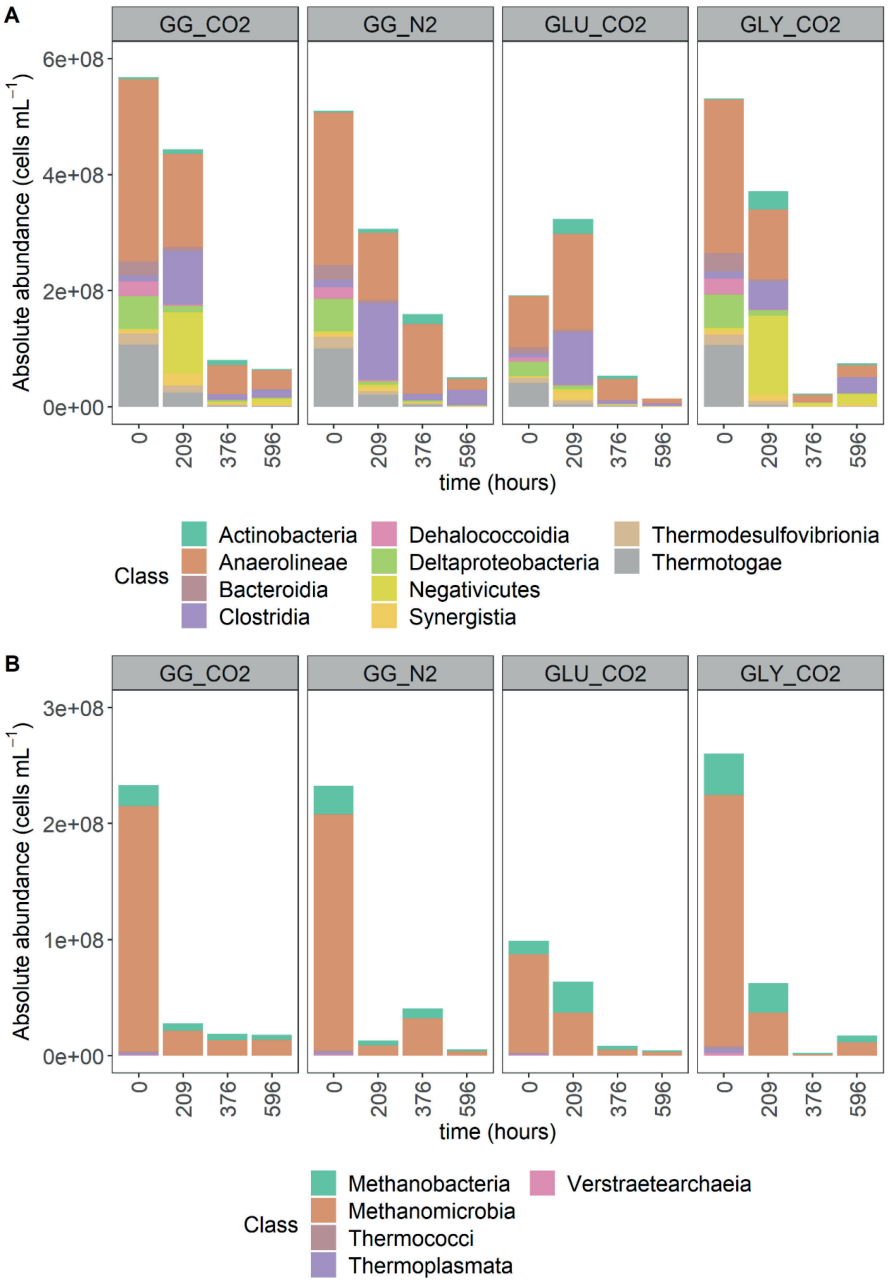

Figure 5-6: Absolute abundances of the top 10 most abundant classes across all samples in A) bacterial community and the top 5 most abundant classes in B) archaeal community. The horizontal axis includes the time points where samples were taken and that correspond to the start of experiment II and the end of phase II-A (209 hours), II-B (376 hours) and II-C (596 hours).

Significant differences were not found in bacterial community richness (p=0.18), but they were found in the archaeal community (p=0.005) when comparing initial and final richness in experiment II. In terms of the beta diversity, significant differences were not found between the bacterial and archaeal community when grouped by type of substrate (p=0.78 and p=0.83) and gas used for headspace pressurization (p=0.63 and p=0.85), respectively. However, bacterial and archaeal communities were significantly different when considering the presence and absence of formate as an additional electron donor (p=0.001 and p=0.03). Total cell density, as the *proxy* of biomass growth, measured carboxylate concentrations, external electron donor (formate) and pCO_2 were included in a Canonical Correspondence Analysis (CCA) to highlight possible correlations between process conditions and the microbial community structure. The constrained variables selected for constructing the model explained 70% (p=0.001) of the variance in the microbial community (Figure 5-7).

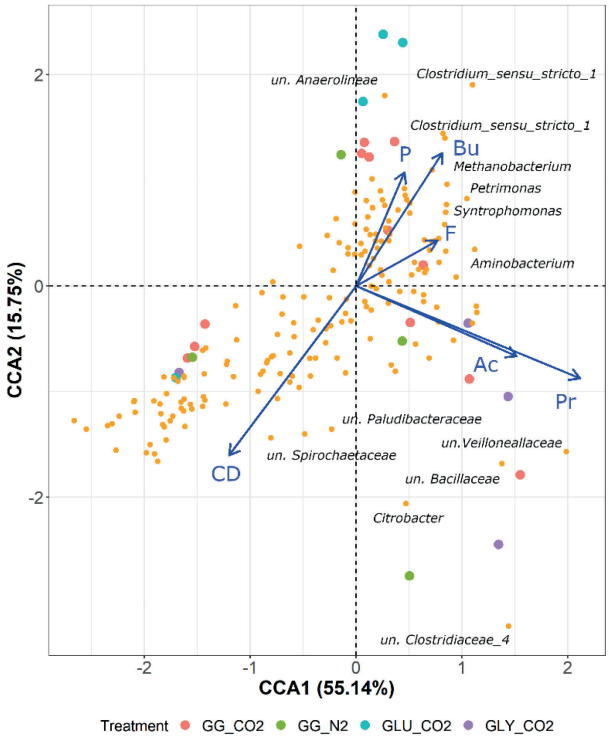

Figure 5-7: Canonical correspondence analysis (CCA) of the microbial community ordinated at the OTU level. Samples correspond to mixed substrate (GG_CO2) at 5 bar pCO_2, mixed substrate control at 5 bar pN_2 (GG_N2) and single substrate controls (glucose GLU_CO2 and glycerol GLY_CO2). Significant correlations between community composition and operational conditions: elevated pCO_2 (P), presence of formate as additional electron donor (F), carboxylate concentrations (acetate (Ac), propionate (Pr), butyrate (Bu)) and cell density concentrations (CD normalized to the $\log_{10}$) are depicted as blue arrows.

5.3.3 Undissociated carboxylic acids

High substrate concentration leading to an increase in the S/X ratio (Phase II-B) could be compatible with enhanced acid production due to disparities in acid production and consumption. Combined with CO_2 dissolution in each phase, it could have led to pH fluctuations despite the provided high buffer concentration. Lowered pH could increase the concentration of undissociated carboxylic acids, which could inhibit microbial activity. A pH value of 6.5 was calculated (Section 1.2.4 Eqs. 5-1 and 5-2) as the lowest equilibrium value achieved in phase II-B, and we used it to estimate the time evolution of undissociated acetic (HAc), propionic (HPr) and butyric (HBu) acids throughout experiment II as depicted in Figure 5-8.

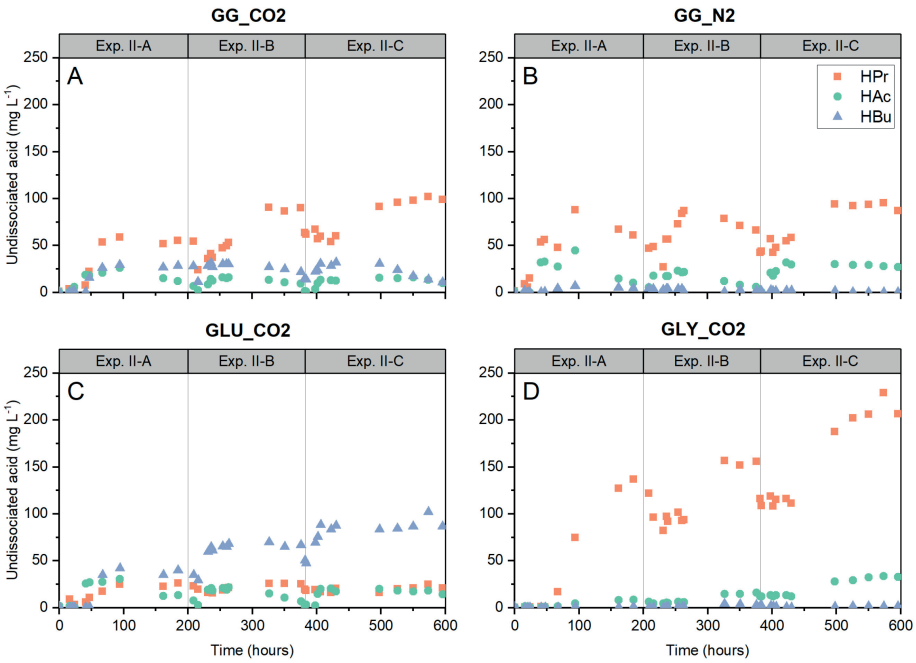

Figure 5-8: Evolution of calculated undissociated carboxylic acid concentrations (acetic - HAc, propionic- HPr and butyric - HBu acids) during experiment II. Data is presented for mixed substrate treatments at 5 bar pCO_2 (GG_CO2) (A), mixed substrate control at 5 bar pN_2 (GG_N2) (B) and single substrate controls (glucose GLU_CO2 and glycerol GLY_CO2) (C and D).

Undissociated carboxylic acid concentrations were employed to investigate possible correlations with changes in the microbial community structure. A significant negative correlation between total undissociated carboxylic acids (expressed as mg HAc equivalents

L^{-1}) and the log-absolute abundance of total archaea (r_s=-0.71, p=0.002) (Figure 5-9A) was found. Both predominant classes, Methanomicrobia and Methanobacteria, were negatively correlated with undissociated carboxylic acids (r_s=-0.73, p=0.001 and r_s=-0.58, p=0.019) (Figure 5-9, B and C).

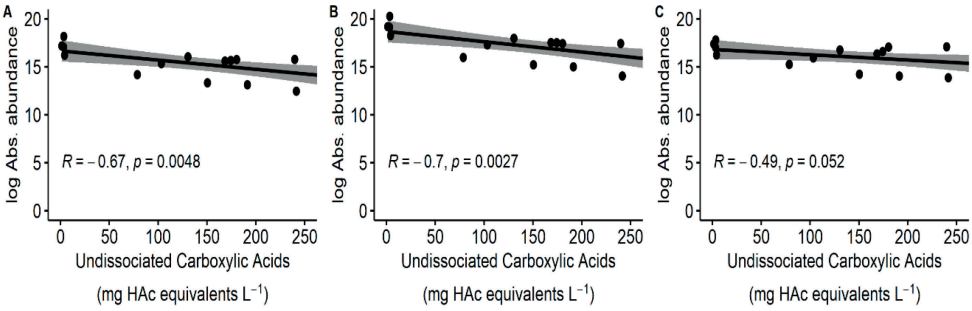

Figure 5-9: Spearman correlation between calculated undissociated carboxylic acids, expressed as mg acetic acid (HAc) equivalents L^{-1}, in Experiment II and log-absolute abundances of A) Total Archaea, B) Class Methanomicrobia and C) Class Methanobacteria.

5.4 Discussion

5.4.1 Interaction effects between elevated pCO_2 - operational conditions steer product formation in anaerobic processes

Previous research has suggested a potential steering role of elevated pCO_2 in anaerobic processes, *e.g.,* AD and mixed culture fermentation, particularly concerning propionate production (Lindeboom et al., 2016). Observed differences in the production/conversion of propionate and butyrate in GG_CO2 and GG_N2 during all phases align with this proposition. However, these differences cannot be exclusively ascribed to elevated pCO_2 since disparities in methanogenic activity also occurred due to the pressurization process when comparing pressurized treatments and atmospheric controls (Chapter 4). The decreased methanogenic activity could have led to the accumulation of reducing equivalents, eventually impacting pathway feasibility. Higher CH_4 production occurred in GG_N2 than in GG_CO2 during phases II-A and II-B (Figure 5-2, B and A), which aligns with results previously presented for glucose and glycerol conversion with non-adapted inoculum at 5 bar pN_2 / pCO_2 (Chapter 4). In Chapter 4, a reduction (53 to 85%) in the final mg COD-CH_4 was reported when reactor

headspace was pressurized with CO_2 rather than N_2. However, in phase II-C, the obtained CH_4 became similar in GG_CO2 and GG_N2, due to a decrease in the methanogenic activity in GG_N2 (Table 5-3) and resumed methanogenic activity in GG_CO2 after decreasing the S/X ratio and adding formate (Figure 5-2A and B). These changes in methanogenic activity occurred despite the overall reduction in absolute archaeal abundances (Figure 5-6B).

Several roles can be attributed to formate in the methanogenesis reestablishment during phase II-C. Formate can be indistinctively used by some hydrogenotrophic methanogens (Dolfing et al., 2008; Stams and Plugge, 2009) and acetogenic bacteria, as an electron donor (Ramió-Pujol et al., 2015). Acetogenic bacteria have shown a higher formate affinity than methanogens when cultivated together; thus, at low formate concentrations, acetogenic bacteria could outcompete methanogens regarding formate utilization (Asanuma et al., 1999). Under conditions of elevated pCO_2, methanogenesis in GG_CO2 could have been reestablished via a "mediated" process. Here formate would have been used by acetogenic bacteria to fix CO_2 into acetate, which, together with acetate from glucose fermentation (Eqs. 3,4,6 Table 5-7), was subsequently consumed by acetoclastic methanogens. The concomitant increase in the absolute abundance of *Clostridium* and *Veillonella* spp. and class Methanomicrobia (genus *Methanosaeta*) in treatments GG_CO2 during phase II-C supports this postulate (Figure 5-6).

The product spectrum in GG_CO2 closely resembled the expected profile from the independent conversion of glycerol and glucose at 5 bar pCO_2, with propionate and butyrate being present (Figure 5-1). Butyrate rather than propionate concentrations were significantly different between GG_CO2 and GG_N2 (see Results). At first, this result diverges from observations presented earlier (Ceron-Chafla et al., 2021; Lindeboom et al., 2016), and it does not align with a direct link between elevated pCO_2 and, *e.g.,* high propionate levels. However, this finding evidences that the relation pCO_2-product spectrum is more complex than initially proposed. The product profile does not seem to be defined by an isolated effect of pCO_2, but rather by interaction effects with operational conditions, such as type of substrate, S/X ratio and presence of additional electron donors (Table 5-2). Furthermore, these changes in the intermediate product spectrum result from a trade-off in terms of reduced substrate consumption rate and establishment of lag-phases due to elevated pCO_2 (Table 5-5, Figure 5-4).

When analyzing the product spectrum for the individual substrates, enhanced propionate production from glycerol was observed in control GLY_CO2 at 5 bar pCO_2 (Figure 5-1). Elevated pCO_2 most likely stimulated carbon fixation in the reductive side of the TCA cycle towards propionate via the higher activity of enzymes, such as pyruvate carboxylase (Parizzi et al., 2012), CoA transferase (Zhang and Yang, 2009) and PEP carboxykinase (Tan et al., 2013). In contrast to earlier results (Ceron-Chafla et al., 2021; Lindeboom et al., 2016), propionate was the main metabolite from glucose conversion under 5.0 and 6.2 bar pCO_2,

respectively, GLU_CO2 presented high butyrate and acetate levels. Increased butyrate production in GLU_CO2 and GG_CO2 could be attributed to the presence of excess acetate and carbohydrates enhancing the activity of butyryl-CoA: acetate CoA-transferase, a key enzyme in the pathway of certain *Clostridium* spp. (van Lingen et al., 2016) (Eq. 5 Table 5-7). Excess acetate may be ascribed to reduced consumption by acetoclastic methanogens, since absolute archaeal abundances were negatively impacted by elevated CO_2 (Figure 5-6B), high S/X ratio (phase II-B) and increasing concentrations of undissociated carboxylic acids (Figure 5-7). *Clostridium* spp. were a predominant bacterial group in GLU_CO2 (Figure 5-5A) and showed a strong positive correlation with butyrate concentrations (Figure 5-7). However, they were less predominant in prior glucose experiments (Ceron-Chafla et al., 2021) and DGGE results from Lindeboom et al. (2016), which helps to explain differences in the reported product spectrum composition.

Table 5-7: Biochemical reactions possibly involved in glucose and glycerol anaerobic conversion experiment at conditions of elevated pCO_2= 5bar, initial pH= 7.5 and T=35°C. The Gibbs free energy change (ΔG_{cat}^1) was corrected for pH and calculated according to (Heijnen and Kleerebezem, 2010). Stoichiometries are adapted from (Fast and Papoutsakis, 2012), (Lee and Rittmann, 2009), (Zeng et al., 1993), (González-Cabaleiro et al., 2016)

No.	Catabolic reactions	ΔG_{cat}^1 (kJ/ Rxn)
1	$Glucose \rightarrow 2\ Lactate + 2\ H^+ + 2\ ATP$	-202.8
2	$Glucose \rightarrow Butyrate + H^+ + 2\ H_2 + 2\ CO_2 + 3\ ATP$	-267.0
3	$Glucose \rightarrow 0.67\ Acetate + 0.67\ Butyrate + 1.33\ H^+ + 2.67\ H_2 + 2\ CO_2 + 3.33\ ATP$	-307.8
4	$Glucose \rightarrow 0.67\ Acetate + 1.33\ Propionate + 2\ H^+ + 0.67\ CO_2 + 2.67\ ATP$	-317.2
5	$Glucose + 2\ Acetate \rightarrow 2\ Butyrate + 2\ CO_2 + 2\ H_2O + 2\ ATP$	-354.3
6	$Glucose + 0.67\ CO_2 \rightarrow 1.33\ Succinate + 0.67\ Acetate + 0.67\ H_2O + 3.5\ H^+ + 2\ ATP$	-292.0
7	$Glycerol \rightarrow Propionate + H_2O + 2\ ATP$	-152.5
8	$Glycerol \rightarrow Lactate + H_2 + 1\ ATP$	-92.4
9	$Glycerol \rightarrow 0.67\ Propionate + 0.33\ Acetate + 0.33\ CO_2 + H_2 + 0.33\ H_2O + 2\ H^+ + 1.67\ ATP$	-149.7
10	$Glycerol + CO_2 \rightarrow Succinate + H_2O + 2\ ATP$	-109.3
11	$3\ Lactate \rightarrow Acetate + 2\ Propionate + 2\ CO_2 + 1.5\ ATP$	-171.3
12	$2\ Lactate + H^+ \rightarrow Butyrate + 2\ H_2 + 2\ CO_2 + 1.5\ ATP$	-64.3
13	$Lactate + Acetate + H^+ \rightarrow Butyrate + CO_2 + H_2O + 0.5\ ATP$	-96.9
14	$Butyrate + 2H_2O \rightarrow 2\ Acetate + H^+ + 2H_2 + 2\ ATP$	+43.9
15	$Propionate + 2H_2O \rightarrow Acetate + 3H_2 + CO_2 + 1\ ATP$	+71.7
16	$4H_2 + 2CO_2 \rightarrow Acetate + H^+ + 2H_2O + 1\ ATP$	-55.0
17	$4H_2 + CO_2 \rightarrow CH_4 + 2H_2O$	-130.7
18	$Acetate + H_2O \rightarrow CH_4 + CO_2$	-31.1
19	$2\ Acetyl - CoA + 2\ NAD(P)H \rightarrow Butyrate + ATP + 2\ NAD(P)^+ + 2\ HS - CoA$	-46.4*
20	$Acetyl - CoA + H_2O \rightarrow Acetate + ATP + HS - CoA$	-52.1*

*Values expressed as kJ mol^{-1} acetyl-CoA

In GG_CO2, succinate production may have become a suitable alternative to dispose of excess reducing equivalents after formate addition if propionate conversion became limited by the predicted high concentrations of undissociated carboxylic acids (Xiao et al., 2016) (Figure 5-8). Stimulating carboxylation activity in pyruvate carboxylase and PEP carboxykinase by elevated CO_2 concentrations has shown positive correlations with succinate production (Lu et al., 2009). In pure cultures of *Actinobacillus succinogenes*, keeping CO_2 concentrations above 17.1% saturation increased succinate levels (Van Der Werf et al., 1997). Besides CO_2 supply, providing an additional electron donor (in this case formate) has been favourable for succinate production (Amulya and Mohan, 2019). As an intermediate metabolite in pressurized anaerobic systems, succinate has only been previously reported by Lindeboom et al. (2014) as a product of the saccharification of gelatinized starch at 30°C and 16 bar. Thus, despite yields being low, *i.e.,* succinate represented <10% of the COD fed to GG_CO2 in phase II_C (Table 5-3), results constitute encouraging evidence of the steering potential of elevated pCO_2.

Other changes in product spectrum after formate addition in phase II-C were related to higher acetate concentrations in the controls (Figure 5-1). Our results suggest, through indirect observations, the occurrence of enhanced CO_2 fixation in phase II-C, due to formate addition. First, a considerable increase in COD-acetate in GLU_CO2 and particularly in GLY_CO2 was observed (Table 5-3). Second, significant differences were detected in the absolute abundances of bacteria with possible acetogenic metabolism in the Firmicutes phylum, such as *Clostridium* spp., ($p<0.05$). Third, an increased relative abundance of *Methanosaeta* (Figure 5-5B) in response to higher acetate levels with concomitant recovered CH_4 production in all pCO_2 treatments (Table 5-3). Finally, high cell densities in GG_CO2 and GLY_CO2 could have resulted from carbon and electron fluxes being directed towards anabolic processes in response to enhanced CO_2 fixation in the presence of organic non-methanised substrate (formate) as electron donor (Figure 5-3, A and C). However, definite proof of enhanced CO_2 fixation shall come from studies with labelled formate and CO_2 to thoroughly track the carbon faith on pressurized anaerobic conversions. In this way, it will be possible to differentiate between acetate produced from CO_2 fixation and acetate accumulated because of reduced methanogenic activity.

Other differences between GG_CO2 and GG_N2 corresponded to measured cell densities and biomass-related products. After two pressurization cycles and formate addition in phase II-C, final cell density (*proxy* of biomass growth) was 1.5 and 4.5 times higher in GG_CO2 than in controls GG_N2 and GLU_CO2, respectively (Figure 5-3). According to the Aligned Rank Transform test, the presence of an additional electron donor was a significant factor to explain differences in cell density (Table 5-4). The additional availability of reducing equivalents from formate could have enhanced CO_2 fixation and, in turn, increased levels of acetyl-CoA, a precursor of anabolic and catabolic products (Pietrocola et al., 2015). Remarkably, there was

an opposite trend between the results from cell density measurements and VSS concentrations in experiment II. When analyzing VSS (expressed as COD-biomass), the values for GG_N2 were the ones 1.7, 2.7 and 2.5 times higher than GG_CO2, GLY_CO2 and GLU_CO2 in phase II-C, respectively (Table 5-3). These results suggest that VSS may not constitute an adequate *proxy* of biomass growth, since it does not distinguish between dead/non-viable cells, extracellular compounds and the biomass corresponding to active microbial cells (Ceron-Chafla et al., 2021; Foladori et al., 2010). Further research shall systematically quantify biomass and biomass-associated products under pressurized headspace to discriminate between enhanced anabolism and higher synthesis of extracellular microbial products.

5.4.2 Interaction effects between elevated pCO_2 – process conditions modify community dynamics and indirectly product spectrum

The interaction between pCO_2 and operational conditions was expected to modify the metabolic activity and microbial community structure, indirectly impacting the product spectrum. Particularly, under relatively "unfavourable" conditions for reactor operation, such as high S/X ratio, increased undissociated carboxylic acids and elevated pCO_2, an increase in the abundance of stress-tolerant microorganisms with metabolic flexibility was expected (Emerson et al., 2008). The absolute abundances of the *par excellence* stress-tolerant *Clostridium* spp. (Figure 5-6A) were significantly different ($p=0.001$) when considering phase (II-A, II-B and II-C) as grouping factor in experiment II. Previous investigations have shown positive effects of formate addition on the growth rates and total carbon fixation of certain acetogenic cultures, particularly in *Clostridium* spp. such as *C. kjundhali* and *C. carboxidivorans* (Jain et al., 2020; Ramió-Pujol et al., 2015), which aligns with the dynamics of *Clostridium* spp. in phase II-C. On the other hand, metabolic pathways for carbohydrate fermentation in *Clostridium* spp. are diverse: at low pH, ABE fermentation, *i.e.,* acetone-butanol- ethanol (Patakova et al., 2013) occurs, whereas, at circumneutral pH, the fermentation pattern could be dominated by butyrate-acetate (Kleerebezem et al., 2015). Propionate production in *Clostridium* spp. is ascribed to the acrylate pathway, *i.e.,* lactate to propionate (Gonzalez-Garcia et al., 2017), occurs in particular strains (*C. propionicum)* and has been evidenced using glucose or glycerol as substrates (Barbirato et al., 1997). Hence, provided that the proper *Clostridium* spp. are selected, the acrylate pathway also constitutes a thermodynamically feasible option for propionate production, with lower dependency on CO_2 availability at circumneutral pH (Eq. 11, Table 5-7), as in the case of GG_N2.

Another remarkable result corresponds to the increase in the absolute abundance of the class Negativicutes, particularly the family Veillonellaceae, when glycerol and elevated pCO_2 were present (GG_CO2 and GLY_CO2, Figure 5-6A). In systems degrading glycerol at

circumneutral pH, a concomitant increase in the abundance of Veillonellaceae and Clostridiaceae has been observed (Moscoviz et al., 2016). Propionate production is the preferred pathway for glycerol conversion in most members of Veillonellaceae (Braz et al., 2019; Ferguson et al., 2018; Xafenias et al., 2015), which also became evident in the strong positive correlation between Veillonellaceae and high propionate concentrations (Figure 5-7). Notably, in this family and the Negativicutes class, the most commonly observed pathway for propionate production is the succinate pathway, *i.e.,* phosphoenolpyruvate (PEP) → succinate → propionate, where CO_2 plays a role. Glycerol conversion experiments with open mixed cultures give limited emphasis to CO_2 evolution in the headspace or liquid medium. Thus, an indirect causal relation between CO_2 levels and enhanced propionate production via the selection of members from the Veillonellacea family, with reported acetogenic nature in the lineage (Aryal et al., 2017), may have been overlooked. However, the observation that Veillonellacea was a less relevant group in GG_N2 (Figure 5-5A) where glycerol was present but not CO_2, supports the hypothesis of CO_2 requirement for Veillonellacea predominance.

The sustained predominance of class Methanomicrobia (genus *Methanosaeta*), particularly in GG_CO2 and GLY_CO2 and to a lower extent in GLU_CO2 (Figure 5-5B), also stands out from the presented results. This observation aligns with our previous results (Chapter 4, Figure 4-3B and Figure 4-7B) and prior pressurized AD studies (Lindeboom et al., 2016). Methanosaetaceae became predominant in the archaeal community, although elevated pCO_2 conventionally results in thermodynamic constraints towards aceticlastic methanogenesis (Chapter 2). In addition, members of Methanosaetaceae are unable to directly utilize hydrogen and formate for CO_2 reduction to CH_4 (Rotaru et al., 2014). However, additional thermodynamics analyses showed that increasing acetate concentrations (phase II-C) (Table 5-3) might compensate for detrimental effects of elevated pCO_2, ultimately helping to develop favourable bioenergetics for aceticlastic methanogenesis (Figure 5-10). In addition, a recent study by Braz et al. (2019) proposed that *Methanosaeta* may be more resilient to increasing carboxylate concentrations, providing a further explanation for the predominance of this group during Experiment II.

A possible link between increased pCO_2 levels and the abundance of members of the class Anaerolinea, whose relative abundance remained high throughout experiment II (Figure 5-5A), remains to be elucidated. On one side, since these microorganisms were highly abundant in the original inoculum (Figure 5-5A) they could be considered part of the core anaerobic microbiome as reported for other close relatives in the Chloroflexi phylum (Bovio-Winkler et al., 2021). On the other side, the observed fluctuations in absolute abundances throughout experiment II (Figure 5-6A) suggest an effect of applied operational conditions on this microbial group. Pressure and higher concentration of carboxylic acids could have selected for Anaerolinea populations due to their adhesive feature enabling attachment, formation of

protective structures and exchange of intermediate products (Xia et al., 2016). Furthermore, recent research in deep-sea sediments has provided evidence of a homoacetogenic lifestyle for members of phylum Chloroflexi (Sewell et al., 2017); thus, elevated pCO_2 could have acted as a selection parameter. When considering links between elevated pCO_2 and community structure, a final point requiring further exploration corresponds to the concomitant increased abundances of Anaerolinea (Chloroflexi phylum) and *Methanosaeta* spp. (Figure 5-6). It remains to be elucidated the occurrence of syntrophic interactions between these two microbial taxa in pressurized systems because both groups have been found co-localized in other anaerobic reactors (Bovio-Winkler et al., 2021; McIlroy et al., 2017). Moreover, Chloroflexi spp. have been described as a microbial population associated with or supporting syntrophic relations in anaerobic digesters (Narihiro et al., 2015).

Combined pH-pCO_2 effects impact pathway feasibility in anaerobic processes

Batch operation at elevated pCO_2, with moderately high substrate concentration, high S/X ratio and relatively short phase durations, led to constrained complete acid conversion (Figure 5-2). Acid accumulation, in turn, could have had a more substantial effect on pH fluctuations than anticipated during the provision of 150 mM buffer as HCO_3^-. Thus, the system could have experienced lower pH than the calculated value of 6.5, leading to higher levels of undissociated carboxylic acids than those predicted in experiment II (Figure 5-8). Propionate conversion is inhibited by concentrations > 80 mg L^{-1} undissociated propionic acid (HPr) and ≈ 3 mg L^{-1} undissociated acetic acid (HAc) at pH=7 (Fukuzaki et al., 1990). Mösche and Jördening (1999) reported limited propionate conversion at a higher HPr concentration of 260 mg L^{-1}, which coincides with the upper boundary for predicted HPr in experiment II (Figure 5-8 D).

Xiao et al. (2013) reported inhibition of the specific acetic acid utilization rate in methanogens at 145 mg HAc L^{-1}, whereas a higher concentration of 1141 mg HAc L^{-1} caused inhibitory effects on hydrogen yield from glucose (Van Ginkel and Logan, 2005). A 37-60% reduction in the net carboxylates production from glucose at 2000 mg HAc L^{-1}, 1400 mg HPr L^{-1} and 120 mg HBu L^{-1} has also been documented (Xiao et al., 2016). Thus, increased undissociated carboxylic acids, as an outcome of combined pH-pCO_2 effects, could help to partially explain carboxylates (*e.g.,* propionate) accumulation and changes in product spectrum at elevated pCO_2 and high S/X ratio. However, it cannot be considered the standalone explanatory mechanism in experiment II since carboxylates accumulation occurred already in phase II-A at lower concentrations of undissociated carboxylic acids (Figure 5-2, Figure 5-8). Therefore, increasing undissociated carboxylic acid concentrations complement the explanatory mechanism for steering product formation in experiment II based on the interaction effects between pCO_2 - process conditions and its modification of microbial community dynamics.

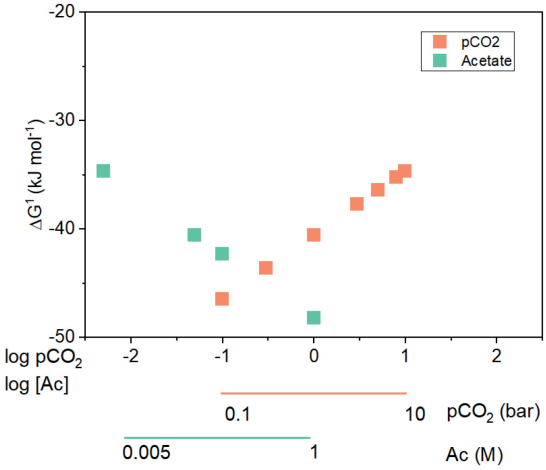

Figure 5-10: Gibbs free energy for aceticlastic methanogenesis at circumneutral pH considering the effect of increased partial pressure of carbon dioxide (pCO_2 in orange) and acetate concentrations (in green)

It is recognized that the total concentration of carboxylates and particularly undissociated ones, could become a strong modifier of microbial community structure (Jia et al., 2019) and activity (H. S. Lee et al., 2008). Hence, in the scenario of increasing undissociated carboxylic acid concentrations in experiment II, dissimilarities in the abundance of syntrophic partners could have occurred, which in turn constrained microbial syntrophy. These dissimilarities were associated with a significant, moderate negative correlation between archaeal abundance and undissociated carboxylic acids (Figure 5-9A) and the significant differences in the abundance of syntrophic organisms from class Synergistia ($p<0.05$) when phase was considered the grouping factor in GG_CO2. Eventually, the constrained syntrophic conversion of propionate and butyrate would have led to the divergence of the pressurized anaerobic system from CH_4 to carboxylates production in a single reactor without the addition of methanogenic inhibitors when elevated pCO_2, pH and high S/X ratio interacted during experiment II.

5.5 Conclusions

The results from this investigation support a potential role of elevated pCO_2 as a steering parameter in anaerobic processes, *e.g.,* mixed culture fermentation and AD. However, they also revealed that its "*modus operandi*" is complex and that the obtained selectivity leads to trade-offs with substrate consumption rates and lag-phases. Changes in product spectrum and cell density, rather than an isolated effect of increasing pCO_2, showed dependency on the interaction with process conditions, such as S/X ratio and availability of external electron donor. In particular, substrate specificity and interaction elevated pCO_2 and process conditions also seem to act as a selection mechanism in the microbial community, *e.g.,* towards acetogenic microorganisms, whose activity further modified the product spectrum. Furthermore, the interaction pCO_2 and formate played a beneficial role in succinate production with mixed substrate after subsequent pressurized cycles, due to the availability of extra reducing equivalents and likely enhanced carbon fixating activity.

6

CHAPTER 6

GENERAL DISCUSSION, SUMMARY AND OUTLOOK

6.1 Summary of relevant findings

The ultimate goal of this thesis was to provide experimental evidence supporting a hypothesized role of elevated pCO_2 as a steering parameter in HPAD. To achieve this goal, this investigation started by understanding the effect of elevated pCO_2 on the kinetics and thermodynamics of syntrophic oxidation of two common intermediate products of the AD process: butyrate and propionate (Chapter 2). This work also aimed to differentiate the effects of mild hydrostatic pressure (MHP) and gas partial pressure and identify possible cross-resistance effects due to prior exposure to environmental stressors, such as non-optimal incubation temperature and high salinity (Chapter 3). Furthermore, the effect of elevated pCO_2 on the anaerobic conversion of energy-rich substrates, such as glycerol and glucose, and the effect of adaptive laboratory evolution (ALE) to increase microbial endurance and enhance CH_4 production were studied (Chapter 4). Finally, interaction effects of elevated pCO_2 and process conditions, such as substrate specificity, substrate to biomass ratio (S/X), and external electron donor, were explored to steer product formation from biogas to carboxylates in a single reactor without methanogenesis inhibitors (Chapter 5). A summary of the main research findings to be further discussed in this chapter is presented in Table 6-1.

Table 6-1: Short summary of main results from this study

Chapter	Objective	Substrate	Main results
2	Elucidate kinetic and thermodynamic effects of elevated pCO_2 in syntrophic anaerobic conversions	Propionate Butyrate	Decreased maximum substrate utilization rate (r_{smax}) at elevated pCO_2 Bioenergetics analysis showed: Direct impact of elevated pCO_2 on syntrophic propionate oxidation and pH-mediated effect on syntrophic butyrate oxidation. Changes in pCO_2, pH have a differentiated impact in the individual reaction feasibility leading to a potential biochemical energy redistribution among syntrophic partners "Energy feasibility niche" for syntrophic conversions at elevated pCO_2 shows interdependence with pH_2 and pH.
3	Determine cross-resistance effects to moderate hydrostatic pressure (MHP) triggered by halotolerance and thermal adaptation	Glucose	MHP did not limit growth and fermentative activity at moderate temperature (20°C) in the inoculum from marine sediment (MSI). Results suggest a cross-resistance effect from mild incubation temperature and halotolerance enhancing piezotolerance. Kinetic and bioenergetic limitations constrained growth and product formation at 10° C in MSI. Product formation was enhanced at 28°C (MSI) and 37°C (anaerobic digester saline inoculum – ADI) with reduced biomass yield due to high maintenance and decay.

Chapter	Objective	Substrate	Main results
4	Study the effect of directional selection under increasing substrate load to restructure microbial community and induce cross-resistance mechanisms to improve conversion under elevated pCO_2	Glucose	Inoculum after adaptive laboratory evolution (ALE) showed: Increase in total and viable cell density and relative abundance of *Smithella* and *Syntrophobacter* (8%). Slight increase in the relative abundance of *Methanosaeta* compared to *Methanobacterium.* Propionate conversion was not constrained when using evolved inoculum and enabled a higher CH_4 yield per archeal cell than using the original inoculum.
		Glycerol	Inoculum after ALE showed: Moderate decrease in final cell density. Highest relative abundance of *Smithella* and *Syntrophobacter* (18%). Relative abundance of *Methanosaeta* and *Methanobacterium* were comparable to original inoculum. Enabled propionate conversion in evolved inoculum led to higher CH_4 yield per archaeal cell than using the original inoculum.
5	Study the interaction effects of elevated pCO_2 and operational conditions in high pressure mixed culture fermentation	Glucose	Fermentation profile was dominated by butyrate and acetate production. Microbial community showed a high relative abundance of *Clostridium* spp.
		Glycerol	High propionate yields are associated with a high relative abundance of family Veillonellacea.
		Glycerol-Glucose	Mixed substrate (1:1 molar ratio) was beneficial for final cell densities with sustained propionate production. Succinate formation after adding formate as external electron donor.

6.2 Take away messages

- Elevated pCO_2 exerts a detrimental effect on substrate conversion rates that cannot be explained by only bioenergetic effects. The mechanistic explanation provided in this thesis needed to be complemented with pH-associated effects occurring when alkalinity is not controlled. Among them, the increasing concentration of undissociated carboxylates and physiological impairments in the activity of syntrophic bacteria were relevant (Chapter 2).

- Depending on the starting inoculum and imposed environmental conditions, such as temperature and salinity, there will be a “trade-off” between biomass growth and intermediate product formation to satisfy increased maintenance requirements under mild hydrostatic pressure (MHP) and high temperature. Between MHP and temperature, the latter proved to be more significant to explain observed changes in microbial community dynamics (Chapter 3).

- The adaptive laboratory evolution (ALE) strategy under increasing substrate to biomass ratio, selected for a more resilient syntrophic community with higher abundances of *Smithella* and *Methanosaeta* spp. CH_4 production under elevated pCO_2 was reinstated via the favoured dismutation pathway with independence from pH_2 in the "evolved" inoculum (Chapter 4).

- Elevated pCO_2 has potential to steer intermediate product formation in anaerobic processes. However, pCO_2 is a complex parameter to tune, due to its role in physicochemical and biological reactions. Thus, a multiparameter approach is required to incorporate pCO_2 into a control strategy targeting selective product formation (Chapter 5).

6.3 Effects of elevated pCO_2 on reaction feasibility: Insights from the utilization of a multi-parameter bioenergetics analysis

6.3.1 The role of increased pCO_2

Syntrophic oxidation of reduced compounds like propionate and butyrate is thermodynamically limited by high pH_2 and occurs at partial pressures lower than 40 and 2 Pa, respectively (Schink, 1997; Worm et al., 2014). Chapter 2 expanded on the existing knowledge through an interactive multi-parameter analysis on bioenergetics, including operational parameters such as pH_2, elevated pCO_2 and pH (Figure 2-6 and Figure 2-8). The employed method calculated the overall energetic feasibility of syntrophic conversions in HPAD and high-pressure mixed culture fermentation (HP-MCF) at conditions of fluctuating pH, pCO_2, pH_2, or combined fluctuations herein. The performed analysis identified a direct effect of elevated pCO_2 on the thermodynamic feasibility of syntrophic propionate oxidation (Figure 2-6) and a pH-mediated effect on syntrophic butyrate oxidation (Figure 2-8).

The bioenergetics analysis in Chapter 2 assumed that the predominant pathway for propionate oxidation was the methyl-malonyl-CoA pathway (Table 4-4). In Chapter 4, the abovementioned multi-parameter analysis was employed to investigate differences in the thermodynamic feasibility of syntrophic propionate oxidation when another pathway, *i.e.,* dismutation pathway, characteristic of the *Smithella* genus (Table 4-4), was considered. The *Smithella* genus became predominant in experiments from Chapter 4 after an adaptive laboratory evolution (ALE) strategy based on serial cultivation under conditions of increased S/X ratio (Section 4.3.3). The multi-parameter bioenergetics analysis evidenced that, from a thermodynamic perspective, the dismutation pathway was more resilient to changes in pCO_2 and pH_2 than the methyl malonyl-CoA pathway (Figure 4-12). This outcome complements previous work that only considered pH_2 as a limiting factor for the thermodynamics of syntrophic propionate oxidation (Dolfing, 2013; Stams and Plugge, 2009). Our results also

support that selection of functional traits, *e.g.,* a pathway for syntrophic propionate oxidation, could be considered as the observable output of an intricate nexus between environmental conditions, thermodynamic feasibility and reorganization of the microbial community.

In Chapter 5, the multi-parameter bioenergetics analysis was employed to further explain the predominance of aceticlastic methanogenesis (AcM) in HPAD despite the Gibbs free energy for catabolism, ΔG_{cat}^{01}, becoming less negative when pCO_2 increases (Chapter 2). In anaerobic processes, some of the production routes for acetate correspond to homoacetogenesis (HA) and syntrophic propionate/ butyrate oxidation. On the other hand, acetate is converted via syntrophic acetate oxidation (SAO) and AcM. The thermodynamic feasibility of these reactions is strongly influenced by changes in pH_2, pCO_2, pH and acetate concentrations (Müller et al., 2010; Worm et al., 2014). SAO and AcM can coexist in anaerobic digesters (Wu et al., 2022). However, a relevant role for SAO was not considered likely in the here presented experiments due to the mesophilic conditions (Petersen and Ahring, 1991) and low ammonia concentrations (Jiang et al., 2018). Calculations in Chapter 5 showed that at high acetate concentrations (500-1000 mM), the ΔG_{cat}^{01} of AcM becomes more negative, whereas it becomes more positive at increasing pCO_2 (0-10 bar). Hence, at acetate concentrations in the range relevant for the experiments presented in this thesis (<20 mM, Chapter 5), the detrimental effects of elevated pCO_2 on AcM are counterbalanced by a favourable thermodynamic effect of increasing acetate concentrations on the ΔG_{cat}^{01} (Figure 5-10).

On the other hand, in the case of HA vs hydrogenotrophic methanogenesis (HyM), there is an evident effect of pH_2 on the thermodynamic feasibility of the reaction (Liu et al., 2016; Tsapekos et al., 2022). It is also observed that at high pH_2 and increasing pCO_2, HA becomes energetically favourable, *i.e.,* more negative ΔG_{cat}^{01} (Figure 4-11). More interestingly, when analyzing HA + AcM reactions in scenarios of increasing pCO_2 and low pH_2 (Figure 6-1A) or high pH_2 (Figure 6-1B), the difference in ΔG_{cat}^{01} with HyM disappears and both reactions become equivalent in terms of available energy (Figure 6-1). The syntrophic interaction between HA and AcM requires an adequate coupling between acetate production and consumption rates because increasing acetate concentrations do have a strong detrimental effect on the energy feasibility of HA (Figure 6-1C). However, various authors suggested that the HA-AcM conversion pathway can be stimulated by the addition of CO_2 to sewage sludge digesters (Bajón Fernández et al., 2019; Muntau et al., 2021). From the thermodynamic point of view, a syntrophic interaction between homoacetogens and aceticlastic methanogens under conditions of elevated pCO_2 constitutes a feasible option for the microbial consortium. In the

aftermath, this syntrophic interaction may improve the biochemical energy allocation for each of the partners involved.

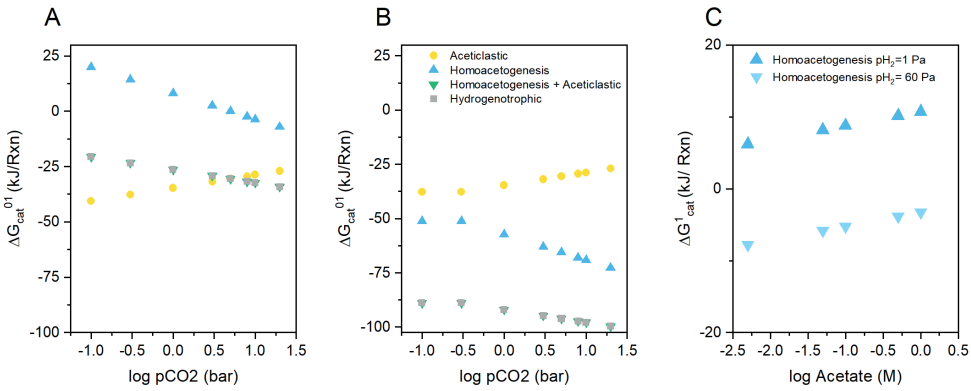

Figure 6-1: Effect of increasing pCO_2 on the available catabolic energy ΔG_{cat}^{01} of aceticlastic methanogenesis, homoacetogenesis, hydrogenotrophic methanogenesis and the proposed syntrophic reaction between homoacetogens and aceticlastic methanogens at different pH_2. A) corresponds to pH_2=1 Pa and B) to pH_2=60 Pa. Plot C) depicts the effect of increasing acetate concentrations on the available catabolic energy during homoacetogenesis at pH_2=1 and 60 Pa

6.3.2 The role of pH

The pH played an important role in defining the energy feasibility of syntrophic conversions in HPAD or HP-MCF, by itself and by its interaction with other process parameters such as pH_2 and evidently with pCO_2 in the carbonate equilibrium (Chapter 2, Figure 2-6 and Figure 2-8). Despite the elevated buffer concentration provided in the batch experiments described in Chapters 2 and 5 (100 and 150 mM, respectively), pH fluctuations in the bulk or at the micro-level environment due to non-uniform mixing could still have occurred in the pressurized reactors. Consequently, these pH fluctuations could have impacted the thermodynamics, conversion kinetics, and microbial physiology. Fluctuations in pH can impact the energy feasibility of biochemical reactions in direct and indirect ways. Direct effects are observed in the reactions that consume or produce protons and indirect effects correspond to the regulation of chemical speciation, *i.e.,* equilibrium between the undissociated and the dissociated forms (Jin and Kirk, 2018b, 2018a).

Increasing concentrations of undissociated carboxylic acids in this thesis became part of the mechanistic explanations provided for carboxylates accumulation (propionate and butyrate) and pathway steering in the pressurized experiments (Chapter 2, Chapter 5). Chapter 2 stated

a limited effect of lowered pH on increasing the concentration of undissociated carboxylic acids in the HPAD experiments. Due to low initial substrate concentrations (<1 g COD L^{-1}), total acid production was low. Therefore, buffer consumption due to acids production was minor and pH remained higher than 6.0 even when initial pCO_2 for headspace pressurization corresponded to 8.0 bar. Conversely, the inhibitory effect of undissociated carboxylic acids may have resulted more critical in the experiments described in Chapter 5 at higher initial COD (5-10 g COD L^{-1}). Considering a theoretical calculation of pH= 6.5 after reaching equilibrium with a headspace at 5 bar pCO_2 (Materials and Methods Chapter 5), accumulation of butyrate and propionate could be partially explained by rising concentrations of undissociated carboxylic acids in the experiments. A high concentration of undissociated acids, resulting from pH fluctuations, the high S/X ratio applied, and limited conversion of intermediates, could have affected the intra–extracellular balance between dissociated and undissociated acid species. This unbalance affected the thermodynamic feasibility of the acid-producing reactions (Richter et al., 2016) on top of the thoroughly described effects of increasing undissociated acid concentrations (Van Ginkel and Logan, 2005; Xiao et al., 2016). Among those detrimental effects are the collapse of the pH gradient, a component of the proton motive force for H^+ translocation across the cellular membrane, and the increased energy allocation into maintenance to preserve homeostasis (Jones and Woods, 1986).

The pH and substrate concentration also contributed to explain the switch between the formation of butyrate + acetate and propionate + acetate observed in the experiments from Chapter 5, which other authors also reported in atmospheric glucose MCF fermentation at 5.5<pH<6 (González-Cabaleiro et al., 2015). From a thermodynamic perspective, these product combinations lead to maximum biochemical energy harvest per unit of glucose or glycerol at circumneutral pH, suggesting an equal biochemical energy gain from both pathways (Figure 6-2). However, preferred pathways will depend on the overall composition of the metabolic network in the HPAD or HP-MCF system and ecological processes such as competition and stochastic colonization (Marsland et al., 2019). Ecological processes will shape the microbial community and the key players/functions involved in the anaerobic process.

The theoretical pH calculations in HPAD and HP-MCF are indicative, requiring more realistic approaches. Modelling tools enabling the development of soft-sensors (Luttmann et al., 2012) are a good starting point to simulate the physicochemical behaviour of the pressurized systems when reaching equilibrium between the headspace and liquid phase. Despite the high investment costs, continuous pH monitoring with pressure-resistant equipment is the only real alternative that will allow for temporal distinction of CO_2 dissolution, equilibrium points, and pH fluctuations due to carboxylates and CH_4 production and reactor decompression. Limited experimental results of pH monitoring in systems safely operating until 10 bars have not been

included in the various thesis chapters (See Annex A). However, those experiments revealed the importance of pH monitoring under pressurized conditions to differentiate pH-associated inhibition effects from elevated pCO_2 effects.

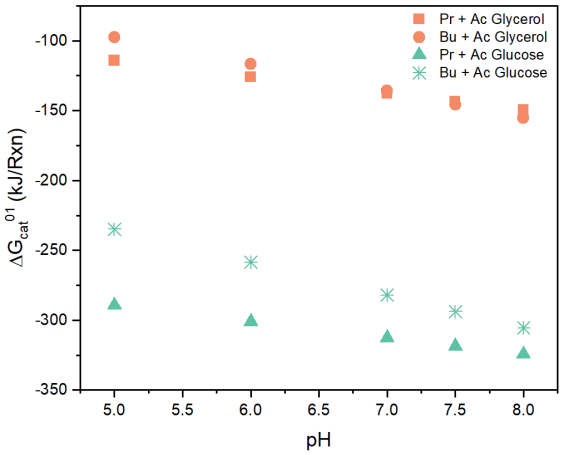

Figure 6-2: pH effect on the catabolic energy of glycerol (green) and glucose (orange) fermentation pathways with propionate + acetate or butyrate + acetate as products

6.3.3 The role of mild hydrostatic pressure (MHP) and temperature

The multi-parameter bioenergetics analysis (Chapter 2) was expanded by including anabolic reactions and used to investigate the combined effects of incubation temperature and MHP on the net available energy. Net available energy from catabolic processes was estimated based on the metabolic pathway contribution calculated from the intermediate product spectrum in pressurized fermentation experiments at 0.1, 5.0 and 8.0 MPa (Chapter 3, Section 3.3.3). A distinctive effect on the ΔG_{cat}^{01} was observed due to temperature changes and it was exacerbated by MHP, particularly at low and moderate temperatures (Figure 3-10A). The individual effect of temperature on energy feasibility (Conrad and Wetter, 1990; Finke and Jørgensen, 2008; Kleerebezem and Van Loosdrecht, 2010) and energy requirements for maintenance (m) (Tijhuis et al., 1993) have been thoroughly documented in literature. The effect of MHP in bioenergetics has been less explored, but the available literature suggests a marginal effect of this operational parameter on ΔG_{cat}^{01} (Amend and Plyasunov, 2001; Mayumi et al., 2013).

Combined effects between temperature and MHP have been discussed for thermophilic and piezophilic microorganisms when analyzing the energetic feasibility of biochemical reactions in extreme environments such as hydrothermal fluids (Amend and Shock, 2001), evidencing a more pivotal role of temperature. The results from Chapter 3, using saline-adapted marine sediment and anaerobic digestion inocula, showed that the combination of low temperature and MHP has a detrimental effect on $Y_{X/S,}$ evidenced by a decreasing trend when pressure increased from 5 to 8 MPa. In contrast, there was no clear trend at increasing temperatures and pressure (Figure 3-10, A-C). Moreover, the trend for $Y_{X/S}$, theoretically derived from thermodynamic analysis (Figure 3-10D), did not resemble the trend observed in the measured $Y_{X/S}$. This disparity implies that besides energy constraints, other process conditions may play a role when explaining the effects on microbial growth and activity associated with the interaction temperature-MHP. These results reflect the usefulness of the developed multi-parameter bioenergetics analysis as a predictive, explanatory tool and its limitations. Furthermore, results from Chapters 2 and 3 support the need to include thermodynamic approaches inside more holistic mechanistic explanations for biomass growth and product formation under stress conditions. Ultimately, our results justify the expansion of the scope of thermodynamic analyses to include the influence of other environmental parameters and their interaction effects.

6.3.4 Thermodynamic feasibility and microbial community structure

Selective pressures, *e.g.,* high S/X, elevated pCO_2, high pH_2, and extreme pH, modify the thermodynamic feasibility of biochemical reactions leading to the selection of robust genera from a diverse anaerobic microbiome, able to cope with a new set of conditions (X. N. Wang et al., 2017; Zhao et al., 2021). Results from Chapter 2 suggested a redistribution of biochemical energy among syntrophic partners in propionate and butyrate oxidation, due to the effects of elevated pCO_2 and pH (Figure 2-7). Environmental conditions determine the thermodynamic feasibility of the biochemical reactions involved in syntrophic conversions. Deviating energy allocations could impact the different growth strategies of syntrophic partners (Junicke et al., 2016, 2015), while provoking metabolic uncoupling and, ultimately, compromising the overall process performance. This "thermodynamic control", in turn, could end up reorganizing the microbial community structure (Junicke et al., 2016; Marsland et al., 2019) or could lead to divergences stimulating new syntrophic interactions. In Chapter 4, the multi-parameter bioenergetics analysis evidenced that the dismutation pathway from *Smithella* genus was more advantageous for syntrophic propionate oxidation than the methyl-malonyl-CoA pathway from *Syntrophobacter* when pH_2 and pCO_2 were increasing.

The "equivalence" in the availability of net biochemical energy from HA + AcM and HyM reactions at conditions of elevated pCO_2 (Figure 6-1) may help to explain the predominance of

bacteria with reported homoacetogenic activity, namely *Clostridium* spp. It is hypothesized that due to enhanced homoacetogenic metabolism, acetate concentrations increased and promoted a shift in syntrophic interactions with acetotrophic microorganisms such as *Methanosaeta* instead of hydrogenotrophic archaea (Figure 4-3, Figure 4-7 and Figure 5-5). Other studies have already suggested a syntrophic interaction between *Clostridium* spp. and *Methanosaeta* (Zhu et al., 2020). The analysis presented in Section 6.2.1 complements the explanations provided in Chapter 5, where the concomitant increase in the absolute abundance of *Clostridium* spp. was attributed to the high S/X ratio and elevated pCO_2 promoting homoacetogenic / mixotrophic activity. On the other hand, as observed in Figure 6-1A, AcM can become more energetically favourable than HyM in a scenario of moderate pCO_2 and low pH_2. This particular "window of opportunity" could explain the sustained predominance of *Methanosaeta* at conditions of elevated pCO_2 in our experiments (Chapter 4 and Chapter 5) and the experiments from Lindeboom et al. (2016).

Zerfaß et al. (2018) suggested that the interplay between electron donors and electron acceptors effectively manipulates community structure and functionality and is compatible with a community engineering process guided by thermodynamic considerations. Chapter 5 evidenced that adding an external electron donor such as formate had an important effect on glycerol and glucose fermentation pattern and triggered rearrangements in the microbial community composition (Figure 5-5). Substrate specificity and concentration in HP-MCF experiments intensified this effect, leading to noteworthy differences in the predominant taxa with glycerol (class Negativicutes, family Veillonellaceae) and glucose (*Clostridium* spp.). Overall, it can be concluded that the relationship between community reorganization and thermodynamic feasibility is complex. Feedback loops between environmental conditions and metabolic activity that further alter the surrounding environment, as well as the feasibility of biochemical reactions, are the main source of this complexity (Zerfaß et al., 2018) (this thesis).

6.3.5 The biokinetics-thermodynamics nexus

The effect of elevated pCO_2 on the substrate conversion rate (r_{smax}) became evident from results presented in Chapter 2. Increasing lag phases and a reduction in the calculated r_{smax} were observed in syntrophic propionate and butyrate oxidation experiments when increasing pCO_2 from 0.3 to 8 bar (93 and 57%, respectively). In Chapter 5, the interaction of elevated pCO_2, increasing S/X ratio and additional electron donor (formate) distinctly influenced the substrate conversion rates (Table 5-5 and Figure 5-4). In Chapter 2, it was postulated that increased availability of biochemical energy from the provision of energy-rich substrates could improve the conversion kinetics. This hypothesis was based on the nexus between kinetics and thermodynamics, *i.e.,* "thermodynamic consistency" or the dependency of the reaction rate on

the thermodynamic driving force (amount of energy available to drive the reaction) (Jin and Bethke, 2007; Jin and Kirk, 2018b). However, lower conversion rates and distinctive lag phases were observed when glucose and glycerol were used as substrates at a moderately-high concentration (5-10 g COD L^{-1}). Thus, overcoming energy limitations by providing energy-rich substrates (ΔG_{cat}^{01} glucose = -957 kJ mol^{-1} and glycerol= -528.4 kJ mol^{-1} upon oxidation to CO_2) (Kleerebezem and Van Loosdrecht, 2010) did not suffice to prevent intermediates accumulation under conditions of elevated pCO_2. However, adding formate as an additional electron donor after two cycles of CO_2-pressurized operation and reducing the S/X ratio led to slight improvements in the conversion rates (Chapter 5).

In Chapter 3, despite the limited collection of useful data points to adequately determine production and consumption rates, a slow-down of intermediates consumption at low temperatures (10°C) and MHP of 8 MPa was evidenced. Under these conditions, lactate accumulation was the most pronounced effect (Figure 3-12). It is well known that temperature changes strongly regulate reaction rates according to the Arrhenius equation (Huang et al., 2011; Infantes et al., 2012). However, pressure and temperature also exert a distinct effect on reaction rates, as described by the Eyring equation (Eq. 1-2). Thus, when envisioning a strategy for carboxylates production in HP-MCF, the interaction effects of environmental conditions (pH, temperature, MHP, pCO_2) need to be investigated first. In this regard, fundamental biochemical principles, *i.e.,* thermodynamics and kinetics, allow a better understanding of the nature of interaction effects. Identified trade-offs in parameters such as $Y_{X/S}$, substrate affinity (*Ks*) and μ_{max} (Chapter 3) could allow for a better interpretation of inter-species dynamics and help to predict microbial activity and shifts in community structure (González-Cabaleiro et al., 2021).

The links between thermodynamics and kinetics are critical to describe the performance of a biological system, especially under conditions of environmental stress. However, as suggested by our results, other considerations such as ecological processes and physiological responses (Hanselmann, 1991) also need to be included when ascribing mechanistic explanations to product formation in HPAD or HP-MCF under conditions of elevated pCO_2.

6.4 Engineering a piezotolerant microbial community

6.4.1 Inoculum selection vs Adaptive Laboratory Evolution (ALE)

In Chapter 2, evidence was provided about the distinctive response of non-adapted inocula to elevated pCO_2. Other authors have previously raised attention to the issue of inoculum selection being crucial for functional stability (De Vrieze et al., 2015a; Franchi et al., 2018),

especially to reduce the start-up period and facilitate operation under stress conditions. Stress tolerance mechanisms at the cell level and the initially present microbial network in the community (*e.g.,* syntrophic partners) are factors likely determining the adaptation and resistance/resilience/redundancy response after environmental disturbances (Allison and Martiny, 2009). Chapter 2 discussed that differences in microbial sensitivity to environmental stressors such as elevated pCO_2 and pH could explain, to a certain extent, kinetic limitations in systems operated at elevated pressure. Physiological differences, *e.g.,* cell membrane composition in bacteria and archaea and pH optimality for growth (Balk et al., 2008; Li et al., 2012) are examples of microbial features that could play a role in the microbial stress response and deserve further attention in open microbiomes exposed to elevated pCO_2.

Chapter 3 exposed clear distinctions in piezotolerance of natural (NMC) and engineered microbial communities (EMC). NMC are exposed to environmental gradients, which differs from the stable operation that EMC adapted to stress conditions usually perform. In this thesis, it was shown that incubation of NMC under diverse sources of environmental disturbances ($T > T_{local}$ and salinity) triggered cross-resistance mechanisms in fermenting NMC (Chapter 3). The proposed cross-resistance may have allowed sustained growth and microbial activity, *i.e.,* carboxylates production, when microorganisms were exposed to a different source of stress, such as MHP. Thus, provided that cultivation bottlenecks are surpassed (Ali et al., 2021), the biotechnological potential of piezotolerant NMC could be exploited to produce compounds of interest, *e.g.,* carboxylates, intracellular polymers, pigments, among others (Valdemarsen and Kristensen, 2010).

However, as other authors have previously stated, proper biomass acclimation under the culture conditions of interest will select for the required specific functionalities rather than for particular microbial genera (Scoma et al., 2017). This postulate was also evaluated in Chapter 4 and Chapter 5, with distinctive results that aligned with the objectives defined for these studies: alleviate hindered syntrophic propionate oxidation for improving CH_4 production (Chapter 4) or increase carboxylates production, while simultaneously limiting methanogenic activity in glycerol-glucose MCF (Chapter 5). As expected, substrate specificity and concentration were key for propionate production. On the other hand, biomass acclimation at increasing S/X ratio in an adaptive laboratory evolution (ALE) strategy at atmospheric conditions selected for more resilient syntrophic microorganisms such as *Smithella* genus. The predominance of *Smithella* + *Methanosaeta* after ALE with glycerol and glucose was remarkable as an enabling factor for propionate oxidation under elevated pCO_2 (Chapter 3). The predominance of *Smithella* needs to be further researched to elucidate if substrate specificity and concentration was the preponderant selection mechanism as suggested by literature (Kim et al., 2015). Alternatively, a postulated detrimental effect of elevated pCO_2 at the physiology level (*e.g.,* hydrogenases activity) may have also triggered the selection of

microorganisms with a different pathway for propionate oxidation, less dependent on hydrogen-mediated interspecies electron transfer.

Inoculum screening with next-generation sequencing techniques may be the first step for inoculum selection (Franchi et al., 2018; Sydney et al., 2018), with monitoring metabolic activity and tuning operational conditions as the accompanying next steps. Following this approach, start-up times could be shortened and direct operation under environmental stress conditions could become possible. Another approach could use bioaugmentation processes with piezotolerant fermenting NMC to target the production of specific carboxylates under pressurized conditions. In this approach, the taxon or taxa of interest with proven piezotolerance could be artificially introduced to the community of a bioreactor, preferably after an adaptation period to the intended cultivation conditions (Schauer-Gimenez et al., 2010). However, it remains to be determined if these "external key players" can thrive in the anaerobic microbiome by establishing syntrophy with the local microbiota or if the native microorganisms easily outcompete them.

6.4.2 Influence of operational conditions

In Chapter 5, incubations under pressurized conditions with subsequent transfers to deliberately increase the S/X ratio and additional electron donor (formate) were selective for propionate producers in the Negativicutes class (Veillonellacea family). Veillonellacea members have been previously associated with glycerol conversion to propionate in AD systems (Braz et al., 2019; Tapia-Venegas et al., 2015). *Clostridium* spp. were also favoured by the conditions applied in Chapter 5. However, it remains to be elucidated if the primary driver for *Clostridium* spp. predominance was the high substrate concentration selecting for organisms with an adequate stress response, *e.g.,* sporulation (Al-Hinai et al., 2015; Bastidas-Oyanedel et al., 2015) or the mixotrophic nature previously reported in this taxon (Braun and Gottschalk, 1981; Sandoval-Espinola et al., 2017). Taxon presence does not necessarily mean activity (De Vrieze and Verstraete, 2016). Thus, complementary metagenomics analyses are required to determine if genes associated with CO_2 fixation are upregulated under elevated pCO_2, high S/X ratio and semi-continuous pressurized operation (Braun and Gottschalk, 1981; Figueroa et al., 2018).

The substrate concentration, high S/X ratio, pressurized incubation and provision of mixed substrate caused distinct differences in the microbial communities between experiments presented in Chapters 4 and 5. These conditions were detrimental to the abundance of syntrophic oxidizers from families Smithellaceae and Synergistaceae, which were absent or present with reduced predominance when comparing results from Chapters 4 and 5 (Figure 4-3, Figure 4-7, Figure 5-5 and Figure 5-6). As explained in Chapter 5, a compromised syntrophic conversion could be attributed to dissimilarities in absolute abundances of

syntrophic partners due to detrimental effects of elevated pCO_2, fluctuating pH, accumulating intermediate products and increasing concentrations of undissociated carboxylic acids.

The predominance of *Methanosaeta*, previously described in HPAD literature (Lindeboom et al., 2016) and under conditions of increasing pCO_2 (Bajón Fernández et al., 2019), was once again highlighted in this research. Results presented in Chapter 4 evidenced a high relative abundance of *Methanosaeta* in HPAD experiments under elevated pCO_2. This predominance, based on our experimental results, is attributed to a) the dismutation pathway (*i.e.,* propionate → butyrate + acetate) being favoured after ALE at increasing S/X ratio b) the provision of glycerol enabling fermentation to propionate (balance reducing equivalents) and acetate (ATP production) and c) elevated pCO_2 promoting homoacetogenesis and aceticlastic methanogenesis as an alternative pathway for CO_2 reduction. Here, the proposed syntrophic interaction is more complex since it would involve three different microorganisms: members of the genus *Smithella*, a butyrate oxidizer probably associated with *Syntrophomonas* or *Syntrophus* spp. and *Methanosaeta* (Puengrang et al., 2020). The results from this thesis need to be complemented with enzymatic analysis of the activity of key enzymes in the methanogenic pathway, such as acetate kinase and coenzyme F_{420} (Zhu et al., 2020). Once this information is available, it will be possible to fully elucidate and confirm that despite the harsh conditions imposed on microorganisms, due to operation under elevated pCO_2, the actively promoted pathway is aceticlastic methanogenesis. This novel insight supports labelling the *Methanosaeta* genus in AD as "resilient" instead of "sensitive" (De Vrieze et al., 2012). Overall, our results align with previous research stating the importance of selecting the "right selective pressure" to restructure the microbial community and achieve a specific functional profile (González-Cabaleiro et al., 2021).

6.4.3 Cross-resistance effects and microbial piezotolerance

Interconnection between resistance to different "environmental extremes" has been observed in "extremophiles," *i.e.,* microorganisms able to grow and thrive in harsh environments (Canganella and Wiegel, 2011), such as the deep sea, where salinity, temperature, and hydrostatic pressure interplay. However, the combined influence of these parameters has been limitedly studied at the laboratory scale. For example, Kaye and Baross (2004), working with piezotolerant and piezosensitive isolates from *Halomonas* spp. showed a predominant effect of hydrostatic pressure (>15 MPa) compared to temperature and salinity fluctuations. Conversely, the results presented in Chapter 3 strongly suggest that temperature acts as an overarching metabolic modulator in psychrotolerant, non-pressure adapted microorganisms with fermentative activity (*e.g., Marinifilum, Psychromonas, Halilactibacillus and Trichococcus*). In contrast, moderate hydrostatic pressure (MHP <10 MPa) has a fine-tuning effect on growth and activity. Moreover, results from Chapter 3 also indicate that incubation at a presumed

optimal temperature for growth (T_{opt} ≈20°C) for psychrotolerant microorganisms may counteract the detrimental effects of MHP on growth and product formation (Figure 3-3 and Figure 3-4). Conversely, deviations from T_{opt} and additional stress conditions result in kinetic or bioenergetic limitations in microbial growth and activity. These limitations are associated with low and high temperature effects on the biochemical reactions, such as slower rates and increased energy requirements for maintenance and decay (Chapter 3).

The validity of the conclusions about the community structure of halotolerant communities being notoriously modified by temperature and, to a lesser extent, by MHP is associated with applied stressor duration and intensity. If experiments had been performed for extended periods and at higher HP, a different outcome in which communities are more or less resilient to MHP could have been observed (Shade et al., 2012). Regarding the functional stability of natural and engineering carbohydrate fermenting communities, it was established that these initially diverse communities showed functional redundancy. Community composition changed due to temperature and MHP (Figure 3-5); however, glucose conversion and acid formation were evidenced in all tested conditions. Conversely, biomass growth was apparently more sensitive to changes in operational conditions (Figure 3-3).

Concerning microbial piezotolerance in microorganisms from open mixed cultures, a result deserving further investigation concerns the predominance of groups such as *Proteiniphilum* and *Ercella* without reported piezotolerance, as far as the author is aware. Microorganisms belonging to these genera remained abundant (absolute abundance) in pressurized treatments with the inoculum initially extracted from a UASB treating petrochemical wastewater (ADI) (Chapter 3). Despite strain isolation being out of the scope of this thesis, it could be of interest for future research to isolate organisms with piezotolerant features from uncommon sources like industrial reactors treating effluents under other extreme conditions. Through this approach, the here suggested cross-resistance effects between salinity, temperature and mild hydrostatic pressure resistance could be further confirmed. Moreover, specific cross-resistance effects could be ascribed to specific features of the strain, *e.g.,* EPS production, presence of cell wall and lipid membrane composition.

Acid and pressure stress responses share commonalities in terms of microbial response. There are reports of increasing concentrations of dissolved CO_2 upregulating genes associated with the stress response in *E. coli* (Baez et al., 2009; Sun et al., 2005). Thus, the backward mechanism, *i.e.,* increased acid levels triggering stress response mechanisms that can be used when exposed to elevated pCO_2, was a logical assumption that needed to be tested. It was hypothesized that deliberate biomass exposure to a progressive increase in the S/X ratio during the atmospheric incubation could induce cross-resistance effects during the pressurized incubation. In turn, this cross-resistance could have been attributed to i) elements of the general

stress response, such as metabolic regulation, repair of macromolecules and altered membrane fluidity conserving membrane integrity and improving cell viability, and ii) modification of the microbial community dynamics with more resilient syntrophic partners. Evaluation of membrane permeability and structure using techniques such as fluorescence microscopy and transmission electron microscopy are required to confirm our postulate regarding the conserved membrane integrity (Prieto-Calvo et al., 2014). Undoubtedly, reduced metabolic heterogeneity (Huang et al., 2016) was achieved with the ALE strategy. Concomitantly, and as a positive side effect, a more resilient pathway for syntrophic propionate oxidation was selected, the dismutation pathway from *Smithella*. Due to higher independence on pH_2 and pCO_2, the dismutation pathway contributed to achieving high CH_4 yields per viable archaeal cell (Chapter 4).

It remains to be investigated if longer incubations under elevated pCO_2 will select a more resilient community able to cope with heterogeneous feeding patterns. Furthermore, it is pivotal to track the temporal occurrence of shifts in microbial community composition and structure. The conditions imposed during short adaptation periods under elevated pCO_2 (Chapter 5) already provided insight into how elevated pCO_2 can distinctively reshape the microbial community (Figure 5-5 and Figure 5-6). However, due to the dynamic interplay of process conditions in Chapter 5, a straightforward distinction between the specific effects of pCO_2, high S/X ratio and formate addition on the microbial structure was rather difficult. Nevertheless, the short-term effect on the community composition is evident, despite the changes in relative abundances resulting from a single parameter (pCO_2) or interaction effects with the studied operational conditions. Conversely, the long-term effect of moderate pCO_2 in high-pressure anaerobic processes needs to be studied in a modified setup, which permits systematic substrate feeding under continuous flow conditions.

6.5 Steering towards different products in high-pressure anaerobic processes

The previous sections show that biomethane and selective carboxylates production in high-pressure AD and MCF will result from applying "proper" selective pressures, such as pCO_2, pH, pH_2, and temperature. Pathway predominance will also result from interaction effects between multiple process conditions impacting thermodynamics, kinetics and microbial physiology. Moreover, substrate specificity, type of inoculum and the feedback responses between environmental conditions and microbial community dynamics will also play an important role when targeting biomethane or carboxylates production. Two clear examples of these complex interactions studied during this research are discussed in the following sections:

biomethane production and steering towards carboxylates production in anaerobic reactors under elevated pCO_2.

6.5.1 Biomethane production

In Chapter 4, it was determined that providing the proper conditions for syntrophic propionate oxidation by applying glycerol as the substrate and ALE to increase microbiome endurance (Carballa et al., 2015) helped to achieve distinctive CH_4 yield per viable archaeal cell (Figure 4-10) under conditions of elevated pCO_2. The selection of more resilient syntrophic partners, *i.e., Smithella* genus, on top of the increased abundance of a traditional syntrophic propionate oxidizer such as *Syntrophobacter,* appears to have been pivotal to sustain biomethane production at elevated pCO_2. This directional selection of syntrophic partners was likely complemented by the occurrence of a stress-tolerant microbial community established after the ALE process at increasing S/X ratio. The clear advantages of the dismutation pathway to enable propionate oxidation under elevated pCO_2 and fluctuating pH_2 corresponded to a) thermodynamic feasibility independent of the "pH_2 bottleneck" (Li et al., 2012; Van Lier et al., 1993) and b) presumably, a better stress response in the microorganisms from this genus, which allowed them to become predominant after ALE at increasing S/X ratio. The overall outcome of the directional selection process was a microbial community for biomethane production with improved performance under elevated pCO_2. Since there are commonalities between the acid resistance stress response and the response to elevated dissolved CO_2 (Section 6.3.2), we speculate that cross-resistance may have also played a key role in this adaptation.

6.5.2 Steering towards carboxylates production

Results from Chapter 4 showed that after the ALE process under increasing S/X ratio, an evolved inoculum was obtained whose "restructured microbial community" could carry out syntrophic propionate oxidation under the imposed environmental conditions. Moreover, we could speculate that a high S/X ratio triggered "stress-tolerance" in the anaerobic inoculum, evidenced by higher final cell densities in the evolved inoculum compared to the original. An increased S/X ratio has been proposed to steer product formation in MCF (Arslan et al., 2016); thus, results from Chapter 4 justified the design of experiments aiming process steering towards carboxylates production.

Chapter 5 studied the interaction effects of elevated pCO_2 with mixed substrate provision, increased S/X ratio, and formate addition in HP-MCF. Overall, the imposed conditions were favourable for carboxylates production with distinctive differences in the subsequential experiments. Propionate production was measured in the control assays with only glycerol and

CO_2 as substrates, whereas butyrate + acetate production was found in the control assays with glucose and CO_2 as substrates. Furthermore, an overall increase in acetate concentrations was observed in experiments in Chapter 5, and was attributed to a likely increased homoacetogenesis and constrained methanogenic activity (Table 5-3). After formate addition, succinate (282 mg L^{-1}) was present in the mixed substrate treatments and CH_4 production was re-established to a certain extent. The interaction between substrate specificity, elevated pCO_2, presence of additional electron donor, and increment in the S/X ratio gave interesting results in the experiments presented in this thesis. However, more research is needed to identify specific relations between applied levels of the various parameters and specific output, *e.g.,* selective propionate or butyrate formation, following a design of experiments (DoE) approach.

Propionate production is an alternative to valorize waste biomass via MCF (Chen et al., 2016). By-products of the biodiesel industry, such as glycerol, can be valorized through its conversion to propionate. Moreover, by imposing appropriate selective pressures, "key players", *e.g.,* members of family Veillonellacea with proven capabilities for glycerol conversion to propionate via the succinate pathway, can be favoured (Chapter 5). If waste carbohydrates are used for propionate production, imposed conditions could instead favour lactate production to concomitantly select for particular *Clostridium* spp. (*Clostridium propionicum*) (Gonzalez-Garcia et al., 2017) and the acrylate pathway for propionate production (Chapter 5). Both options could be explored in pressurized and atmospheric systems.

Fermentative succinate production constitutes a viable alternative to the traditional petrochemical process (Cao et al., 2013), with high selectivity and yield and open culture utilization as highly desirable features (Chen et al., 2016; Ferreira et al., 2020). The addition of formate as an additional electron donor was associated with succinate production in treatments with mixed substrate and elevated pCO_2, which positively affected the final cell densities (Figure 5-2 and Figure 5-3). Our results indicated the effect of specific operational conditions to trigger succinate production: a) high S/X ratio, b) presence of formate as additional electron donor, c) biomass adaptation under pressurized conditions d) propionate accumulation until non-inhibitory levels. Applying the mentioned operational conditions in a continuous mode of operation, or as a periodical disturbance, could lead to a high-yielding succinate process using anaerobic microbiomes with restructured microbial communities. Additionally, studies to describe competitive formate utilization in artificially assembled consortia could increase our understanding of formate utilization by bacteria such as *Clostridium* spp. and hydrogenotrophic archaea. In this way, clarity will be given to the possible fate of formate in anaerobic systems under elevated pCO_2.

On the other hand, in Chapter 3, a slightly different approach was taken to promote carboxylate production using marine sediment and saline adapted biomass from an anaerobic digester as

inocula. First, during the enrichment, *i.e.,* subsequential transfers in serum bottles, conditions of high S/X ratio were imposed during short periods in between transfers to generate unfavourable conditions for methanogens proliferation. The high S/X ratio was particularly extreme considering the carbon availability in the natural settings of the inoculum's origin (Weston and Joye, 2005); thus, this was already a preliminary strong selective pressure for the inoculum from the marine sediment (MSI). The short inter-cycle periods imposed unfavourable conditions for syntrophic partners with low growth rates and high sensitivity to high acid concentrations, *e.g.,* methanogenic archaea, whose abundance was significantly reduced. Afterwards, when exposed to a stronger combination of selective pressures, *i.e.,* high temperature and MHP, this saline-fermenting-enriched inoculum produced more carboxylates. The exacerbated carboxylates production was likely associated with increased energy requirements for maintenance (*m*), enhanced decay and constrained growth, as discussed in Chapter 3. In the aftermath, the "right" combination of selective pressures in NMC and EMC was favourable for carboxylates production as initially hypothesized.

6.5.3 The role of glucose and glycerol as steering parameters

In Chapter 2, limitations in propionate and butyrate syntrophic oxidation occurred under conditions of elevated pCO_2, leading to their accumulation. It was proposed that those limitations were associated with kinetic, bioenergetic, and physiological aspects and, to a minor degree, with the presence of undissociated carboxylates. Chapter 2 also suggested that using energy-rich substrates such as glucose and glycerol and biomass adaptation could help to relieve the observed constraints in the syntrophic oxidations, while working under elevated pCO_2.

Glucose and glycerol can be fermented to the carboxylates, acetate, propionate, and butyrate, to other organic acids, such as succinate, lactate, and formate, as well as to alcohols, H_2 and CO_2 (Freguia et al., 2008). In syntrophic propionate and butyrate oxidation (Chapter 2), elevated pCO_2 was slightly detrimental to the bioenergetics of aceticlastic methanogenesis due to product inhibition. Conversely, it was favorable for hydrogenotrophic methanogenesis due to higher substrate availability. It was hypothesized that the production of additional acetate, H_2, and formate from the acidogenic pathways of glycerol and glucose fermentation could stimulate the activity and growth of homoacetogenic bacteria and methanogens, enabling the syntrophic conversion of acetate (Detman et al., 2021). Moreover, acidogenesis from glycerol and glucose was expected to influence environmental conditions, such as the bulk pH, impacting the feasibility of H^+-consuming reactions, such as aceticlastic methanogenesis and, ultimately, the actual energy harvested by the microorganisms (González-Cabaleiro et al., 2021). Also, the differences in the degree of reduction between glucose and glycerol (-0.67 and 0 electron equivalents/C-mol) would generate different quantities of reducing equivalents

(Hoelzle et al., 2014). Depending on the prevailing fermentation pathway and the enzymatic machinery of the microorganism, reducing equivalents could be transported outside the cell by different electron carriers (H_2, formate), enabling specific interactions with syntrophic methanogenic partners (Müller et al., 2010). These mechanisms were expected to relieve limitations in the syntrophic oxidation of propionate and butyrate under elevated pCO_2. However, the results presented in Chapter 4 (Figure 4-4 and Figure 4-9) evidenced that propionate oxidation was still limited at elevated pCO_2 in experiments with glucose and glycerol (1 g COD L^{-1}) as the substrate.

On the other hand, the ALE process at increasing S/X ratio was seemingly favourable for methane production under elevated pCO_2 since the highest CH_4 yield per viable cell was obtained in experiments at 5 bar pCO_2, particularly in the case of glycerol as the substrate (Figure 4-10). Building upon results from Chapters 2 and 4, it was decided to test the effects of moderately high substrate concentrations (5-10 g COD L^{-1}), leading to noteworthy differences in the S/X ratio, to steer the pressurized system towards carboxylates production. A high S/X ratio was accompanied by mixed substrate provision. Glycerol was provided to promote reduced product formation and glucose to satisfy the anabolic energy requirements via an increased ATP yield from products such as acetate. The mixed substrate was provided under the assumption that glucose and glycerol could be used by microorganisms without any of them triggering a strong catabolite repression on the assimilation of the other (Malaoui and Marczak, 2001) (Chapter 5). However, it was later observed that each substrate resulted in the selection of reported glycerol fermenting organisms (family Veillonellaceae) and glucose fermenting organisms (*Clostridium* spp.). Hence, both Veillonellaceae and *Clostridium* spp. became predominant in mixed substrate experiments. Furthermore, propionate and butyrate syntrophic oxidation were limited during all phases of the sequential pressurized incubations. Immediately following the dosing of formate as additional electron donor, methanogenesis was re-established (Chapter 5).

Glycerol and glucose share the glycolytic pathway (Sauer and Eikmanns, 2005) for their conversion under anaerobic conditions. Despite this feature, carbon and reducing equivalents (electrons) distribution over the different pathways will depend on the imposed environmental conditions and the functional diversity of the microbial community. From the results of this thesis (Chapters 4 and 5), it is evidenced that glycerol is a suitable carbon and energy source for selective propionate production under a particular set of conditions: elevated pCO_2, elevated alkalinity to keep pH around circumneutral values, moderate S/X ratio, presence of formate as additional electron donor, and a microbial community with a distinctive presence of the family *Veillonellaceae.* However, if the fermentation process targets succinate rather than propionate production, it is worth investigating mixed substrate provision, such as glycerol + glucose. Results from Chapter 5 evidenced the appearance of succinate as an important intermediate of

the fermentation (≈10% of the COD fed) in the reactors with glycerol and glucose in a 1:1 molar ratio. Succinate was observed in pressurized reactors after formate addition and after two incubation cycles with subsequential transfers to increase the S/X ratio.

In the experiments presented in Chapter 5, the use of glucose as fermentation substrate under conditions of elevated pCO_2 led to the production of significant amounts of butyrate. Enhanced butyrate production was ascribed to a likely promoted activity of butyryl-CoA: acetate CoA-transferase in the presence of excess acetate and carbohydrates (van Lingen et al., 2016; Zhang et al., 2013) and to thermodynamically favourable acetate-lactate chain elongation processes (Eq. 13 Table 5-7) (Candry et al., 2020; Spirito et al., 2014). Our results align with previous research from Arslan et al. (2013, 2012). These authors already demonstrated the feasibility of steering the glucose product spectrum towards selective butyrate formation by increasing pCO_2 and substrate concentration under batch conditions (as performed in Chapter 5) and continuous flow conditions. The studies from Arslan et al. (2013, 2012) also postulated lactate-acetate chain elongation, directional selection of the community, and high S/X ratio as possible explanatory mechanisms for the product profile dominated by butyrate. However, the specific role of hydrogen in MCF under elevated pCO_2 remains to be elucidated. Continuous monitoring of the headspace composition over time under pressurized conditions, coupled with thermodynamic calculations based on the dynamic changes in partial pressures and intermediates concentrations, could help to unravel the particular role of pH_2.

6.6 Outlook

6.6.1 Research follow up

Complex substrates, rate modulation and syngas fermentation

From Lindeboom et al. (2016, 2014, 2013a, 2012) and our present study, we could make a representative overview of the effects of pressure and elevated pCO_2 on AD and MCF. However, this knowledge needs to be translated to the actual treatment of solid and liquid wastes, where increased pressure could be beneficial. For example, biodiesel by-products containing high levels of crude glycerol (Posada et al., 2011) are an interesting feedstock for propionate production under elevated pCO_2 following up on the results from Chapters 4 and 5. Nonetheless, the effect of possible inhibitory compounds such as salts and methanol needs to be concomitantly addressed (Dietz and Zeng, 2014).

From a more technological perspective, due to the rate modulation effect of MHP and elevated pCO_2 (Chapters 2, 3 and 5), these operational parameters could be applied to two-stage systems

to control acid production rate when using carbohydrate-rich substrates from the food and beverages industry (Labatut et al., 2011). Furthermore, rate modulation could also lead to a better temporal coupling between acidogenesis and methanogenesis in phased AD. Hydrolysis improvement at more cost-effective milder conditions than supercritical CO_2, independently or in combination with other physicochemical alternatives, can also be explored to enhance posterior enzymatic hydrolysis and, in consequence, overall CH_4 yield (Navarro et al., 2021).

In pressure reactors, syngas fermentation to acetic acid, ethanol, and formic acid or bio-methanation with adapted open microbiomes needs further investigation. Gas transfer rates could be distinctly improved due to the elevated pressure operation. However, optimized operational conditions, namely reactor design, the biomass-gas ratio and increased external H_2 supply, need to be further explored (Figueras et al., 2021; C. Li et al., 2021; Sivalingam and Dinamarca, 2021). Furthermore, possible inhibition of key microbial groups due to increased gaseous substrate availability needs to be addressed. For example, carboxydotrophs, *i.e.,* CO-utilizing microorganisms, have shown to be sensitive to CO pressure > 2 bar (Figueras et al., 2021). In single-stage biogas upgrading applications, H_2 transfer, which is considered the limiting factor in substrate conversion, can benefit from pressurized operation combined with adequate reactor configurations, including bubble columns, airlift and stirred tank reactors (Díaz et al., 2020; Van Hecke et al., 2019). Moreover, the presented multi-parameter analysis on bioenergetics (Chapter 2) could help to identify thermodynamic limitations in syngas fermentation, in which the headspace composition is subject to temporal changes due to fluctuations in the partial pressures of gaseous substrates/products.

Utilization of natural communities to enhance performance under elevated pressure and pCO_2

The addition of microorganisms with a desired functionality trait to enhance process performance (Herrero and Stuckey, 2015), has been employed to accelerate the recovery of temporarily intoxicated anaerobic digesters (Schauer-Gimenez et al., 2010). Our present work showed that natural communities (NMC) might be more resilient to specific environmental stressors due to their continuous exposure to environmental gradients (Chapter 3). Depending on the prevailing relations in the original incubations, namely competition vs syntrophy, and the adaptability potential of the added biomass to operational conditions, the overall piezotolerance and/or tolerance to elevated pCO_2 could be enhanced. Preliminary studies on the co-cultivation of hydrocarbon-degrading piezotolerant isolates at atmospheric and high-pressure conditions indicates the possibility to “synthesize” piezotolerant communities (Van Landuyt et al., 2020). Moreover, provided that reducing equivalents are available, incorporating highly specialized microorganisms, such as homoacetogens and

hydrogenotrophic archaea, which are able to grow under the operational conditions of interest, could improve the overall conversion process due to their CO_2-utilization capabilities.

Direct interspecies electron transfer (DIET) in high-pressure anaerobic systems

DIET may be an option worth investigating in pressurized systems since the feasibility of syntrophic reactions may gain independence from mass transfer phenomena associated with interspecies electron transfer. Liu et al. (2020) thoroughly examined the energy feasibility of syntrophic methanogenesis using ethanol as a carbon source and including DIET as part of syntrophic reactions in addition to aceticlastic and hydrogenotrophic methanogenesis. Under product and reactant concentrations of 1 M and after corrections for T=305 K and gas partial pressures of 1 atm, the net available energies (ΔG_{cat}^{01} in kJ mol^{-1}) were comparable (-91.44 kJ mol_{ED}^{-1}) when considering syntrophic ethanol oxidation with a) hydrogenotrophic methanogenesis or b) DIET. However, a pH_2 in the order of magnitude suggested by these authors, is difficult to obtain by microbial fermentative activity only. Thus, this oversimplified assumption may mask other underlying issues, such as mass transfer limitations, that define the real hydrogen concentration to which microbes are exposed and ultimately the available ΔG_{cat}^{01}. In this regard, DIET appears as a more resilient and effective process for syntrophic oxidation due to its independence from the concentration gradient, diffusion of mediators (hydrogen) and the associated thermodynamic constraints in reaction feasibility (Storck et al., 2016).

From a thermodynamic perspective, in methanogenesis DIET has a competitive advantage over interspecies electron transfer via hydrogen, since it avoids energy losses in production, consumption and diffusion of electron carriers (Baek et al., 2018). A digester supported by DIET can be envisioned to directly enhance CH_4 production by utilizing the electrons, protons and CO_2 from the oxidation of intermediates such as propionate and butyrate. Instead of hydrogenotrophic methanogenesis as electron sink, electroactive bacteria might be favored, which are cooperating in syntrophy with aceticlastic methanogens. One of the observed effects of elevated pCO_2 in this research was the lowered relative abundance of hydrogenotrophic archaea and increased relative abundance of aceticlastic archaea (Figure 5-5). Therefore, elevated pCO_2 could indirectly facilitate DIET via amendments in the microbial community as the ones observed in this thesis. In terms of the microbial community and enhanced DIET, the recently postulated DIET between *Chloroflexi* and *Methanosaeta* (J. Li et al., 2021; Wang et al., 2020) could also be studied in HPAD reactors since the applied and established conditions in Chapter 5 (elevated pCO_2 and high S/X ratio) were favourable for the predominance of both taxa (Figure 5-5).

In addition to tailor-made adaptive laboratory evolution procedures to favour the predominance of taxa of interest (Chapter 4), the usage of conductive materials, namely magnetite, biochar, could also be tested in pressurized systems to achieve more direct management of the available electrons (Martins et al., 2018). Recent studies have found that members of *Ercella*, one of the prevalent genera under pressurized conditions when using adapted inoculum from a UASB treating petrochemical wastewater with high salinity (Chapter 3), can transfer electrons to extracellular acceptors. More remarkable, *Ercella* members have successfully used conductive materials, *e.g.,* carbon cloth, to transfer electrons to methanogens (Feng et al., 2021).

Affordability to increase reproducibility

High-pressure operation, either in fermentation, pre-treatment or downstream applications, is usually perceived as expensive (Noppawan et al., 2021). However, contrasting evidence comes from techno-economic analyses addressing these technologies, making a case for economic and environmental sustainability benefits (Wu et al., 2020). Furthermore, recent investigations have shown that increased product yields are associated with stage-wise use of elevated pCO_2. For example, operation under moderate supercritical CO_2 (T >31°C and P > 74 bar) can help to enhance enzymatic hydrolysis and overall biogas production (Navarro et al., 2021). Supercritical-CO_2-assisted enzymatic hydrolysis, when integrated into a biorefinery concept, can lead to cuts in production costs in the order of 40% (Wu et al., 2020). Pressurized treatment (*e.g.,* supercritical CO_2) can also help to increase sustainability in processes such as bioethanol production by reducing the total energy consumption due to enhanced hydrolysis. Recent studies show that alternative hydrolysis processes making use of harsher conditions are associated with a higher energy consumption for achieving similar product yields than supercritical CO_2-based hydrolysis (Ge et al., 2020; Wu et al., 2020).

On the other hand, high-pressure operation has been included inside recent techno-economical assessments and life cycle cost analysis. In the case of biogas upgrading with pressure swing adsorption (PSA) and High-Pressure Water Scrubbing (HPWS), the operation occurs inside a pressure range comparable to the one employed in this thesis (≤ 10bar). It was established that PSA and HPWS are slightly more cost-effective for small and medium-size gas-producing plants (350-500 Nm^3 biogas h^{-1}) than traditional alternatives (Lombardi and Francini, 2020).

Considering the current natural gas crisis, HPAD with elevated pCO_2 is a technology that could support a resilient, decentralized energy supply. HPAD is particularly relevant in direct biogas upgrading to biomethane. According to the European Biogas Association, biomethane will play an important role to achieve energy independence since it shall cover 20% of current European Union gas imports from Russia by 2030 (2022). Furthermore, when envisioning a hydrogen-based bioeconomy (De Vrieze et al., 2020), indirect biogas upgrading can be considered an

additional energy storage process, where high-pressure operation could play a pivotal role. Pressurized operation can enhance the mass transfer of renewably produced H_2, externally added to AD reactors, and the solubilization of CO_2 from the produced biogas. Due to the positive effect of pressure on indirect biogas upgrading, the overall CH_4 production is increased (Lai et al., 2021). Based on these scenarios, upscaling of HPAD at elevated pCO_2 should be pursued independently of preliminary cost-effectiveness calculations.

Soft-sensor applications can further reduce costs in environmental bioprocesses operating under pressure (Luttmann et al., 2012). Soft-sensors are software-based and use mathematical models fed with available online data to estimate the value of a specific process variable that is challenging to measure. This thesis investigated a simplified approach for pH estimation in pressurized systems via soft-sensors (See Annex A). However, estimating other variables of interest, such as biomass growth and gas transfer rate, could be derived from more complex dynamic mass balance models (Luttmann et al., 2012). The rapid growth of the Internet-of-Things (IoT) and open-source electronic prototyping platforms (Arduino®, Raspberry Pi) for process monitoring and control could further help to decrease operational costs. However, specific calibration procedures and extensive testing will be required to achieve research-grade scientific instrumentation, but with the advantage of increasing process monitoring capabilities for a fraction of the costs (Chan et al., 2021). The selection of affordable materials for reactor construction, such as PVC (See Annex A) and novel tools such as 3D printing for reactor customization, could further improve process economics (Dursun et al., 2021). The mentioned approaches will help advance moderate and high-pressure research and speed up bioprocess innovation.

Monitoring biomass growth, microbial community dynamics and microbial activity in high-pressure operation: novel approaches

This thesis (Chapter 3) has limitedly shown the potential for incorporating new techniques to describe microbial growth and community dynamics, namely flow cytometry (FCM). This technique has been recently compared with more well-established alternatives such as Illumina sequencing, metabolomics and metaproteomics. According to the authors, FCM shows promising results in describing community composition (beta diversity) in a shorter and less biased way (De Vrieze et al., 2021). However, its application in high-pressure systems remains challenging because FCM analyses are being carried out in depressurized samples, which likely affects cell viability despite the decompression process being done at conservative rates (Zhang et al., 2020). The alternative, *i.e.,* to carry out continuous real-time data acquisition with FCM equipment in pressurized reactors, is technically complex. Nevertheless, experiences with custom-built continuous staining devices for analysis of microbial communities are already available for drinking water monitoring (Props et al., 2018). Thus, if technical challenges are

overcome, such a system could also operate at moderate pressures, significantly improving our monitoring capabilities.

One of the current bottlenecks in high-pressure systems, in general, is in-situ monitoring. Traditionally, samples are taken from pressurized equipment and measured at atmospheric conditions, which might introduce biases in the measurement. Non-invasive, non-destructive techniques, such as in-situ Raman and X-ray spectroscopy, have already been used to monitor in-situ microbial activity in high-pressure reactors/cells via quantification of liquid and gas metabolites (Knebl et al., 2020; Oger et al., 2010; Picard et al., 2007). These technologies could potentially be used to further elucidate the effect of high pressure on the activity of open microbiomes. However, specially designed reactors with optical fibers or transparent openings need to become available. Provided these reactor innovations occur, Raman and X-ray spectroscopy can be used as a suitable option to corroborate the conclusions reached so far with traditional biomass monitoring schemes (Oger et al., 2010).

Isolated strains with proven stress tolerance and biopolymer production capabilities could be used in bioprocesses, where pressure has shown interesting modifying effects, *e.g.,* in biopolymer production (Mota et al., 2019). Furthermore, for the particular case of biocellulose production, the use of glycerol as a substrate has shown a positive effect on the yield and properties of the obtained material (Kato et al., 2007; Zhong et al., 2013). Thus, biopolymer production under pressurized conditions with open cultures or strains isolated from open cultures under extremes conditions using (waste) glycerol as a substrate is an avenue worth exploring.

Regarding the ALE process (Chapter 4), additional experiments in parallel where ALE at increasing S/X ratio is carried out with a headspace of a) just H_2, b) mixture H_2:CO_2 and c) just CO_2 at the same buffer capacity are required. Through these experiments, we could discriminate pH effects and further elucidate the role of elevated CO_2 on hydrogen consumption/production in HPAD and HP-MCF. Subsequently, the obtained inoculum could be incubated in parallel at pressurized conditions with i) headspace composition of origin and ii) alternative compositions tested in ALE. This set of experiments could help depict additional cross-resistance effects due to fluctuating headspace composition.

Effects of elevated pCO_2 on membrane permeability

It has been postulated that elevated pCO_2 effects on substrate uptake depend on the transport systems found in microorganisms converting glucose or glycerol: PTS vs facilitated diffusion (Carruthers, 1991; Mitchell, 2016). Thus, it remains to be proven if an enhanced membrane permeability due to elevated pCO_2 facilitated substrate uptake. In the chain of events, this could

have triggered pathways such as lactate uptake for immediate use of reducing equivalents (Hoelzle et al., 2021) but also could have resulted in the uncoupling of catabolism and anabolism. Therefore, studies on cell membrane permeability under elevated pCO_2 in mixed cultures or artificially assembled syntrophic consortia are required to determine the synergistic effects of elevated pCO_2 and high S/X ratio on substrate uptake rates.

Pressure effects in AD and MCF need to be addressed

Pressure is an operational parameter not considered at the same level of importance as temperature, pH, OLR, SRT in AD or MCF. However, with the deployment of high-rate anaerobic digesters (*e.g.,* expanded granular sludge bed - EGSB) biomass can be exposed to pressures between 1-2.5 bar. EGSB reactors are characterized by a higher height-to-diameter ratio than conventional anaerobic reactors, such as the upflow anaerobic sludge blanket (UASB) reactor (Seghezzo et al., 1998). The operational pressure range of 1-2.5 bar is estimated from the correspondence between pressure increase and depth (1 bar per 10 m). Depending on the biogas composition, this could imply exposure to pCO_2 in the range from 0.5-0.8 bar. Despite being in the low range of pressures studied in this research, these values have been already associated with kinetic limitations and shifts in microbial community structure (Chapters 2 and 4). Operational problems observed in EGSB reactors could also be associated with pressurization, depressurization, volume compression and biomass recirculation cycles. Some of the results presented here could justify further studies on the effect of these cycles on biomass activity and growth in high-rate AD reactors at the pilot or industrial scale.

The usage of elevated pCO_2 has also been investigated inside AD-associated technologies such as Dissolved Air Flotation (DAF) for microbubble generation to achieve optimal performance in solid-liquid separation (research with Super-W consortium partner Paques Technology B.V.). Preliminary results were promising regarding particle separation[2]. However, due to the elevated pCO_2 employed in the DAF system (2-3 bar), when compared to pCO_2 in traditional AD, it is crucial to address the effects of biomass exposure to high levels of dissolved CO_2 if biomass recirculation from the DAF to the main digestion unit is intended.

[2] Data not shown due to confidentiality agreement

AD and CO_2 sequestration – towards negative carbon systems

The usage of AD as a technology for carbon (CO_2) sequestration has been recently reviewed by Xu et al. (2021) and distinctive approaches have been presented. For example, CO_2 bio-conversion mediated by exogenous H_2 can occur in a separate bioreactor (ex-situ biogas upgrading) (Angelidaki et al., 2018; Díaz et al., 2015) or the same digester (in-situ upgrading) (Deschamps et al., 2021; Zabranska and Pokorna, 2018). However, in-situ biogas upgrading might impact overall process stability due to CO_2 consumption modifying operational pH (Kougias et al., 2017). Moreover, thermodynamic limitations in syntrophic propionate and butyrate oxidation could become evident due to increased pH_2 when exogenous H_2 is added to the reactors. As well, high pH_2 may lead to a transition of the dominant syntrophic interaction in the digester: at high pH_2, homoacetogens may become predominant, due to their higher H_2 threshold (350-700 nM) and can outcompete hydrogenotrophic methanogens (Xu et al., 2021). Thus, at high pH_2, H_2 and CO_2 are transitorily converted into acetate, subsequently consumed by aceticlastic methanogens (Aryal et al. 2018). This process could further take advantage of the mixotrophic capacity of acetogens (Chapter 5) such as *Clostridium* spp., *Eubacterium limosum* and *Moorella thermoacetica* to achieve high acetate levels due to heterotrophic sugar conversion and autotrophic CO_2 fixation (Jones et al., 2016).

Another alternative for CO_2 sequestration is based on electromethanogenesis. In this process, external energy is supplied to drive the non-spontaneous reaction of CO_2 to CH_4 (Cheng et al., 2009; Van Eerten-Jansen et al., 2012). Electromethanogenesis can occur by direct electron transfer from the cathode to the microbe via outer membrane redox proteins such as cytochromes and conductive pili (Choi and Sang, 2016). Furthermore, electromethanogenesis can indirectly occur via the formation of H_2 in the cathodic compartment from free H^+ and posterior utilization by hydrogenotrophic methanogens (Blasco-Gómez et al., 2017). In the latter work, the performance of electromethanogenic systems could be improved by enhanced mass transfer of gaseous substrates (CO_2) due to increased operational pressures. The practical usage of the gaseous substrate seems to be preferred, due to pH stabilization under continuous flushing and potential financial savings compared to the utilization of carbonates (Jiang and Zeng, 2018). Other opportunities for CO_2 utilization in AD include CO_2 reduction coupled with increased electron transfer due to DIET in digesters where electroconductive materials such as magnetite, biochar and activated carbon are present (Xiao et al., 2019). CH_4 production rates might be improved, due to the higher substrate availability (CO_2) for electromethanogenesis (Guo et al., 2021) associated with high pressure operation, and the aforementioned increased electron transfer rate.

On the other hand, the production of multi-carbon compounds from CO_2 constitutes a form of energy storage. Through microbial electrosynthesis (Rabaey and Rozendal, 2010), CO_2 can be

converted into acetate (Patil et al., 2015) or butyrate (Ntagia et al., 2021), which are precursors for the chemical industry (Nevin et al., 2010). Other researchers have proposed "microbial electrolytic carbon capture" as a suitable alternative for CO_2 capture and utilized this concept already at full scale at a wastewater treatment plant (Lu et al., 2015). In this technology, the organic matter present in high-salinity wastewater from the petrochemical industry is used to produce protons. Protons, in turn, interact with metal hydroxides formed in the cathode compartment, transforming CO_2 into metal-bicarbonate. Bicarbonate can be further used for alkalinity regulation in the plant, helping to reduce operational costs (Lu et al., 2015).

Another possibility for CO_2 valorization in two-stage AD systems may come from using H_2 and CO_2-rich off-gas from the acidogenic reactor, while controlling the partial pressures in the stoichiometric ratio of 4:1, to stimulate the hydrogenotrophic methanogenic pathway in the second stage (Xu et al., 2021). CO_2-enriched gaseous streams also can be obtained after pre-treatment of flue gases from cement production, fossil fuel-fired power plants with gas separation membranes. The CO_2-enriched stream could be used for selective acetate production by simultaneous CO_2 sequestration in AD reactors with enriched homoacetogenic activity, provided hydrogen or formate are present as electron donors (Liu et al., 2017). In their investigation, Liu et al. (2017) also mentioned the importance of inoculum enrichment for homoacetogenic activity using sodium formate and the CO_2 content in the headspace. Chapter 5 suggested an important role of formate and CO_2 for enhancing acetogenic activity in AD. However, more research is needed to clarify the specific role of formate in enhancing homoacetogenic activity under pressurized conditions.

From a circular economy perspective, a photosynthetic route for CO_2 capture with microalgae could be explored for biogas upgrading to biomethane. In this process, light-driven CO_2 fixation is carried out by microalgae in coexistence with sulfur-oxidizing bacteria that can oxidize the H_2S from the biogas to sulfate using the oxygen produced by the microalgae (Franco-Morgado et al., 2018; Passos et al., 2018). By moderately increasing the operating pressure of transparent photobioreactors, CO_2 gas transfer can positively improve, impacting the overall productivity. Moreover, pressure and CO_2 could also be used in harvesting the microalgae via pressure-induced coagulation (Lee et al., 2015). As well, when going towards the supercritical CO_2 conditions (*e.g.,* 50 MPa and 80°C), the recovery of industrially relevant pigments (β-carotene, chlorophyll) can be assisted (Kitada et al., 2009). Similar to the research line concerning photo-CO_2-valorization, investigations with purple phototrophic bacteria (PPB), a type of β-Proteobacteria capable of hetero/ auto/ and mixotrophic metabolisms, are gaining momentum (Kondaveeti et al., 2020). The capability of PPB for CO_2-fixation via the Calvin-Benson-Bassham cycle is of particular interest. PBB can assimilate CO_2 via photoheterotrophy of reduced substrates (propionate, butyrate, valerate, caproate) in the presence of infrared light. CO_2 can also be fixed by photo-autotrophy, where the electron donor

could be H_2, produced via more sustainable alternatives such as water hydrolysis driven by solar or wind (Angelidaki et al., 2018; Puyol et al., 2017a). Due to their versatile metabolism, PBB potentially could be used to produce high-quality microbial protein (MP) and other by-products such as fatty acids, carotenoids, phytohormones and vitamins from residual waters, such as domestic sewage. MP production combining anaerobic fermentation and PPB is an alternative worth exploring inside the resource recovery agenda coupled with increased sustainability in protein production (Capson-Tojo et al., 2020). However, these technologies are immature, and further research is needed (Alloul et al., 2021; Capson-Tojo et al., 2020; Puyol et al., 2017a; Spanoghe et al., 2021).

Some of the envisioned / previously reported technological integrations keeping AD/MCF as a core technology but oriented towards CO_2 sequestration and utilization are presented in Figure 6-3.

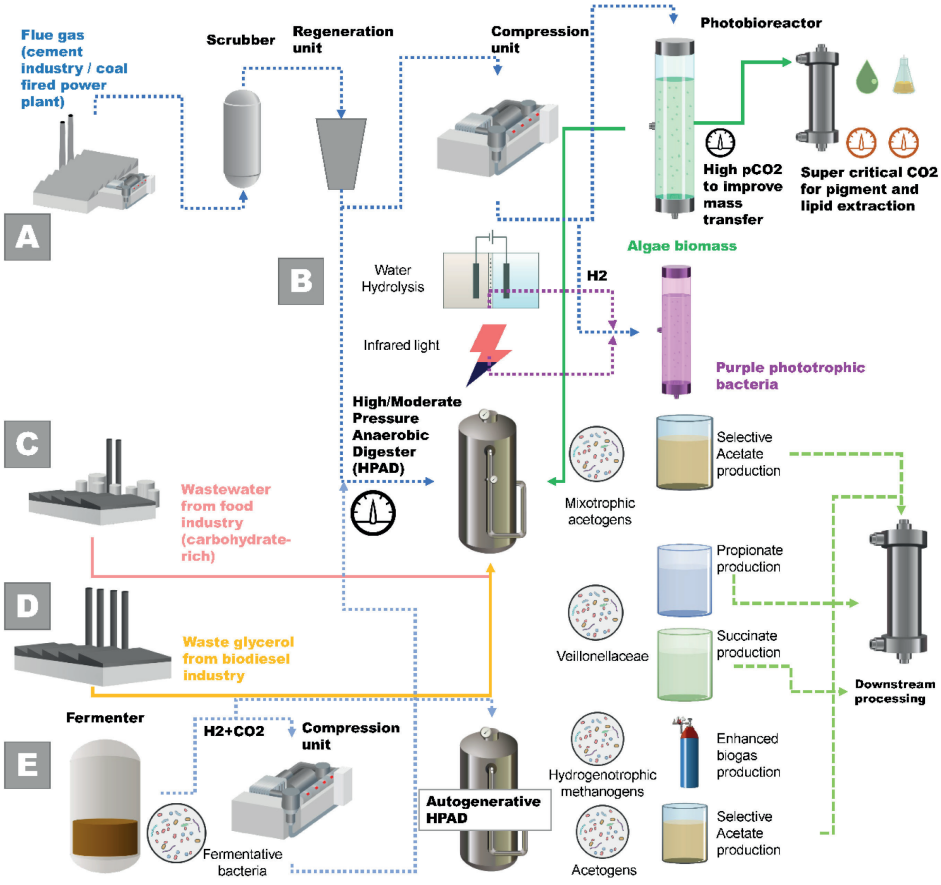

Figure 6-3: Proposed/ envisioned technology integration for CO_2 sequestration and utilization in anaerobic digestion (AD) systems

A

APPENDIX A

FRUGAL PRESSURE RESISTANT BIOREACTORS AND pH MONITORING

This section is based on:

Application of soft-sensor for pH monitoring in High-Pressure reactors used for Mixed Culture fermentation
P.S. Ceron-Chafla, R.E.F Lindeboom, K. Rabaey and J.B van Lier
Conference proceedings: ADTech-SAB2018: The 2nd InternationalConference on Anaerobic Digestion Technology. Sustainable Alternative Bioenergy for a Stable Life, 4-7 June 2018, Chiang Mai, Thailand

Effects of selected operational parameters on pH of anaerobic biological systems working under elevated CO_2 partial pressures
Additional thesis
Yiyi Zhang (4701542)

Frugalizing engineering solutions for recovery of resources from wastewater
Pamela Ceron-Chafla, Ralph E.F. Lindeboom
Chapter in Handbook on Frugal Innovation – International Center for Frugal Innovation
Leiden University - TU Delft - Erasmus University

A.1 Introduction

In a research area where high equipment costs have limited the expansion of the field, *e.g.,* high-pressure operation (Sauer et al., 2012), developing systems with lower production and monitoring costs while achieving process robustness is desirable. The use of soft-sensors, *i.e.,* software-based estimation of process variables, is gaining attention in the bioprocesses field due to the advantages of cost reduction and simplification of process monitoring. However, concerns regarding data pre-processing, accuracy, robustness, calibration, validation have limited widespread usage of frugal equipment and monitoring applications (Luttmann et al., 2012). This section summarizes the experiences concerning the development of a) low-cost reactors for pressure operation and b) soft-sensor for pH monitoring in pressurized systems employed for anaerobic bioconversions.

A.2 Materials and Methods

A.2.1 Development of "frugal" pressurized reactors

In-house pressure reactors for operation until 10 bar

The preliminary experiments of anaerobic bioconversions under elevated partial pressure of CO_2 (pCO_2) were carried out using a set-up consisting of three in-house developed reactors (790 mL), assembled with low-cost bulk produced components and two custom made stainless-steel parts. Although the commercially available vessel (paintball bottle Tippman 0.79 L HP tank) was certified to 200 bar, the set-up was tested in a range from 3 to 10 bar (Figure A-2 A). The liquid sampling port was comparable to a "dip tube" commonly present in high-pressure equipment. The accompanying "marker" was used for pressurization via its adaptation to a compressed CO_2 bottle (>99%) instead of a paintball gun. The quick-fit connection (now installed sideways in the pressure bottle) was used for gas sampling using plastic syringes (10 mL) coupled with 3-way valves.

Soft-sensor for pH estimation on pressurized systems carrying out anaerobic conversions

This application was developed based on an experimental and simplified model component. The pH in experiments pCO_2 was monitored using the set-up described in the previous section. In brief, the set-up consisted of an in-house developed PVC reactor (500 mL) able to withstand pressures until 12 bar (Figure A-2 D). A pressure-resistant pH probe (16 bar CPS11D, Endress

and Hauser, Switzerland) with a pressure sensor (B+B Thermo-Techniek, Germany) and a gas inlet were installed in the top part of the reactor. In the side-bottom of the reactor, a liquid sampling port was installed. Temperature was controlled with an incubator at 35±1°C and mixing was provided with a magnetic stirrer. Data from the pH probe was retrieved every 5 seconds, converted using a multichannel transmitter (Endress and Hauser, Switzerland), and visualized through a Lab-view interface. Pressure signal was monitored with a microcontroller (Arduino Uno©, Italy) and recorded at 3 seconds intervals. Three different mesophilic inocula with confirmed propionate oxidation activity at atmospheric pressure were used. The inocula were collected from A) sludge digester treating excess sewage sludge, B) UASB reactor treating sugar beet wastewater and C) AnMBR treating wastewater from the food and feed industry.

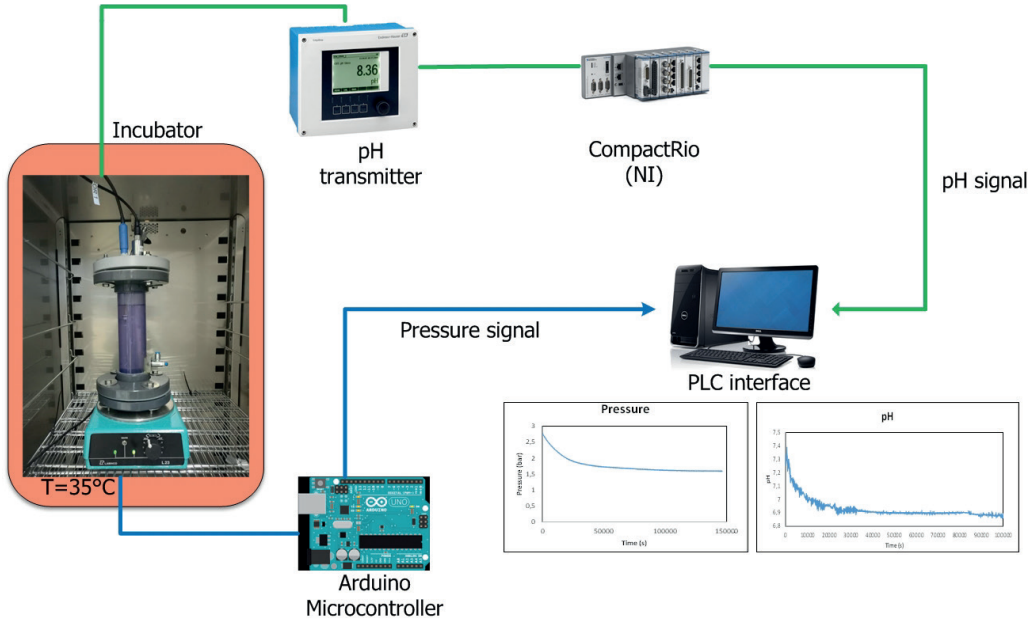

Figure A-1: Schematic representation of the used set-up for development of soft-sensor for pH monitoring in anaerobic pressurized systems

Frugal innovation: pressurized bioreactor

Despite the affordability of the paintball bottles system for pressurized operation, its reliability was not satisfactory to carry out high-quality research. Thus, a set of industrially produced high-pressure reactors ((Nantong Vasia, China) suitable for pressures up to 600 bar in combination with the Arduino soft-sensor was employed for some of the further experiments

in this study (Figure A-2 B). These reactors were equipped with the aforementioned “dip tube” for liquid sampling retrieval. Gas samples were taken via a self-developed gas-sampling device constructed with a pressure-resistant valve (Festo, Germany) and stainless steel connectors (Swagelok, US).

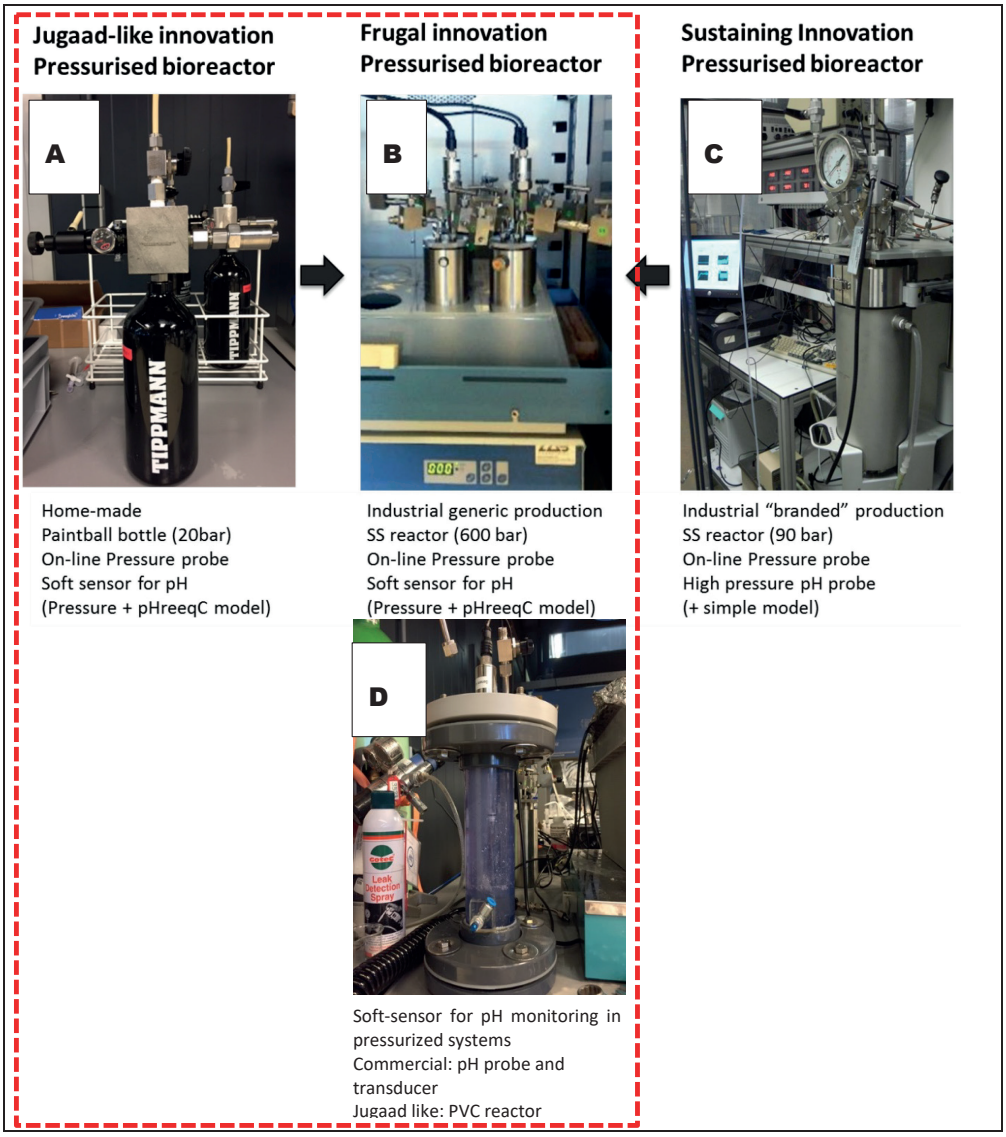

Figure A-2: Overview of the development of a hybrid frugal pressurized bioreactor. Figure adapted from (Ceron-Chafla and Lindeboom, 2022). The set-ups presented in the dotted rectangle were developed inside the scope of this thesis.

The equilibrium pH in the pressurized reactor was calculated using the geochemical equilibrium software PHREEQC (USGS, Version3). Total pressure, gas type, and initial medium composition were considered for the calculation. A simplified kinetic model was constructed in Phreeqc to simulate the substrate bioconversion effect on equilibrium pH of the pressurized system. The model incorporated complex ionic matrices, acid-base equilibria, ion-pairing, solubility and Monod kinetics for biomass growth.

A.3 Results soft-sensor development

A.3.1 Simulation of the physicochemical system

Discrepancies were found between the calculated pH with the Phreeqc model and the measured pH in the experiments without inoculum at pCO_2=3 bar (Figure A-3). This observation suggests the existence of additional alkalinity sources, which accounted for approximately 2.5 mM based on additional calculations. However, when considering a buffer concentration of 100 mM as HCO_3^-, results obtained with the Phreeqc model and measured experimentally were close to each other.

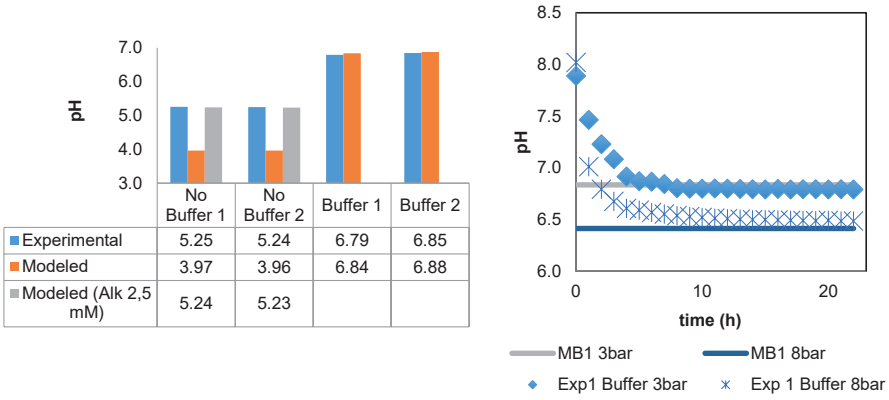

Figure A-3: Experimental and simulated values for equilibrium pH in physicochemical system at 3 bar pCO_2 B) pH evolution on a pressurized system at 3 and 8 bar pCO_2. Points represent measured experimental data and lines the calculated equilibrium pH using a PhreeqC developed model

A.3.2 Biomass addition effect on the pH of pressurized systems

Results obtained from the PhreeqC calculations and experiments with the pressurized system described in the Materials and Methods sections indicate a close correspondence in the calculated pH values when alkalinity (100 mM as HCO_3^-) is included (Figure A-4). The effect of increasing pCO_2 from 3 to 8 bar was studied with inoculum B. Calculated pH values were slightly lower than measured ones, suggesting that other possible buffering systems, e.g., ammonium, need to be further evaluated (Figure A-5).

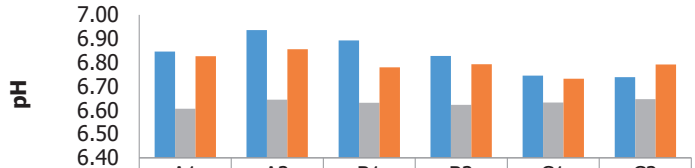

	A1	A2	B1	B2	C1	C2
Experimental	6.85	6.94	6.89	6.83	6.75	6.74
Modeled (Alk solution)	6.61	6.64	6.63	6.62	6.63	6.65
Modeled (Alk solution + buffer)	6.83	6.86	6.78	6.79	6.73	6.79

Figure A-4: Experimental and simulated results for equilibrium pH in physicochemical system at 3 bar pCO_2 using a different types of inoculum: A) Sludge from UASB treating waste activated sludge from a domestic wastewater treatment plant B) sludge from a UASB treating effluent from a sugar beet factory and C) Sludge from an AnMBR treating wastewater from the food and feed industry

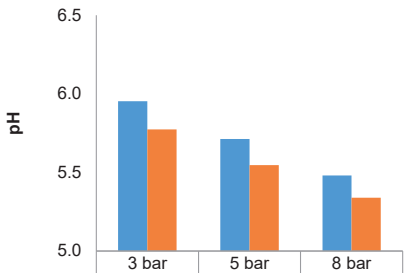

	3 bar	5 bar	8 bar
Experimental	5.95	5.71	5.48
Modeled	5.77	5.55	5.34

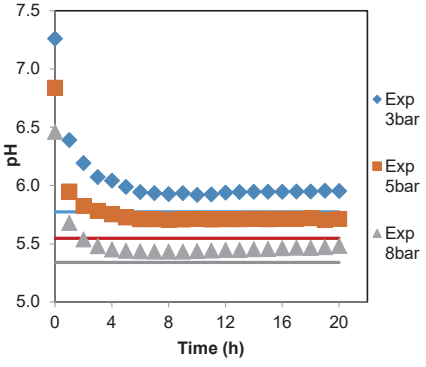

Figure A-5: Effect of increasing pCO_2 in equilibrium pH of the pressurized system B) pH evolution in the pressurized system. Points represent experimental data and lines the calculated equilibrium pH using a PhreeqC developed model

A.4 Conclusions

The alternative use of "commercially available" equipment (paintball bottles) and open-source prototyping platforms (Arduino©) for laboratory research can help to reduce equipment and monitoring costs considerably. Furthermore, it can become an alternative option for the simultaneous training of groups of students. Reliability is still an issue with the frugal equipment and monitoring presented to study pressurized anaerobic conversions. The right level of simplification of a complex system as anaerobic conversions occurring under pressurized conditions is still required. However, if overcome via more extensive calibration and validation, these frugal innovations could turn pressurized digestion research into a more accessible field for a wider academic audience.

References

Abe, F., 2007. Exploration of the effects of high hydrostatic pressure on microbial growth, physiology and survival: Perspectives from piezophysiology. Biosci. Biotechnol. Biochem. 71, 2347–2357. https://doi.org/10.1271/bbb.70015

Abe, F., Horikoshi, K., 2001. The biotechnological potential of piezophiles. Trends Biotechnol. 19, 102–108. https://doi.org/10.1016/S0167-7799(00)01539-0

Adnan, A.I., Ong, M.Y., Nomanbhay, S., Chew, K.W., Show, P.L., 2019. Technologies for biogas upgrading to biomethane: A review. Bioengineering 6, 1–23. https://doi.org/10.3390/bioengineering6040092

Aertsen, A., Meersman, F., Hendrickx, M.E.G., Vogel, R.F., Michiels, C.W., 2009. Biotechnology under high pressure: applications and implications. Trends Biotechnol. 27, 434–441. https://doi.org/10.1016/j.tibtech.2009.04.001

Agler, M.T., Wrenn, B.A., Zinder, S.H., Angenent, L.T., 2011. Waste to bioproduct conversion with undefined mixed cultures: the carboxylate platform. Trends Biotechnol. 29, 70–78. https://doi.org/10.1016/j.tibtech.2010.11.006

Agoda-Tandjawa, G., Dieudé-Fauvel, E., Girault, R., Baudez, J.C., 2013. Using water activity measurements to evaluate rheological consistency and structure strength of sludge. Chem. Eng. J. 228, 799–805. https://doi.org/10.1016/j.cej.2013.05.012

Ahrendt, S.R., Mobberley, J.M., Visscher, P.T., Koss, L.L., Foster, J.S., 2014. Effects of elevated carbon dioxide and salinity on the microbial diversity in lithifying microbial mats. Minerals 4, 145–169. https://doi.org/10.3390/min4010145

Al-Hinai, M.A., Jones, S.W., Papoutsakis, E.T., 2015. The Clostridium Sporulation Programs: Diversity and Preservation of Endospore Differentiation. Microbiol. Mol. Biol. Rev. 79, 19–37. https://doi.org/10.1128/mmbr.00025-14

Albers, S.V., Meyer, B.H., 2011. The archaeal cell envelope. Nat. Rev. Microbiol. 9, 414–426. https://doi.org/10.1038/nrmicro2576

Ali, R., Saravia, F., Hille-reichel, A., Härrer, D., Gescher, J., Horn, H., 2021. Enhanced production of propionic acid through acidic hydrolysis by choice of inoculum. https://doi.org/10.1002/jctb.6529

Ali, S., Hua, B., Huang, J.J., Droste, R.L., Zhou, Q., Zhao, W., Chen, L., 2019. Effect of different initial low pH conditions on biogas production, composition, and shift in the aceticlastic methanogenic population. Bioresour. Technol. 289, 121579. https://doi.org/10.1016/j.biortech.2019.121579

Allen, E.E., Bartlett, D.H., 2000. FabF is required for piezoregulation of cis-vaccenic acid levels and piezophilic growth of the deep-sea bacterium Photobacterium profundum strain SS9. J. Bacteriol. 182, 1264–1271. https://doi.org/10.1128/JB.182.5.1264-1271.2000

Allison, S.D., Martiny, J.B.H., 2009. Resistance, resilience, and redundancy in microbial communities. Light Evol. 2, 149–166. https://doi.org/10.17226/12501

Alloul, A., Cerruti, M., Adamczyk, D., Weissbrodt, D.G., Vlaeminck, S.E., 2021. Operational strategies to selectively produce purple bacteria for microbial protein in raceway reactors. Environ. Sci. Technol. 55, 8278–8286. https://doi.org/10.1021/acs.est.0c08204

Amend, J.P., Plyasunov, A. V., 2001. Carbohydrates in thermophile metabolism: Calculation of the standard molal thermodynamic properties of aqueous pentoses and hexoses at elevated temperatures and pressures. Geochim. Cosmochim. Acta 65, 3901–3917. https://doi.org/10.1016/S0016-7037(01)00707-4

Amend, J.P., Shock, E.L., 2001. Energetics of overall metabolic reactions of thermophilic and hyperthermophilic Archaea and Bacteria. FEMS Microbiol. Rev. 25, 175–243. https://doi.org/10.1111/j.1574-6976.2001.tb00576.x

American Public Health Association, 2017. Standard methods for the examination of water and wastewater, 23rd ed. APHA, Washington, D.C.

Ammar, E.M., Jin, Y., Wang, Z., Yang, S.T., 2014. Metabolic engineering of Propionibacterium freudenreichii: Effect of expressing phosphoenolpyruvate carboxylase on propionic acid production. Appl. Microbiol.

Biotechnol. 98, 7761–7772. https://doi.org/10.1007/s00253-014-5836-y

Amorim, N.C.S., Amorim, E.L.C., Kato, M.T., Florencio, L., Gavazza, S., 2018. The effect of methanogenesis inhibition, inoculum and substrate concentration on hydrogen and carboxylic acids production from cassava wastewater. Biodegradation 29, 41–58. https://doi.org/10.1007/s10532-017-9812-y

Amulya, K., Kopperi, H., Venkata Mohan, S., 2020. Tunable production of succinic acid at elevated pressures of CO2 in a high pressure gas fermentation reactor. Bioresour. Technol. 309, 123327. https://doi.org/10.1016/j.biortech.2020.123327

Amulya, K., Mohan, S.V., 2019. Fixation of CO2 , electron donor and redox microenvironment regulate succinic acid production in Citrobacter amalonaticus. Sci. Total Environ. 695, 133838. https://doi.org/10.1016/j.scitotenv.2019.133838

Angelidaki, I., Treu, L., Tsapekos, P., Luo, G., Campanaro, S., Wenzel, H., Kougias, P.G., 2018. Biogas upgrading and utilization: Current status and perspectives. Biotechnol. Adv. 36, 452–466. https://doi.org/10.1016/j.biotechadv.2018.01.011

Angenent, L.T., Kleerebezem, R., 2011. Bioproducts from undefined mixed cultures: electron pushing. Microb. Biotechnol. 4, 109–137. https://doi.org/10.1111/j.1751-7915.2010.00245.x

Angenent, L.T., Richter, H., Buckel, W., Spirito, C.M., Steinbusch, K.J.J., Plugge, C.M., Strik, D.P.B.T.B., Grootscholten, T.I.M., Buisman, C.J.N., Hamelers, H.V.M., 2016. Chain Elongation with Reactor Microbiomes: Open-Culture Biotechnology To Produce Biochemicals. Environ. Sci. Technol. 50, 2796–2810. https://doi.org/10.1021/acs.est.5b04847

Angenent, L.T., Wrenn, B.A., 2008. Optimizing Mixed-Culture Bioprocessing To Convert Wastes into Bioenergy, in: Bioenergy. pp. 179–194. https://doi.org/10.1128/9781555815547.ch15

Appels, L., Lauwers, J., Degrve, J., Helsen, L., Lievens, B., Willems, K., Van Impe, J., Dewil, R., 2011. Anaerobic digestion in global bio-energy production: Potential and research challenges. Renew. Sustain. Energy Rev. 15, 4295–4301. https://doi.org/10.1016/j.rser.2011.07.121

Ariesyady, H.D., Ito, T., Yoshiguchi, K., Okabe, S., 2007. Phylogenetic and functional diversity of propionate-oxidizing bacteria in an anaerobic digester sludge. Appl. Microbiol. Biotechnol. 75, 673–683. https://doi.org/10.1007/s00253-007-0842-y

Arnosti, C., Jørgensen, B., Sagemann, J., Thamdrup, B., 1998. Temperature dependence of microbial degradation of organic matter in marine sediments:polysaccharide hydrolysis, oxygen consumption, and sulfate reduction. Mar. Ecol. Prog. Ser. 165, 59–70. https://doi.org/10.3354/meps165059

Arslan, D., Steinbusch, K.J.J., Diels, L., De Wever, H., Hamelers, H.V.M., Buisman, C.J.N., 2013. Selective carboxylate production by controlling hydrogen, carbon dioxide and substrate concentrations in mixed culture fermentation. Bioresour. Technol. 136, 452–460. https://doi.org/10.1016/j.biortech.2013.03.063

Arslan, D., Steinbusch, K.J.J., Diels, L., Hamelers, H.V.M., Strik, D.P.B.T.B., Buisman, C.J.N., De Wever, H., 2016. Selective short-chain carboxylates production: A review of control mechanisms to direct mixed culture fermentations. Crit. Rev. Environ. Sci. Technol. 46, 592–634. https://doi.org/10.1080/10643389.2016.1145959

Arslan, D., Steinbusch, K.J.J.J., Diels, L., De Wever, H., Buisman, C.J.N.J.N., Hamelers, H.V.M.V.M., 2012. Effect of hydrogen and carbon dioxide on carboxylic acids patterns in mixed culture fermentation. Bioresour. Technol. 118, 227–234. https://doi.org/10.1016/j.biortech.2012.05.003

Aryal, N., Tremblay, P.L., Lizak, D.M., Zhang, T., 2017. Performance of different Sporomusa species for the microbial electrosynthesis of acetate from carbon dioxide. Bioresour. Technol. 233, 184–190. https://doi.org/10.1016/j.biortech.2017.02.128

Asanuma, N., Iwamoto, M., Hino, T., 1999. Effect of the addition of fumarate on methane production by ruminal microorganisms in vitro. J. Dairy Sci. 82, 780–787. https://doi.org/10.3168/jds.S0022-0302(99)75296-3

Aslam, S.N., Cresswell-Maynard, T., Thomas, D.N., Underwood, G.J.C., 2012. Production and Characterization of the Intra- and Extracellular Carbohydrates and Polymeric Substances (Eps) of Three Sea-Ice Diatom Species, and Evidence for a Cryoprotective Role for Eps. J. Phycol. 48, 1494–1509. https://doi.org/10.1111/jpy.12004

Augelletti, R., Conti, M., Annesini, M.C., 2017. Pressure swing adsorption for biogas upgrading. A new process configuration for the separation of biomethane and carbon dioxide. J. Clean. Prod. 140, 1390–1398.

https://doi.org/10.1016/j.jclepro.2016.10.013

Baek, G., Kim, Jaai, Kim, Jinsu, Lee, C., 2018. Role and Potential of Direct Interspecies Electron Transfer in Anaerobic Digestion. Energies 11, 107. https://doi.org/10.3390/en11010107

Baez, A., Flores, N., Bolívar, F., Ramírez, O.T., 2009. Metabolic and transcriptional response of recombinant Escherichia coli to elevated dissolved carbon dioxide concentrations. Biotechnol. Bioeng. 104, 102–110. https://doi.org/10.1002/bit.22379

Bajón Fernández, Y., Green, K., Schuler, K., Soares, A., Vale, P., Alibardi, L., Cartmell, E., 2015. Biological carbon dioxide utilisation in food waste anaerobic digesters. Water Res. 87, 467–475. https://doi.org/10.1016/j.watres.2015.06.011

Bajón Fernández, Y., Soares, A., Vale, P., Koch, K., Masse, A.L., Cartmell, E., 2019. Enhancing the anaerobic digestion process through carbon dioxide enrichment: initial insights into mechanisms of utilization. Environ. Technol. (United Kingdom) 40, 1744–1755. https://doi.org/10.1080/09593330.2019.1597173

Bajón Fernández, Y., Soares, A., Villa, R., Vale, P., Cartmell, E., 2014. Carbon capture and biogas enhancement by carbon dioxide enrichment of anaerobic digesters treating sewage sludge or food waste. Bioresour. Technol. 159, 1–7. https://doi.org/10.1016/j.biortech.2014.02.010

Bakermans, C., Nealson, K.H., 2004. Relationship of Critical Temperature to Macromolecular Synthesis and Growth Yield in Psychrobacter cryopegella. J. Bacteriol. 186, 2340–2345. https://doi.org/10.1128/JB.186.8.2340-2345.2004

Baleeiro, F.C.F., Kleinsteuber, S., Sträuber, H., 2021. Hydrogen as a Co-electron Donor for Chain Elongation With Complex Communities. Front. Bioeng. Biotechnol. 9, 1–15. https://doi.org/10.3389/fbioe.2021.650631

Balk, M., Altinbaş, M., Rijpstra, W.I.C., Damsté, J.S.S., Stams, A.J.M., 2008. Desulfatirhabdium butyrativorans gen. nov., sp. nov., a butyrate-oxidizing, sulfate-reducing bacterium isolated from an anaerobic bioreactor. Int. J. Syst. Evol. Microbiol. 58, 110–115. https://doi.org/10.1099/ijs.0.65396-0

Ban, Q., Zhang, L., Li, J., 2015. Shift of Propionate-Oxidizing Bacteria with HRT Decrease in an UASB Reactor Containing Propionate as a Sole Carbon Source. Appl. Biochem. Biotechnol. 175, 274–286. https://doi.org/10.1007/s12010-014-1265-8

Bär, K., Merkle, W., Tuczinski, M., Saravia, F., Horn, H., Ortloff, F., Graf, F., Lemmer, A., Kolb, T., 2018. Development of an innovative two-stage fermentation process for high-calorific biogas at elevated pressure. Biomass and Bioenergy 115, 186–194. https://doi.org/10.1016/j.biombioe.2018.04.009

Barbirato, F., Chedaille, D., Bories, A., 1997. Propionic acid fermentation from glycerol: comparison with conventional substrates. Appl. Microbiol. Biotechnol. 47, 441–446. https://doi.org/10.1007/s002530050953

Bastidas-Oyanedel, J.-R., Bonk, F., Thomsen, M.H., Schmidt, J.E., 2015. Dark fermentation biorefinery in the present and future (bio)chemical industry. Rev. Environ. Sci. Bio/Technology 14, 473–498. https://doi.org/10.1007/s11157-015-9369-3

Bataille, C., Åhman, M., Neuhoff, K., Nilsson, L.J., Fischedick, M., Lechtenböhmer, S., Solano-Rodriquez, B., Denis-Ryan, A., Stiebert, S., Waisman, H., Sartor, O., Rahbar, S., 2018. A review of technology and policy deep decarbonization pathway options for making energy-intensive industry production consistent with the Paris Agreement. J. Clean. Prod. 187, 960–973. https://doi.org/10.1016/j.jclepro.2018.03.107

Bauer, F., Persson, T., Hulteberg, C., Tamm, D., 2013. Biogas upgrading – technology overview, comparison and perspectives for the future. Biofuels, Bioprod. Biorefining 7, 499–511. https://doi.org/https://doi.org/10.1002/bbb.1423

Benazzi, T., Calgaroto, S., Astolfi, V., Dalla Rosa, C., Oliveira, J.V., Mazutti, M.A., 2013. Pretreatment of sugarcane bagasse using supercritical carbon dioxide combined with ultrasound to improve the enzymatic hydrolysis. Enzyme Microb. Technol. 52, 247–250. https://doi.org/10.1016/j.enzmictec.2013.02.001

Beney, L., Gervais, P., 2001. Influence of the fluidity of the membrane on the response of microorganisms to environmental stresses. Appl. Microbiol. Biotechnol. 57, 34–42. https://doi.org/10.1007/s002530100754

Berríos-Rivera, S.J., Bennett, G.N., San, K.Y., 2002. The effect of increasing NADH availability on the redistribution of metabolic fluxes in Escherichia coli chemostat cultures. Metab. Eng. 4, 230–237. https://doi.org/10.1006/mben.2002.0228

Bertoloni, G., Bertucco, A., De Cian, V., Parton, T., 2006. A study on the inactivation of micro-organisms and

enzymes by high pressure CO2. Biotechnol. Bioeng. 95, 155–160. https://doi.org/10.1002/bit.21006

Bertucco, A., Spilimbergo, S., 2001. Treating micro-organisms with high pressure 9, 626–640. https://doi.org/10.1016/S0926-9614(01)80036-8

Bethke, C.M., Sanford, R.A., Kirk, M.F., Jin, Q., Flynn, T.M., 2011. The thermodynamic ladder in Geomicrobiology. Am. J. Sci. 311, 183–210. https://doi.org/10.2475/03.2011.01

Bhatia, S.K., Bhatia, R.K., Jeon, J.M., Kumar, G., Yang, Y.H., 2019. Carbon dioxide capture and bioenergy production using biological system – A review. Renew. Sustain. Energy Rev. 110, 143–158. https://doi.org/10.1016/j.rser.2019.04.070

Bhattarai, S., Zhang, Y., Lens, P.N.L., 2018. Effect of pressure and temperature on anaerobic methanotrophic activities of a highly enriched ANME-2a community. Environ. Sci. Pollut. Res. 25, 30031–30043. https://doi.org/10.1007/s11356-018-2573-2

Biselli, E., Schink, S.J., Gerland, U., 2020. Slower growth of Escherichia coli leads to longer survival in carbon starvation due to a decrease in the maintenance rate. Mol. Syst. Biol. 16, 1–13. https://doi.org/10.15252/msb.20209478

Blasco-Gómez, R., Batlle-Vilanova, P., Villano, M., Balaguer, M.D., Colprim, J., Puig, S., 2017. On the edge of research and technological application: A critical review of electromethanogenesis. Int. J. Mol. Sci. 18, 1–32. https://doi.org/10.3390/ijms18040874

Bokulich, N.A., Subramanian, S., Faith, J.J., Gevers, D., Gordon, J.I., Knight, R., Mills, D.A., Caporaso, J.G., 2013. Quality-filtering vastly improves diversity estimates from Illumina amplicon sequencing. Nat. Methods 10, 57–59. https://doi.org/10.1038/nmeth.2276

Bonk, F., Popp, D., Harms, H., Centler, F., 2018. PCR-based quantification of taxa-specific abundances in microbial communities: Quantifying and avoiding common pitfalls. J. Microbiol. Methods 153, 139–147. https://doi.org/10.1016/j.mimet.2018.09.015

Bonk, F., Popp, D., Weinrich, S., Sträuber, H., Becker, D., Kleinsteuber, S., Harms, H., Centler, F., 2019. Determination of microbial maintenance in acetogenesis and methanogenesis by experimental and modeling techniques. Front. Microbiol. 10, 1–13. https://doi.org/10.3389/fmicb.2019.00166

Boock, J.T., Freedman, A.J.E., Tompsett, G.A., Muse, S.K., Allen, A.J., Jackson, L.A., Castro-Dominguez, B., Timko, M.T., Prather, K.L.J., Thompson, J.R., 2019. Engineered microbial biofuel production and recovery under supercritical carbon dioxide. Nat. Commun. 10. https://doi.org/10.1038/s41467-019-08486-6

Booker, A.E., Borton, M.A., Daly, R.A., Welch, S.A., Nicora, C.D., Hoyt, D.W., Wilson, T., Purvine, S.O., Wolfe, R.A., Sharma, S., Mouser, P.J., Cole, D.R., Lipton, M.S., Wrighton, K.C., Wilkins, M.J., 2017. Sulfide Generation by Dominant Halanaerobium Microorganisms in Hydraulically Fractured Shales . mSphere 2, 1–13. https://doi.org/10.1128/mspheredirect.00257-17

Booker, A.E., Hoyt, D.W., Meulia, T., Eder, E., Nicora, C.D., Purvine, S.O., Daly, R.A., Moore, J.D., Wunch, K., Pfiffner, S.M., Lipton, M.S., Mouser, P.J., Wrighton, K.C., Wilkins, M.J., 2019. Deep-Subsurface Pressure Stimulates Metabolic Plasticity in Shale-Colonizing Halanaerobium spp. Appl. Environ. Microbiol. 85, 18–19. https://doi.org/10.1128/AEM.00018-19

Bothun, G.D.D., Knutson, B.L.L., Berberich, J.A.A., Strobel, H.J.J., Nokes, S.E.E., 2004. Metabolic selectivity and growth of Clostridium thermocellum in continuous culture under elevated hydrostatic pressure. Appl. Microbiol. Biotechnol. 65, 149–157. https://doi.org/10.1007/s00253-004-1554-1

Bovio-Winkler, P., Cabezas, A., Etchebehere, C., 2021. Database Mining to Unravel the Ecology of the Phylum Chloroflexi in Methanogenic Full Scale Bioreactors. Front. Microbiol. 11. https://doi.org/10.3389/fmicb.2020.603234

Bradley, J.A., Amend, J.P., LaRowe, D.E., 2018. Bioenergetic controls on microbial ecophysiology in marine sediments. Front. Microbiol. 9, 1–8. https://doi.org/10.3389/fmicb.2018.00180

Braun, K., Gottschalk, G., 1981. Effect of molecular hydrogen and carbon dioxide on chemo-organotrophic growth of Acetobacterium woodii and Clostridium aceticum. Arch. Microbiol. 128, 294–298. https://doi.org/10.1007/BF00422533

Bray, J.R., Curtis, J.T., 1957. An Ordination of the Upland Forest Communities of Southern Wisconsin. Ecol. Monogr. 27, 325–349. https://doi.org/10.2307/1942268

Braz, G.H.R., Fernandez-Gonzalez, N., Lema, J.M., Carballa, M., 2019. Organic overloading affects the microbial

interactions during anaerobic digestion in sewage sludge reactors. Chemosphere 222, 323–332. https://doi.org/10.1016/j.chemosphere.2019.01.124

Brehmer, B., Boom, R.M., Sanders, J., 2009. Maximum fossil fuel feedstock replacement potential of petrochemicals via biorefineries. Chem. Eng. Res. Des. 87, 1103–1119. https://doi.org/10.1016/j.cherd.2009.07.010

Bruce, K.D., Jones, T.H., Bezemer, T.M., Thompson, L.J., Ritchie, D.A., 2000. The effect of elevated atmospheric carbon dioxide levels on soil bacterial communities. Glob. Chang. Biol. 6, 427–434. https://doi.org/10.1046/j.1365-2486.2000.00320.x

Bruins, M.E., Janssen, A.E.M., Boom, R.M., 2006. Equilibrium shifts in enzyme reactions at high pressure. J. Mol. Catal. B Enzym. 39, 124–127. https://doi.org/10.1016/j.molcatb.2006.01.033

Campanaro, S., Treu, L., Kougias, P.G., Zhu, X., Angelidaki, I., 2018. Taxonomy of anaerobic digestion microbiome reveals biases associated with the applied high throughput sequencing strategies. Sci. Rep. 8, 1–12. https://doi.org/10.1038/s41598-018-20414-0

Candry, P., Radić, L., Favere, J., Carvajal-Arroyo, J.M., Rabaey, K., Ganigué, R., 2020. Mildly acidic pH selects for chain elongation to caproic acid over alternative pathways during lactic acid fermentation. Water Res. 186, 116396. https://doi.org/10.1016/j.watres.2020.116396

Canganella, F., Wiegel, J., 2011. Extremophiles: From abyssal to terrestrial ecosystems and possibly beyond. Naturwissenschaften 98, 253–279. https://doi.org/10.1007/s00114-011-0775-2

Cao, Y., Zhang, R., Sun, C., Cheng, T., Liu, Y., Xian, M., 2013. Fermentative succinate production: An emerging technology to replace the traditional petrochemical processes. Biomed Res. Int. 2013. https://doi.org/10.1155/2013/723412

Caporaso, J.G., Kuczynski, J., Stombaugh, J., Bittinger, K., Bushman, F.D., Costello, E.K., Fierer, N., Peña, A.G., Goodrich, J.K., Gordon, J.I., Huttley, G.A., Kelley, S.T., Knights, D., Koenig, J.E., Ley, R.E., Lozupone, C.A., McDonald, D., Muegge, B.D., Pirrung, M., Reeder, J., Sevinsky, J.R., Turnbaugh, P.J., Walters, W.A., Widmann, J., Yatsunenko, T., Zaneveld, J., Knight, R., 2010. QIIME allows analysis of high-throughput community sequencing data. Nat. Methods 7, 335–336. https://doi.org/10.1038/nmeth.f.303

Caporaso, J.G., Lauber, C.L., Walters, W.A., Berg-Lyons, D., Lozupone, C.A., Turnbaugh, P.J., Fierer, N., Knight, R., 2011. Global patterns of 16S rRNA diversity at a depth of millions of sequences per sample. Proc. Natl. Acad. Sci. U. S. A. 108, 4516–4522. https://doi.org/10.1073/pnas.1000080107

Capson-Tojo, G., Batstone, D.J., Grassino, M., Vlaeminck, S.E., Puyol, D., Verstraete, W., Kleerebezem, R., Oehmen, A., Ghimire, A., Pikaar, I., Lema, J.M., Hülsen, T., 2020. Purple phototrophic bacteria for resource recovery: Challenges and opportunities. Biotechnol. Adv. 43, 107567. https://doi.org/10.1016/j.biotechadv.2020.107567

Carballa, M., Regueiro, L., Lema, J.M., 2015. Microbial management of anaerobic digestion: Exploiting the microbiome-functionality nexus. Curr. Opin. Biotechnol. 33, 103–111. https://doi.org/10.1016/j.copbio.2015.01.008

Carruthers, A., 1991. Mechanisms for the Facilitated Diffusion of Substrates across Cell Membranes. Biochemistry 30, 3898–3906. https://doi.org/10.1021/bi00230a014

CBS, 2022. Gemiddelde energietarieven voor consumenten [WWW Document]. StatLine. URL https://opendata.cbs.nl/#/CBS/nl/dataset/84672NED/table

Ceron-Chafla, P., Chang, Y., Rabaey, K., van Lier, J.B., Lindeboom, R.E.F., 2021. Directional Selection of Microbial Community Reduces Propionate Accumulation in Glycerol and Glucose Anaerobic Bioconversion Under Elevated pCO2. Front. Microbiol. 12, 1583. https://doi.org/10.3389/fmicb.2021.675763

Ceron-Chafla, P., Kleerebezem, R., Rabaey, K., B. van Lier, J., E. F. Lindeboom, R., 2020. Direct and Indirect Effects of Increased CO2 Partial Pressure on the Bioenergetics of Syntrophic Propionate and Butyrate Conversion. Environ. Sci. Technol. 54, 12583–12592. https://doi.org/10.1021/acs.est.0c02022

Ceron-Chafla, P., Lindeboom, R.E.F., 2022. Frugalizing engineering solutions for recovery of resources from wastewater, in: Handbook of Frugal Innovation.

Chan, K., Schillereff, D.N., Baas, A.C.W., Chadwick, M.A., Main, B., Mulligan, M., O'Shea, F.T., Pearce, R., Smith, T.E.L., van Soesbergen, A., Tebbs, E., Thompson, J., 2021. Low-cost electronic sensors for

environmental research: Pitfalls and opportunities, Progress in Physical Geography. https://doi.org/10.1177/0309133320956567

Cheah, Y.K., Vidal-Antich, C., Dosta, J., Mata-Álvarez, J., 2019. Volatile fatty acid production from mesophilic acidogenic fermentation of organic fraction of municipal solid waste and food waste under acidic and alkaline pH. Environ. Sci. Pollut. Res. 26, 35509–35522. https://doi.org/10.1007/s11356-019-05394-6

Chen, J.S., Balaban, M.O., Wei, C. i., Marshall, M.R., Hsu, W.Y., 1992. Inactivation of Polyphenol Oxidase by High-Pressure Carbon Dioxide. J. Agric. Food Chem. 40, 2345–2349. https://doi.org/10.1021/jf00024a005

Chen, Y., Rößler, B., Zielonka, S., Lemmer, A., Wonneberger, A.-M., Jungbluth, T., 2014a. The pressure effects on two-phase anaerobic digestion. Appl. Energy 116, 409–415. https://doi.org/10.1016/j.apenergy.2013.11.012

Chen, Y., Rößler, B., Zielonka, S., Wonneberger, A.-M., Lemmer, A., 2014b. Effects of Organic Loading Rate on the Performance of a Pressurized Anaerobic Filter in Two-Phase Anaerobic Digestion. Energies 7, 736–750. https://doi.org/10.3390/en7020736

Chen, Y., Wang, T., Shen, N., Zhang, F., Zeng, R.J., 2016. High-purity propionate production from glycerol in mixed culture fermentation. Bioresour. Technol. 219, 659–667. https://doi.org/10.1016/j.biortech.2016.08.026

Chen, Y.Y., Temelli, F., Gänzle, M.G., 2017. Mechanisms of inactivation of dry Escherichia coli by high-pressure carbon dioxide. Appl. Environ. Microbiol. 83, 1–10. https://doi.org/10.1128/AEM.00062-17

Cheng, C.L., Che, P.Y., Chen, B.Y., Lee, W.J., Chien, L.J., Chang, J.S., 2012. High yield bio-butanol production by solvent-producing bacterial microflora. Bioresour. Technol. 113, 58–64. https://doi.org/10.1016/j.biortech.2011.12.133

Cheng, S., Xing, D., Call, D.F., Logan, B.E., 2009. Direct biological conversion of electrical current into methane by electromethanogenesis. Environ. Sci. Technol. 43, 3953–3958. https://doi.org/10.1021/es803531g

Cherubini, F., 2010. The biorefinery concept: Using biomass instead of oil for producing energy and chemicals. Energy Convers. Manag. 51, 1412–1421. https://doi.org/10.1016/j.enconman.2010.01.015

Choi, O., Sang, B.I., 2016. Extracellular electron transfer from cathode to microbes: Application for biofuel production. Biotechnol. Biofuels 9, 1–14. https://doi.org/10.1186/s13068-016-0426-0

Christodoulou, X., Okoroafor, T., Parry, S., Velasquez-Orta, S.B., 2017. The use of carbon dioxide in microbial electrosynthesis: Advancements, sustainability and economic feasibility. J. CO2 Util. 18, 390–399. https://doi.org/10.1016/j.jcou.2017.01.027

Coelho, M.M.H., Morais, N.W.S., Pereira, E.L., Leitão, R.C., dos Santos, A.B., 2020. Potential assessment and kinetic modeling of carboxylic acids production using dairy wastewater as substrate. Biochem. Eng. J. 156, 107502. https://doi.org/10.1016/j.bej.2020.107502

Coma, M., Vilchez-Vargas, R., Roume, H., Jauregui, R., Pieper, D.H., Rabaey, K., 2016. Product Diversity Linked to Substrate Usage in Chain Elongation by Mixed-Culture Fermentation. Environ. Sci. Technol. 50, 6467–6476. https://doi.org/10.1021/acs.est.5b06021

Connell, S.D., Kroeker, K.J., Fabricius, K.E., Kline, D.I., Russell, B.D., 2013. The other ocean acidification problem: CO2 as a resource among competitors for ecosystem dominance. Philos. Trans. R. Soc. B Biol. Sci. 368. https://doi.org/10.1098/rstb.2012.0442

Conrad, R., 2020. Importance of hydrogenotrophic, aceticlastic and methylotrophic methanogenesis for methane production in terrestrial, aquatic and other anoxic environments: A mini review. Pedosphere 30, 25–39. https://doi.org/10.1016/S1002-0160(18)60052-9

Conrad, R., Wetter, B., 1990. Influence of temperature on energetics of hydrogen metabolism in homoacetogenic, methanogenic, and other anaerobic bacteria. Arch. Microbiol. 155, 94–98. https://doi.org/10.1007/BF00291281

Cooper, V.S., Lenski, R.E., 2000. The population genetics of ecological specialization in evolving Escherichia coli populations. Nature 407, 736–739. https://doi.org/10.1038/35037572

Coquelle, N., Fioravanti, E., Weik, M., Vellieux, F., Madern, D., Cedex, G., 2007. Activity , Stability and Structural Studies of Lactate Dehydrogenases Adapted to Extreme Thermal Environments 547–562. https://doi.org/10.1016/j.jmb.2007.09.049

Cord-Ruwisch, R., Seitz, H.J., Conrad, R., 1988. The capacity of hydrogenotrophic anaerobic bacteria to compete for traces of hydrogen depends on the redox potential of the terminal electron acceptor. Arch. Microbiol. 149, 350–357. https://doi.org/10.1007/BF00411655

Dai, K., Wen, J.-L., Zhang, F., Zeng, R.J., 2017. Valuable biochemical production in mixed culture fermentation: fundamentals and process coupling. Appl. Microbiol. Biotechnol. 101, 6575–6586. https://doi.org/10.1007/s00253-017-8441-z

Danevčič, T., Stopar, D., 2011. Asymmetric Response of Carbon Metabolism at High and Low Salt Stress in Vibrio sp. DSM14379. Microb. Ecol. 62, 198–204. https://doi.org/10.1007/s00248-011-9870-3

Dareioti, M.A., Vavouraki, A.I., Kornaros, M., 2014. Effect of pH on the anaerobic acidogenesis of agroindustrial wastewaters for maximization of bio-hydrogen production: A lab-scale evaluation using batch tests. Bioresour. Technol. 162, 218–227. https://doi.org/10.1016/j.biortech.2014.03.149

Darvekar, P., Liang, C., Karim, M.N., Holtzapple, M.T., 2019. Effect of headspace gas composition on carboxylates production in open-culture fermentation of corn stover. Biomass and Bioenergy 126, 57–61. https://doi.org/10.1016/j.biombioe.2019.04.019

De Kok, S., Meijer, J., Van Loosdrecht, M.C.M.M., Kleerebezem, R., 2013. Impact of dissolved hydrogen partial pressure on mixed culture fermentations. Appl. Microbiol. Biotechnol. 97, 2617–2625. https://doi.org/10.1007/s00253-012-4400-x

De Sitter, K., Garcia-Gonzalez, L., Matassa, C., Bertin, L., De Wever, H., 2018. The use of membrane based reactive extraction for the recovery of carboxylic acids from thin stillage. Sep. Purif. Technol. 206, 177–185. https://doi.org/10.1016/j.seppur.2018.06.001

De Vrieze, J., Christiaens, M.E.R., Walraedt, D., Devooght, A., Ijaz, U.Z., Boon, N., 2017. Microbial community redundancy in anaerobic digestion drives process recovery after salinity exposure. Water Res. 111, 109–117. https://doi.org/10.1016/j.watres.2016.12.042

De Vrieze, J., Gildemyn, S., Vilchez-Vargas, R., Jáuregui, R., Pieper, D.H., Verstraete, W., Boon, N., 2015a. Inoculum selection is crucial to ensure operational stability in anaerobic digestion. Appl. Microbiol. Biotechnol. 99, 189–199. https://doi.org/10.1007/s00253-014-6046-3

De Vrieze, J., Hennebel, T., Boon, N., Verstraete, W., 2012. Methanosarcina: The rediscovered methanogen for heavy duty biomethanation. Bioresour. Technol. 112, 1–9. https://doi.org/10.1016/j.biortech.2012.02.079

De Vrieze, J., Heyer, R., Props, R., Van Meulebroek, L., Gille, K., Vanhaecke, L., Benndorf, D., Boon, N., 2021. Triangulation of microbial fingerprinting in anaerobic digestion reveals consistent fingerprinting profiles. Water Res. 202, 117422. https://doi.org/10.1016/j.watres.2021.117422

De Vrieze, J., Regueiro, L., Props, R., Vilchez-Vargas, R., Jáuregui, R., Pieper, D.H., Lema, J.M., Carballa, M., 2016. Presence does not imply activity: DNA and RNA patterns differ in response to salt perturbation in anaerobic digestion. Biotechnol. Biofuels 9, 1–13. https://doi.org/10.1186/s13068-016-0652-5

De Vrieze, J., Saunders, A.M., He, Y., Fang, J., Nielsen, P.H., Verstraete, W., Boon, N., 2015b. Ammonia and temperature determine potential clustering in the anaerobic digestion microbiome. Water Res. 75, 312–323. https://doi.org/10.1016/j.watres.2015.02.025

De Vrieze, J., Verbeeck, K., Pikaar, I., Boere, J., Van Wijk, A., Rabaey, K., Verstraete, W., 2020. The hydrogen gas bio-based economy and the production of renewable building block chemicals, food and energy. N. Biotechnol. 55, 12–18. https://doi.org/10.1016/j.nbt.2019.09.004

De Vrieze, J., Verstraete, W., 2016. Perspectives for microbial community composition in anaerobic digestion: from abundance and activity to connectivity. Environ. Microbiol. 18, 2797–2809. https://doi.org/10.1111/1462-2920.13437

Decho, A.W., 1990. Microbial exopolymer secretions in ocean environments: their role(s) in food webs and marine processes. Oceanogr. Mar. Biol. 28, 73–153.

Decho, A.W., Gutierrez, T., 2017. Microbial extracellular polymeric substances (EPSs) in ocean systems. Front. Microbiol. 8, 1–28. https://doi.org/10.3389/fmicb.2017.00922

Degeest, B., Janssens, B., De Vuyst, L., 2001. Exopolysaccharide (EPS) biosynthesis by Lactobacillus sakei 0-1: Production kinetics, enzyme activities and EPS yields. J. Appl. Microbiol. 91, 470–477. https://doi.org/10.1046/j.1365-2672.2001.01404.x

Demirel, B., Scherer, P., 2008. The roles of acetotrophic and hydrogenotrophic methanogens during anaerobic

conversion of biomass to methane: A review. Rev. Environ. Sci. Biotechnol. 7, 173–190. https://doi.org/10.1007/s11157-008-9131-1

Deschamps, L., Imatoukene, N., Lemaire, J., Mounkaila, M., Filali, R., Lopez, M., Theoleyre, M.A., 2021. In-situ biogas upgrading by bio-methanation with an innovative membrane bioreactor combining sludge filtration and H2 injection. Bioresour. Technol. 337. https://doi.org/10.1016/j.biortech.2021.125444

Detman, A., Bucha, M., Treu, L., Chojnacka, A., Pleśniak, Ł., Salamon, A., Łupikasza, E., Gromadka, R., Gawor, J., Gromadka, A., Drzewicki, W., Jakubiak, M., Janiga, M., Matyasik, I., Błaszczyk, M.K., Jędrysek, M.O., Campanaro, S., Sikora, A., 2021. Evaluation of acidogenesis products ' effect on biogas production performed with metagenomics and isotopic approaches. Biotechnol. Biofuels 14, 1–25. https://doi.org/10.1186/s13068-021-01968-0

Díaz, I., Fdz-Polanco, F., Mutsvene, B., Fdz-Polanco, M., 2020. Effect of operating pressure on direct biomethane production from carbon dioxide and exogenous hydrogen in the anaerobic digestion of sewage sludge. Appl. Energy 280, 115915. https://doi.org/10.1016/j.apenergy.2020.115915

Díaz, I., Pérez, C., Alfaro, N., Fdz-Polanco, F., 2015. A feasibility study on the bioconversion of CO2 and H2 to biomethane by gas sparging through polymeric membranes. Bioresour. Technol. 185, 246–253. https://doi.org/10.1016/j.biortech.2015.02.114

Dietz, D., Zeng, A.P., 2014. Efficient production of 1,3-propanediol from fermentation of crude glycerol with mixed cultures in a simple medium. Bioprocess Biosyst. Eng. 37, 225–233. https://doi.org/10.1007/s00449-013-0989-0

Dixon, N.M., Kell, D.B., 1989. The inhibition by CO 2 of the growth and metabolism of micro-organisms. J. Appl. Bacteriol. 67, 109–136. https://doi.org/10.1111/j.1365-2672.1989.tb03387.x

Do, H., Lim, J., Shin, S.G., Wu, Y.-J., Ahn, J.-H., Hwang, S., 2008. Simultaneous effect of temperature, cyanide and ammonia-oxidizing bacteria concentrations on ammonia oxidation. J. Ind. Microbiol. Biotechnol. 35, 1331–1338. https://doi.org/10.1007/s10295-008-0415-9

Doi, Y., Ikegami, Y., 2014. Pyruvate formate-lyase is essential for fumarate-independent anaerobic glycerol utilization in the Enterococcus faecalis strain W11. J. Bacteriol. 196, 2472–2480. https://doi.org/10.1128/JB.01512-14

Dolfing, J., 2013. Syntrophic propionate oxidation via butyrate: A novel window of opportunity under methanogenic conditions. Appl. Environ. Microbiol. 79, 4515–4516. https://doi.org/10.1128/AEM.00111-13

Dolfing, J., Jiang, B., Henstra, A.M., Stams, A.J.M., Plugge, C.M., 2008. Syntrophic growth on formate: A new microbial niche in anoxic environments. Appl. Environ. Microbiol. 74, 6126–6131. https://doi.org/10.1128/AEM.01428-08

Dong, L., Cao, G., Wu, J., Yang, S., Ren, N., 2019. Reflux of acidizing fluid for enhancing biomethane production from cattle manure in plug flow reactor. Bioresour. Technol. 284, 248–255. https://doi.org/10.1016/j.biortech.2019.03.092

Dong, X., Greening, C., Rattray, J.E., Chakraborty, A., Chuvochina, M., Mayumi, D., Dolfing, J., Li, C., Brooks, J.M., Bernard, B.B., Groves, R.A., Lewis, I.A., Hubert, C.R.J., 2019. Metabolic potential of uncultured bacteria and archaea associated with petroleum seepage in deep-sea sediments. Nat. Commun. 10, 1–12. https://doi.org/10.1038/s41467-019-09747-0

Dong, Y., Jiang, H., 2016. Microbial production of metabolites and associated enzymatic reactions under high pressure. World J. Microbiol. Biotechnol. 32. https://doi.org/10.1007/s11274-016-2136-y

Dragosits, M., Mattanovich, D., 2013. Adaptive laboratory evolution – principles and applications for biotechnology. Microb. Cell Fact. 12, 64. https://doi.org/10.1186/1475-2859-12-64

Dumbrell, A.J., Ferguson, R.M.W., Clark, D.R., 2016. Microbial Community Analysis by Single-Amplicon High-Throughput Next Generation Sequencing: Data Analysis – From Raw Output to Ecology 155–206. https://doi.org/10.1007/8623_2016_228

Dursun, G., Umer, M., Markert, B., Stoffel, M., 2021. Designing of an advanced compression bioreactor with an implementation of a low-cost controlling system connected to a mobile application. Processes 9. https://doi.org/10.3390/pr9060915

Edgar, R.C., 2013. UPARSE: highly accurate OTU sequences from microbial amplicon reads. Nat. Methods 10,

996–998. https://doi.org/10.1038/nmeth.2604

Edgar, R.C., 2004. MUSCLE: multiple sequence alignment with high accuracy and high throughput. Nucleic Acids Res. 32, 1792–1797. https://doi.org/10.1093/nar/gkh340

Edgar, R.C., Haas, B.J., Clemente, J.C., Quince, C., Knight, R., 2011. UCHIME improves sensitivity and speed of chimera detection. Bioinformatics 27, 2194–2200. https://doi.org/10.1093/bioinformatics/btr381

Eisenmenger, M.J., Reyes-De-Corcuera, J.I., 2009. High pressure enhancement of enzymes: A review. Enzyme Microb. Technol. 45, 331–347. https://doi.org/10.1016/j.enzmictec.2009.08.001

Emerson, J.E., Stabler, R.A., Wren, B.W., Fairweather, N.F., 2008. Microarray analysis of the transcriptional responses of Clostridium difficile to environmental and antibiotic stress. J. Med. Microbiol. 57, 757–764. https://doi.org/10.1099/jmm.0.47657-0

European Biogas Association, 2022. The biomethane sector will deliver 20% of current EU gas imports from Russia by 2030 [WWW Document]. URL https://www.europeanbiogas.eu/the-biomethane-sector-will-deliver-20-of-current-eu-gas-imports-from-russia-by-2030/#:~:text=News-,The biomethane sector will deliver 20%25 of current EU gas,the biomethane industry in Europe. (accessed 3.11.22).

Eyring, H., 1935. The Activated Complex and the absolute rate of chemical reactions. Chem. Rev. 17.

Falkowski, P., Scholes, R.J., Boyle, E., Canadell, J., Canfield, D., Elser, J., Gruber, N., Hibbard, K., Hogberg, P., Linder, S., Mackenzie, F.T., Moore, B., Pedersen, T., Rosental, Y., Seitzinger, S., Smetacek, V., Steffen, W., 2000. The global carbon cycle: A test of our knowledge of earth as a system. Science (80-.). 290, 291–296. https://doi.org/10.1126/science.290.5490.291

Fasca, H., de Castilho, L.V.A., de Castilho, J.F.M., Pasqualino, I.P., Alvarez, V.M., de Azevedo Jurelevicius, D., Seldin, L., 2018. Response of marine bacteria to oil contamination and to high pressure and low temperature deep sea conditions. Microbiologyopen 7, 1–10. https://doi.org/10.1002/mbo3.550

Fast, A.G., Papoutsakis, E.T., 2012. Stoichiometric and energetic analyses of non-photosynthetic CO2-fixation pathways to support synthetic biology strategies for production of fuels and chemicals. Curr. Opin. Chem. Eng. 1, 380–395. https://doi.org/10.1016/j.coche.2012.07.005

Fast, A.G., Schmidt, E.D., Jones, S.W., Tracy, B.P., 2015. Acetogenic mixotrophy : novel options for yield improvement in biofuels and biochemicals production. Curr. Opin. Biotechnol. 33, 60–72. https://doi.org/10.1016/j.copbio.2014.11.014

Fazi, S., Ungaro, F., Venturi, S., Vimercati, L., Cruz Viggi, C., Baronti, S., Ugolini, F., Calzolari, C., Tassi, F., Vaselli, O., Raschi, A., Aulenta, F., 2019. Microbiomes in Soils Exposed to Naturally High Concentrations of CO2 (Bossoleto Mofette Tuscany, Italy). Front. Microbiol. 10. https://doi.org/10.3389/fmicb.2019.02238

Feng, D., Xia, A., Liao, Q., Nizami, A.S., Sun, C., Huang, Y., Zhu, Xianqing, Zhu, Xun, 2021. Carbon cloth facilitates semi-continuous anaerobic digestion of organic wastewater rich in volatile fatty acids from dark fermentation. Environ. Pollut. 272, 116030. https://doi.org/10.1016/j.envpol.2020.116030

Ferguson, R.M.W., Coulon, F., Villa, R., 2018. Understanding microbial ecology can help improve biogas production in AD. Sci. Total Environ. 642, 754–763. https://doi.org/10.1016/j.scitotenv.2018.06.007

Fernando-Foncillas, C., Varrone, C., 2021. Effect of reactor operating conditions on carboxylate production and chain elongation from co-fermented sludge and food waste. J. Clean. Prod. 292, 126009. https://doi.org/10.1016/j.jclepro.2021.126009

Ferreira, R.M., Mota, M.J., Lopes, R.P., Sousa, S., Gomes, A.M., Delgadillo, I., Saraiva, J.A., 2019. Adaptation of Saccharomyces cerevisiae to high pressure (15, 25 and 35 MPa) to enhance the production of bioethanol. Food Res. Int. https://doi.org/10.1016/j.foodres.2018.11.027

Ferreira, T.B., Rego, G.C., Ramos, L.R., de Menezes, C.A., Silva, E.L., 2020. Improved dark fermentation of cane molasses in mesophilic and thermophilic anaerobic fluidized bed reactors by selecting operational conditions. Int. J. Energy Res. 44, 10442–10452. https://doi.org/10.1002/er.5673

Fichtel, K., Logemann, J., Fichtel, J., Rullkötter, J., Cypionka, H., Engelen, B., 2015. Temperature and pressure adaptation of a sulfate reducer from the deep subsurface. Front. Microbiol. 6, 1078. https://doi.org/10.3389/fmicb.2015.01078

Figueras, J., Benbelkacem, H., Dumas, C., Buffiere, P., 2021. “Biomethanation of syngas by enriched mixed anaerobic consortium in pressurized agitated column.” Bioresour. Technol. 338, 125548. https://doi.org/10.1016/j.biortech.2021.125548

Figueroa, I.A., Barnum, T.P., Somasekhar, P.Y., Carlström, C.I., Engelbrektson, A.L., Coates, J.D., 2018. Metagenomics-guided analysis of microbial chemolithoautotrophic phosphite oxidation yields evidence of a seventh natural CO2 fixation pathway. Proc. Natl. Acad. Sci. U. S. A. 115, E92–E101. https://doi.org/10.1073/pnas.1715549114

Finke, N., Jørgensen, B.B., 2008. Response of fermentation and sulfate reduction to experimental temperature changes in temperate and Arctic marine sediments. ISME J. 2, 815–829. https://doi.org/10.1038/ismej.2008.20

Foladori, P., Bruni, L., Tamburini, S., Ziglio, G., 2010. Direct quantification of bacterial biomass in influent, effluent and activated sludge of wastewater treatment plants by using flow cytometry. Water Res. 44, 3807–3818. https://doi.org/10.1016/j.watres.2010.04.027

Franchi, O., Rosenkranz, F., Chamy, R., 2018. Key microbial populations involved in anaerobic degradation of phenol and p-cresol using different inocula. Electron. J. Biotechnol. 35, 33–38. https://doi.org/10.1016/j.ejbt.2018.08.002

Franco-Morgado, M., Toledo-Cervantes, A., González-Sánchez, A., Lebrero, R., Muñoz, R., 2018. Integral (VOCs, CO2, mercaptans and H2S) photosynthetic biogas upgrading using innovative biogas and digestate supply strategies. Chem. Eng. J. 354, 363–369. https://doi.org/10.1016/j.cej.2018.08.026

Freguia, S., Rabaey, K., Yuan, Z., Keller, J., 2008. Syntrophic processes drive the conversion of glucose in microbial fuel cell anodes. Environ. Sci. Technol. 42, 7937–7943. https://doi.org/10.1021/es800482e

Friedlingstein, P., O'Sullivan, M., Jones, M.W., Andrew, R.M., Hauck, J., Olsen, A., Peters, G.P., Peters, W., Pongratz, J., Sitch, S., Le Quéré, C., Canadell, J.G., Ciais, P., Jackson, R.B., Alin, S., Aragão, L.E.O.C., Arneth, A., Arora, V., Bates, N.R., Becker, M., Benoit-Cattin, A., Bittig, H.C., Bopp, L., Bultan, S., Chandra, N., Chevallier, F., Chini, L.P., Evans, W., Florentie, L., Forster, P.M., Gasser, T., Gehlen, M., Gilfillan, D., Gkritzalis, T., Gregor, L., Gruber, N., Harris, I., Hartung, K., Haverd, V., Houghton, R.A., Ilyina, T., Jain, A.K., Joetzjer, E., Kadono, K., Kato, E., Kitidis, V., Korsbakken, J.I., Landschützer, P., Lefèvre, N., Lenton, A., Lienert, S., Liu, Z., Lombardozzi, D., Marland, G., Metzl, N., Munro, D.R., Nabel, J.E.M.S., Nakaoka, S.I., Niwa, Y., O'Brien, K., Ono, T., Palmer, P.I., Pierrot, D., Poulter, B., Resplandy, L., Robertson, E., Rödenbeck, C., Schwinger, J., Séférian, R., Skjelvan, I., Smith, A.J.P., Sutton, A.J., Tanhua, T., Tans, P.P., Tian, H., Tilbrook, B., Van Der Werf, G., Vuichard, N., Walker, A.P., Wanninkhof, R., Watson, A.J., Willis, D., Wiltshire, A.J., Yuan, W., Yue, X., Zaehle, S., 2020. Global Carbon Budget 2020. Earth Syst. Sci. Data 12, 3269–3340. https://doi.org/10.5194/essd-12-3269-2020

Fry, J.C., 1990. Direct Methods and Biomass Estimation, Methods in Microbiology. https://doi.org/10.1016/S0580-9517(08)70239-3

Fu, S., Angelidaki, I., Zhang, Y., 2021. In situ Biogas Upgrading by CO2-to-CH4 Bioconversion. Trends Biotechnol. 39, 336–347. https://doi.org/10.1016/j.tibtech.2020.08.006

Fu, T., Jia, C., Fu, L., Zhou, S., Yao, P., Du, R., Sun, H., Yang, Z., Shi, X., Zhang, X.H., 2018. Marinifilum breve sp. nov., a marine bacterium isolated from the yongle blue hole in the south China sea and emended description of the genus marinifilum. Int. J. Syst. Evol. Microbiol. 68, 3540–3545. https://doi.org/10.1099/ijsem.0.003027

Fu, Z., Holtzapple, M.T., 2010. Fermentation of sugarcane bagasse and chicken manure to calcium carboxylates under thermophilic conditions. Appl. Biochem. Biotechnol. 162, 561–578. https://doi.org/10.1007/s12010-009-8748-z

Fukuzaki, S., Nishio, N., Shobayashi, M., Nagai, S., 1990. Inhibition of the fermentation of propionate to methane by hydrogen, acetate, and propionate. Appl. Environ. Microbiol. 56, 719–23.

Gao, X., Kong, J., Zhu, H., Mao, B., Cui, S., Zhao, J., 2021. Lactobacillus, Bifidobacterium and Lactococcus response to environmental stress: Mechanisms and application of cross-protection to improve resistance against freeze-drying. J. Appl. Microbiol. 1–20. https://doi.org/10.1111/jam.15251

Garcia-Gonzalez, L., Geeraerd, A.H., Mast, J., Briers, Y., Elst, K., Van Ginneken, L., Van Impe, J.F., Devlieghere, F., 2010. Membrane permeabilization and cellular death of Escherichia coli, Listeria monocytogenes and Saccharomyces cerevisiae as induced by high pressure carbon dioxide treatment. Food Microbiol. 27, 541–549. https://doi.org/10.1016/j.fm.2009.12.004

García Rea, V.S., Muñoz Sierra, J.D., Fonseca Aponte, L.M., Cerqueda-Garcia, D., Quchani, K.M., Spanjers, H., van Lier, J.B., 2020. Enhancing Phenol Conversion Rates in Saline Anaerobic Membrane Bioreactor Using Acetate and Butyrate as Additional Carbon and Energy Sources. Front. Microbiol. 11.

https://doi.org/10.3389/fmicb.2020.604173

Ge, S., Wu, Y., Peng, W., Xia, C., Mei, C., Cai, L., Shi, S.Q., Sonne, C., Lam, S.S., Tsang, Y.F., 2020. High-pressure CO2 hydrothermal pretreatment of peanut shells for enzymatic hydrolysis conversion into glucose. Chem. Eng. J. 385, 123949. https://doi.org/10.1016/j.cej.2019.123949

Ghasimi, D.S.M., Aboudi, K., de Kreuk, M., Zandvoort, M.H., van Lier, J.B., 2016. Impact of lignocellulosic-waste intermediates on hydrolysis and methanogenesis under thermophilic and mesophilic conditions. Chem. Eng. J. 295, 181–191. https://doi.org/10.1016/j.cej.2016.03.045

Ghimire, A., Frunzo, L., Pirozzi, F., Trably, E., Escudie, R., Lens, P.N.L., Esposito, G., 2015. A review on dark fermentative biohydrogen production from organic biomass: Process parameters and use of by-products. Appl. Energy 144, 73–95. https://doi.org/10.1016/j.apenergy.2015.01.045

Gillen, R.G., 1971. The effect of pressure on muscle lactate dehydrogenase activity of some deep-sea and shallow-water fishes. Mar. Biol. 8, 7–11. https://doi.org/10.1007/BF00349340

Girbal, L., Soucaille, P., 1994. Regulation of Clostridium acetobutylicum metabolism as revealed by mixed-substrate steady-state continuous cultures: Role of NADH/NAD ratio and ATP pool. J. Bacteriol. 176, 6433–6438. https://doi.org/10.1128/jb.176.21.6433-6438.1994

Goel, A., Wortel, M.T., Molenaar, D., Teusink, B., 2012. Metabolic shifts: A fitness perspective for microbial cell factories. Biotechnol. Lett. 34, 2147–2160. https://doi.org/10.1007/s10529-012-1038-9

González-Cabaleiro, R., Lema, J.M., Rodríguez, J., 2015. Metabolic energy-based modelling explains product yielding in anaerobic mixed culture fermentations. PLoS One 10, 1–17. https://doi.org/10.1371/journal.pone.0126739

González-Cabaleiro, R., Lema, J.M., Rodríguez, J., Kleerebezem, R., 2013. Linking thermodynamics and kinetics to assess pathway reversibility in anaerobic bioprocesses. Energy Environ. Sci. 6, 3780. https://doi.org/10.1039/c3ee42754d

González-Cabaleiro, R., Martinez-Rabert, E., Argiz, L., van Kessel, M.A., Smith, C.J., 2021. A framework based on fundamental biochemical principles to engineer microbial community dynamics. Curr. Opin. Biotechnol. 67, 111–118. https://doi.org/10.1016/j.copbio.2021.01.001

González-Cabaleiro, R., Ofiţeru, I.D., Lema, J.M., Rodríguez, J., 2016. Microbial catabolic activities are naturally selected by metabolic energy harvest rate. ISME J. 9, 2630–2641. https://doi.org/10.1038/ismej.2015.69

Gonzalez-Garcia, R.A., McCubbin, T., Navone, L., Stowers, C., Nielsen, L.K., Marcellin, E., 2017. Microbial propionic acid production. Fermentation 3, 1–20. https://doi.org/10.3390/fermentation3020021

Guan, N., Liu, L., 2020. Microbial response to acid stress: mechanisms and applications. Appl. Microbiol. Biotechnol. 104, 51–65. https://doi.org/10.1007/s00253-019-10226-1

Gulliver, D.M., Lowry, G. V, Gregory, K.B., 2014. CO2 concentration and pH alters subsurface microbial ecology at reservoir temperature and pressure. RSC Adv. 4, 17443–17453. https://doi.org/10.1039/C4RA02139H

Guo, X., Chen, H., Zhu, X., Xia, A., Liao, Q., 2021. Revealing the role of conductive materials on facilitating direct interspecies electron transfer in syntrophic methanogenesis : A thermodynamic analysis. Energy 229, 120747. https://doi.org/10.1016/j.energy.2021.120747

Gustafsson, L., Larsson, K., Larsson, C., Adler, L., 1993. Maintenance Energy Requirements Under Stress Conditions 65, 1893–1898.

Hakobyan, B., Pinske, C., Sawers, G., Trchounian, A., Trchounian, K., 2018. PH and a mixed carbon-substrate spectrum influence FocA- and FocB-dependent, formate-driven H2 production in Escherichia coli. FEMS Microbiol. Lett. 365, 1–8. https://doi.org/10.1093/femsle/fny233

Han, S.K., Shin, H.S., 2004. Performance of an innovative two-stage process converting food waste to hydrogen and methane? J. Air Waste Manag. Assoc. 54, 242–249. https://doi.org/10.1080/10473289.2004.10470895

Han, Y., Green, H., Tao, W., 2020. Reversibility of propionic acid inhibition to anaerobic digestion: Inhibition kinetics and microbial mechanism. Chemosphere 255, 126840. https://doi.org/10.1016/j.chemosphere.2020.126840

Hanselmann, K.W., 1991. Microbial energetics appfied to waste repositories. Rev. Exp. 47.

Hansson, Gora, Molin, N., 1981. End product inhibition in methane fermentations: effects of carbon dioxide on

fermentative and acetogenic bacteria. Eur. J. Appl. Microbiol. … 236–241. https://doi.org/10.1007/BF00499165

Hansson, Goran, Molin, N., 1981. End product inhibition in methane fermentations: Effects of carbon dioxide and methane on methanogenic bacteria utilizing acetate. Eur. J. Appl. Microbiol. Biotechnol. 13, 236–241. https://doi.org/10.1007/BF00500105

Hao, L., Bize, A., Conteau, D., Chapleur, O., Courtois, S., Kroff, P., Desmond-Le Quéméner, E., Bouchez, T., Mazéas, L., 2016. New insights into the key microbial phylotypes of anaerobic sludge digesters under different operational conditions. Water Res. 102, 158–169. https://doi.org/10.1016/j.watres.2016.06.014

Harrison, J.P., Gheeraert, N., Tsigelnitskiy, D., Cockell, C.S., 2013. The limits for life under multiple extremes. Trends Microbiol. 21, 204–212. https://doi.org/10.1016/j.tim.2013.01.006

Heffernan, J.K., Valgepea, K., de Souza Pinto Lemgruber, R., Casini, I., Plan, M., Tappel, R., Simpson, S.D., Köpke, M., Nielsen, L.K., Marcellin, E., 2020. Enhancing CO2-Valorization Using Clostridium autoethanogenum for Sustainable Fuel and Chemicals Production. Front. Bioeng. Biotechnol. 8, 1–10. https://doi.org/10.3389/fbioe.2020.00204

Heijnen, J.J., Kleerebezem, R.R., 2010. Bioenergetics of Microbial Growth, in: Encyclopedia of Industrial Biotechnology. John Wiley & Sons, Inc., Hoboken, NJ, USA, pp. 1–66.

Henze, M., 2008. Biological wastewater treatment : principles, modelling and design. IWA Pub.

Herrero, M., Stuckey, D.C., 2015. Bioaugmentation and its application in wastewater treatment: A review. Chemosphere 140, 119–128. https://doi.org/10.1016/j.chemosphere.2014.10.033

Heuer, V.B., Pohlman, J.W., Torres, M.E., Elvert, M., Hinrichs, K.U., 2009. The stable carbon isotope biogeochemistry of acetate and other dissolved carbon species in deep subseafloor sediments at the northern Cascadia Margin. Geochim. Cosmochim. Acta 73, 3323–3336. https://doi.org/10.1016/j.gca.2009.03.001

Hickey, R.F., Switzenbaum, M.S., 1991. Thermodynamics of volatile fatty acid accumulation in anaerobic digesters subject to increases in hydraulic and organic loading. Res. J. Water Pollut. Control Fed. 63, 141–144.

Hill, M.O., 1973. Diversity and Evenness: A Unifying Notation and Its Consequences. Ecology 54, 427–432. https://doi.org/10.2307/1934352

Hoelzle, R.D., Puyol, D., Virdis, B., Batstone, D., 2021. Substrate availability drives mixed culture fermentation of glucose to lactate at steady state. Biotechnol. Bioeng. bit.27678. https://doi.org/10.1002/bit.27678

Hoelzle, R.D., Virdis, B., Batstone, D.J., 2014. Regulation mechanisms in mixed and pure culture microbial fermentation. Biotechnol. Bioeng. 111, 2139–2154. https://doi.org/10.1002/bit.25321

Holtzapple, M.T., Granda, C.B., 2009. Carboxylate platform: The MixAlco process part 1: Comparison of three biomass conversion platforms. Appl. Biochem. Biotechnol. 156, 95–106. https://doi.org/10.1007/s12010-008-8466-y

Holtzapple, M.T., Wu, H., Weimer, P.J., Dalke, R., Granda, C.B., Mai, J., Urgun-Demirtas, M., 2022. Microbial communities for valorizing biomass using the carboxylate platform to produce volatile fatty acids: A review. Bioresour. Technol. 344, 126253. https://doi.org/10.1016/j.biortech.2021.126253

Hong, S.-I., Pyun, Y.-R., 1999. Inactivation Kinetics of Lactobacillus plantarum by High Pressure Carbon Dioxide. J. Food Sci. 64, 728–733. https://doi.org/10.1111/j.1365-2621.1999.tb15120.x

Hu, J., Wang, L., Zhang, S., Fu, X., Le, Y., 2010. Matching different inorganic compounds as mixture of electron donors to improve CO2 fixation by nonphotosynthetic microbial community without hydrogen. Environ. Sci. Technol. 44, 6364–6370. https://doi.org/10.1021/es1002499

Huang, L., Hwang, A., Phillips, J., 2011. Effect of Temperature on Microbial Growth Rate-Mathematical Analysis: The Arrhenius and Eyring-Polanyi Connections. J. Food Sci. 76. https://doi.org/10.1111/j.1750-3841.2011.02377.x

Huang, Z., Yu, J., Xiao, X., Miao, H., Ren, H., Zhao, M., Ruan, W., 2016. Directional regulation of the metabolic heterogeneity in anaerobic mixed culture to enhance fermentative hydrogen production by adaptive laboratory evolution. Int. J. Hydrogen Energy 41, 10145–10151. https://doi.org/10.1016/j.ijhydene.2016.05.012

IEA, 2020. Outlook for biogas and biomethane. Prospects for organic growth. World Energy Outlook Special

Report. 93.

Infantes, D., González del Campo, A., Villaseñor, J., Fernández, F.J., 2012. Kinetic model and study of the influence of pH, temperature and undissociated acids on acidogenic fermentation. Biochem. Eng. J. 66, 66–72. https://doi.org/10.1016/J.BEJ.2012.04.017

Ishikawa, H., Shimoda, M., Yonekura, A., Osajima, Y., 1996. Inactivation of Enzymes and Decomposition of α-Helix Structure by Supercritical Carbon Dioxide Microbubble Method. J. Agric. Food Chem. 44, 2646–2649. https://doi.org/10.1021/jf9602075

Iwahashi, H., Odani, M., Ishidou, E., Kitagawa, E., 2005. Adaptation of Saccharomyces cerevisiae to high hydrostatic pressure causing growth inhibition. FEBS Lett. 579, 2847–2852. https://doi.org/10.1016/j.febslet.2005.03.100

Jain, S., Dietrich, H.M., Müller, V., Basen, M., 2020. Formate Is Required for Growth of the Thermophilic Acetogenic Bacterium Thermoanaerobacter kivui Lacking Hydrogen-Dependent Carbon Dioxide Reductase (HDCR). Front. Microbiol. 11. https://doi.org/10.3389/fmicb.2020.00059

Jajesniak, P., Omar Ali, H.E.M., Wong, T.S., 2014. Carbon Dioxide Capture and Utilization using Biological Systems: Opportunities and Challenges. J. Bioprocess. Biotech. 04. https://doi.org/10.4172/2155-9821.1000155

Jankowska, E., Chwialkowska, J., Stodolny, M., Oleskowicz-Popiel, P., 2017. Volatile fatty acids production during mixed culture fermentation – The impact of substrate complexity and pH. Chem. Eng. J. 326, 901–910. https://doi.org/10.1016/j.cej.2017.06.021

Jebbar, M., Franzetti, B., Girard, E., Oger, P., 2015. Microbial diversity and adaptation to high hydrostatic pressure in deep-sea hydrothermal vents prokaryotes. Extremophiles 19, 721–740. https://doi.org/10.1007/s00792-015-0760-3

Ji, Q., Fan, Y., 2012. How does oil price volatility affect non-energy commodity markets? Appl. Energy 89, 273–280. https://doi.org/10.1016/j.apenergy.2011.07.038

Jia, X., Wang, Y., Ren, L., Li, M., Tang, R., Jiang, Y., Hou, J., 2019. Early warning indicators and microbial community dynamics during unstable stages of continuous hydrogen production from food wastes by thermophilic dark fermentation. Int. J. Hydrogen Energy 44, 30000–30013. https://doi.org/10.1016/j.ijhydene.2019.08.082

Jiang, J., Zhang, Y., Li, K., Wang, Q., Gong, C., Li, M., 2013. Volatile fatty acids production from food waste: Effects of pH, temperature, and organic loading rate. Bioresour. Technol. 143, 525–530. https://doi.org/10.1016/j.biortech.2013.06.025

Jiang, Y., Banks, C., Zhang, Y., Heaven, S., Longhurst, P., 2018. Quantifying the percentage of methane formation via acetoclastic and syntrophic acetate oxidation pathways in anaerobic digesters. Waste Manag. 71, 749–756. https://doi.org/10.1016/j.wasman.2017.04.005

Jiang, Y., Zeng, R.J., 2018. Expanding the product spectrum of value added chemicals in microbial electrosynthesis through integrated process design — A review. Bioresour. Technol. 269, 503–512. https://doi.org/10.1016/j.biortech.2018.08.101

Jin, Q., Bethke, C.M., 2007. The thermodynamics and kinetics of microbial metabolism. Am. J. Sci. 307, 643–677. https://doi.org/10.2475/04.2007.01

Jin, Q., Kirk, M.F., 2018a. pH as a Primary Control in Environmental Microbiology : 2 . Kinetic Perspective 6, 1–16. https://doi.org/10.3389/fenvs.2018.00101

Jin, Q., Kirk, M.F., 2018b. pH as a Primary Control in Environmental Microbiology : 1 . Thermodynamic Perspective 6, 1–15. https://doi.org/10.3389/fenvs.2018.00021

Jin, Q., Kirk, M.F., 2016. Thermodynamic and kinetic response of microbial reactions to high CO2. Front. Microbiol. 7, 1696. https://doi.org/10.3389/fmicb.2016.01696

Johnson, K., Kleerebezem, R., van Loosdrecht, M.C.M., 2009. Model-based data evaluation of polyhydroxybutyrate producing mixed microbial cultures in aerobic sequencing batch and fed-batch reactors. Biotechnol. Bioeng. 104, 50–67. https://doi.org/10.1002/bit.22380

Jones, D.T., Woods, D.R., 1986. Acetone-butanol fermentation revisited. Microbiol. Rev. 50, 484–524. https://doi.org/10.1128/mmbr.50.4.484-524.1986

Jones, S.W., Fast, A.G., Carlson, E.D., Wiedel, C.A., Au, J., Antoniewicz, M.R., Papoutsakis, E.T., Tracy, B.P., 2016. CO2 fixation by anaerobic non-photosynthetic mixotrophy for improved carbon conversion. Nat. Commun. 7, 12800. https://doi.org/10.1038/ncomms12800

Junicke, H., Feldman, H., van Loosdrecht, M.C.M., Kleerebezem, R., 2015. Impact of the hydrogen partial pressure on lactate degradation in a coculture of Desulfovibrio sp. G11 and Methanobrevibacter arboriphilus DH1. Appl. Microbiol. Biotechnol. 99, 3599–3608. https://doi.org/10.1007/s00253-014-6241-2

Junicke, H., van Loosdrecht, M.C.M., Kleerebezem, R., 2016. Kinetic and thermodynamic control of butyrate conversion in non-defined methanogenic communities. Appl. Microbiol. Biotechnol. 100, 915–925. https://doi.org/10.1007/s00253-015-6971-9

Kato, N., Sato, T., Kato, C., Yajima, M., Sugiyama, J., Kanda, T., Mizuno, M., Nozaki, K., Yamanaka, S., Amano, Y., 2007. Viability and cellulose synthesizing ability of Gluconacetobacter xylinus cells under high-hydrostatic pressure. Extremophiles 11, 693–698. https://doi.org/10.1007/s00792-007-0085-y

Kato, S., Yoshida, R., Yamaguchi, T., Sato, T., Yumoto, I., Kamagata, Y., 2014. The effects of elevated CO2 concentration on competitive interaction between aceticlastic and syntrophic methanogenesis in a model microbial consortium. Front. Microbiol. 5, 1–8. https://doi.org/10.3389/fmicb.2014.00575

Kay, M., Elkin, L., Higgins, J., Wobbrock, J., 2021. ARTool: Aligned Rank Transform for Nonparametric Factorial ANOVAs. https://doi.org/10.5281/zenodo.594511

Kaye, J.Z., Baross, J.A., 2004. Synchronous Effects of Temperature, Hydrostatic Pressure, and Salinity on Growth, Phospholipid Profiles, and Protein Patterns of Four Halomonas Species Isolated from Deep-Sea Hydrothermal-Vent and Sea-Surface Environments. Appl. Environ. Mi 70, 6220–6229. https://doi.org/10.1128/AEM.70.10.6220

Kehrein, P., van Loosdrecht, M., Osseweijer, P., Posada, J., Dewulf, J., 2020. The SPPD-WRF framework: A novel and holistic methodology for strategical planning and process design of water resource factories. Sustain. 12. https://doi.org/10.3390/su12104168

Khan, M.A.A., Ngo, H.H.H., Guo, W.S.S., Liu, Y., Nghiem, L.D.D., Hai, F.I.I., Deng, L.J.J., Wang, J., Wu, Y., 2016. Optimization of process parameters for production of volatile fatty acid, biohydrogen and methane from anaerobic digestion. Bioresour. Technol. 219, 738–748. https://doi.org/10.1016/j.biortech.2016.08.073

Kim, B.H., Gadd, G.M., 2008. Bacterial Physiology and Metabolism, Second. ed. Cambridge University Press, New York.

Kim, S., Mostafa, A., Im, S., Lee, M.K., Kang, S., Na, J.G., Kim, D.H., 2021. Production of high-calorific biogas from food waste by integrating two approaches: Autogenerative high-pressure and hydrogen injection. Water Res. 194. https://doi.org/10.1016/j.watres.2021.116920

Kim, W., Shin, S.G., Han, G., Cho, K., Hwang, S., 2015. Structures of microbial communities found in anaerobic batch runs that produce methane from propionic acid-Seeded from full-scale anaerobic digesters above a certain threshold. J. Biotechnol. 214, 192–198. https://doi.org/10.1016/j.jbiotec.2015.09.040

Kirk, M.F., 2011. Variation in Energy Available to Populations of Subsurface Anaerobes in Response to Geological Carbon Storage 6676–6682. https://doi.org/10.1021/es201279e

Kish, A., Griffin, P.L., Rogers, K.L., Fogel, M.L., Hemley, R.J., Steele, A., 2012. High-pressure tolerance in Halobacterium salinarum NRC-1 and other non-piezophilic prokaryotes. Extremophiles 16, 355–361. https://doi.org/10.1007/s00792-011-0418-8

Kitada, K., Machmudah, S., Sasaki, M., Goto, M., Nakashima, Y., Kumamoto, S., Hasegawa, T., 2009. Supercritical CO2 extraction of pigment components with pharmaceutical importance from Chlorella vulgaris. J. Chem. Technol. Biotechnol. 84, 657–661. https://doi.org/10.1002/jctb.2096

Kleerebezem, R., Joosse, B., Rozendal, R., Van Loosdrecht, M.C.M., 2015. Anaerobic digestion without biogas? Rev. Environ. Sci. Bio/Technology 14, 787–801. https://doi.org/10.1007/s11157-015-9374-6

Kleerebezem, R., Stams, A.J.M., 2000. Kinetics of syntrophic cultures: A theoretical treatise on butyrate fermentation. Biotechnol. Bioeng. 67, 529–543. https://doi.org/10.1002/(SICI)1097-0290(20000305)67:5<529::AID-BIT4>3.0.CO;2-Q

Kleerebezem, R., van Loosdrecht, M.C.M., 2007. Mixed culture biotechnology for bioenergy production. Curr. Opin. Biotechnol. 18, 207–12. https://doi.org/10.1016/j.copbio.2007.05.001

Kleerebezem, R., Van Loosdrecht, M.C.M., 2010. A Generalized Method for Thermodynamic State Analysis of Environmental Systems. Crit. Rev. Environ. Sci. Technol. 40, 1–54. https://doi.org/10.1080/10643380802000974

Klindworth, A., Pruesse, E., Schweer, T., Peplies, J., Quast, C., Horn, M., Glöckner, F.O., 2013. Evaluation of general 16S ribosomal RNA gene PCR primers for classical and next-generation sequencing-based diversity studies. Nucleic Acids Res. 41, 1–11. https://doi.org/10.1093/nar/gks808

Knebl, A., Domes, R., Wolf, S., Domes, C., Popp, J., Frosch, T., 2020. Fiber-Enhanced Raman Gas Spectroscopy for the Study of Microbial Methanogenesis. Anal. Chem. 92, 12564–12571. https://doi.org/10.1021/acs.analchem.0c02507

Knoblauch, C., Jorgensen, B.B., 1999. Effect of temperature on sulphate reduction, growth rate and growth yield in five psychrophilic sulphate-reducing bacteria from Arctic sediments. Environ. Microbiol. 1, 457–467. https://doi.org/10.1046/j.1462-2920.1999.00061.x

Kobayashi, H., Nagashima, A., Kouyama, M., Fu, Q., Ikarashi, M., Maeda, H., Sato, K., 2017. High-pressure thermophilic electromethanogenic system producing methane at 5 MPa, 55°C. J. Biosci. Bioeng. 124, 327–332. https://doi.org/10.1016/j.jbiosc.2017.04.001

Kondaveeti, S., Abu-Reesh, I.M., Mohanakrishna, G., Bulut, M., Pant, D., 2020. Advanced Routes of Biological and Bio-electrocatalytic Carbon Dioxide (CO2) Mitigation Toward Carbon Neutrality. Front. Energy Res. 8, 1–24. https://doi.org/10.3389/fenrg.2020.00094

Kondo, R., Nishijima, T., Hata, Y., 1993. Effect of Temperature on the Production of Low Molecular Fatty Acids within an Anoxic Marine Sediment Slurry. Nippon SUISAN GAKKAISHI 59, 1189–1194. https://doi.org/10.2331/suisan.59.1189

Kougias, P.G., Treu, L., Benavente, D.P., Boe, K., Campanaro, S., Angelidaki, I., 2017. Ex-situ biogas upgrading and enhancement in different reactor systems. Bioresour. Technol. 225, 429–437. https://doi.org/10.1016/j.biortech.2016.11.124

Kraemer, J.T., Bagley, D.M., 2007. Improving the yield from fermentative hydrogen production. Biotechnol. Lett. 29, 685–695. https://doi.org/10.1007/s10529-006-9299-9

Kujawa-Roeleveld, K., Zeeman, G., 2006. Anaerobic Treatment in Decentralised and Source-Separation-Based Sanitation Concepts. Rev. Environ. Sci. Bio/Technology 5, 115–139. https://doi.org/10.1007/s11157-005-5789-9

Kumagai, H., Hata, C., Nakamura, K., 1997. CO2 sorption by microbial cells and sterilization by high-pressure CO2. Biosci. Biotechnol. Biochem. 61, 931–935. https://doi.org/10.1271/bbb.61.931

Kwon, Y.D., Kim, S., Lee, S.Y., Kim, P., 2011. Long-term continuous adaptation of Escherichia coli to high succinate stress and transcriptome analysis of the tolerant strain. J. Biosci. Bioeng. 111, 26–30. https://doi.org/10.1016/j.jbiosc.2010.08.007

Labatut, R.A., Angenent, L.T., Scott, N.R., 2011. Biochemical methane potential and biodegradability of complex organic substrates. Bioresour. Technol. 102, 2255–2264. https://doi.org/10.1016/j.biortech.2010.10.035

Lai, C.Y., Zhou, L., Yuan, Z., Guo, J., 2021. Hydrogen-driven microbial biogas upgrading: Advances, challenges andsolutions. Water Res. 197, 117120. https://doi.org/10.1016/j.watres.2021.117120

Lam, M.K., Lee, K.T., 2012. Microalgae biofuels: A critical review of issues, problems and the way forward. Biotechnol. Adv. 30, 673–690. https://doi.org/10.1016/j.biotechadv.2011.11.008

Lanciotti, R., Gardini, F., Sinigaglia, M., Guerzoni, M.E., 1996. Effects of growth conditions on the resistance of some pathogenic and spoilage species to high pressure homogenization. Lett. Appl. Microbiol. 22, 165–168. https://doi.org/10.1111/j.1472-765X.1996.tb01134.x

Latif, M.A., Mehta, C.M., Batstone, D.J., 2018. Enhancing soluble phosphate concentration in sludge liquor by pressurised anaerobic digestion. Water Res. 145, 660–666. https://doi.org/10.1016/j.watres.2018.08.069

Lee, H.S., Rittmann, B.E., 2009. Evaluation of metabolism using stoichiometry in fermentative biohydrogen. Biotechnol. Bioeng. 102, 749–758. https://doi.org/10.1002/bit.22107

Lee, H.S., Salerno, M.B., Rittmann, B.E., 2008. Thermodynamic Evaluation on H2 Production in Glucose Fermentation. Environ. Sci. Technol. 42, 2401–2407. https://doi.org/10.1021/es702610v

Lee, M., Hidaka, T., Tsuno, H., 2008. Effect of temperature on performance and microbial diversity in

hyperthermophilic digester system fed with kitchen garbage. Bioresour. Technol. 99, 6852–6860. https://doi.org/10.1016/j.biortech.2008.01.038

Lee, M.K., Sivagurunathan, P., Yun, Y.M., Kang, S., Na, J.G., Kim, D.H., 2018. High-calorific bio-hydrogen production under self-generated high-pressure condition. Bioresour. Technol. 264, 174–179. https://doi.org/10.1016/j.biortech.2018.05.074

Lee, R., Jessop, P.G., Champagne, P., 2015. Carbon dioxide pressure-induced coagulation of microalgae. Philos. Trans. R. Soc. A Math. Phys. Eng. Sci. 373, 1–8. https://doi.org/10.1098/rsta.2015.0016

Lemaire, O.N., Jespersen, M., Wagner, T., 2020. CO2-Fixation Strategies in Energy Extremophiles: What Can We Learn From Acetogens? Front. Microbiol. 11, 1–8. https://doi.org/10.3389/fmicb.2020.00486

Lemmer, A., Chen, Y., Lindner, J., Wonneberger, A.M., Zielonka, S., Oechsner, H., Jungbluth, T., 2015a. Influence of different substrates on the performance of a two-stage high pressure anaerobic digestion system. Bioresour. Technol. 178, 313–318. https://doi.org/10.1016/j.biortech.2014.09.118

Lemmer, A., Chen, Y., Wonneberger, A.M., Graf, F., Reimert, R., 2015b. Integration of a water scrubbing technique and two-stage pressurized anaerobic digestion in one process. Energies 8, 2048–2065. https://doi.org/10.3390/en8032048

Lemmer, A., Merkle, W., Baer, K., Graf, F., 2017. Effects of high-pressure anaerobic digestion up to 30 bar on pH-value, production kinetics and specific methane yield. Energy 138, 659–667. https://doi.org/10.1016/j.energy.2017.07.095

Leng, L., Yang, P., Mao, Y., Wu, Z., Zhang, T., Lee, P.H., 2017. Thermodynamic and physiological study of caproate and 1,3-propanediol co-production through glycerol fermentation and fatty acids chain elongation. Water Res. 114, 200–209. https://doi.org/10.1016/j.watres.2017.02.023

Leng, L., Yang, P., Singh, S., Zhuang, H., Xu, L., Chen, W.-H., Dolfing, J., Li, D., Zhang, Y., Zeng, H., Chu, W., Lee, P.-H., 2018. A review on the bioenergetics of anaerobic microbial metabolism close to the thermodynamic limits and its implications for digestion applications. Bioresour. Technol. 247, 1095–1106. https://doi.org/10.1016/J.BIORTECH.2017.09.103

Li, C., Lin, J., Gao, L., Lin, H., Lin, J., 2018. Modeling and simulation of enzymatic gluconic acid production using immobilized enzyme and CSTR–PFTR circulation reaction system. Biotechnol. Lett. 40, 649–657. https://doi.org/10.1007/s10529-018-2509-4

Li, C., Zhu, X., Angelidaki, I., 2021. Syngas biomethanation: effect of biomass-gas ratio, syngas composition and pH buffer. Bioresour. Technol. 342, 125997. https://doi.org/10.1016/j.biortech.2021.125997

Li, J., Ban, Q., Zhang, L., Jha, A.K., 2012. Syntrophic propionate degradation in anaerobic digestion: A review. Int. J. Agric. Biol. 14, 843–850.

Li, J., Chen, T., Yin, J., Shen, D., 2021. Effect of nano-magnetite on the propionic acid degradation in anaerobic digestion system with acclimated sludge. Bioresour. Technol. 334, 125143. https://doi.org/10.1016/j.biortech.2021.125143

Li, L., He, Q., Ma, Y., Wang, X., Peng, X., 2016. A mesophilic anaerobic digester for treating food waste: Process stability and microbial community analysis using pyrosequencing. Microb. Cell Fact. 15, 1–11. https://doi.org/10.1186/s12934-016-0466-y

Li, Y., Liu, H., Yan, F., Su, D., Wang, Y., Zhou, H., 2017. High-calorific biogas production from anaerobic digestion of food waste using a two-phase pressurized biofilm (TPPB) system. Bioresour. Technol. 224, 56–62. https://doi.org/10.1016/j.biortech.2016.10.070

Li, Y., Sun, Y., Li, L., Yuan, Z., 2018. Acclimation of acid-tolerant methanogenic propionate-utilizing culture and microbial community dissecting. Bioresour. Technol. 250, 117–123. https://doi.org/10.1016/j.biortech.2017.11.034

Li, Y.F., Abraham, C., Nelson, M.C., Chen, P.H., Graf, J., Yu, Z., 2015. Effect of organic loading on the microbiota in a temperature-phased anaerobic digestion (TPAD) system co-digesting dairy manure and waste whey. Appl. Microbiol. Biotechnol. 99, 8777–8792. https://doi.org/10.1007/s00253-015-6738-3

Lim, S.J., Kim, B.J., Jeong, C.M., Choi, J. dal rae, Ahn, Y.H., Chang, H.N., 2008. Anaerobic organic acid production of food waste in once-a-day feeding and drawing-off bioreactor. Bioresour. Technol. 99, 7866–7874. https://doi.org/10.1016/j.biortech.2007.06.028

Lin, H., Cao, N., Chen, L.-F., 1994. Antimicrobial Effect of Pressurized Carbon Dioxide on Listeria

monocytogenes. J. Food Sci. 59, 657–659. https://doi.org/10.1111/j.1365-2621.1994.tb05587.x

Lindeboom, R.E.F., 2014. Autogenerative high pressure digestion: biogass production and upgrading in a single step. Wageningen University.

Lindeboom, R.E.F., Ding, L., Weijma, J., Plugge, C.M., van Lier, J.B., 2014. Starch hydrolysis in autogenerative high pressure digestion: Gelatinisation and saccharification as rate limiting steps. Biomass and Bioenergy 71, 256–265. https://doi.org/10.1016/j.biombioe.2014.07.031

Lindeboom, R.E.F., Fermoso, F.G., Weijma, J., Zagt, K., van Lier, J.B., 2011. Autogenerative high pressure digestion: Anaerobic digestion and biogas upgrading in a single step reactor system. Water Sci. Technol. 64, 647–653. https://doi.org/10.2166/wst.2011.664

Lindeboom, R.E.F., Ferrer, I., Weijma, J., van Lier, J.B., 2013a. Effect of substrate and cation requirement on anaerobic volatile fatty acid conversion rates at elevated biogas pressure. Bioresour. Technol. 150, 60–66. https://doi.org/10.1016/j.biortech.2013.09.100

Lindeboom, R.E.F., Ferrer, I., Weijma, J., van Lier, J.B., 2013b. Silicate minerals for CO2 scavenging from biogas in Autogenerative High Pressure Digestion. Water Res. 47, 3742–3751. https://doi.org/10.1016/j.watres.2013.04.028

Lindeboom, R.E.F., Ilgrande, C., Carvajal-Arroyo, J.M., Coninx, I., Van Hoey, O., Roume, H., Morozova, J., Udert, K.M., Sas, B., Paille, C., Lasseur, C., Ilyin, V., Clauwaert, P., Leys, N., Vlaeminck, S.E., 2018. Nitrogen cycle microorganisms can be reactivated after Space exposure. Sci. Rep. 8, 8–14. https://doi.org/10.1038/s41598-018-32055-4

Lindeboom, R.E.F., Shin, S.G., Weijma, J., van Lier, J.B., Plugge, C.M., 2016. Piezo-tolerant natural gas-producing microbes under accumulating pCO2. Biotechnol. Biofuels 9, 98–127. https://doi.org/10.1186/s13068-016-0634-7

Lindeboom, R.E.F., Weijma, J., Van Lier, J.B., 2012. High-calorific biogas production by selective CO 2 retention at autogenerated biogas pressures up to 20 bar. Environ. Sci. Technol. 46, 1895–1902. https://doi.org/10.1021/es202633u

Lipson, D.A., 2015. The complex relationship between microbial growth rate and yield and its implications for ecosystem processes. Front. Microbiol. 6, 1–5. https://doi.org/10.3389/fmicb.2015.00615

Liu, B., Kleinsteuber, S., Centler, F., Harms, H., Sträuber, H., 2020. Competition Between Butyrate Fermenters and Chain-Elongating Bacteria Limits the Efficiency of Medium-Chain Carboxylate Production. Front. Microbiol. 11, 1–13. https://doi.org/10.3389/fmicb.2020.00336

Liu, H.H., Shi, J., Zhan, X., Zhang, L., Fu, B., Liu, H.H., 2017. Selective acetate production with CO 2 sequestration through acetogen-enriched sludge inoculums in anaerobic digestion. Biochem. Eng. J. 121, 163–170. https://doi.org/10.1016/j.bej.2017.02.008

Liu, R., Hao, X., Wei, J., 2016. Function of homoacetogenesis on the heterotrophic methane production with exogenous H2/CO2 involved. Chem. Eng. J. 284, 1196–1203. https://doi.org/10.1016/j.cej.2015.09.081

Liu, Y., Gu, M., Yin, Q., Du, J., Wu, G., 2020. Thermodynamic analysis of direct interspecies electron transfer in syntrophic methanogenesis based on the optimized energy distribution. Bioresour. Technol. 297, 122345. https://doi.org/10.1016/j.biortech.2019.122345

Lohri, C.R., Diener, S., Foundation, B., 2014. Anaerobic Digestion of Biowaste in Developing Countries Practical Information and Case Studies. https://doi.org/10.13140/2.1.2663.1045

Lombardi, L., Francini, G., 2020. Techno-economic and environmental assessment of the main biogas upgrading technologies. Renew. Energy 156, 440–458. https://doi.org/10.1016/j.renene.2020.04.083

Lopes, R.P., Mota, M.J., Sousa, S., Gomes, A.M., Delgadillo, I., Saraiva, J.A., 2019. Combined effect of pressure and temperature for yogurt production. Food Res. Int. 122, 222–229. https://doi.org/10.1016/j.foodres.2019.04.010

Low, P.S., Somero, G.N., 1975. Activation volumes in enzymic catalysis: their sources and modification by low molecular weight solutes. Proc. Natl. Acad. Sci. U. S. A. 72, 3014–3018. https://doi.org/10.1073/pnas.72.8.3014

Lu, L., Huang, Z., Rau, G.H., Ren, Z.J., 2015. Microbial Electrolytic Carbon Capture for Carbon Negative and Energy Positive Wastewater Treatment. Environ. Sci. Technol. 49, 8193–8201. https://doi.org/10.1021/acs.est.5b00875

Lu, S., Eiteman, M.A., Altman, E., 2009. Effect of CO2 on succinate production in dual-phase Escherichia coli fermentations. J. Biotechnol. 143, 213–223. https://doi.org/10.1016/j.jbiotec.2009.07.012

Luttmann, R., Bracewell, D.G., Cornelissen, G., Gernaey, K. V., Glassey, J., Hass, V.C., Kaiser, C., Preusse, C., Striedner, G., Mandenius, C.F., 2012. Soft sensors in bioprocessing: A status report and recommendations. Biotechnol. J. 7, 1040–1048. https://doi.org/10.1002/biot.201100506

Ma, H., Liu, He, Zhang, L., Yang, M., Fu, B., Liu, Hongbo, 2017. Novel insight into the relationship between organic substrate composition and volatile fatty acids distribution in acidogenic co-fermentation. Biotechnol. Biofuels 10, 137. https://doi.org/10.1186/s13068-017-0821-1

Macdonald, A.G., 1984. The effects of pressure on the molecular structure and physiological functions of cell membranes. Philos. Trans. R. Soc. Lond. B. Biol. Sci. 304, 47–68. https://doi.org/10.1098/rstb.1984.0008

Magoc, T., Salzberg, S.L., Magoč, T., Salzberg, S.L., 2011. FLASH: fast length adjustment of short reads to improve genome assemblies. Bioinformatics 27, 2957–2963. https://doi.org/10.1093/bioinformatics/btr507

Maillacheruvu, K.Y., Parkin, G.F., Ma, K.Y., 2013. Kinetics and of sulfide growth , substrate utilization utilizers acetate , for toxicity and hydrogen in anaerobic systems. Water Environ. Fed. 68, 1099–1106. https://doi.org/10.2175/106143096X128126

Malaoui, H., Marczak, R., 2001. Influence of glucose on glycerol metabolism by wild-type and mutant strains of Clostridium butyricum E5 grown in chemostat culture. Appl. Microbiol. Biotechnol. 55, 226–233. https://doi.org/10.1007/s002530000495

Mand, T., Metcalf, W., 2019. Energy conservation and Hydrogenase Function in Methanogenic Archaea, in particular the Genus Methanosarcina. Microbiol. Mol. Biol. Rev. 1–22.

Manzocco, L., Ignat, A., Valoppi, F., Burrafato, K.R., Lippe, G., Spilimbergo, S., Nicoli, M.C., 2016. Inactivation of mushroom polyphenoloxidase in model systems exposed to high-pressure carbon dioxide. J. Supercrit. Fluids 107, 669–675. https://doi.org/10.1016/j.supflu.2015.07.029

Manzocco, L., Plazzotta, S., Spilimbergo, S., Nicoli, M.C., 2017. Impact of high-pressure carbon dioxide on polyphenoloxidase activity and stability of fresh apple juice. LWT - Food Sci. Technol. 85, 363–371. https://doi.org/10.1016/j.lwt.2016.11.052

Mao, C., Feng, Y., Wang, X., Ren, G., 2015. Review on research achievements of biogas from anaerobic digestion. Renew. Sustain. Energy Rev. 45, 540–555. https://doi.org/10.1016/j.rser.2015.02.032

Marietou, A., Bartlett, D.H., 2014. Effects of high hydrostatic pressure on coastal bacterial community abundance and diversity. Appl. Environ. Microbiol. 80, 5992–6003. https://doi.org/10.1128/AEM.02109-14

Marshall, C.W., LaBelle, E. V, May, H.D., 2013. Production of fuels and chemicals from waste by microbiomes. Curr. Opin. Biotechnol. 24, 391–7. https://doi.org/10.1016/j.copbio.2013.03.016

Marsland, R., Cui, W., Goldford, J., Sanchez, A., Korolev, K., Mehta, P., 2019. Available energy fluxes drive a transition in the diversity, stability, and functional structure of microbial communities. PLoS Comput. Biol. 15, 1–18. https://doi.org/10.1371/journal.pcbi.1006793

Martin, D.D., Bartlett, D.H., Roberts, M.F., 2002. Solute accumulation in the deep-sea bacterium Photobacterium profundum. Extremophiles 6, 507–514. https://doi.org/10.1007/s00792-002-0288-1

Martinez-Monteagudo, S.I., Saldaña, M.D.A., 2014. Chemical Reactions in Food Systems at High Hydrostatic Pressure. Food Eng. Rev. 6, 105–127. https://doi.org/10.1007/s12393-014-9087-6

Martins, G., Salvador, A.F., Pereira, L., Alves, M.M., 2018. Methane Production and Conductive Materials: A Critical Review. Environ. Sci. Technol. 52, 10241–10253. https://doi.org/10.1021/acs.est.8b01913

Maru, B.T., Munasinghe, P.C., Gilary, H., Jones, S.W., Tracy, B.P., 2018. Fixation of CO2 and CO on a diverse range of carbohydrates using anaerobic, non-photosynthetic mixotrophy. FEMS Microbiol. Lett. 365, 1–8. https://doi.org/10.1093/femsle/fny039

Mauerhofer, L.M., Zwirtmayr, S., Pappenreiter, P., Bernacchi, S., Seifert, A.H., Reischl, B., Schmider, T., Taubner, R.S., Paulik, C., Rittmann, S.K.M.R., 2021. Hyperthermophilic methanogenic archaea act as high-pressure CH4 cell factories. Commun. Biol. 4, 1–12. https://doi.org/10.1038/s42003-021-01828-5

Mawson, A.J., Earle, R.L., Larsen, V.F., 1991. Degradation of acetic and propionic acids in the methane fermentation. Water Res. 25, 1549–1554. https://doi.org/10.1016/0043-1354(91)90187-U

Mayumi, D., Dolfing, J., Sakata, S., Maeda, H., Miyagawa, Y., Ikarashi, M., Tamaki, H., Takeuchi, M., Nakatsu,

C.H., Kamagata, Y., 2013. Carbon dioxide concentration dictates alternative methanogenic pathways in oil reservoirs. Nat. Commun. 4, 1998. https://doi.org/10.1038/ncomms2998

McMahon, K.D., Zheng, D., Stams, A.J.M., Mackie, R.I., Raskin, L., 2004. Microbial population dynamics during start-up and overload conditions of anaerobic digesters treating municipal solid waste and sewage sludge. Biotechnol. Bioeng. 87, 823–834. https://doi.org/10.1002/bit.20192

McMurdie, P.J., Holmes, S., 2013. phyloseq: An R Package for Reproducible Interactive Analysis and Graphics of Microbiome Census Data. PLoS One 8, e61217. https://doi.org/10.1371/journal.pone.0061217

Merkel, W., Krauth, K., 1999. Mass transfer of carbon dioxide in anaerobic reactors under dynamic substrate loading conditions. Water Res. 33, 2011–2020. https://doi.org/10.1016/S0043-1354(98)00434-5

Merkle, W., Baer, K., Haag, N.L., Zielonka, S., Ortloff, F., Graf, F., Lemmer, A., 2017a. High-pressure anaerobic digestion up to 100 bar: influence of initial pressure on production kinetics and specific methane yields. Environ. Technol. 38, 337–344. https://doi.org/10.1080/09593330.2016.1192691

Merkle, W., Baer, K., Lindner, J., Zielonka, S., Ortloff, F., Graf, F., Kolb, T., Jungbluth, T., Lemmer, A., 2017b. Influence of pressures up to 50bar on two-stage anaerobic digestion. Bioresour. Technol. 232, 72–78. https://doi.org/10.1016/j.biortech.2017.02.013

Mikkelsen, M., Jørgensen, M., Krebs, F.C., 2010. The teraton challenge. A review of fixation and transformation of carbon dioxide. Energy Environ. Sci. 3, 43–81. https://doi.org/10.1039/b912904a

Millero, F.J., Feistel, R., Wright, D.G., McDougall, T.J., 2008. The composition of Standard Seawater and the definition of the Reference-Composition Salinity Scale. Deep. Res. Part I Oceanogr. Res. Pap. 55, 50–72. https://doi.org/10.1016/j.dsr.2007.10.001

Min, K., Khan, A., Kwon, M., Jung, Y., Yun, Z., Kiso, Y., 2005. Acidogenic fermentation of blended food-waste in combination with primary sludge for the production of volatile fatty acids. J. Chem. Technol. Biotechnol. 80, 909–915. https://doi.org/10.1002/jctb.1261

Mitchell, W.J., 2016. Sugar uptake by the solventogenic clostridia. World J. Microbiol. Biotechnol. 32, 1–10. https://doi.org/10.1007/s11274-015-1981-4

Miyazawa, T., Funazukuri, T., 2005. Polysaccharide Hydrolysis Accelerated by Adding Carbon Dioxide under Hydrothermal Conditions. Biotechnol. Prog. 21, 1782–1785. https://doi.org/10.1021/bp050214q

Molina-Höppner, A., Sato, T., Kato, C., Gänzle, M.G., Vogel, R.F., 2003. Effects of pressure on cell morphology and cell division of lactic acid bacteria. Extremophiles 7, 511–516. https://doi.org/10.1007/s00792-003-0349-0

Monot, F., Engasser, J.-M., Petitdemange, H., 1984. Influence of pH and undissociated butyric acid on the production of acetone and butanol in batch cultures of Clostridium acetobutylicum. Appl. Microbiol. Biotechnol. 19, 422–426.

Morild, E., 1981. The theory of pressure effects on enzymes. Adv. Protein Chem. 34, 93–166. https://doi.org/10.1016/S0065-3233(08)60519-7

Mösche, M., Jördening, H.J., 1999. Comparison of different models of substrate and product inhibition in anaerobic digestion. Water Res. 33, 2545–2554. https://doi.org/10.1016/S0043-1354(98)00490-4

Moscoviz, R., Trably, E., Bernet, N., 2016. Consistent 1,3-propanediol production from glycerol in mixed culture fermentation over a wide range of pH. Biotechnol. Biofuels 9, 32. https://doi.org/10.1186/s13068-016-0447-8

Mota, M.J., Lopes, R.P., Delgadillo, I., Saraiva, J.A., 2015. Probiotic yogurt production under high pressure and the possible use of pressure as an on/off switch to stop/start fermentation. Process Biochem. 50, 906–911. https://doi.org/10.1016/j.procbio.2015.03.016

Mota, M.J., Lopes, R.P., Delgadillo, I., Saraiva, J.A., 2013. Microorganisms under high pressure - Adaptation, growth and biotechnological potential. Biotechnol. Adv. 31, 1426–1434. https://doi.org/10.1016/j.biotechadv.2013.06.007

Mota, M.J., Lopes, R.P., Koubaa, M., Roohinejad, S., Barba, F.J., Delgadillo, I., Saraiva, J.A., 2017. Fermentation at non-conventional conditions in food- and bio-sciences by application of advanced processing technologies. Crit. Rev. Biotechnol. 38, 122–140. https://doi.org/10.1080/07388551.2017.1312272

Mota, M.J., Lopes, R.P., Simões, M.M.Q., Delgadillo, I., Saraiva, J.A., 2019. Effect of High Pressure on

Paracoccus denitrificans Growth and Polyhydroxyalkanoates Production from Glycerol. Appl. Biochem. Biotechnol. 188, 810–823. https://doi.org/10.1007/s12010-018-02949-0

Mota, M.J., Lopes, R.P., Sousa, S., Gomes, A.M., Lorenzo, J.M., Barba, F.J., Delgadillo, I., Saraiva, J.A., 2018. Utilization of glycerol during consecutive cycles of Lactobacillus reuteri fermentation under pressure: The impact on cell growth and fermentation profile. Process Biochem. 75, 39–48. https://doi.org/10.1016/j.procbio.2018.08.034

Müller, N., Worm, P., Schink, B., Stams, A.J.M., Plugge, C.M., 2010. Syntrophic butyrate and propionate oxidation processes: from genomes to reaction mechanisms. Environ. Microbiol. Rep. 2, 489–499. https://doi.org/10.1111/j.1758-2229.2010.00147.x

Muñoz Sierra, J.D., García Rea, V.S., Cerqueda-García, D., Spanjers, H., van Lier, J.B., 2020. Anaerobic Conversion of Saline Phenol-Containing Wastewater Under Thermophilic Conditions in a Membrane Bioreactor. Front. Bioeng. Biotechnol. 8, 1–12. https://doi.org/10.3389/fbioe.2020.565311

Muntau, M., Lebuhn, M., Polag, D., Bajón-Fernández, Y., Koch, K., 2021. Effects of CO2 enrichment on the anaerobic digestion of sewage sludge in continuously operated fermenters. Bioresour. Technol. 332. https://doi.org/10.1016/j.biortech.2021.125147

Nakasaki, K., Nguyen, K.K., Ballesteros, F.C., Maekawa, T., Koyama, M., 2020. Characterizing the microbial community involved in anaerobic digestion of lipid-rich wastewater to produce methane gas. Anaerobe 61, 102082. https://doi.org/10.1016/j.anaerobe.2019.102082

Narihiro, T., Nobu, M.K., Kim, N.K., Kamagata, Y., Liu, W.T., 2015. The nexus of syntrophy-associated microbiota in anaerobic digestion revealed by long-term enrichment and community survey. Environ. Microbiol. 17, 1707–1720. https://doi.org/10.1111/1462-2920.12616

Navarro, A., Montiel, C., Gracia-Fadrique, J., Tecante, A., Bárzana, E., 2021. Supercritical carbon dioxide "explosion" on blue agave bagasse to enhance enzymatic digestibility. Biomass Convers. Biorefinery. https://doi.org/10.1007/s13399-021-01557-z

Nedwell, D.B., Rutter, M., 1994. Influence of temperature on growth rate and competition between two psychrotolerant antarctic bacteria: Low temperature diminishes affinity for substrate uptake. Appl. Environ. Microbiol. 60, 1984–1992. https://doi.org/10.1128/aem.60.6.1984-1992.1994

Nevin, K.P., Woodard, T.L., Franks, A.E., Summers, Z.M., Lovley, D.R., Colwell, R.R., 2010. Microbial Electrosynthesis: Feeding Microbes Electricity To Convert Carbon Dioxide and Water to Multicarbon Extracellular Organic Compounds. MBio 1, e00103-10. https://doi.org/10.1128/mBio.00103-10

Nichols, C.M., Bowman, J.P., Guezennec, J., 2005. Effects of incubation temperature on growth and production of exopolysaccharides by an antarctic sea ice bacterium grown in batch culture. Appl. Environ. Microbiol. 71, 3519–3523. https://doi.org/10.1128/AEM.71.7.3519-3523.2005

Nobu, M.K., Narihiro, T., Mei, R., Kamagata, Y., Lee, P.K.H., Lee, P.H., McInerney, M.J., Liu, W.T., 2020. Catabolism and interactions of uncultured organisms shaped by eco-thermodynamics in methanogenic bioprocesses. Microbiome 8, 1–16. https://doi.org/10.1186/s40168-020-00885-y

Noppawan, P., Lanctôt, A.G., Magro, M., Navarro, P.G., Supanchaiyamat, N., Attard, T.M., Hunt, A.J., 2021. High pressure systems as sustainable extraction and pre-treatment technologies for a holistic corn stover biorefinery. BMC Chem. 15, 1–11. https://doi.org/10.1186/s13065-021-00762-1

Ntagia, E., Chatzigiannidou, I., Carvajal-Arroyo, J.M., Arends, J.B.A., Rabaey, K., 2021. Continuous H2/CO2 fermentation for acetic acid production under transient and continuous sulfide inhibition. Chemosphere 285, 131536. https://doi.org/10.1016/j.chemosphere.2021.131536

Oger, P.M., Daniel, I., Picard, A., 2010. In situ Raman and X-ray spectroscopies to monitor microbial activities under high hydrostatic pressure. Ann. N. Y. Acad. Sci. 1189, 113–120. https://doi.org/10.1111/j.1749-6632.2009.05176.x

Oger, P.M., Jebbar, M., 2010. The many ways of coping with pressure. Res. Microbiol. 161, 799–809. https://doi.org/10.1016/j.resmic.2010.09.017

Oksanen, J., Blanchet, F.G., Kindt, R., Legendre, P., Minchin, P.R., R.B., O., Simpson, G.L., Solymos, P., Stevens, M.H.H., Wagner, H., 2016. Vegan: Community ecology package. R package version 2.3-4.

Oppermann, B.I., Michaelis, W., Blumenberg, M., Frerichs, J., Schulz, H.M., Schippers, A., Beaubien, S.E., Krüger, M., 2010. Soil microbial community changes as a result of long-term exposure to a natural CO2

vent. Geochim. Cosmochim. Acta 74, 2697–2716. https://doi.org/10.1016/j.gca.2010.02.006

Oren, A., 2011. Thermodynamic limits to microbial life at high salt concentrations. Environ. Microbiol. 13, 1908–1923. https://doi.org/10.1111/j.1462-2920.2010.02365.x

OriginLab Corporation, 2019. OriginPro.

Oswald, F., Stoll, I.K., Zwick, M., Herbig, S., Sauer, J., Boukis, N., Neumann, A., 2018. Formic acid formation by Clostridium ljungdahlii at elevated pressures of carbon dioxide and hydrogen. Front. Bioeng. Biotechnol. 6, 6. https://doi.org/10.3389/fbioe.2018.00006

Pagaling, E., Strathdee, F., Spears, B.M., Cates, M.E., Allen, R.J., Free, A., 2014. Community history affects the predictability of microbial ecosystem development. ISME J. 8, 19–30. https://doi.org/10.1038/ismej.2013.150

Pagán, R., Mackey, B., 2000. Relationship between membrane damage and cell death in pressure-treated Escherichia coli cells: Differences between exponential- and stationary-phase cells and variation among strains. Appl. Environ. Microbiol. 66, 2829–2834. https://doi.org/10.1128/AEM.66.7.2829-2834.2000

Pan, X., Zhao, L., Li, C., Angelidaki, I., Lv, N., Ning, J., Cai, G., Zhu, G., 2021. Deep insights into the network of acetate metabolism in anaerobic digestion: focusing on syntrophic acetate oxidation and homoacetogenesis. Water Res. 190, 116774. https://doi.org/10.1016/j.watres.2020.116774

Parizzi, L.P., Grassi, M.C.B., Llerena, L.A., Carazzolle, M.F., Queiroz, V.L., Lunardi, I., Zeidler, A.F., Teixeira, P.J., Mieczkowski, P., Rincones, J., Pereira, G.A., 2012. The genome sequence of Propionibacterium acidipropionici provides insights into its biotechnological and industrial potential. BMC Genomics 13, 562. https://doi.org/10.1186/1471-2164-13-562

Park, C.B., Clark, D.S., 2002. Rupture of the cell envelope by decompression of the deep-sea methanogen Methanococcus jannaschii. Appl. Environ. Microbiol. 68, 1458–1463. https://doi.org/10.1128/AEM.68.3.1458-1463.2002

Park, C.Y., Ryu, Y.W., Kim, C., 2001. Kinetics and Rate of Enzymatic Hydrolysis of Cellulose in Supercritical Carbon Dioxide. Korean J. Chem. Eng. 18, 475–478. https://doi.org/10.1007/BF02698293

Park, S., Kwon, H.S., Lee, C.H., Ahn, I.S., 2020. Correlation between fixation of high-concentration CO2 and glutamate accumulation in Sulfurovum lithotrophicum 42BKTT. J. Ind. Eng. Chem. 92, 56–61. https://doi.org/10.1016/j.jiec.2020.08.015

Parkhurst, D.L., Appelo, C.A.J., 1999. USER'S GUIDE TO PHREEQC (VERSION 2).

Passos, F., Mota, C., Donoso-Bravo, A., Astals, S., Jeison, D., Muñoz, R., 2018. Biofuels from Microalgae: Biomethane. Green Energy Technol. 0, 247–270. https://doi.org/10.1007/978-3-319-69093-3_12

Patakova, P., Linhova, M., Rychtera, M., Paulova, L., Melzoch, K., 2013. Novel and neglected issues of acetone-butanol-ethanol (ABE) fermentation by clostridia: Clostridium metabolic diversity, tools for process mapping and continuous fermentation systems. Biotechnol. Adv. 31, 58–67. https://doi.org/10.1016/j.biotechadv.2012.01.010

Patil, S.A., Arends, J.B.A.A., Vanwonterghem, I., van Meerbergen, J., Guo, K., Tyson, G.W., Rabaey, K., 2015. Selective Enrichment Establishes a Stable Performing Community for Microbial Electrosynthesis of Acetate from CO2. Environ. Sci. Technol. 49, 8833–8843. https://doi.org/10.1021/es506149d

Patón, M., Rodríguez, J., 2019. A compilation and bioenergetic evaluation of syntrophic microbial growth yields in anaerobic digestion. Water Res. 159, 176–183. https://doi.org/10.1016/j.watres.2019.05.013

Patterson, M.F., Linton, M., 2008. Factors Affecting Inactivation of Food-Borne Bacteria by High Pressure, in: High-Pressure Microbiology. American Society of Microbiology, pp. 181–193. https://doi.org/10.1128/9781555815646.ch10

Pavlovic, M., Hörmann, S., Vogel, R.F., Ehrmann, M.A., 2008. Characterisation of a piezotolerant mutant of Lactobacillus sanfranciscensis. Zeitschrift fur Naturforsch. - Sect. B J. Chem. Sci. 63, 791–797. https://doi.org/10.1515/znb-2008-0630

Perez Calderon, L.J., Gontikaki, E., Potts, L.D., Shaw, S., Gallego, A., Anderson, J.A., Witte, U., 2019. Pressure and temperature effects on deep-sea hydrocarbon-degrading microbial communities in subarctic sediments. Microbiologyopen 8. https://doi.org/10.1002/mbo3.768

Petersen, S.P., Ahring, B.K., 1991. Acetate oxidation in a thermophilic anaerobic sewage-sludge digestor: the

importance of non-aceticlastic methanogenesis from acetate. FEMS Microbiol. Lett. 86, 149–158. https://doi.org/10.1111/j.1574-6968.1991.tb04804.x

Picard, A., Daniel, I., Montagnac, G., Oger, P., 2007. In situ monitoring by quantitative Raman spectroscopy of alcoholic fermentation by Saccharomyces cerevisiae under high pressure. Extremophiles 11, 445–452. https://doi.org/10.1007/s00792-006-0054-x

Pietrocola, F., Galluzzi, L., Bravo-San Pedro, J.M., Madeo, F., Kroemer, G., 2015. Acetyl coenzyme A: a central metabolite and second messenger. Cell Metab. 21, 805–21. https://doi.org/10.1016/j.cmet.2015.05.014

Pikuta, E. V., Hoover, R.B., 2014. The genus Trichococcus, in: Holzapfel, W.H., Wood, B.J.B. (Eds.), Lactic Acid Bacteria: Biodiversity and Taxonomy. John Wiley & Sons, Ltd., pp. 135–145. https://doi.org/10.1002/9781118655252.ch12

Portnoy, V.A., Bezdan, D., Zengler, K., 2011. Adaptive laboratory evolution-harnessing the power of biology for metabolic engineering. Curr. Opin. Biotechnol. 22, 590–594. https://doi.org/10.1016/j.copbio.2011.03.007

Posada, J. a., Naranjo, J.M., López, J. a., Higuita, J.C., Cardona, C. a., 2011. Design and analysis of poly-3-hydroxybutyrate production processes from crude glycerol. Process Biochem. 46, 310–317. https://doi.org/10.1016/j.procbio.2010.09.003

Post, W., Peng, T.-H., Emanuel, W.R., King, A.W., Dale, V.H., DeAngelis, D.L., 1990. The Global Carbon Cycle. Am. Sci. 78, 310–326. https://doi.org/10.1007/978-3-642-84608-3

Potier, P., Drevet, P., Gounot, A.M., Hipkiss, A.R., 1990. Temperature-dependent changes in proteolytic activities and protein composition in the psychotrophic bacterium Arthrobacter globiformis S155. J. Gen. Microbiol. 136, 283–291. https://doi.org/10.1099/00221287-136-2-283

Prieto-Calvo, M., Prieto, M., López, M., Alvarez-Ordóñez, A., 2014. Effects of high hydrostatic pressure on Escherichia coli ultrastructure, membrane integrity and molecular composition as assessed by ftir spectroscopy and microscopic imaging techniques. Molecules 19, 21310–21323. https://doi.org/10.3390/molecules191221310

Props, R., Kerckhof, F.M., Rubbens, P., Vrieze, J. De, Sanabria, E.H., Waegeman, W., Monsieurs, P., Hammes, F., Boon, N., 2017. Absolute quantification of microbial taxon abundances. ISME J. 11, 584–587. https://doi.org/10.1038/ismej.2016.117

Props, R., Monsieurs, P., Mysara, M., Clement, L., Boon, N., 2016. Measuring the biodiversity of microbial communities by flow cytometry. Methods Ecol. Evol. 7, 1376–1385. https://doi.org/10.1111/2041-210X.12607

Props, R., Rubbens, P., Besmer, M., Buysschaert, B., Sigrist, J., Weilenmann, H., Waegeman, W., Boon, N., Hammes, F., 2018. Detection of microbial disturbances in a drinking water microbial community through continuous acquisition and advanced analysis of flow cytometry data. Water Res. 145, 73–82. https://doi.org/10.1016/j.watres.2018.08.013

Puengrang, P., Suraraksa, B., Prommeenate, P., Boonapatcharoen, N., Cheevadhanarak, S., Tanticharoen, M., Kusonmano, K., 2020. Diverse microbial community profiles of propionate-degrading cultures derived from different sludge sources of anaerobic wastewater treatment plants. Microorganisms 8. https://doi.org/10.3390/microorganisms8020277

Puyol, D., Barry, E.M., Hülsen, T., Batstone, D.J., 2017a. A mechanistic model for anaerobic phototrophs in domestic wastewater applications: Photo-anaerobic model (PAnM). Water Res. 116, 241–253. https://doi.org/10.1016/j.watres.2017.03.022

Puyol, D., Batstone, D.J., Hülsen, T., Astals, S., Peces, M., Krömer, J.O., 2017b. Resource Recovery from Wastewater by Biological Technologies: Opportunities, Challenges, and Prospects. Front. Microbiol. 7, 2106. https://doi.org/10.3389/fmicb.2016.02106

Qiao, W., Takayanagi, K., Li, Q., Shofie, M., Gao, F., Dong, R., Li, Y.-Y., 2016. Thermodynamically enhancing propionic acid degradation by using sulfate as an external electron acceptor in a thermophilic anaerobic membrane reactor. Water Res. 106, 320–329. https://doi.org/10.1016/j.watres.2016.10.013

Quast, C., Pruesse, E., Yilmaz, P., Gerken, J., Schweer, T., Yarza, P., Peplies, J., Glöckner, F.O., 2012. The SILVA ribosomal RNA gene database project: improved data processing and web-based tools. Nucleic Acids Res. 41, D590–D596. https://doi.org/10.1093/nar/gks1219

R Core Team 2019, 2019. R: A language and environment for statistical computing.

Rabaey, K., Rozendal, R.A., 2010. Microbial electrosynthesis - Revisiting the electrical route for microbial production. Nat. Rev. Microbiol. 8, 706–716. https://doi.org/10.1038/nrmicro2422

Ragsdale, S.W., Pierce, E., 2008. Acetogenesis and the Wood-Ljungdahl pathway of CO2 fixation. Biochim. Biophys. Acta - Proteins Proteomics 1784, 1873–1898. https://doi.org/10.1016/j.bbapap.2008.08.012

Ramió-Pujol, S., Ganigué, R., Bañeras, L., Colprim, J., 2015. Impact of formate on the growth and productivity of Clostridium ljungdahlii PETC and Clostridium carboxidivorans P7 grown on syngas. Int. Microbiol. 17, 195–204. https://doi.org/10.2436/20.1501.01.222

Regueiro, L., Veiga, P., Figueroa, M., Alonso-Gutierrez, J., Stams, A.J.M., Lema, J.M., Carballa, M., 2012. Relationship between microbial activity and microbial community structure in six full-scale anaerobic digesters. Microbiol. Res. 167, 581–589. https://doi.org/10.1016/j.micres.2012.06.002

Richter, H., Molitor, B., Wei, H., Chen, W., Aristilde, L., Angenent, L.T., 2016. Ethanol production in syngas-fermenting: Clostridium ljungdahlii is controlled by thermodynamics rather than by enzyme expression. Energy Environ. Sci. 9, 2392–2399. https://doi.org/10.1039/c6ee01108j

Rillig, M.C., Rolff, J., Tietjen, B., Wehner, J., Andrade-Linares, D.R., 2015. Community priming-Effects of sequential stressors on microbial assemblages. FEMS Microbiol. Ecol. 91, 1–7. https://doi.org/10.1093/femsec/fiv040

Rittmann, S., Seifert, A., Herwig, C., 2015. Essential prerequisites for successful bioprocess development of biological CH4 production from CO2 and H2. Crit. Rev. Biotechnol. 35, 141–151. https://doi.org/10.3109/07388551.2013.820685

Rodríguez, J., Kleerebezem, R., Lema, J.M., van Loosdrecht, M.C.M.M., 2006. Modeling product formation in anaerobic mixed culture fermentations. Biotechnol. Bioeng. 93, 592–606. https://doi.org/10.1002/bit.20765

Roger, M., Brown, F., Gabrielli, W., Sargent, F., 2018. Efficient Hydrogen-Dependent Carbon Dioxide Reduction by Escherichia coli. Curr. Biol. 28, 140-145.e2. https://doi.org/10.1016/j.cub.2017.11.050

Rognes, T., Flouri, T., Nichols, B., Quince, C., Mahé, F., 2016. VSEARCH: A versatile open source tool for metagenomics. PeerJ 2016, e2584. https://doi.org/10.7717/peerj.2584

Rombouts, J.L., Kranendonk, E.M.M., Regueira, A., Weissbrodt, D.G., Kleerebezem, R., van Loosdrecht, M.C.M., 2020. Selecting for lactic acid producing and utilising bacteria in anaerobic enrichment cultures. Biotechnol. Bioeng. 117, 1281–1293. https://doi.org/10.1002/bit.27301

Rotaru, A.E., Shrestha, P.M., Liu, F., Shrestha, M., Shrestha, D., Embree, M., Zengler, K., Wardman, C., Nevin, K.P., Lovley, D.R., 2014. A new model for electron flow during anaerobic digestion: Direct interspecies electron transfer to Methanosaeta for the reduction of carbon dioxide to methane. Energy Environ. Sci. 7, 408–415. https://doi.org/10.1039/c3ee42189a

Rotunno, P., Lanzini, A., Leone, P., 2017. Energy and economic analysis of a water scrubbing based biogas upgrading process for biomethane injection into the gas grid or use as transportation fuel. Renew. Energy 102, 417–432. https://doi.org/10.1016/j.renene.2016.10.062

Rouviere, P.E., Wolfe, R.S., 1988. Novel biochemistry of methanogenesis. J. Biol. Chem. 263, 7913–7916. https://doi.org/10.1016/s0021-9258(18)68417-0

Saint-Amans, S., Girbal, L., Andrade, J., Ahrens, K., Soucaille, P., 2001. Regulation of Carbon and Electron Flow in Clostridium butyricum VPI 3266 Grown on Glucose-Glycerol Mixtures. J. Bacteriol. 183, 1748–1754. https://doi.org/10.1128/JB.183.5.1748

Salek, S.S., van Turnhout, A.G., Kleerebezem, R., van Loosdrecht, M.C.M., Turnhout, A.G. van, Kleerebezem, R., Loosdrecht, M.C.M. van, van Turnhout, A.G., Kleerebezem, R., van Loosdrecht, M.C.M., 2015. pH control in biological systems using calcium carbonate. Biotechnol. Bioeng. 112, 905–913. https://doi.org/10.1002/bit.25506

Sander, R., 2015. Compilation of Henry's law constants (version 4.0) for water as solvent. Atmos. Chem. Phys. 15, 4399–4981. https://doi.org/10.5194/acp-15-4399-2015

Sandoval-Espinola, W.J., Chinn, M.S., Thon, M.R., Bruno-Bárcena, J.M., 2017. Evidence of mixotrophic carbon-capture by n-butanol-producer Clostridium beijerinckii. Sci. Rep. 7, 1–13. https://doi.org/10.1038/s41598-017-12962-8

Sarvenoei, F.F., Zinatizadeh, A.A., Zangeneh, H., 2018. A novel technique for waste sludge solubilization using a combined magnetic field and CO2 injection as a pretreatment prior anaerobic digestion. J. Clean. Prod.

172, 2182–2194. https://doi.org/10.1016/j.jclepro.2017.11.195

Sauer, P., Glombitza, C., Kallmeyer, J., Teske, A., Bartlett, D., 2012. A system for incubations at high gas partial pressure. https://doi.org/10.3389/fmicb.2012.00025

Sauer, U., Eikmanns, B.J., 2005. The PEP-pyruvate-oxaloacetate node as the switch point for carbon flux distribution in bacteria. FEMS Microbiol. Rev. 29, 765–794. https://doi.org/10.1016/j.femsre.2004.11.002

Sawers, R.G., Clark, D.P., 2004. Fermentative Pyruvate and Acetyl-Coenzyme A Metabolism. EcoSal Plus 1. https://doi.org/10.1128/ecosalplus.3.5.3

Schauer-Gimenez, A.E., Zitomer, D.H., Maki, J.S., Struble, C.A., 2010. Bioaugmentation for improved recovery of anaerobic digesters after toxicant exposure. Water Res. 44, 3555–3564. https://doi.org/10.1016/j.watres.2010.03.037

Scheyhing, C.H., Hörmann, S., Ehrmann, M.A., Vogel, R.F., 2004. Barotolerance is inducible by preincubation under hydrostatic pressure cold-, osmotic- and acid-stress conditions in Lactobacillus sanfranciscensis DSM 20451T. Lett. Appl. Microbiol. 39, 284–289. https://doi.org/10.1111/j.1472-765X.2004.01578.x

Schink, B., 1997. Energetics of syntrophic cooperation in methanogenic degradation. Microbiol. Mol. Biol. Rev. 61, 262–280. https://doi.org/1092-2172/97/$04.0010

Schink, B., 1984. Fermentation of tartrate enantiomers by anaerobic bacteria, and description of two new species of strict anaerobes, Ruminococcus pasteurii and Ilyobacter tartaricus. Arch. Microbiol. 139, 409–414. https://doi.org/10.1007/BF00408388

Schlesinger, W.H., 2005. The Global Carbon Cycle and Climate Change. Adv. Econ. Environ. Resour. 5, 31–53. https://doi.org/10.1016/S1569-3740(05)05002-9

Schloss, P.D., Westcott, S.L., Ryabin, T., Hall, J.R., Hartmann, M., Hollister, E.B., Lesniewski, R.A., Oakley, B.B., Parks, D.H., Robinson, C.J., Sahl, J.W., Stres, B., Thallinger, G.G., Van Horn, D.J., Weber, C.F., 2009. Introducing mothur: Open-source, platform-independent, community-supported software for describing and comparing microbial communities. Appl. Environ. Microbiol. 75, 7537–7541. https://doi.org/10.1128/AEM.01541-09

Schweitzer, H., Aalto, N.J., Busch, W., Chat Chan, D.T., Chiesa, M., Elvevoll, E.O., Gerlach, R., Krause, K., Mocaer, K., Moran, J.J., Noel, J.P., Patil, S.K., Schwab, Y., Wijffels, R.H., Wulff, A., Øvreås, L., Bernstein, H.C., 2021. Innovating carbon-capture biotechnologies through ecosystem-inspired solutions. One Earth 4, 49–59. https://doi.org/10.1016/j.oneear.2020.12.006

Scoma, A., Boon, N., 2016. Osmotic Stress Confers Enhanced Cell Integrity to Hydrostatic Pressure but Impairs Growth in Alcanivorax borkumensis SK2. Front. Microbiol. 7. https://doi.org/10.3389/fmicb.2016.00729

Scoma, A., Coma, M., Kerckhof, F.M., Boon, N., Rabaey, K., 2017. Efficient molasses fermentation under high salinity by inocula of marine and terrestrial origin. Biotechnol. Biofuels 10. https://doi.org/10.1186/s13068-017-0701-8

Scoma, A., Garrido-Amador, P., Nielsen, S.D., Røy, H., Kjeldsen, K.U., 2019. The Polyextremophilic Bacterium Clostridium paradoxum Attains Piezophilic Traits by Modulating Its Energy Metabolism and Cell Membrane Composition. Appl. Environ. Microbiol. 85. https://doi.org/10.1128/AEM.00802-19

Seghezzo, L., Zeeman, G., Van Lier, J.B., Hamelers, H.V.M., Lettinga, G., 1998. A review: The anaerobic treatment of sewage in UASB and EGSB reactors. Bioresour. Technol. 65, 175–190. https://doi.org/10.1016/S0960-8524(98)00046-7

Sewell, H.L., Kaster, A.-K., Sporman, A.M., 2017. Homoacetogenesis in Deep-Sea Chloroflexi, as Inferred by Single-Cell Genomics, Provides a Link to Reductive Dehalogenation in Terrestrial Dehalococcoidetes. MBio.

Shade, A., Peter, H., Allison, S.D., Baho, D.L., Berga, M., Bürgmann, H., Huber, D.H., Langenheder, S., Lennon, J.T., Martiny, J.B.H., Matulich, K.L., Schmidt, T.M., Handelsman, J., 2012. Fundamentals of Microbial Community Resistance and Resilience. Front. Microbiol. 3. https://doi.org/10.3389/fmicb.2012.00417

Shi, J., Jiang, Y., Jiang, Z., Wang, Xueyan, Wang, Xiaoli, Zhang, S., Han, P., Yang, C., 2015. Enzymatic conversion of carbon dioxide. Chem. Soc. Rev. 44, 5981–6000. https://doi.org/10.1039/c5cs00182j

Šibanc, N., Dumbrell, A.J., Mandić-Mulec, I., Maček, I., 2014. Impacts of naturally elevated soil CO2 concentrations on communities of soil archaea and bacteria. Soil Biol. Biochem. 68, 348–356. https://doi.org/10.1016/j.soilbio.2013.10.018

Siliakus, M.F., van der Oost, J., Kengen, S.W.M., 2017. Adaptations of archaeal and bacterial membranes to variations in temperature, pH and pressure. Extremophiles 21, 651–670. https://doi.org/10.1007/s00792-017-0939-x

Sivalingam, V., Dinamarca, C., 2021. High pressure moving bed biofilm reactor for syngas fermentation. Chem. Eng. Trans. 86, 1483–1488. https://doi.org/10.3303/CET2186248

Sivalingam, V., Haugen, T., Wentzel, A., Dinamarca, C., 2021. Effect of Elevated Eydrogen Partial Pressure on Mixed Culture Homoacetogenesis. Chem. Eng. Sci. X 12, 100118. https://doi.org/10.1016/j.cesx.2021.100118

Slonczewski, J.L., Fujisawa, M., Dopson, M., Krulwich, T.A., 2009. Cytoplasmic pH Measurement and Homeostasis in Bacteria and Archaea. Adv. Microb. Physiol. 55, 1-79,317. https://doi.org/10.1016/S0065-2911(09)05501-5

Somero, G.N., 1990. Life at low volume change: Hydrostatic pressure as a selective factor in the aquatic environment. Integr. Comp. Biol. 30, 123–135. https://doi.org/10.1093/icb/30.1.123

Song, H., Lee, J.W., Choi, S., You, J.K., Hong, W.H., Lee, S.Y., 2007. Effects of dissolved CO2 levels on the growth of Mannheimia succiniciproducens and succinic acid production. Biotechnol. Bioeng. 98, 1296–1304. https://doi.org/10.1002/bit.21530

Spanoghe, J., Vermeir, P., Vlaeminck, S.E., 2021. Microbial food from light, carbon dioxide and hydrogen gas: Kinetic, stoichiometric and nutritional potential of three purple bacteria. Bioresour. Technol. 337, 125364. https://doi.org/10.1016/j.biortech.2021.125364

Spilimbergo, S., Bertucco, A., 2003. Non-Thermal Bacteria Inactivation with Dense CO2. Biotechnol. Bioeng. 84, 627–638. https://doi.org/10.1002/bit.10783

Spirito, C.M., Richter, H., Stams, A.J., Angenent, L.T., 2014. Chain elongation in anaerobic reactor microbiomes to recover resources from waste. Curr. Opin. Biotechnol. 27, 115–122. https://doi.org/10.1016/j.copbio.2014.01.003

Stamatopoulou, P., Malkowski, J., Conrado, L., Brown, K., Scarborough, M., 2020. Fermentation of organic residues to beneficial chemicals: A review of medium-chain fatty acid production. Processes 8, 1–25. https://doi.org/10.3390/pr8121571

Stams, A.J.M., Dijkema, C., Plugge, C.M., Lens, P., 1998. Contribution of 13C-NMR spectroscopy to the elucidation of pathways of propionate formation and degradation in methanogenic environments. Biodegradation 9, 463–473. https://doi.org/10.1023/A:1008342130938

Stams, A.J.M., Plugge, C.M., 2009. Electron transfer in syntrophic communities of anaerobic bacteria and archaea. Nat. Rev. Microbiol. 7, 568–577. https://doi.org/10.1038/nrmicro2166

Stoll, K.I., Herbig, S., Zwick, M., Boukis, N., Sauer, J., Neumann, A., Oswald, F., 2018. Fermentation of H2 and CO2 with Clostridium ljungdahlii at Elevated Process Pressure-First Experimental Results, in: CHEMICAL ENGINEERING TRANSACTIONS. https://doi.org/10.3303/CET1864026

Storck, T., Virdis, B., Batstone, D.J., 2016. Modelling extracellular limitations for mediated versus direct interspecies electron transfer. ISME J. 10, 621–631. https://doi.org/10.1038/ismej.2015.139

Stumm, W., Morgan, J.J., 1996. Aquatic chemistry: chemical equilibria and rates in natural waters, Third edit. ed, Environmental science and technology. John Wiley & Sons, Inc, New York Chichester Brisbane Toronto SIngapore.

Sun, L., Fukamachi, T., Saito, H., Kobayashi, H., 2005. Carbon dioxide increases acid resistance in Escherichia coli. Lett. Appl. Microbiol. 40, 397–400. https://doi.org/10.1111/j.1472-765X.2005.01714.x

Tamburini, C., Boutrif, M., Garel, M., Colwell, R.R., Deming, J.W., 2013. Prokaryotic responses to hydrostatic pressure in the ocean - a review. Environ. Microbiol. 15, 1262–1274. https://doi.org/10.1111/1462-2920.12084

Tamburini, C., Garel, M., Al Ali, B., Mérigot, B., Kriwy, P., Charrière, B., Budillon, G., 2009a. Distribution and activity of Bacteria and Archaea in the different water masses of the Tyrrhenian Sea. Deep. Res. Part II Top. Stud. Oceanogr. 56, 700–712. https://doi.org/10.1016/j.dsr2.2008.07.021

Tamburini, C., Goutx, M., Guigue, C., Garel, M., Lefèvre, D., Charrière, B., Sempéré, R., Pepa, S., Peterson, M.L., Wakeham, S., Lee, C., 2009b. Effects of hydrostatic pressure on microbial alteration of sinking fecal pellets. Deep. Res. Part II Top. Stud. Oceanogr. 56, 1533–1546. https://doi.org/10.1016/j.dsr2.2008.12.035

Tamis, J., Joosse, B.M.M., van Loosdrecht, M.C.M., Kleerebezem, R., Loosdrecht, M.C.M. va., Kleerebezem, R., 2015. High-rate volatile fatty acid (VFA) production by a granular sludge process at low pH. Biotechnol. Bioeng. 112, 2248–2255. https://doi.org/10.1002/bit.25640

Tan, Z., Zhu, X., Chen, J., Li, Q., Zhanga, X., 2013. Activating phosphoenolpyruvate carboxylase and phosphoenolpyruvate carboxykinase in combination for improvement of succinate production. Appl. Environ. Microbiol. 79, 4838–4844. https://doi.org/10.1128/AEM.00826-13

Tapia-Venegas, E., Cabrol, L., Brandhoff, B., Hamelin, J., Trably, E., Steyer, J.P., Ruiz-Filippi, G., 2015. Adaptation of acidogenic sludge to increasing glycerol concentrations for biohydrogen production. Appl. Microbiol. Biotechnol. 99, 8295–8308. https://doi.org/10.1007/s00253-015-6832-6

Temudo, M.F., Kleerebezem, R., van Loosdrecht, M., 2007. Influence of the pH on (open) mixed culture fermentation of glucose: A chemostat study. Biotechnol. Bioeng. 98, 69–79. https://doi.org/10.1002/bit.21412

Thauer, R.K., 2012. The Wolfe cycle comes full circle. Proc. Natl. Acad. Sci. U. S. A. 109, 15084–15085. https://doi.org/10.1073/pnas.1213193109

Thauer, R.K., Jungermann, K., Decker, K., 1977. Energy conservation in chemotrophic anaerobic bacteria. Bacteriol. Rev. 41, 100–180. https://doi.org/10.1128/br.41.1.100-180.1977

Tholosan, O., Garcin, J., Bianchi, A., 1999. Effects of hydrostatic pressure on microbial activity through a 2000 m deep water column in the NW Mediterranean Sea. Mar. Ecol. Prog. Ser. 183, 49–57.

Tijhuis, L., Van Loosdrecht, M.C.M., Heijnen, J.J., 1993. A thermodynamically based correlation for maintenance gibbs energy requirements in aerobic and anaerobic chemotrophic growth. Biotechnol. Bioeng. 42, 509–519. https://doi.org/10.1002/bit.260420415

Tonanzi, B., Gallipoli, A., Gianico, A., Montecchio, D., Pagliaccia, P., Di Carlo, M., Rossetti, S., Braguglia, C.M., 2018. Long-term anaerobic digestion of food waste at semi-pilot scale: Relationship between microbial community structure and process performances. Biomass and Bioenergy 118, 55–64. https://doi.org/10.1016/j.biombioe.2018.08.001

Town, J.R., Dumonceaux, T.J., 2016. Laboratory-scale bioaugmentation relieves acetate accumulation and stimulates methane production in stalled anaerobic digesters. Appl. Microbiol. Biotechnol. 100, 1009–1017. https://doi.org/10.1007/s00253-015-7058-3

Treu, L., Campanaro, S., Kougias, P.G., Sartori, C., Bassani, I., Angelidaki, I., 2018. Hydrogen-fueled microbial pathways in biogas upgrading systems revealed by genome-centric metagenomics. Front. Microbiol. 9, 1–16. https://doi.org/10.3389/fmicb.2018.01079

Tsapekos, P., Alvarado-Morales, M., Angelidaki, I., 2022. H2 competition between homoacetogenic bacteria and methanogenic archaea during biomethanation from a combined experimental-modelling approach. J. Environ. Chem. Eng. 10, 107281. https://doi.org/10.1016/j.jece.2022.107281

Ullrich, T., Lindner, J., Bär, K., Mörs, F., Graf, F., Lemmer, A., 2018. Influence of operating pressure on the biological hydrogen methanation in trickle-bed reactors. Bioresour. Technol. 247, 7–13. https://doi.org/10.1016/j.biortech.2017.09.069

Valdemarsen, T., Kristensen, E., 2010. Degradation of dissolved organic monomers and short-chain fatty acids in sandy marine sediment by fermentation and sulfate reduction. Geochim. Cosmochim. Acta 74, 1593–1605. https://doi.org/10.1016/j.gca.2009.12.009

van Bodegom, P., 2007. Microbial Maintenance: A Critical Review on Its Quantification. Microb. Ecol. 53, 513–523. https://doi.org/10.1007/s00248-006-9049-5

van de Velde, S., Lesven, L., Burdorf, L.D.W., Hidalgo-Martinez, S., Geelhoed, J.S., Van Rijswijk, P., Gao, Y., Meysman, F.J.R., 2016. The impact of electrogenic sulfur oxidation on the biogeochemistry of coastal sediments: A field study. Geochim. Cosmochim. Acta 194, 211–232. https://doi.org/10.1016/j.gca.2016.08.038

Van De Vossenberg, J.L.C.M., Driessen, A.J.M., Konings, W.N., 2000. Adaptations of the Cell Membrane for Life in Extreme Environments, in: Environmental Stressors and Gene Responses. pp. 71–88.

Van Der Werf, M.J., Guettler, M. V, Jain, M.K., Zeikus, J.G., 1997. Environmental and physiological factors affecting the succinate product ratio during carbohydrate fermentation by Actinobacillus sp. 130Z. Arc 332–342.

Van Eerten-Jansen, M.C.A.A., Heijne, A. Ter, Buisman, C.J.N., Hamelers, H.V.M., 2012. Microbial electrolysis cells for production of methane from CO2: long-term performance and perspectives. Int. J. Energy Res. 36, 809–819. https://doi.org/https://doi.org/10.1002/er.1954

van Gelder, A.H., Sousa, D.Z., Rijpstra, W.I.C., Sinninghe Damsté, J.S., Stams, A.J.M., Sánchez-Andrea, I., 2014. Ercella succinigenes gen. nov., sp. nov., an anaerobic succinate-producing bacterium. Int. J. Syst. Evol. Microbiol. 64, 2449–2454. https://doi.org/10.1099/ijs.0.058966-0

Van Ginkel, S., Logan, B.E., 2005. Inhibition of Biohydrogen Production by Undissociated Acetic and Butyric Acids. Environ. Sci. Technol. 39, 9351–9356.

Van Hecke, W., Bockrath, R., De Wever, H., 2019. Effects of moderately elevated pressure on gas fermentation processes. Bioresour. Technol. 293, 122129. https://doi.org/10.1016/j.biortech.2019.122129

Van Landuyt, J., Cimmino, L., Dumolin, C., Chatzigiannidou, I., Taveirne, F., Mattelin, V., Zhang, Y., Vandamme, P., Scoma, A., Williamson, A., Boon, N., 2020. Microbial enrichment, functional characterization and isolation from a cold seep yield piezotolerant obligate hydrocarbon degraders. FEMS Microbiol. Ecol. 96, 1–15. https://doi.org/10.1093/femsec/fiaa097

Van Lier, J.B., Grolle, K.C., Frijters, C.T., Stams, A.J., Lettinga, G., 1993. Effects of acetate, propionate, and butyrate on the thermophilic anaerobic degradation of propionate by methanogenic sludge and defined cultures. Appl. Environ. Microbiol. 59, 1003–11.

van Lier, J.B., Mahmoud, N., Zeeman, G., 2020. Anaerobic wastewater treatment, in: Chen, G., Ekama, G.A., van Loosdrecht, M.C.M., Brdjanovic, D. (Eds.), Biological Wastewater Treatment: Principles, Modeling and Design. IWA Publishing, pp. 701–756. https://doi.org/10.2166/9781789060362

Van Lier, J.B., Mahmoud, N., Zeeman, G., 2008. Anaerobic Wastewater Treatment, in: Biological Wastewater Treatment : Principles, Modelling and Design. pp. 401–442. https://doi.org/10.1021/es00154a002

van Lingen, H.J., Plugge, C.M., Fadel, J.G., Kebreab, E., Bannink, A., Dijkstra, J., 2016. Thermodynamic Driving Force of Hydrogen on Rumen Microbial Metabolism: A Theoretical Investigation. PLoS One 11, e0161362. https://doi.org/10.1371/journal.pone.0161362

Van Walsum, G.P., Shi, H., 2004. Carbonic acid enhancement of hydrolysis in aqueous pretreatment of corn stover. Bioresour. Technol. 93, 217–226. https://doi.org/10.1016/j.biortech.2003.11.009

Vanlint, D., Mitchell, R., Bailey, E., Meersman, F., McMillan, P.F., Michiels, C.W., Aertsen, A., 2011. Rapid acquisition of gigapascal-high-pressure resistance by Escherichia coli. MBio 2, 1–3. https://doi.org/10.1128/mBio.00130-10

Vanwonterghem, I., Jensen, P.D., Ho, D.P., Batstone, D.J., Tyson, G.W., 2014. Linking microbial community structure, interactions and function in anaerobic digesters using new molecular techniques. Curr. Opin. Biotechnol. 27, 55–64. https://doi.org/10.1016/j.copbio.2013.11.004

Vasconcelos, I., Girbal, L., Soucaille, P., 1994. Regulation of carbon and electron flow in Clostridium acetobutylicum grown in chemostat culture at neutral pH on mixtures of glucose and glycerol. J. Bacteriol. 176, 1443–1450. https://doi.org/10.1128/jb.176.5.1443-1450.1994

Voolapalli, R.K., Stuckey, D.C., 1999. Relative importance of trophic group concentrations during anaerobic degradation of volatile fatty acids. Appl. Environ. Microbiol. 65, 5009–5016. https://doi.org/10.1128/aem.65.11.5009-5016.1999

Vossmeyer, A., Deusner, C., Kato, C., Inagaki, F., Ferdelman, T.G., 2012. Substrate-specific pressure-dependence of microbial sulfate reduction in deep-sea cold seep sediments of the Japan Trench. Front. Microbiol. 3, 1–12. https://doi.org/10.3389/fmicb.2012.00253

Wainaina, S., Lukitawesa, Kumar Awasthi, M., Taherzadeh, M.J., 2019. Bioengineering of anaerobic digestion for volatile fatty acids, hydrogen or methane production: A critical review. Bioengineered 10, 437–458. https://doi.org/10.1080/21655979.2019.1673937

Wan, R., Chen, Y., Zheng, X., Su, Y., Huang, H., 2018. Effect of CO2on NADH production of denitrifying microbes via inhibiting carbon source transport and its metabolism. Sci. Total Environ. 627, 896–904. https://doi.org/10.1016/j.scitotenv.2018.01.315

Wan, R., Chen, Y., Zheng, X., Su, Y., Li, M., 2016. Effect of CO2 on Microbial Denitrification via Inhibiting Electron Transport and Consumption. Environ. Sci. Technol. 50, 9915–9922. https://doi.org/10.1021/acs.est.5b05850

Wang, Chen, Wang, Caiqin, Liu, J., Han, Z., Xu, Q., Xu, X., Zhu, L., 2020. Role of magnetite in methanogenic degradation of different substances. Bioresour. Technol. 314, 123720. https://doi.org/10.1016/j.biortech.2020.123720

Wang, G., Post, W.M., 2012. A theoretical reassessment of microbial maintenance and implications for microbial ecology modeling. FEMS Microbiol. Ecol. 81, 610–617. https://doi.org/10.1111/j.1574-6941.2012.01389.x

Wang, J., Li, J., Dasgupta, S., Zhang, L., Golovko, M.Y., Golovko, S.A., Fang, J., 2014. Alterations in membrane phospholipid fatty acids of gram-positive piezotolerant bacterium sporosarcina sp. DSK25 in response to growth pressure. Lipids 49, 347–356. https://doi.org/10.1007/s11745-014-3878-7

Wang, Q., Garrity, G.M., Tiedje, J.M., Cole, J.R., 2007. Naive Bayesian Classifier for Rapid Assignment of rRNA Sequences into the New Bacterial Taxonomy. Appl. Environ. Microbiol. 73, 5261–5267. https://doi.org/10.1128/AEM.00062-07

Wang, S., Hou, X., Su, H., 2017. Exploration of the relationship between biogas production and microbial community under high salinity conditions. Sci. Rep. 7, 1–10. https://doi.org/10.1038/s41598-017-01298-y

Wang, X.N., Sun, G.X., Zhu, Y.G., 2017. Thermodynamic energy of anaerobic microbial redox reactions couples elemental biogeochemical cycles. J. Soils Sediments 17, 2831–2846. https://doi.org/10.1007/s11368-017-1767-4

Wannicke, N., Frindte, K., Gust, G., Liskow, I., Wacker, A., Meyer, A., Grossart, H.-P., 2015. Measuring bacterial activity and community composition at high hydrostatic pressure using a novel experimental approach: a pilot study. FEMS Microbiol. Ecol. 91. https://doi.org/10.1093/femsec/fiv036

Watanabe, T., Furukawa, S., Kawarai, T., Wachi, M., Ogihara, H., Yamasaki, M., 2007. Cytoplasmic Acidification May Occur in High- Pressure Carbon Dioxide-Treated Escherichia coli. Biosci. Biotechnol. Biochem. ISSN 71, 2522–2526. https://doi.org/10.1271/bbb.70313

Wei, T., Simko, V., 2017. R package "corrplot": Visualization of a Correlation Matrix (Version 0.84) [WWW Document]. URL https://github.com/taiyun/corrplot

Weiland, P., 2010. Biogas production: Current state and perspectives. Appl. Microbiol. Biotechnol. 85, 849–860. https://doi.org/10.1007/s00253-009-2246-7

Wemekamp-Kamphuis, H.H., Karatzas, A.K., Wouters, J. a, Abee, T., 2002. Enhanced Levels of Cold Shock Proteins in Listeria monocytogenes LO28 upon Exposure to Low Temperature and High Hydrostatic Pressure. Appl. Environ. Microbiol. 68, 456–463. https://doi.org/10.1128/AEM.68.2.456

Werner, J.J., Knights, D., Garcia, M.L., Scalfone, N.B., Smith, S., Yarasheski, K., Cummings, T.A., Beers, A.R., Knight, R., Angenent, L.T., 2011. Bacterial community structures are unique and resilient in full-scale bioenergy systems. Proc. Natl. Acad. Sci. U. S. A. 108, 4158–4163. https://doi.org/10.1073/pnas.1015676108

Westcott, S.L., Schloss, P.D., 2017. OptiClust, an Improved Method for Assigning Amplicon-Based Sequence Data to Operational Taxonomic Units. mSphere 2. https://doi.org/10.1128/mspheredirect.00073-17

Weston, N.B., Joye, S.B., 2005. Temperature-driven decoupling of key phases of organic matter degradation in marine sediments. Proc. Natl. Acad. Sci. 102, 17036–17040.

Winter, R., Jeworrek, C., 2009. Effect of pressure on membranes. Soft Matter 5, 3157–3173. https://doi.org/10.1039/b901690b

Worm, P., Koehorst, J.J., Visser, M., Sedano-Núñez, V.T., Schaap, P.J., Plugge, C.M., Sousa, D.Z., Stams, A.J.M.M., 2014. A genomic view on syntrophic versus non-syntrophic lifestyle in anaerobic fatty acid degrading communities. Biochim. Biophys. Acta - Bioenerg. 1837, 2004–2016. https://doi.org/10.1016/j.bbabio.2014.06.005

Wu, D., Li, L., Zhen, F., Liu, H., Xiao, F., Sun, Y., Peng, X., Li, Y., Wang, X., 2022. Thermodynamics of volatile fatty acid degradation during anaerobic digestion under organic overload stress: The potential to better identify process stability. Water Res. 214. https://doi.org/10.1016/j.watres.2022.118187

Wu, H., Dalke, R., Mai, J., Holtzapple, M., Urgun-Demirtas, M., 2021. Arrested methanogenesis digestion of high-strength cheese whey and brewery wastewater with carboxylic acid production. Bioresour. Technol. 332, 125044. https://doi.org/10.1016/j.biortech.2021.125044

Wu, Y., Ge, S., Xia, C., Cai, L., Mei, C., Sonne, C., Park, Y.K., Kim, Y.M., Chen, W.H., Chang, J.S., Lam, S.S., 2020. Using low carbon footprint high-pressure carbon dioxide in bioconversion of aspen branch waste for

sustainable bioethanol production. Bioresour. Technol. 313, 123675. https://doi.org/10.1016/j.biortech.2020.123675

Wu, Y., Yao, S.-J., Guan, Y.-X., 2007. Inactivation of Microorganisms in Carbon Dioxide at Elevated Pressure and Ambient Temperature. Ind. Eng. Chem. Res. 46, 6345–6352. https://doi.org/10.1021/ie0702330

Xafenias, N., Anunobi, M.S.O., Mapelli, V., 2015. Electrochemical startup increases 1,3-propanediol titers in mixed-culture glycerol fermentations. Process Biochem. 50, 1499–1508. https://doi.org/10.1016/j.procbio.2015.06.020

Xia, Y., Wang, Yubo, Wang, Yi, Chin, F.Y.L., Zhang, T., 2016. Cellular adhesiveness and cellulolytic capacity in Anaerolineae revealed by omics-based genome interpretation. Biotechnol. Biofuels 9, 1–13. https://doi.org/10.1186/s13068-016-0524-z

Xiao, F., Li, Y., Sun, Y., 2020. Novel thermodynamic early warning method for anaerobic digestion failure of energy crops. Bioresour. Technol. 310, 123440. https://doi.org/10.1016/j.biortech.2020.123440

Xiao, K., Zhou, Y., Guo, C., Maspolim, Y., Ng, W.J., 2016. Impact of undissociated volatile fatty acids on acidogenesis in a two-phase anaerobic system. J. Environ. Sci. 42, 196–201. https://doi.org/10.1016/J.JES.2015.06.015

Xiao, K.K., Guo, C.H., Zhou, Y., Maspolim, Y., Wang, J.Y., Ng, W.J., 2013. Acetic acid inhibition on methanogens in a two-phase anaerobic process. Biochem. Eng. J. 75, 1–7. https://doi.org/10.1016/J.BEJ.2013.03.011

Xiao, L., Sun, R., Zhang, P., Zheng, S., Tan, Y., Li, J., Zhang, Y., Liu, F., 2019. Simultaneous intensification of direct acetate cleavage and CO2 reduction to generate methane by bioaugmentation and increased electron transfer. Chem. Eng. J. 378, 122229. https://doi.org/10.1016/j.cej.2019.122229

Xu, M., He, Z., Deng, Y., Wu, L., Van Nostrand, J.D., Hobbie, S.E., Reich, P.B., Zhou, J., 2013. Elevated CO2 influences microbial carbon and nitrogen cycling. BMC Microbiol. 13. https://doi.org/10.1186/1471-2180-13-124

Xu, R., Xu, S., Florentino, A.P., Zhang, L., Yang, Z., Liu, Y., 2019. Enhancing blackwater methane production by enriching hydrogenotrophic methanogens through hydrogen supplementation. Bioresour. Technol. 278, 481–485. https://doi.org/10.1016/j.biortech.2019.01.014

Xu, S., Qiao, Z., Luo, L., Sun, Y., Wong, J.W.C., Geng, X., Ni, J., 2021. On-site CO2 bio-sequestration in anaerobic digestion: Current status and prospects. Bioresour. Technol. 332, 125037. https://doi.org/10.1016/j.biortech.2021.125037

Xu, Y., Nogi, Y., Kato, C., Liang, Z., Rüger, H.-J.J., De Kegel, D., Glansdorff, N., Nogi, Y., Kato, C., Liang, Z., Rüger, H.-J.J., De Kegel, D., Glansdorff, N., 2003. Psychromonas profunda sp. nov., a psychropiezophilic bacterium from deep Atlantic sediments. Int. J. Syst. Evol. Microbiol. 53, 527–532. https://doi.org/10.1099/ijs.0.02227-0

Yao, C., Li, X., Bi, W., Jiang, C., 2014. Relationship between membrane damage, leakage of intracellular compounds, and inactivation of *Escherichia coli* treated by pressurized CO_2. J. Basic Microbiol. 54, 858–865. https://doi.org/10.1002/jobm.201200640

Yin, W., Wang, Y., Liu, L., He, J., 2019. Biofilms: The microbial “protective clothing” in extreme environments. Int. J. Mol. Sci. 20. https://doi.org/10.3390/ijms20143423

Yu, T., Chen, Y., 2019. Effects of elevated carbon dioxide on environmental microbes and its mechanisms: A review. Sci. Total Environ. 655, 865–879. https://doi.org/10.1016/j.scitotenv.2018.11.301

Zabranska, J., Pokorna, D., 2018. Bioconversion of carbon dioxide to methane using hydrogen and hydrogenotrophic methanogens. Biotechnol. Adv. 36, 707–720. https://doi.org/10.1016/j.biotechadv.2017.12.003

Zeng, A.P., Biebl, H., Schlieker, H., Deckwer, W.D., 1993. Pathway analysis of glycerol fermentation by Klebsiella pneumoniae: Regulation of reducing equivalent balance and product formation. Enzyme Microb. Technol. 15, 770–779. https://doi.org/10.1016/0141-0229(93)90008-P

Zerfaß, C., Chen, J., Soyer, O.S., 2018. Engineering microbial communities using thermodynamic principles and electrical interfaces. Curr. Opin. Biotechnol. 50, 121–127. https://doi.org/10.1016/j.copbio.2017.12.004

Zhang, A., Sun, J., Wang, Z., Yang, S.-T., Zhou, H., 2015. Effects of carbon dioxide on cell growth and propionic acid production from glycerol and glucose by Propionibacterium acidipropionici. Bioresour. Technol. 175,

374–381. https://doi.org/10.1016/J.BIORTECH.2014.10.046

Zhang, A., Yang, S.-T., 2009. Propionic acid production from glycerol by metabolically engineered Propionibacterium acidipropionici. Process Biochem. 44, 1346–1351. https://doi.org/10.1016/j.procbio.2009.07.013

Zhang, F., Zhang, Y., Chen, M., Van Loosdrecht, M.C.M., Zeng, R.J., 2013. A modified metabolic model for mixed culture fermentation with energy conserving electron bifurcation reaction and metabolite transport energy. Biotechnol. Bioeng. 110, 1884–1894. https://doi.org/10.1002/bit.24855

Zhang, K., Ren, N.Q., Cao, G.L., Wang, A.J., 2011. Biohydrogen production behavior of moderately thermophile Thermoanaerobacterium thermosaccharolyticum W16 under different gas-phase conditions. Int. J. Hydrogen Energy 36, 14041–14048. https://doi.org/10.1016/j.ijhydene.2011.04.056

Zhang, L., Zhu, K., Li, A., 2016. Differentiated effects of osmoprotectants on anaerobic syntrophic microbial populations at saline conditions and its engineering aspects. Chem. Eng. J. 288, 116–125. https://doi.org/10.1016/j.cej.2015.11.100

Zhang, Y., Delbrück, A.I., Off, C.L., Benke, S., Mathys, A., 2020. Flow Cytometry Combined With Single Cell Sorting to Study Heterogeneous Germination of Bacillus Spores Under High Pressure. Front. Microbiol. 10, 1–13. https://doi.org/10.3389/fmicb.2019.03118

Zhao, J., Li, Y., Marandola, C., Krooneman, J., Euverink, G.J.W., 2020. Comparison of the microbial communities in anaerobic digesters treating high alkalinity synthetic wastewater at atmospheric and high-pressure (11 bar). Bioresour. Technol. 318. https://doi.org/10.1016/j.biortech.2020.124101

Zhao, J.Y., Hu, B., Dolfing, J., Li, Y., Tang, Y.Q., Jiang, Y., Chi, C.Q., Xing, J., Nie, Y., Wu, X.L., 2021. Thermodynamically favorable reactions shape the archaeal community affecting bacterial community assembly in oil reservoirs. Sci. Total Environ. 781. https://doi.org/10.1016/j.scitotenv.2021.146506

Zheng, Y., Lin, H.M., Tsao, G.T., 1998. Pretreatment for cellulose hydrolysis by carbon dioxide explosion. Biotechnol. Prog. 14, 890–896. https://doi.org/10.1021/bp980087g

Zhong, C., Zhang, G.C., Liu, M., Zheng, X.T., Han, P.P., Jia, S.R., 2013. Metabolic flux analysis of Gluconacetobacter xylinus for bacterial cellulose production. Appl. Microbiol. Biotechnol. 97, 6189–6199. https://doi.org/10.1007/s00253-013-4908-8

Zhou, M., Zhou, J., Tan, M., Du, J., Yan, B., Wong, J.W.C., Zhang, Y., 2017. Enhanced carboxylic acids production by decreasing hydrogen partial pressure during acidogenic fermentation of glucose. Bioresour. Technol. 245, 44–51. https://doi.org/10.1016/J.BIORTECH.2017.08.152

Zhu, C., Nomura, C.T., Perrotta, J. a, Stipanovic, A.J., Nakas, J.P., 2009. Production and characterization of poly-3-hydroxybutyrate from biodiesel-glycerol by Burkholderia cepacia ATCC 17759. Biotechnol. Prog. 26, 424–30. https://doi.org/10.1002/btpr.355

Zhu, X., Chen, L., Chen, Y., Cao, Q., Liu, X., Li, D., 2020. Effect of H2 addition on the microbial community structure of a mesophilic anaerobic digestion system. Energy 198, 117368. https://doi.org/10.1016/j.energy.2020.117368

Zhuo, G., Yan, Y., Tan, X., Dai, X., Zhou, Q., 2012. Ultrasonic-pretreated waste activated sludge hydrolysis and volatile fatty acid accumulation under alkaline conditions: Effect of temperature. J. Biotechnol. 159, 27–31. https://doi.org/10.1016/j.jbiotec.2012.01.005

Ziels, R.M., Nobu, M.K., Sousa, D.Z., 2019. Elucidating Syntrophic Butyrate-Degrading Populations in Anaerobic Digesters Using Stable-Isotope-Informed Genome-Resolved Metagenomics. mSystems 4, 1–16. https://doi.org/10.1128/msystems.00159-19

Ziganshin, A.M., Liebetrau, J., Pröter, J., Kleinsteuber, S., 2013. Microbial community structure and dynamics during anaerobic digestion of various agricultural waste materials. Appl. Microbiol. Biotechnol. 97, 5161–5174. https://doi.org/10.1007/s00253-013-4867-0

Zoetemeyer, R.J.J., van den Heuvel, J.C.C., Cohen, A., 1982. pH influence on acidogenic dissimilation of glucose in an anaerobic digestor. Water Res. 16, 303–311. https://doi.org/10.1016/0043-1354(82)90190-7

Acknowledgements

"Be strong enough to stand alone, smart enough to know when you need help, and brave enough to ask for it."

Ziad K. Abdelnour

The take-home message of this thesis could be summarized as follows: "in order to thrive under pressure (or elevated pCO_2), the right (operational) conditions, nutrients and symbiotic interactions are needed". This, for me, constitutes the perfect analogy of how to survive and succeed in a PhD, *i.e.,* the extreme condition to which a "highly skilled" macroorganism is exposed. Thus, you need a suitable inoculum (PhD candidate with a good supporting network), the right conditions (budget for research, technical support) and a mind eager to be nurtured (conferences, colloquiums, Red lab and MeCAT meetings). Moreover, symbiotic interactions with colleagues and academic peers are needed for personal and project development, which ultimately would increase the research outreach.

In my long list of acknowledgments, I would like to start thanking my family. Gracias a mis padres, mi hermana y mi abuelita por siempre apoyarme, confiar en mis decisiones, nunca cortarme las alas y por alimentar la mentalidad de que yo era capaz de conseguir grandes cosas en la vida pero que nunca debía olvidarme de mis orígenes. Gracias a mis tíos, primos en Ecuador y Colombia por siempre tenerme presente a pesar de la distancia, su cariño incondicional y por motivarme a seguir adelante al saber lo orgullosos que se sienten por mis logros.

I would like to express my deepest gratitude to my supervisory team in Delft for all their help and support throughout these years. Thanks to Jules for his trust, for constantly challenging the direction I wanted to take on my research project and for the critical feedback to improve my scientific writing. To Ralph, for becoming more of a mentor than a supervisor, the motivation and support and for being an example that you can find your way in the world to do things that matter. Having another "idealist" guiding your way in the sinuous path of academia was an extra source of motivation. Following the tradition from Ralph's project, mine was also not easy. I faced difficulties that none of my PhD fellows did. Fortunately, Jules and Ralph were there to back me up. A special thanks to Robbert Kleerebezem, for showing me the "complex beauty" of thermodynamics in environmental biotechnology. Also, my deep appreciation to the committee members for the time and effort dedicated to assessing my dissertation. I feel very honoured that recognized scientists showed interest in the work performed during my PhD.

I'm grateful for the symbiotic interactions that I established during my PhD at different levels. Thanks to my "office-mates", who evolved to become "my friends" throughout the years. To Victor, for his genuine friendship, all the practical help in the lab, the Mexican food, the dancing parties and showing how much he cares about me, sometimes in his very "particularly annoying" way. BTW, I miss you in the office. To Magela, for showing me the perks of the "obsessive-compulsive personality", for keeping the social interaction alive now that we don't see each other that often and for jumping into the waters of the life-changing decisions before me and showing that everything is going to be okay. To Niels, "the wanna-be-latino" from the office S3.02.030, thanks for being the personification of the "peer pressure" and changing my initial opinion about you after starting with the wrong foot (the lab experience conversation). Thank you guys for the ups and downs and for keeping track of everything with the potential to be used against us in the "board of shame".

Some words for Sara Toja, the strongest basque that I know (from 5 at least). Thanks not only for showing off your physical strength when I needed in the lab but also for your easy-going personality, you're a breeze of "different" air in our circle. Also, to Javier, the honorary member of the S3.02.030 office and currently my new "office-mate". Thanks for being a Mr.-Know-it-all, for the (wanted) technical help and (unwanted) singing demonstrations in the lab and for supplying us with the most random list of discussion topics ever.

Special thanks to Adrian for his friendship and for showing the importance of commitment and hard work in the lab. To Hongxiao, for his excellent disposition to work in the lab and to join the latin parties. To Anto, for saving my internship, letting me use her column two summers ago, for the easy-going chats, her charisma and decisive attitude. To my (old and contemporary) colleagues in the Red and Green Lab: Julian, Steef, Lenno, Saqr, Emiel, Carina, Bruno, thanks for being great scientists, for the times that we have discussed scientific or day-to-day issues and for always being willing to give a hand during difficult times. I cannot forget to express my gratitude to Alexander; thanks for all the scientific discussions, the reading recommendations and the initial guidance in the complex world of microbial fermentation. Sorry if I don't mention all the names here; space is limited, but I'm sure I expressed my gratitude to you back in the day. If I didn't, I would like to use these lines to recognize the big and small contributions that, in one way or the other, brought me to the completion of my PhD.

I'm also incredibly thankful to all the students that contributed with their work to this research project. Thanks to Maria Paola, Judith, Yiyi (Annie), Roberta, Charlotte, Jessie, Yu-ting (Kelly), and Yuan for being the other hands and brains of this operation.

My deep appreciation to the support team in the Water lab, especially to Armand and back on the day to Mohammed; without your help, the bumpy ride from idea to a working experiment

would not have become smooth. Also, to the secretaries, Mariska, Tamara and Rielle, for helping us navigate the world of immigration and university-related paperwork.

To the SuPER-W program and the European Union's Horizon 2020 research and innovation program for funding the project and allowing my development as an early-stage researcher in a competitive environment. To the Super-W people, thanks for sharing with me the initial three years of the chaotic journey that implies being a Marie-Curie fellow. In particular to the other latins in the program, Juan and Larissa, for all the fun moments and the shared distress, and to Mojtaba, for being an incredibly nice person.

To my friends in The Netherlands, Ecuador and around the world, thanks for always reminding me that life is not only about science and work but also is important to have fun and a good laugh with people that cares about you. Al ingeniero (David), por uno de los mejores tres leches que he probado en la vida, por las encomiendas ida y vuelta de Ecuador y por ser de esas personas que están ahí cuando en verdad los necesitas. Ana O, por ser una persona con super buena vibra que hizo que el primer año en Delft fuera más llevadero con las fiestas, viajes y barbacoas. Gracias a mis amigas de toda la vida, Anita, Angie, Yepitas y Gaby por siempre creer en mis capacidades y por instantáneamente incorporarme a sus vidas cuando estoy en Ecuador. Andre, por ser mi amiga ecuatoriana del clic instantáneo en Holanda, gracias por las historias, los encuentros en tierra neutral y las cervezas compartidas. Una mención especial a Gaby y Pauwel, gracias por ser mi pequeña familia en Gante, fue muy especial haber tenido la oportunidad de volver a ser "compis de depar".

A mis amigos de la U (Diego, Rommel, Chepo, Toscaine, Cha, Lore, Dani, Ana Gaby, Liz, Ale, Pablito, Lupo, Marieli), gracias por mantener el contacto y por de cuando en cuando revivir esas historias épicas aunque sea por chat. A mis amigos de la maestría Chupete, Belencita, Rosi gracias por mantener el contacto, las posadas en Cuenca y por su interés sincero en saber de mi vida a pesar de que ya no tengo Facebook. Al otro oso (Paúl B) por ser un amigo incondicional que siempre se acuerda de mi cumpleaños y por los mensajes random para saber si sigo viva. Rafa V, gracias por tu ayuda en mi última visita a Ecuador y por no haber desaparecido del mapa de los amigos a pesar de los años.

Thanks to all the people in Ghent that made my CMET experience worth remembering. To Korneel Rabaey for the fast-paced scientific discussions and his workarounds to make things feasible in such a short time. To Nico Boon and Ramon Ganigué for their valuable contributions to my experimental designs and manuscript. A big thanks to Jo de Vrieze for jumping into the project out of honest interest and the incredible help with the microbial community analysis together with Tim Lacoere, who was always willing to help even on short notice. Whichever thing I manage to do now on my own is thanks to you both. To Frederiek-Maarten for his help with statistics and flow cytometry. A la comunidad ecuatoriana: Naya,

Suanny, Katty, Adri, Byron gracias por volverme parte del grupo y por traer a Ecuador un poquito más cerca de mí. My sincere gratitude to Cristina Garcia for all her help with the flow cytometry and always being critical and supportive. To Myrsini, for being an example of a hard-working-warm-hearted person. To Funda, for always starting a conversation and not allowing awkward silences. To Jose and Pieter Candry, for their interest in my topic and the valuable discussions. To Camille, for her help and the good talks while preparing samples for VFA measurement. To Josefien, for borrowing me her pressure reactors and sharing the chore of "putting things under pressure." To Tyler, thanks a lot for the discussions, sediment samples for my experiments and your fine test in beer. To Cindy, Lotte, Eleftheria, Xiaoting, Xiaofei, Rui, Antonin and Amanda, thanks for all your help when I needed it and for a kind word when I was not having the best of days. Thank you to the secretaries and the supporting staff for all your help with the administrative paperwork and solving the day-to-day issues.

My gratitude also to René Rozendal for being my first contact point in Paques and for his initial contributions to this project. To Dhaval Mehta and Carla Frijters for being reasonable and flexible regarding the challenges that an internship during COVID times implied. Unfortunately, I couldn't grasp the real experience of "working at Paques," but I hope the performed work was somehow valuable for you.

Een grote dank aan Frans en Froukje. Jullie hebben goed voor mij gezorgd ook al was het niet nodig. Bedankt voor de hartelijke ontvangst in jullie familie en jullie vriendelijkheid. Ook aan mijn favoriete nederlanders Robin, Ilonka, Joris en Chris bedankt voor de gezelligheid, de biertjes, het geouwehoer en dat ik deel uit mocht maken van de groep. Ik heb altijd veel plezier gehad als jullie er waren.

Last but not least, I want to thank Daniel for all that he has done for me during these years. I know that I'm not easy to handle and always overthink things. So, it was evident that I wanted to find just the right words to express my love and gratitude for his constant support. Fortunately, the great RBG (Ruth Bader Ginsburg) already thought them for me: "If you have a caring (not yet) partner, you help the other person when that person needs it. I have a (not yet) partner who thinks my work is as important as his, and I think that makes all the difference for me."

About the author

Pamela Ceron-Chafla was born in Riobamba, Ecuador on April 8th, 1989. Pamela completed her Environmental Engineering degree (Summa Cum Laude), together with a minor in Chemical Engineering, at Universidad San Francisco de Quito (Ecuador) in 2012. Her bachelor's project focused in the development of a physicochemical system for the primary treatment of tannery effluents. Afterwards, she decided to pursue a Master degree in Environmental Technology and Engineering (IMETE) offered as a joint program by Unesco IHE, UCT Prague and Ghent University (2012-2014), from where she graduated with the highest distinction. For her master thesis, she worked in the optimization of a two-stage fermentation process for PHB production. This study was carried out in the Department of Biosystems Engineering (Ghent University) and the Flemish Institute for Technological Research (VITO).

After her master's, she went back to Ecuador where she worked as an environmental consultant for Walsh-Ecuador. Later on, she collaborated as an advisor on the implementation of low-cost environmental technologies for national and international development projects in Africa and South-America for Sun Mountain International.

Due to her career aspirations, she decided to go back to the academia to pursue a PhD in the area of resource recovery from wastewater. She joined the Sanitary Engineering section (Delft University of Technology) as PhD researcher in 2016 working on the topic "Steering Product formation in High-Pressure Anaerobic Systems". This research was developed under the framework of the European Joint Doctorate SuPER-W (Sustainable Product and Energy Recovery from Wastewater). This project was funded by the European Union's Horizon 2020 Research and Innovation program, which granted her the status of Marie Curie fellow. During her PhD, she also worked as visiting researcher at the Center for Microbial Ecology and Technology (CMET) in Ghent University (2019). Also, she carried out a two-months internship for the company Paques NL (2020).

She currently works as a post-doctoral researcher for the Water Management Department (Delft University of Technology) and the International Center for Frugal Innovation. Her research aims to develop and optimize "frugal" anaerobic wastewater treatment systems in the Global South. Her professional interests are linked to resource recovery from wastewater, waste-to-energy solutions and improving sanitation via decentralized systems.

List of publications

Scientific Articles

Ceron-Chafla, P., De Vrieze, J., Rabaey, K., van Lier, J. B., & Lindeboom, R. E. F. Potentials and limitations of elevated pCO_2 as steering parameter in anaerobic processes. *Submitted to Biotechnology for Biofuels and Bioproducts.*

Ceron-Chafla, P., García-Timermans, C., Vrieze, J., Ganigué, R., Boon, N., Rabaey, K., Lier, J.B., Lindeboom, R.E.F., 2022. Pre-incubation conditions determine the fermentation pattern and microbial community structure in fermenters at mild hydrostatic pressure. Biotechnol. Bioeng. 1–16. https://doi.org/10.1002/bit.28085

Crescenzo, D., Crescenzo, C. De, Marzocchella, A., Karatza, D., Molino, A., **Ceron-Chafla, P.,** Lindeboom, R.E.F., Lier, J.B. Van, Chianese, S., Musmarra, D., 2022. Biotechnology for Biofuels Modelling of autogenerative high - pressure anaerobic digestion in a batch reactor for the production of pressurised biogas. Biotechnol. Biofuels Bioprod. 1–14.

Wasajja, H., Al-Muraisy, S. A. A., Piaggio, A. L. ., **Ceron-Chafla, P.,** Aravind, P. V., Spanjers, H., van Lier, J. B. ., & Lindeboom, R. E. F. (2021). Improvement of Biogas Quality and Quantity for Small-Scale Biogas-Electricity Generation Application in off-Grid Settings: A Field-Based Study. Energies, 14(11), 3088.

Ceron-Chafla, P., Chang, Y., Rabaey, K., van Lier, J. B., & Lindeboom, R. E. F. (2021). Directional Selection of Microbial Community Reduces Propionate Accumulation in Glycerol and Glucose Anaerobic Bioconversion Under Elevated pCO_2. Frontiers in Microbiology, 12(June), 1583.

Ceron-Chafla, P., Kleerebezem, R., Rabaey, K., B. van Lier, J., & E. F. Lindeboom, R. (2020). Direct and Indirect Effects of Increased CO_2 Partial Pressure on the Bioenergetics of Syntrophic Propionate and Butyrate Conversion. Environmental Science & Technology, 54(19), 12583–12592.

Book chapters

Ceron-Chafla, P., & Lindeboom, R. E. F. (2022). Frugalizing engineering solutions for recovery of resources from wastewater. In Handbook of Frugal Innovation.

Oral presentations

Ceron-Chafla, P., García-Timermans, C., Vrieze, J., Ganigué, R., Boon, N., Rabaey, K., Lier, J.B., Lindeboom, R.E.F., (2022, May 9-11). Moderate hydrostatic pressure modifies the metabolic flux distribution in natural and adapted high-salinity anaerobic mixed cultures. 4th International Conference on Biogas Microbiology, Braga, Portugal

Ceron-Chafla, P., Rabaey, K., B. van Lier, J., & E. F. Lindeboom, R. (2019, June 23-27). Effects of elevated pCO_2 in mixed culture fermentation. IWA - 16th World Conference on Anaerobic Digestion, Delft, The Netherlands

Ceron-Chafla, P., Rabaey, K., B. van Lier, J., & E. F. Lindeboom, R. (2018, June 4-7). Application of soft sensor for pH monitoring in high-pressure reactors used for mixed culture fermentation. 2nd International Conference on Anaerobic Digestion Technology:Sustainable Alternative Bioenergy for a Stable Life, Chiang Mai, Thailand.

Poster presentations

Ceron-Chafla, P., Rabaey, K., B. van Lier, J., & E. F. Lindeboom, R. (2019, September 8-12). Impact of elevated CO_2 partial pressure on the thermodynamics and kinetics of syntrophic propionate oxidation. 3rd IWA Resource Recovery Conference, Venice, Italy.